

ENGINE EFFICIENCY TECHNOLOGY STUDY

FINAL REPORT

SwRI® Project No. 03.26457

Prepared for:

**Argonne National Laboratory
9700 South Cass Avenue
Lemont, IL 60439**

**Prepared by:
Thomas E. Reinhart
Institute Engineer**

November 30, 2021

ENGINE EFFICIENCY TECHNOLOGY STUDY

FINAL REPORT

SwRI® Project No. 03.26457

Prepared for:

**Argonne National Laboratory
9700 South Cass Avenue
Lemont, IL 60439**

November 30, 2021

Prepared by:

**Thomas E. Reinhart
Institute Engineer
Design & Development Department
Powertrain Engineering Division**

Approved by:

**Chris Hennessey
Director
Design & Development Department
Powertrain Engineering Division**

Reviewed by:

**David Branyon
Staff Engineer
Design & Development Department
Powertrain Engineering Division**

Reviewed by:

**Kevin Hoag
Institute Engineer
Design & Development Department
Powertrain Engineering Division**

POWERTRAIN ENGINEERING DIVISION

This report shall not be reproduced, except in full, without the written approval of Southwest Research Institute®. Results and discussion given in this report relate only to the test items described in this report.

EXECUTIVE SUMMARY

The purpose of this project is to evaluate a range of potential efficiency technologies that could be applied to light, medium, and heavy-duty truck engines. Four engines were studied in the course of the work:

1. Cummins B6.7 medium duty truck diesel engine
2. Detroit DD15 heavy-duty truck diesel engine
3. GM Duramax 3.0-liter light duty diesel for Class 2a pickup trucks
4. Ford 7.3 liter medium-duty gasoline V-8 engine

Two of these engines, the B6.7 and the DD15, had been evaluated in a previous study conducted by Southwest Research Institute (SwRI) for the National Highway Traffic Safety Administration (NHTSA) [1, 2]. The other two engines are new to the market in just the last few years. For each engine, a list of potential BSFC reduction technologies was drawn up and agreed between SwRI, Argonne National Laboratory (ANL), and NHTSA.

Each engine was modeled in GT-Power®, and the models were calibrated and validated against test data available at SwRI or provided by the Original Equipment Manufacturers (OEMs). Once the models achieved satisfactory results, the technology evaluation began. Engine performance was mapped over the speed and load range, and fuel maps suitable for use with the vehicle simulation program Autonomie were provided to ANL.

The B6.7 engine was evaluated with the 2019 baseline configuration and with 8 additional technology options. Cylinder deactivation (CDA) provided fuel consumption reductions at light load of 7% at low speed to 12% at high speed. The maximum load where CDA could be used ranged from just under 2 bar brake mean effective pressure (BMEP) at low and high speeds, up to about 3.5 bar in the middle of the speed range. A reduction in engine friction (FMEP) offers less than a 1% improvement above half load, but more benefit at light load. Implementation of a mild Miller cycle using fixed valve events did not offer any benefit. The use of an EGR pump with a high efficiency fixed geometry turbo provided a small benefit across most of the speed and load range, and the best overall result was obtained by combining the exhaust gas recirculation (EGR) pump and high efficiency turbo with CDA.

The DD15 was evaluated with the 2019 baseline hardware configuration, along with a total of 19 additional technology options. This engine comes with a form of CDA built into the baseline configuration and adding the more complex full CDA with valve deactivation did not provide a measurable benefit. The engine has already had downspeeding applied to it, with the peak torque being available as low as 900 rpm. Further reduction in torque peak speed appeared unrealistic, so an increase in peak torque level was used to reduce the speed at which rated power is available. This approach will still allow the vehicle to be geared taller, providing a lower engine speed at vehicle cruise speed with no loss in available power.

As with the B6.7, mild Miller with fixed valve events provided no benefit to the DD15. On the DD15, a more radical Miller cycle with two stage turbocharging and variable valve events was evaluated, and this technology does provide 1% to 3% benefit across a broad area of the engine

map, and much more at light load. An additional benefit is an increase in exhaust temperatures at low and moderate loads which bodes well for thermal management of the exhaust aftertreatment system without the use of additional fuel or other approaches that result in low engine efficiency. Reduction in engine friction provided very similar benefits as in the B6.7, with less than 1% reduction above half load and more than 1% at light loads. Two downsizing options were explored, one with the same power and torque as the baseline engine (using higher BMEP to achieve this), and another with constant BMEP that would reduce vehicle performance. Both options appear to offer potential benefit, which needs to be explored in the vehicle simulations.

The Rankine cycle waste heat recovery system (WHR) offered the largest benefit of any technology on the DD15, with benefits ranging from 2% to 5.5% except at very light load. These benefits and the associated fuel maps need to be treated carefully, however. WHR has a very slow transient response, because one source of waste heat is the exhaust flow after the aftertreatment system, and the aftertreatment has a very high thermal inertia. As a result, the actual benefit from WHR on a given drive cycle will almost certainly be less than what the steady state map would predict. SwRI recommends a future task, building a transient model of WHR in GT that includes the effects of thermal inertia, to allow for more accurate simulation of WHR performance over different drive cycles.

The EGR pump provides 1% to 3% benefit on the DD15, with higher values at light load. As was found in a previous project, turbocompound technology does not provide a useful benefit, regardless of whether the power turbine is coupled back to the engine mechanically or electrically.

Two technology combinations were evaluated for the DD15. The first included the strong Miller cycle with two-stage boost and VVA. The second added WHR to the first. The second combination reduced the best point BSFC from 183.7 g/kW-hr to 171.8, a 6.5% improvement. Even larger improvements were obtained at other points on the operating map.

The GM Duramax 3.0-liter diesel is a new light duty diesel that shares design features with many high BMEP light duty diesels sold in Europe. One of these features is the combination of high-pressure loop EGR with low pressure loop EGR, which reduces the pumping work required to flow EGR. The engine also uses very little EGR at high load, which helps it run a high 26 bar BMEP at a relatively modest cylinder pressure limit of 180 bar. The Duramax also has very low friction for a diesel engine, limiting the potential for further FMEP reduction. These features meant that several of the technologies explored on the other two diesel engines would not provide the same benefits, so the technology list was revised. The 2020 production baseline and seven technology options were evaluated.

A flat 20% reduction in friction of the Duramax, which would be very difficult to achieve in practice, provided less than 1% BSFC benefit in the portion of the map where most drive cycle time resides. Cylinder deactivation performed better, with a 5% to 30% benefit at light loads below about 3 bar BMEP. Since this is a 26-bar engine, CDA's benefits are limited to operation at about 12% load and below. As with some of the other technologies, CDA also provides an aftertreatment thermal management benefit without incurring a fuel consumption penalty.

The variable geometry turbocharger of the Duramax was replaced with a series sequential combination of two fixed geometry turbochargers. This change provided a 1% to 3% benefit in the portion of the fuel map where most drive time would be spent. Another option considered was the use of a single fixed geometry turbo with an e-booster to fill in the boost required at low speed and medium to high load. This option provided 2% to 8% benefit in the most heavily used portions of the fuel map. However, these values assume that power for the e-booster are provided by a hybrid system or other external source. If the engine is required to generate the electricity required by the e-booster, the benefit will be significantly reduced.

Another option for the Duramax was increasing the BMEP from 26 to 30 bar, in combination with the fixed geometry turbo and e-boost. This allowed rated speed to be moved down 500 rpm, which in turn allows the transmission shift points and axle ratio to be revised in ways that should reduce fuel consumption. Vehicle simulation will be required to determine the benefit of this approach. The final technology combination added CDA to the 30 bar BMEP variant. This provides a significant additional benefit at loads below about 3 bar BMEP.

The Ford 7.3-liter gasoline engine was exercised over the widest range of technologies in both naturally aspirated and turbocharged form, and both 2-valve and 4-valve cylinder head designs. The baseline engine is naturally aspirated with port fuel injection and a 2-valve head. Addition of GDI allowed the engine to increase compression ratio from 10.5 to 11.5, which provided a benefit of about 2% over much of the map. Application of GDI and a 4-valve head allowed an additional compression ratio to increase to 12, and about a 1% reduction in fuel consumption. The benefit was larger at high loads, but zero or slightly negative below 1500 RPM and below 7 bar BMEP. Dual independent cam phasers were added in place of the single cam and phaser of the baseline engine on the 11.5 CR GDI variant. The dual phasers provided significant low speed, light load benefit, but little to no benefit at higher speeds and loads.

Lean burn operation offers the largest benefit of any technology applied. Below 6 bar BMEP, benefits of 5% to over 10% were found. The benefit tapers to zero at full load, since the naturally aspirated engine must run stoichiometric to make full load. Note, however, that lean burn would require development of a NO_x aftertreatment system that could handle sustained high exhaust temperatures. Low pressure loop EGR was added to the 11.5 CR GDI engine. This provided 3 to 9% benefits across the full speed range at low and medium load, tapering to zero near full load. A 10% reduction in friction was applied to the LPL EGR engine. The benefit was 1% or less across most of the speed / load range, but there were benefits at low speed and high load due to improved combustion phasing made possible by the reduced IMEP for a given BMEP. Adding CDA to the 11.5 CR GDI engine provides significant benefits below 4 bar BMEP, and double-digit percentage fuel consumption reductions below about 3 bar BMEP. However, CDA has no effect above 4 bar, where it cannot be used.

Hybrid operation allows the use of an electric motor to compensate for reduced power from the ICE. This opens the door to higher compression ratios and resulting lower torque curves. The Ford 7.3-liter engine is somewhat unusual in that it suffers from high speed knock in addition to low speed knock. As a result, substantial electric assist is required at rated power. Increasing CR to 12.5 provided about a 1% benefit over much of the map, while a 13.5 CR gave 1% to 2% benefit.

More radical CR increases could be considered if the exhaust system was less restrictive, since the restrictive exhaust causes high residuals at high speed and load, which is a factor promoting knock.

Several turbocharged options were evaluated in both 2-valve and 4-valve form. A minimum compression ratio of 9.5 was selected to minimize the efficiency penalty of the boosted engines. The use of 4 valves allowed a higher BMEP level, and thus a lower rated speed than could be obtained from the 2-valve configuration. The potential benefit of boosted engines is that with their narrower speed range, they will run at a lower engine RPM and a higher BMEP level. Under light load conditions, this pushes the boosted engine BMEP up into a more efficient portion of the map compared to the naturally aspirated baseline. Thus, any efficiency benefits to be seen will come from vehicle simulation, not from the engine results. Benefits from the higher BMEP 4-valve configuration should be greater.

Lean burn technology on boosted engines can stay lean up to full load, cylinder pressure limits permitting. The limitation at low speed is turbocharger boost capacity, and at higher speeds a misfire limit of $\Lambda = 1.6$ was applied. As with the naturally aspirated engine, lean burn offers large efficiency improvements, especially at lower engine speeds. Unfortunately, the cost and complexity of lean NOx aftertreatment may preclude production applications. Full authority VVA provided the naturally aspirated GDI engine with large fuel reductions at light load, but below 2% above 4 bar BMEP.

Independent cam phasers provided benefits only under 2 bar BMEP, and penalties above that. Because of different park positions, the independent phasers could not match the results of a single cam phaser above 2 bar. Low pressure loop EGR provided a 1% to 3% benefit across much of the map, but between about 2 bar and 4 bar BMEP, the benefit was zero or slightly negative. Application of D-EGR on the boosted engines provided 3% to 6% benefits across most of the map, with less at full load and larger benefits at loads below 2 bar BMEP. Full authority VVA provided 2% to 4% benefit to the turbocharged engines at medium to high loads, but much larger benefits at low speed, light load.

TABLE OF CONTENTS

	<u>Page</u>
EXECUTIVE SUMMARY	iii
LIST OF FIGURES	x
LIST OF TABLES	xv
LIST OF ABBREVIATIONS AND ACRONYMS	xvi
1.0 INTRODUCTION.....	1
2.0 6.7 LITER MEDIUM-DUTY DIESEL ENGINE	5
2.1 Baseline Model Match	5
2.2 Zero EGR with Variable Geometry Turbine	10
2.3 Fixed Valve Timing Mild Miller Cycle	13
2.4 Cylinder Deactivation.....	13
2.5 Mechanical Friction Reduction	15
2.6 Zero EGR with High-Efficiency Fixed Geometry Turbo.....	Error! Bookmark not defined.
2.7 EGR Pump with High-Efficiency Fixed Geometry Turbo.....	17
2.8 Technology Combo: EGR Pump and Cylinder Deactivation with High-Efficiency Fixed Geometry Turbo.....	21
3.0 DD15 HEAVY-DUTY DIESEL ENGINE	23
3.1 DD15 Baseline Validation	23
3.2 Reduced Engine Friction (FMEP).....	29
3.3 Down Speeding with Increased BMEP	31
3.4 Downsizing with Constant BMEP	34
3.5 Downsizing with Constant Torque.....	37
3.6 Waste Heat Recovery.....	41
3.7 Electric EGR Pump with High Efficiency Turbo	43
3.8 Cylinder Deactivation.....	47
3.9 Mild Miller Cycle	47
3.10 Strong Miller with EGR Pump, VVA, and 2-Stage Turbocharger	49
3.11 Mechanical Turbocompound	53
3.12 Electric Turbocompound	54
3.13 Base Engine Turbo with EGR Delete.....	Error! Bookmark not defined.
3.14 High Efficiency Turbo with EGR Delete	Error! Bookmark not defined.
3.15 Best Build Combination Models	57
4.0 GM DURAMAX 3.0 LITER LIGHT DUTY DIESEL	62

4.1	Baseline Model Match	62
4.2	Reduced Friction.....	66
4.3	Cylinder Deactivation.....	68
4.4	Series Sequential with High Efficiency Fixed Geometry Turbos	70
4.5	Zero EGR with Series Sequential High Efficiency Fixed Geometry Turbos ...Error! Bookmark not defined.	
4.6	High-Efficiency Fixed Geometry Turbocharger with e-Compressor	73
4.7	High-Efficiency Fixed Geometry Turbocharger with e-Compressor and Moderate Down Speeding.....	76
4.8	High-Efficiency Fixed Geometry Turbocharger with e-Compressor, Moderate Down Speeding and CDA.....	78
5.0	FORD 7.3 LITER MEDIUM DUTY GASOLINE ENGINE.....	81
5.1	Baseline Engine Validation	81
5.2	Changes to Model to Predict Engine Technology Performance	84
5.3	GDI with CR 10.5.....	85
5.4	GDI with 11.5 CR.....	87
5.5	GDI with CR 12 and 4V Head	89
5.6	Lean Burn NA Engine with GDI	91
5.7	NA GDI with Independent Cam Phasers (VVT)	93
5.8	NA GDI with LPL EGR	96
5.9	Technology Combo: NA GDI with LPL EGR and 10% Lower Friction	99
5.10	NA GDI with Higher CR for Hybrid Applications.....	103
5.10.1	CR 13.5.....	107
5.11	Turbocharged Versions with a Narrower Speed Range	109
5.11.1	Turbocharged and Downsped with GDI 2V.....	111
5.11.2	Turbocharged Downsped with GDI 4V	113
5.11.3	Turbocharged Downsped with GDI 2V, Lean Burn	114
5.11.4	Turbocharged Downsped with GDI 4V, Lean Burn	117
5.11.5	Turbocharged Downsped with GDI 2V, Independent Cam Phasers (VVT).....	119
5.11.6	Turbocharged Downsped with GDI 4V, Independent Cam Phasers (VVT).....	121
5.11.7	Turbocharged Downsped with GDI 2V, VVT and LPL EGR	123
5.11.8	Turbocharged Downsped with GDI 4V, Cam Phasers, and LPL EGR.....	125
5.12	NA GDI with CDA and 11.5 CR.....	127
5.13	Turbocharged Downsped with GDI 2V, Independent Cam Phasers, D-EGR	129
5.14	Turbocharged Downsped with GDI 4V, VVT, D-EGR, CDA	131
5.15	NA GDI with Full Authority Variable Valve Timing and Duration (VVA)	132
5.16	TC GDI 2V, with Full Authority Variable Valve Timing and Duration (VVA) and LPL EGR.....	134
5.17	TC GDI 4V, with Full Authority Variable Valve Timing and Duration (VVA) + LPL EGR.....	136

6.0	CONCLUSIONS AND RECOMMENDATIONS.....	138
6.1	B6.7 Medium Duty Diesel.....	138
6.2	Detroit DD15 Heavy-Duty Diesel.....	139
6.3	GM Duramax 3.0 Liter Light Duty Diesel.....	140
6.4	Ford 7.3 Liter Medium-Duty Gasoline Engine	141
6.5	Recommendations for Future Work	142

APPENDICES	<u>No. of Pages</u>
A	WASTE HEAT RECOVERY SYSTEM DETAILS..... 7

LIST OF FIGURES

<u>Figure</u>	<u>Page</u>
Figure 1. GT-Power® Model of the Cummins 6.7L Engine	6
Figure 2. Measured Versus Modeled BSFC at Various Operating Points.....	7
Figure 3. Fuel Efficiency Percentage Difference Between Measurement and GT Model	7
Figure 4. EGR Map Used in the Engine Model (Not Verified with Actual Engine Data)	8
Figure 5. Compressor Map Used in the 6.7 Liter Engine Model.....	9
Figure 6. No-Load Fueling with Projection to 600 rpm Idle	10
Figure 7. BSFC Percentage Improvement with Zero EGR and Retaining the VGT	12
Figure 8. Effect of Eliminating EGR on 1600 rpm Compressor Operation	12
Figure 9. BSFC Percentage Improvement with Three Cylinder Deactivation	14
Figure 10. CDA Transition Load and Fuel Efficiency Change versus Engine Speed	15
Figure 11. Friction Reduction Rationale Applied to Heavy- and Medium-Duty Engines	16
Figure 12. BSFC Percentage Improvement From Baseline with Reduced Friction.....	17
Figure 13. Fixed Geometry Turbine Compressor Efficiency Map with Zero-EGR.....	Error! Bookmark not defined.
Figure 14. Wastegate Operation to Maintain 160-bar or Lower PCP.....	Error! Bookmark not defined.
Figure 15. Percentage Fueling Change over Baseline Using Fixed Geometry Turbo with Wastegate and Zero-EGR	Error! Bookmark not defined.
Figure 16. Pressure Differential and Resulting EGR Flow Using a Fixed Geometry Turbo	17
Figure 17. EGR Pump Power Consumption or Production	19
Figure 18. Fueling Change over Baseline, Hybrid EGR Pump Approach (top) and Conventional EGR Pump Approach (bottom)	20
Figure 19. Percentage Fueling Change over Baseline when Combining the Conventional EGR Pump with Cylinder Deactivation.....	21
Figure 20. CDA Fueling Changes Added to the Conventional EGR Pump Model.....	22
Figure 21. BSFC Comparisons for the Fixed Geometry Turbo Configurations Compared to Baseline (top left).....	22
Figure 22. DD15 GT Baseline Model.....	24
Figure 23. DD15 GT Baseline Operating Points	25
Figure 24. Comparison of BSFC Predicted by the GT Model Against 2019 Engine Test Data ..	26
Figure 25. (Part 1) Baseline Model Data Correlation at Full Load. Note that where only one line can be seen, there is a near-perfect match between model and test data.	27
Figure 26. (Part 2) Baseline Model Data Correlation at Full Load	28
Figure 27. (Part 3) Baseline Model Data Correlation at Full Load	29
Figure 28. Friction (FMEP) Reduction Assumptions	30
Figure 29. Friction reduction BSFC Improvement over Baseline	30
Figure 30. Effect of DownSpeed 'A' on Engine Performance at Full Load.....	31
Figure 31. DownSpeed 'A' BSFC improvement. Green and blue areas represent an improvement, while orange and red show an increase in fuel consumption.	32
Figure 32. Effect of DownSpeed 'B' on Engine Performance at Full Load.....	33
Figure 33. DownSpeed 'B' BSFC improvement. Green and blue areas show a reduction in fuel consumption compared to the baseline, while orange and red show an increase.	33

Figure 34. BSFC Improvement of Downsized 5 Cyl. Engine with Constant BMEP. Pale Green, Yellow, and Orange Reflect Increases in Fuel Consumption, While Dark Green and Blue Represent Improvements	35
Figure 35. Comparison of 6 Cyl. vs. 5 Cyl. BSFC Maps	36
Figure 36. Comparison of 6 Cyl. vs. 5 Cyl. BSFC Maps – Zoomed to Look at 300 to 1200 Nm Torque	36
Figure 37. BSFC improvement of Downsize Engine with Constant Torque	38
Figure 38. Comparison of 6 Cyl. vs. 5 Cyl. BSFC Maps.	39
Figure 39. Comparison of 6 Cyl vs. 5 Cyl. BSFC on a Torque Basis – Zoomed to Look at 300 to 1200 Nm Torque.	39
Figure 40. (Part 1). Comparison of 6 Cyl vs. 5 Cyl. Full Load Performance with Constant Power and Torque (Increased BMEP).	40
Figure 41. (Part 2). Comparison of 6 Cyl vs. 5 Cyl. Full Load Performance.	41
Figure 42. Power Recovered by WHR	42
Figure 43. BSFC Improvement From WHR	43
Figure 44. BSFC Improvement With Electric EGR Pump. Pale Green and Yellow Indicate an Increase in Fuel Consumption, While Dark Green and Blue Shades Show a Benefit.....	45
Figure 45. Operating Parameters of Electric EGR Pump	46
Figure 46. BSFC Improvement From Mild Miller Valve Event and Revised Turbocharger Match	48
Figure 47. Inlet Valvetrain Scaling Range.....	50
Figure 48. Resulting Inlet Valve Opening & Closing Optimised.....	50
Figure 49. Strong Miller Cylinder Pressures & Air Fuel Ratios	51
Figure 50. Strong Miller BSFC Improvement vs. Base Engine. Yellow and Orange Areas Show Increased Fuel Consumption, Green and Blue Areas Show Reduced Fuel Consumption.	52
Figure 51. Strong Miller BSFC Improvement vs. EGR Pump + High Efficiency Turbo Engine	53
Figure 52. BSFC Improvement from Mechanical APT	54
Figure 53. BSFC Improvement of Electric Turbocompound With Base Engine EGR	55
Figure 54. BSFC Improvement of Electric Turbocompound With Reduced EGR	56
Figure 55. Comparison of Electric Turbocompound EGR Rates	56
Figure 56. BSFC Improvement of EGR delete on Base Engine... Error! Bookmark not defined.	
Figure 57. Full Load Engine Performance of EGR Delete on Base Engine Error! Bookmark not defined.	
Figure 58. BSFC Improvement of EGR Delete with High Efficiency Turbo ... Error! Bookmark not defined.	
Figure 59. Full Load Engine Performance of EGR Delete with High Efficiency Turbo Error! Bookmark not defined.	
Figure 60. BSFC of Base Engine vs Technology Combinations 1 & 2.....	57
Figure 61. BSFC of Base Engine vs Technology Combinations 1 & 2 at Low Load	58
Figure 62. BSFC & BSFC Improvement of Technology Combination 1	59
Figure 63. BSFC & BSFC Improvement of Technology Combination 2 vs. Baseline	59
Figure 64. Full Load Performance of Base v Downsped v Combination Build Engines	60
Figure 65. Argonne Data for Operating Region of Sleeper Truck (ARB Transient Cycle)	61
Figure 66. GT-Power® Model of the Duramax 3.0L Engine.....	63

Figure 67. Fuel Flow Rate Percentage Difference at Various Operating Points. Yellow and Red Values Indicate That the Model Overpredicts Fuel Consumption, While Blue Areas Under-Predict Fuel Consumption. Green Areas Show Good Agreement Between Model and Test.	64
Figure 68. BTE / BSFC Percentage Difference between Measurement and Model.....	64
Figure 69. Low Pressure Loop EGR Map Used in the Engine Model	65
Figure 70. High Pressure Loop EGR Map Used in the Engine Model.....	65
Figure 71. Duramax 3.0 Motoring / Minimum Torque Curve.....	66
Figure 72. Friction Reduction Rationale Applied to Light-Duty Engine	67
Figure 73. BSFC Percentage Improvement from Baseline with Reduced Friction.....	67
Figure 74. Cylinder Deactivation Boundary	68
Figure 75. BSFC Percentage Fuel Consumption Reduction with Three Cylinder Deactivation..	69
Figure 76. BSFC Percentage Fuel Consumption Reduction with Three Cylinder Deactivation (Zoomed in to Light Load)	69
Figure 77. Reduction in Pumping Losses with Three Cylinder Deactivation	70
Figure 78. GT-Power® Model Modifications for Series Sequential Arrangement.....	71
Figure 79. Valve Control Modes for Series Sequential Turbocharging	72
Figure 80. BSFC Percentage Improvement from Baseline with Series Sequential Turbos.....	73
Figure 81. Valve Control Modes for Series Sequential Turbocharging with Zero EGR..... Error! Bookmark not defined.	
Figure 82. BSFC Percentage Improvement from Baseline with Series Sequential Turbos and Zero EGR. Red Hatched or Dotted Areas Have an Increase in Fuel Consumption, But All Other Areas See a Reduction. Error! Bookmark not defined.	
Figure 83. Fixed Geometry Turbo Compressor Efficiency Map.....	74
Figure 84. Percentage BSFC Improvement Compared to the Baseline, with Fixed Geometry Turbo and e-Compressor.....	75
Figure 85. e-Compressor Power Consumption.....	75
Figure 86. Baseline and Down-Speed Power and Torque Curves.....	77
Figure 87. BSFC Comparison for Fixed Geometry Turbo w/e-Compressor, With and Without Down Speeding.....	77
Figure 88. e-Compressor Power Consumption Over Down Speed Map	78
Figure 89. BSFC Map When Combining Fixed Geometry Turbocharger Model with e-Compressor and Down Speeding with CDA	79
Figure 90. BSFC Comparison at Light loads for Down Speed Configuration with CDA Compared to Configuration without CDA.....	79
Figure 91. e-Compressor Power Consumption for Down Speed Configuration With CDA.....	80
Figure 92. Difference Between Model and Test Data for BTE / BSFC. Green areas show good agreement, while blue areas show the model to under-predict fuel consumption, and yellow or red areas are where the model over-predicts fuel consumption.	82
Figure 93. Equivalence Ratio of the Base Engine, Showing Power Enrichment and Component Protection	82
Figure 94. Ford 7.3 Baseline BTE, from GT Model.....	83
Figure 95. 7.3 V-8 Baseline CA50 Timing.....	83
Figure 96. Friction Model Correlation.....	84
Figure 97. BTE Map for GDI with 10.5 CR	85
Figure 98. CA50 Timing for GDI with 10.5 CR	86

Figure 99. BTE Improvement of GDI with 10.5 CR Relative to Baseline.....	86
Figure 100. BTE Map for GDI with 11.5 CR.....	87
Figure 101. CA50 Timing for GDI with 11.5 CR	88
Figure 102. BTE Improvement of GDI with 11.5 CR Relative to Baseline PFI with CR 10.5....	88
Figure 103. BTE Map for 4-Valve GDI with 12.0 CR	89
Figure 104. CA50 Timing for 4-valve GDI with 12.0 CR.....	90
Figure 105. BTE Improvement of 4-valve GDI with 12.0 CR, Relative to GDI with 11.5 CR ...	90
Figure 106. BTE Map for Lean Burn GDI with 11.5 CR.....	92
Figure 107. AFR Map for Lean Burn GDI with 11.5 CR.....	92
Figure 108. CA50 Map of Lean Burn GDI with 11.5 CR	93
Figure 109. BTE Improvement of Lean Burn GDI with 11.5 CR, Relative to GDI 11.5 CR	93
Figure 110. BTE Map for GDI with 11.5 CR and Independent Cam Phasers.....	94
Figure 111. CA50 Map of GDI with 11.5 CR and Independent Cam Phasers.....	95
Figure 112. BTE Improvement of GDI with 11.5 CR and Independent Cam Phasers, Relative to GDI with 11.5 CR	95
Figure 113. BTE Map for GDI with 11.5 CR and LPL EGR	96
Figure 114. EGR Rate Map for GDI with 11.5 CR and LPL EGR	97
Figure 115. CA50 Map for GDI with 11.5 CR and LPL EGR	97
Figure 116. BTE Improvement of GDI with 11.5 CR and LPL EGR, Relative to GDI 11.5 CR	98
Figure 117. BTE Map for GDI with 11.5 CR, LPL EGR, and FMEP Reduction	99
Figure 118. CA50 Map for GDI with 11.5 CR, LPL EGR, and FMEP Reduction	100
Figure 119. Change in BSFC of for GDI with 11.5 CR, LPL EGR, and FMEP Reduction, Relative to Baseline	100
Figure 120. BTE Improvement for GDI with 11.5 CR, LPL EGR, and FMEP Reduction, Relative to the Same Engine without FMEP Reduction, Showing the Incremental Benefit of Friction Reduction	101
Figure 121. FMEP Map for the Baseline Engine.....	101
Figure 122. FMEP Map for GDI with 11.5 CR and LPL EGR	102
Figure 123. FMEP Map for GDI with 11.5 CR, LPL EGR, and Reduced FMEP.....	102
Figure 124. Engine Derate Options for 25, 75, and 100 kW e-motors.....	104
Figure 125. Engine Torque Curves for 11.5, 12.5, and 13.5 CR with GDI.....	104
Figure 126. BTE Map for GDI with 12.5 CR for Hybrid Applications.....	105
Figure 127. CA50 Map for GDI with 12.5 CR for Hybrid Applications.....	106
Figure 128 BTE Improvement of for GDI with 12.5 CR Relative to GDI with 11.5 CR	106
Figure 129. BTE Map for GDI with 13.5 CR for Hybrid Applications.....	107
Figure 130. CA50 Map for GDI with 13.5 CR for Hybrid Applications.....	108
Figure 131. BTE Improvement for GDI with 13.5 CR Relative to GDI with 11.5 CR.....	108
Figure 132. Torque Curve Options Considered for a Boosted Version with Downspeeding.....	109
Figure 133. Comparison of Turbocharged (2V and 4V) and NA (Base) Torque Curves.....	110
Figure 134. Comparison of Turbocharged (2V and 4V) and NA (Base) Power Curves	110
Figure 135. BTE Map of Turbocharged GDI 2V Engine	112
Figure 136. CA50 Map of Turbocharged GDI 2V Engine	112
Figure 137. BTE Map of Turbocharged GDI 4V Engine	113
Figure 138. CA50 Map of Turbocharged GDI 4V Engine	114
Figure 139. Lambda Map of the TC lean GDI 4V Engine	115
Figure 140. BTE Map of Turbocharged, Lean Burn GDI 2V Engine	115

Figure 141. CA50 Map of Turbocharged GDI, Lean Burn 2V Engine	116
Figure 142. Change in BSFC of for Turbocharged GDI, Lean Burn 2V Engine Relative to the Turbocharged GDI Stoichiometric 2V Engine	116
Figure 143. BTE Map of Turbocharged, Lean Burn GDI 4V Engine	117
Figure 144. CA50 Map of Turbocharged, Lean Burn GDI 4V Engine	118
Figure 145. Change in BSFC for Turbocharged GDI, Lean Burn 4V Engine Relative to the Turbocharged GDI, Stoichiometric 4V Engine	118
Figure 146. BTE Map of Turbocharged, GDI 2V Engine with Independent Cam Phasers	119
Figure 147. CA50 Map of Turbocharged, GDI 2V Engine with Independent Cam Phasers	120
Figure 148. BTE Improvement for Turbocharged, GDI 2V Engine with Independent Cam Phasers, Relative to Turbocharged GDI Stoichiometric 2V Engine.....	120
Figure 149. BTE Map of Turbocharged, GDI 4V Engine with Independent Cam Phasers	121
Figure 150. CA50 Map of Turbocharged, GDI 4V Engine with Independent Cam Phasers	122
Figure 151. BTE Improvement for Turbocharged, GDI 4V Engine with Independent Cam Phasers, Relative to Turbocharged GDI Stoichiometric 4V Engine.....	122
Figure 152. BTE Map for Turbocharged GDI 2V with Cam Phasers and LPL EGR	123
Figure 153. BTE Map for Turbocharged GDI 2V with Cam Phasers and LPL EGR	124
Figure 154. BTE Improvement Turbocharged GDI 2V with Cam Phasers and LPL EGR, Relative to the Turbocharged GDI Stoichiometric 2V Engine.....	124
Figure 155. BTE Map for Turbocharged GDI 4V with Cam Phasers and LPL EGR	125
Figure 156. BTE Map for Turbocharged GDI 4V with Cam Phasers and LPL EGR	126
Figure 157. BTE Improvement Turbocharged GDI 4V with Cam Phasers and LPL EGR, Relative to the Turbocharged GDI Stoichiometric 4V Engine.....	126
Figure 158. BTE Map for GDI with 11.5 CR and CDA.....	127
Figure 159. CA50 Map for GDI with 11.5 CR and CDA.....	128
Figure 160. BTE Improvement for GDI with 11.5 CR and CDA, Relative to GDI and 11.5 CR without CDA	128
Figure 161. BTE for the 2V D-EGR CR 11 Map	129
Figure 162. CA50 Map for the 2V D-EGR CR 11 Model.....	130
Figure 163. BTE Improvement for the 2V D-EGR CR 11 vs the Turbocharged GDI 2V CR 9.5 Engine	130
Figure 165. CA50 Map for the 4V D-EGR Engine with CR 11	131
Figure 166. BTE Improvement for the 4V D-EGR Model Relative to the Turbocharged GDI 4V CR 9.5 Model.....	132
Figure 167. BTE Map for the NA GDI 11.5 CR with VVA.....	133
Figure 168. CA50 Map for the NA GDI 11.5 CR with VVA.....	133
Figure 169. BTE Improvement for the NA GDI 11.5 CR with VVA Relative to the NA GDI 11.5 CR	134
Figure 170. BTE Map for the TC GDI 2V Model with VVA	135
Figure 171. CA50 Map for the TC GDI 2V Model with VVA	135
Figure 172. BTE Improvement for the TC GDI 2V Model with VVA Relative to the Turbocharged GDI 2V Engine.....	136
Figure 173. BTE Map for the Turbocharged GDI 4V Model with VVA.....	136
Figure 174. CA50 Map for the Turbocharged GDI 4V Model with VVA	137
Figure 175. BTE Improvement for the Turbocharged GDI 4V Model with VVA Relative to the Turbocharged GDI 4V Engine.....	137

LIST OF TABLES

<u>Table</u>	<u>Page</u>
Table 1. Mild Miller Simulation Results	13

LIST OF ABBREVIATIONS AND ACRONYMS

AFR.....	Air/Fuel Ratio
AMT.....	Automated Manual Transmission
ANL	Argonne National Laboratory
APT	Auxiliary Power Turbine (part of a turbocompound system)
APU.....	Auxiliary Power Unit
B6.7.....	Cummins 6.7 Liter Medium Duty Truck Engine
BMEP.....	Brake Mean Effective Pressure (A unit to compare the relative load on engines of different size)
BSFC.....	Brake Specific Fuel Consumption
BTE.....	Brake Thermal Efficiency
CAFE	Corporate Average Fuel Economy
CARB.....	California Air Resources Board
CDA	Cylinder Deactivation
CFD.....	Computational Fluid Dynamics
CO	Carbon Monoxide
CO ₂	Carbon Dioxide
DD15.....	Detroit 15 liter heavy duty truck engine (formerly Detroit Diesel)
DEF.....	Diesel Exhaust Fluid (Urea mixture used in SCR catalysts)
DPF	Diesel Particulate Filter
EGR.....	Exhaust Gas Recirculation
EPA	United States Environmental Protection Agency
EEVC	Early Exhaust Valve Closing (Valve timing)
EEVO	Early Exhaust Valve Opening (Valve timing)
EIVC	Early Intake Valve Closing (Valve timing)
EIVO	Early Intake Valve Opening (Valve timing)
EVO	Exhaust Valve Opening (Valve timing)
FMEP	Friction Mean Effective Pressure (Unit for comparison of friction between different engines)
GDI	Gasoline Direct Injection
GHG.....	Greenhouse Gas (CO ₂ , N ₂ O, CH ₄ , and others. In this report, CO ₂ is the focus)
GT-POWER.....	Commercial 1-dimensional engine simulation code. Part of GT-SUITE, sold by Gamma Technologies
HD.....	Heavy Duty (Typically refers to Class 8 trucks with engine of 10 liters or more displacement)
HPCR	High Pressure Common Rail (Diesel fuel system)
IVC.....	Intake Valve Closing (Valve timing)
IMEP	Indicated Mean Effective Pressure (would be the same as BMEP if friction was zero)
LD	Light Duty (Typically refers to Class 2b and 3 trucks. Note that to passenger car manufacturers, Class 2b and 3 are called “Heavy Duty”. This leads to considerable confusion between people with car and truck backgrounds.
MD	Medium Duty (Typically refers to Class 4 through “Baby 8” trucks with engine displacements below 10 liters)
mm	millimeter

MY	Model Year
N ₂	Nitrogen
N ₂ O	Nitrous Oxide
NO _x	Nitrogen Oxides
NHTSA	National Highway Traffic Safety Administration (Responsible for fuel economy regulations)
NO	Nitric Oxide
NO ₂	Nitrogen Dioxide
NO _x	Oxides of Nitrogen
O ₂	Oxygen
DOC	Diesel Oxidation Catalyst
OEM	Original Equipment Manufacturers
PCP	Peak Cylinder Pressure
PMEP	Pumping Mean Effective Pressure (Unit for comparison of pumping work between different displacement engines)
ppm	Parts per Million
PFI	Port Fuel Injection
PM	Particulate Matter
rpm	revolutions per minute
SCR	Selective Catalytic Reduction
SwRI	Southwest Research Institute
TCPD	Turbocompound
VG or VGT	Variable Geometry Turbocharger
VVA	Variable Valve Actuation (Fully variable lift and duration)
VVT	Variable Valve Timing (Typically dual independent cam phasing, but with constant lift & duration)
WHR	Waste Heat Recovery

1.0 INTRODUCTION

In 2016, the National Highway Traffic Safety Administration (NHTSA) and Environmental Protection Agency (EPA) jointly issued a second phase of fuel efficiency and greenhouse gas (GHG) standards that apply to medium- and heavy-duty on-highway engines and vehicles for model years (MY) 2021 to 2027. For engines, there are requirements that are introduced in stages (2021, 2024, and 2027). These regulations are commonly referred to as “Phase 2” of the Heavy-Duty National Program. The standards cover all vehicles in weight classes 2b through 8, which encompasses most vehicles with gross vehicle weight ratings (GVWR) over 8,500 pounds except for a limited number of passenger vehicles covered under the light duty corporate average fuel economy (CAFE) standards, and recreational vehicles, which were included in EPA’s GHG standards but not NHTSA’s fuel efficiency standards. The Phase 2 GHG and fuel consumption standards were developed using input from numerous studies which evaluated the fuel saving technologies that are available, including three studies conducted by SwRI for NHTSA [1, 2, 3]. In these studies, SwRI evaluated using computer models and simulations for engine technologies that could be used to comply with what became the Phase 2 standards.

For this work, a different approach is being used. Argonne National Laboratory (Argonne) has a large collection of validated medium and heavy-duty vehicle models, so ANL has been tasked with the vehicle simulation work, while SwRI performs the engine simulations. Four engines were selected for the project as the baseline engines:

1. Cummins B6.7 medium duty truck diesel engine
2. Detroit DD15 heavy-duty truck diesel engine
3. Ford 7.3 liter medium-duty gasoline V-8 engine
4. GM Duramax 3.0-liter light duty diesel for Class 2a pickup trucks

Two of these engines, the B6.7 and the DD15, had been evaluated in a previous study conducted by SwRI for the National Highway Traffic Safety Administration (NHTSA) [1, 2]. The other two engines are new to the market in just the last few years. For each engine, a list of potential BSFC reduction technologies was drawn up and agreed between SwRI, Argonne, and NHTSA.

Each engine was modeled in GT-Power, and the models were calibrated and validated against test data available at SwRI and/or provided by Ford and General Motors. Once the models achieved satisfactory results, the technology evaluation began. For each new technology application, engine performance was mapped over the speed and load range, and fuel consumption maps suitable for use with the vehicle simulation program Autonomie were provided to ANL.

It is important to emphasize that the objective of this study does not require an exact match of the GT model to a specific engine. The technologies to be evaluated need to be applied to an engine model that well represents current technology in medium trucks. A near-exact match between the model and the engine would have required far more intrusive measurements beyond the scope of the program, or data supplied directly by the manufacturer. The match achieved and the judgements made in addressing unknown information are well suited to the objectives of the project. Some engines had more data available from testing at SwRI than others.

Section 2 provides details and results for the 6.7-liter medium duty diesel, and the following technology options were evaluated:

- 2019 production baseline
- Reduced FMEP
- EGR pump driven by engine power
- EGR pump driven by external power (such as a mild or full hybrid system)
- Cylinder deactivation (CDA)
- Mild Miller cycle with fixed valve events
- Combination of engine driven EGR pump and CDA

Section 3 describes the details and results for the heavy-duty DD15, which could potentially support the cost of more complex fuel saving technologies. This, the DD15 has a longer list of technologies that were evaluated (items in **blue font** are carried over from the B6.7 evaluation):

- 2019 production baseline
- Reduced FMEP
- Downspeed torque curve with 1850 lb-ft peak torque (2508 Nm)
- Downspeed torque curve with 2050 lb-ft peak torque (2780 Nm)
- Downsize (5-cylinder) with the same power and torque as the baseline
- Downsize (5-cylinder) with the same BMEP as the baseline (reduced power and torque)
- Rankine cycle waste heat recovery system (WHR)
- EGR pump driven by engine power
- EGR pump driven by external power (such as a mild or full hybrid system)
- Cylinder deactivation (CDA)
- Mild Miller cycle with fixed valve events
- Strong Miller cycle with two stage boost system, EGR pump, and variable valve events
- Mechanical turbocompound
- Electric turbocompound with the stock EGR rates
- Electric turbocompound with reduced EGR rates
- Combination of Strong Miller and 2050 lb-ft downspeed
- Combination of Strong Miller, 2050 lb-ft downspeed, and WHR

Section 4 provides details and results for the 3.0-liter GM Duramax light duty diesel. This engine had its technology list revised during the project, as it became apparent that several of the original technologies did not offer the prospect of a worthwhile fuel consumption benefit. The following technologies were evaluated on this engine (items in **blue font** are carried over from the B6.7 evaluation):

- 2020 baseline
- Reduced FMEP
- Cylinder deactivation (CDA)
- Series sequential fixed geometry turbos with stock EGR rate
- Single stage fixed geometry turbo + e-boost
- Single stage fixed geometry turbo + e-boost + reduced speed range (higher BMEP)

Single stage fixed geometry turbo + e-boost + reduced speed range (higher BMEP) + CDA

Section 5 provides details and results for the Ford 7.3 liter medium-duty gasoline V-8, which was evaluated with a long list of technology options that was increased by a contract modification signed in June 2021. First, a series of naturally aspirated (NA) technologies were evaluated, all based on the current production engine:

2020 Baseline NA 2V with PFI and 10.5 CR
GDI fuel system NA 2V at 10.5 CR
GDI fuel system NA 2V at 11.5 CR
NA 2V lean burn with SCR
NA 2V with GDI, and dual independent cam phasers
NA 2V with GDI, and full authority VVA
NA 2V stoich GDI with LPL EGR
Reduced FMEP NA 2V combo with LPL EGR
Reduced torque NA 2V for hybrid with 12.5 CR
Reduced torque NA 2V for hybrid with 13.5 CR
GDI + CDA, NA 2V, 11.5 CR
4V NA GDI with 12:1 compression

All these technologies used the current production 2-valve cylinder head layout, except for the final one. For the 4-valve layout, SwRI assumed a pent roof, high tumble combustion chamber arrangement that would provide faster combustion and better knock resistance than the original 2-valve configuration. The 4-valve high tumble configuration was considered because it also allows higher BMEP in the turbocharged versions at a given compression ratio. Because the 4-valve high tumble arrangement is less prone to knock, it can also operate at a higher compression ratio in the naturally aspirated variant.

Several turbocharged technology options were then evaluated in both 2-valve and 4-valve configuration. Because of knock limitations, the 2-valve versions ran at a lower maximum BMEP than the 4-valve versions. To provide comparable vehicle performance, the 2-valve engines had a higher rated speed to reach the same rated power. All turbocharged configurations had lower peak torque and peak power speeds than the naturally aspirated engines:

2V turbocharged GDI with 9.5:1 CR
4V turbocharged GDI with 9.5:1 CR
4V turbocharged GDI with 12:1 CR
2V turbo lean burn
4V turbo lean burn
2V turbo, stoich with dual cam phasers
4V turbo, stoich with dual cam phasers
2V turbo, stoich with full authority VVT
4V turbo, stoich with full authority VVT
2V turbo with dual cam phasers, and LPL EGR
4V turbo with dual cam phasers, and LPL EGR

2V turbo with dual cam phasers, D-EGR
4V turbo with dual cam phasers, D-EGR

Section 6 provides conclusions and recommendations for future work.

DRAFT

2.0 6.7 LITER MEDIUM-DUTY DIESEL ENGINE

The engine recommended by SwRI as representative of North American medium-duty truck applications is the Cummins 6.7-liter ISB series, now called simply the B6.7. This engine enjoys more than a 50% market share in North American medium-duty trucks, according to data provided by ACT Research. It is an in-line six-cylinder four-stroke engine with a 107 mm bore and 124 mm stroke. The engine uses a high-pressure-loop EGR system with a variable geometry turbine turbocharger and air-to-air charge cooling.

The engine is produced in a variety of ratings for different vehicle applications, with torque curves optimized for manual and automatic transmissions, and with two sets of hardware and controls for either maximum fuel-efficiency or maximum power emphases. The rating chosen for this project produces 200 kW at 2400 rpm and maximum torque of 920 N-m at 1600 rpm. The torque curve is relatively flat from 1900 to 1300 rpm and is tailored for automatic transmission installations. This is the highest rating available in the Cummins “fuel efficiency” series and has a compression ratio of 19:1.

2.1 Baseline Model Match

All the engine configurations evaluated were simulated using an existing Gamma Technologies GT Power® model depicted in Figure 1. This model was developed for a similar study conducted by SwRI for NHTSA in 2012-2015 [DOT HS 812 146], and the first step in the current project was to update the model to be representative of current production engine performance. For this matching and validation effort SwRI utilized an internally produced performance and emissions dataset from 2019. Current production 2021 model year engines remain largely unchanged from the 2019 engine that SwRI tested. Available measurements included air and fuel flow versus engine speed and load, and intake system pressure at the charge air cooler outlet. It is important to note that EGR mass flow rate and peak cylinder pressure measurements were not available, nor were temperatures and pressures throughout the intake and exhaust systems. Compressor and turbine performance maps were also not available. Engineering judgement was required to ensure reasonable values were applied, and the model validation focused on matching the baseline fuel efficiency and air-to-fuel ratio (AFR).

The resulting fuel efficiency match achieved with the model is presented in Figures 2 and 3. In Figure 2 the brake specific fuel consumption (BSFC) is identified at specific points throughout the operating map. Measured BSFC is shown in red while the model results are shown in blue. In each case the specific operating point is shown as the solid dot at one corner of the box in which the number is reported. No-load fueling versus engine speed is also reported for both measured and modeling conditions.

In Figure 3 the percent difference between measured and modeled points is presented throughout the speed and load map. The match was within four percent throughout the shaded region, with mid- and high-load operation and low-speed, low load operation often within two percent. The difference between measured and modeled results exceeded four percent only under light-load, high-rpm conditions, where it was deemed that little or no time would be spent in an efficiency-

sensitive installation. Results were previously reviewed and accepted prior to evaluating the effects of the various technologies.

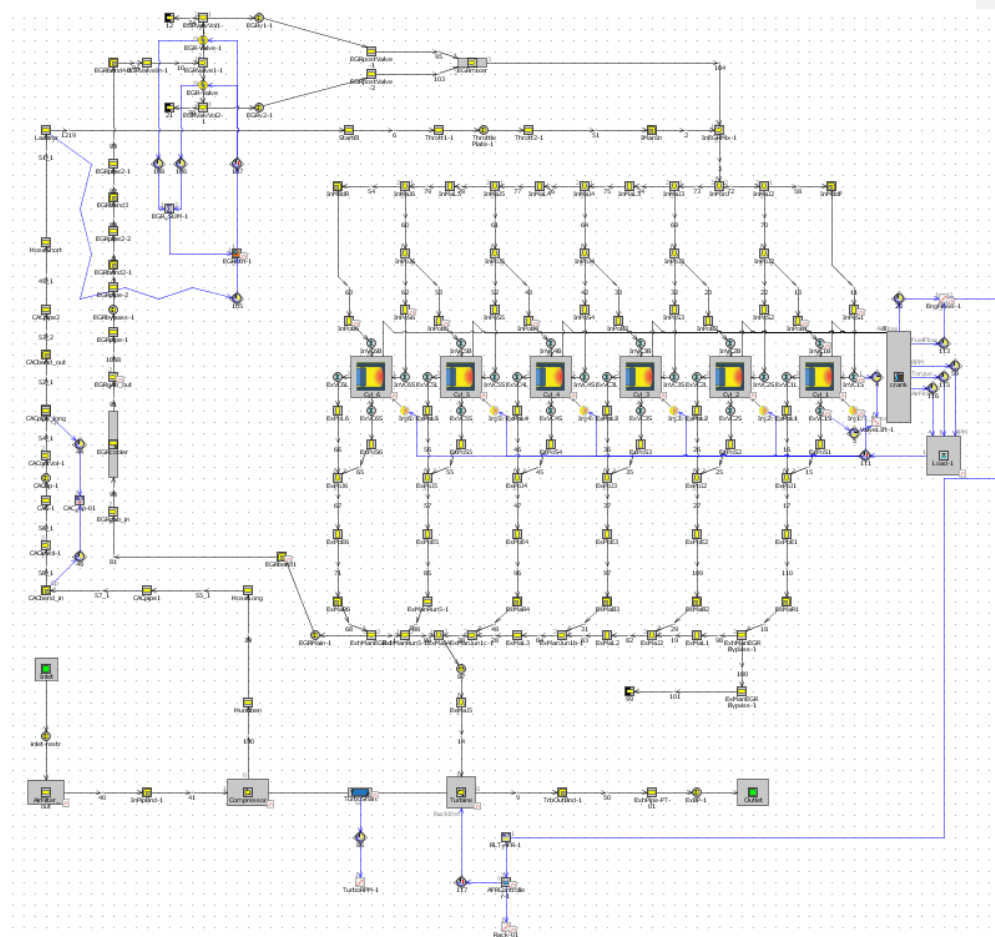


Figure 1. GT-Power® Model of the Cummins 6.7L Engine

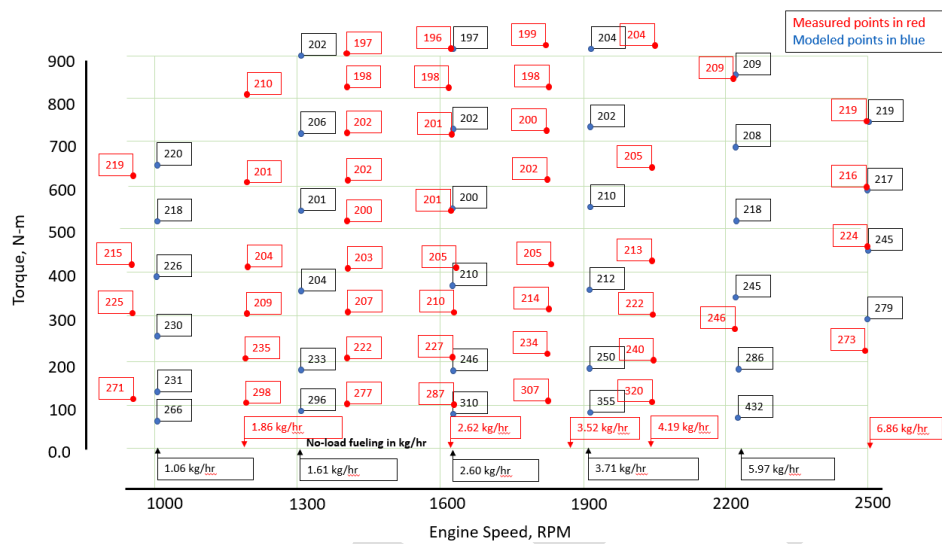


Figure 2. Measured Versus Modeled BSFC at Various Operating Points

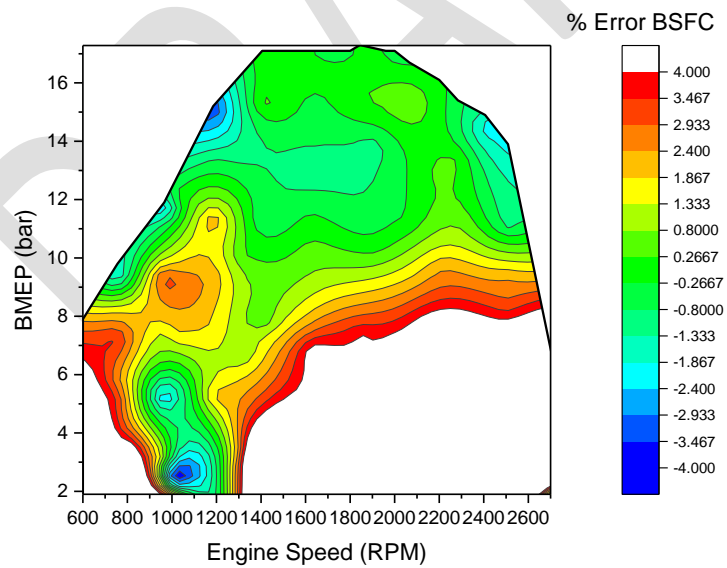


Figure 3. Fuel Efficiency Percentage Difference Between Measurement and GT Model

The EGR map applied to the model is presented in Figure 4. As noted previously, actual EGR map data was not available for the study. The EGR rates were reduced slightly throughout the map as compared to the maps used in the 2012 study. This is believed reflective of advances achieved in aftertreatment systems, based on SwRI's experience with development and certification of on-highway diesel engines. A peak EGR rate of 18 to 19 percent was applied at intermediate loads over most of the engine speed range. The EGR rate was reduced slightly at high loads, and reduced further under low speed, high load conditions where the turbocharger compressor capability limits the maximum EGR rate.

It should also be noted in Figure 4 that an EGR rate reduction was necessary in the 1300 to 1600 rpm range to match the measured engine performance. Throughout the study, this speed range was found to be optimal for engine performance and efficiency. It was deemed plausible that a reduced EGR rate in conjunction with an optimized aftertreatment system would be utilized. SwRI does not have measured EGR rates for the current B6.7 engine, but SwRI's experience with other engines shows that as SCR system effectiveness has improved since 2010, engine makers have taken advantage of this by reducing EGR rates and increasing engine-out NO_x. [Insert reference here](#): Hoag, Kevin L., "An Exploratory Look at an Aggressive Miller Cycle for High-BMEP Heavy-Duty Diesel Engines," SAE 2019-01-0231, 2019.

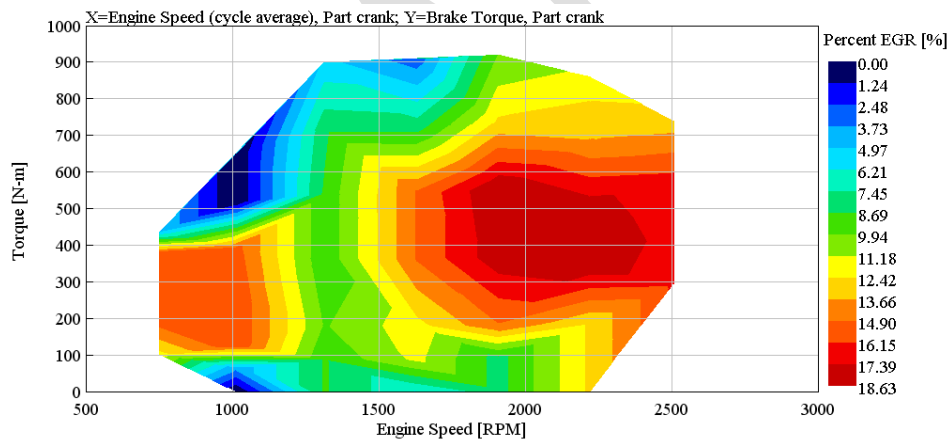


Figure 4. EGR Map Used in the Engine Model (Not Verified with Actual Engine Data)

Turbine and compressor maps, and the variable geometry control map were also not available as parameters from the test of the 2019 engine. A representative compressor map was selected in which the 1600 rpm engine breathing line ran through the heart of the map. The compressor map is shown in Figure 5, with the 1600 rpm full-load operating point at sea level encircled. The peak efficiency on this compressor map was just above 78 percent.

Another important requirement of this project is to provide no-load fueling versus engine speed, including idle fueling. Engine simulation programs such as GT Power[®] have received very little development at light load, and the required sub-models for friction, heat release, and heat transfer are not well validated for light load conditions. The approach taken here was to extrapolate to no-load conditions at each engine speed, and at constant load to minimum speed. Good agreement with measured points was sought whenever available, noting as well that measurement accuracy at light loads is also challenging. The resulting projection to idle fueling is shown in Figure 6. Also shown are the measured no-load fueling points.

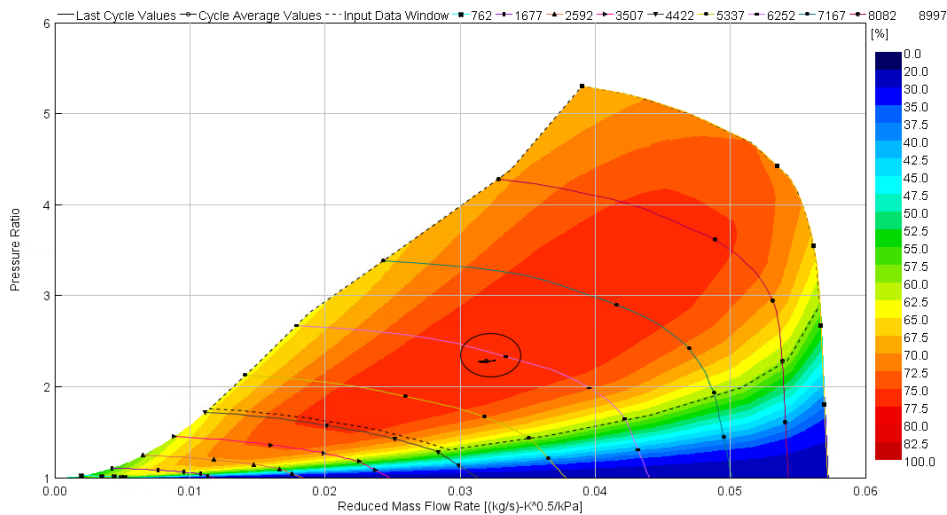


Figure 5. Compressor Map Used in the 6.7 Liter Engine Model

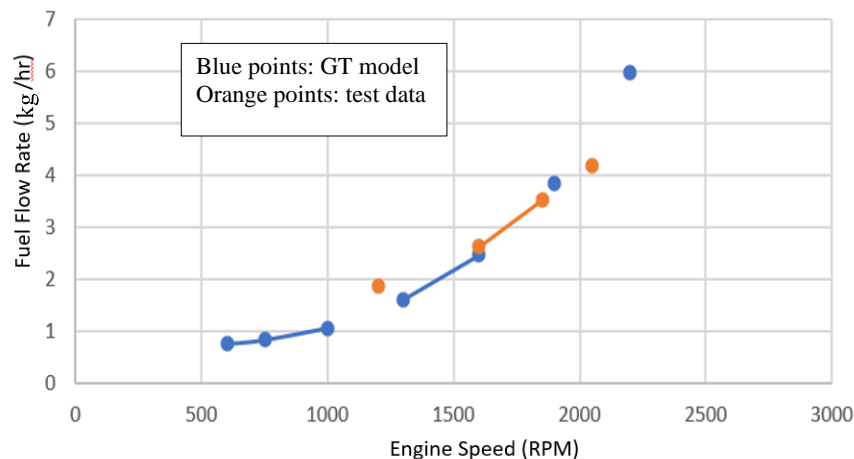


Figure 6. No-Load Fueling with Projection to 600 rpm Idle

Finally, it is important to note that peak cylinder pressure limits for this engine were not available. Good high-load agreement achieved between measured and modeled conditions indicates a maximum cylinder pressure of approximately 160 bar. This number resulted from optimizing the injection timing for best efficiency at the loads at which minimum measured BSFC was seen. Retarding the injection timing to maintain this cylinder pressure at full load resulted in good agreement between measured and modeled fuel efficiency. Historical experience also shows that medium-duty ratings of this engine use a 160 bar PCP limit.

2.2 Zero EGR with Variable Geometry Turbine

The first approach that was taken to evaluate potential fuel efficiency improvements was to assume that the aftertreatment system could be improved to the point where EGR could be eliminated. This assumption is theoretically possible under current emissions regulations but is not compatible with future 2024/2027 CARB requirements. Note that no engine manufacturer has attempted to use a no-EGR approach for an on-highway engine, but there are many engines using this approach for off-highway applications, where the tailpipe NO_x limit is slightly higher. Note that the reduction or elimination of EGR will increase engine-out NO_x. The variable geometry turbocharger turbine was retained, but vane positions were selected solely to maximize fuel efficiency. For this study the fresh air-fuel ratio and the peak cylinder pressure were maintained at their baseline values. Vane position and fuel injection timing were adjusted for minimum fueling at each speed and load point.

The results are summarized in Figure 7 as percentage BSFC reduction in comparison with the baseline engine. The biggest improvements were seen at light loads, where the turbine restriction can be minimized, reducing engine back pressure. The best performance under these light load conditions occurred when the turbine vanes were fully open. The gains dropped to zero or near-zero at high loads, where the inherent boost-to-back pressure ratio had been sufficient to drive the

EGR flow, and the vane positions changed very little when EGR was reduced to zero. Slight pumping improvements and slight injection advances were offset by the higher combustion temperatures and resulting heat transfer losses. Note that the lack of EGR and the advanced injection timings used would result in very high engine-out NO_x on the order of 20 g/kW-hr or more.

When reviewing the data presented in Figure 7, it was initially surprising to see that the fuel efficiency improvement seen at 1600 rpm was less than what is observed at higher and lower speeds, especially at loads below 5 bar BMEP. This is explained by the fact noted in the baseline model match section that the baseline engine breathing line at 1600 rpm passes through the heart of the compressor map. When EGR is eliminated, the breathing lines at each engine speed shift to the right. At 1600 rpm for the baseline engine with EGR, the compressor is operating at or near its best efficiency regardless of pressure ratio. When the breathing line shifts to the right, the resulting compressor efficiency drops, especially at low pressure ratios (which occur at low engine load), as depicted in Figure 8. This trade-off reduces the efficiency gain at this speed. It's important to note that in development of a zero EGR engine, the compressor match would be quite likely to change, either eliminating the effect seen here or transferring it to a different engine speed.

There are no engines certified today for on-highway applications that use no EGR, but this would theoretically be possible if very high efficiency aftertreatment is used. In off-highway applications, where the tailpipe NO_x standard is slightly more relaxed, there are many examples of engines that do not use EGR. Looking forward to future CARB and EPA emissions standards, however, a no-EGR approach will not be feasible. This evaluation was done to see what could be achieved under the current 2010 emissions standards.

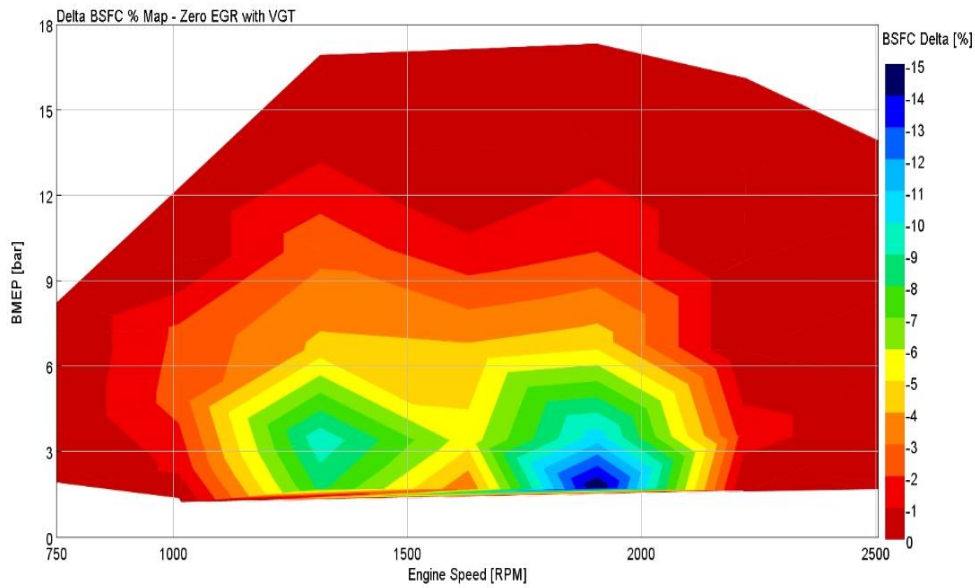


Figure 7. BSFC Percentage Improvement with Zero EGR and Retaining the VGT

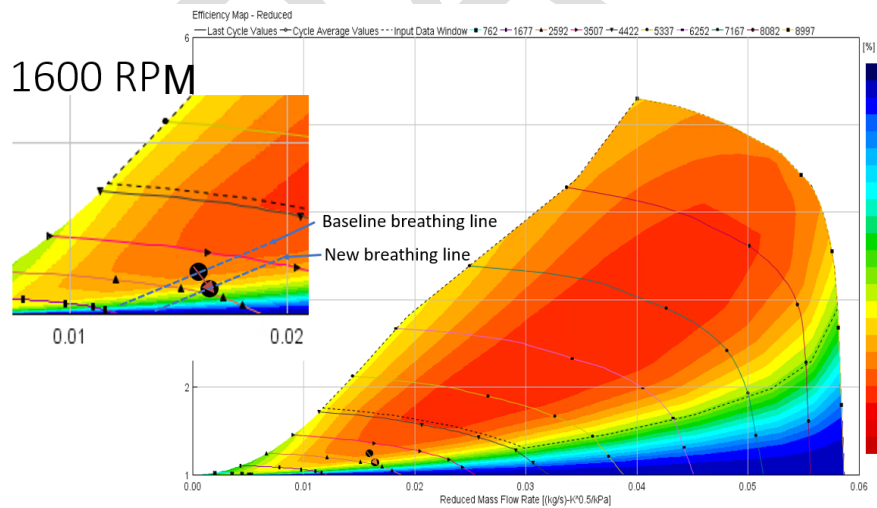


Figure 8. Effect of Eliminating EGR on 1600 rpm Compressor Operation

2.3 Fixed Valve Timing Mild Miller Cycle

The objective of this exercise was to assess the impact of applying a mild Miller Cycle to the baseline engine. A mild application is one in which a fixed intake valve closing timing is used with only a moderate compressor pressure ratio increase to maintain the baseline air-fuel ratio, such as can still be managed by a single stage turbocharger. Geometric compression ratio is increased, accomplishing the desired goal of greater expansion ratio than effective compression ratio. For this study, the constraints were to maintain constant EGR rate and AFR. The injection timing was advanced if this could be done without increasing the peak cylinder pressure. This more advanced injection timing would lead to an increase in engine-out NO_x.

Both early and late intake valve closure were assessed. The late intake valve closure was assessed by applying a range of dwell at the maximum valve lift condition. Dwell at peak lift was then varied to seek the optimum condition. The early intake valve closure option required reducing the peak valve lift to avoid valve train dynamics issues. The variable geometry turbocharger was adjusted to achieve the higher boost pressure required by the Miller cycle.

A range of speed and load conditions were assessed. For each case the modeled engine responded as anticipated, but the fuel efficiency remained unchanged within small fractions of a percent. An example result is tabulated below at 1600 rpm and full load. This result is typical, and other cases can be provided upon request. It should also be noted that not only were the improvements extremely small but the best intake valve closing timings shifted strongly with speed (twenty crank degrees or more), precluding a fixing valve timing approach. A more aggressive approach to the Miller Cycle, with two-stage turbocharging, intercooling, and variable valve actuation has been shown in published studies to provide greater fuel efficiency opportunities, but this is not considered economically feasible for medium-duty applications. **Insert reference:** Hoag, Kevin L., “An Exploratory Look at an Aggressive Miller Cycle for High-BMEP Heavy-Duty Diesel Engines,” SAE 2019-01-0231, 2019. This portion of the study was concluded without providing a fuel efficiency improvement map.

Commented [A1]: Can you put the reference for these studies here?

TABLE 1. MILD MILLER SIMULATION RESULTS

Intake Dwell	Baseline	5	10	15	20	25	30
Torque (N-m)	909.8	909.8	909.8	909.8	909.9	909.9	909.8
BSFC (gm/kW-hr)	195.55	195.53	195.50	195.54	195.68	195.81	196.00
A/F	21.16	21.13	21.11	21.16	20.98	20.78	20.35
Comp PR	2.293	2.297	2.312	2.350	2.382	2.432	2.480
PCP (bar)	155.6	154.9	154.3	154.3	153.2	152.3	150.1
Comp. Eff.	76.70	76.70	76.70	76.70	76.70	76.70	76.70

2.4 Cylinder Deactivation

In all applications, diesel engines spend at least some time at light load or at idle. In long-haul applications, the portion of time at light load and idle is relatively small, while in urban operations and construction applications, well over half of an engine’s operating time may occur at light load or idle. The light load cycle was developed by CARB for implementation in 2024 and is expected

to be implemented on a national basis by EPA in 2027. The light load cycle is designed to address issues related to extended operation at light load and idle. Cylinder deactivation (CDA) serves two purposes during light load operation. First, it reduces exhaust mass flow and increases exhaust temperature, which helps keep the SCR system active without the need for adding heat in ways that increase engine fuel consumption. Second, CDA allows the active cylinders to run more efficiently, resulting in measurable reductions in fuel consumption. Reinhart et al. [“Vibration and Emissions Quantification Over Key Drive Cycles Using Cylinder Deactivation”, Thomas Reinhart, Andrew Matheaus, Chris Sharp, Bryar Peters, Matthew Pieczko, and James McCarthy Jr., International Journal of Powertrains, Volume 9, No. 4, 2020] shows that the use of cylinder deactivation can provide BSFC reduction of 0.8% to 8%, depending on the drive cycle. This paper also provides numerous references to other papers describing CDA. Note that the B6.7 engine is used in applications that often have a large portion of operating time at light load or idle.

Commented [A2]: This needs to be a footnote.

The cylinder deactivation study was conducted using three-cylinder deactivation at light loads and switching to normal six-cylinder operation at higher loads. An intermediate step of four firing cylinders was considered but was ruled out, since further gains would be minimal, and vibration could be problematic with an in-line six-cylinder engine configuration. The approach taken was to operate three cylinders and incrementally increase fueling at each engine speed, from no-load until the air-fuel ratio dropped below 20:1. At this load operation shifted to six cylinders. The resulting light-load fuel efficiency improvement is shown in Figure 9.

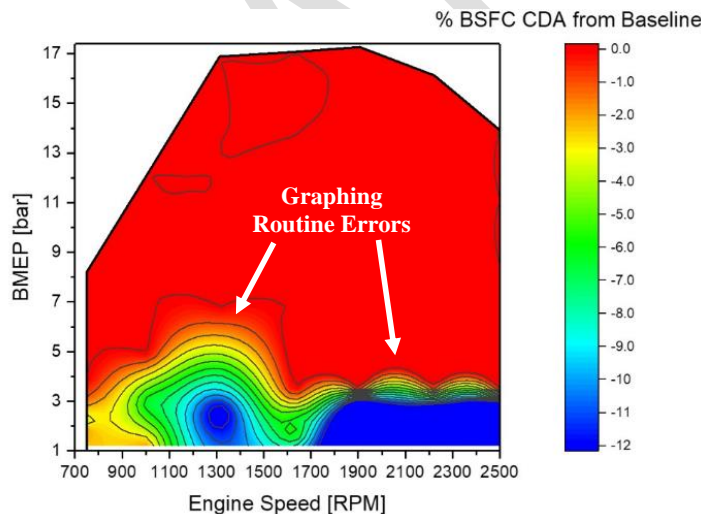


Figure 9. BSFC Percentage Improvement with Three Cylinder Deactivation

As has been noted earlier, the engine operates at its optimal efficiency when near 1600 rpm. Further efficiency improvements were again smaller at this speed but still significant. Also noted in Figure 9 is the graphing software challenge of reporting a step change in BSFC between three- and six-cylinder operation. The plot shows a very tight transition at three modeled speeds (1900, 2200,

and 2500 rpm), but the graphing routine attempts to relax the transition at speeds in between the modeled points and around the 1300 rpm data point.

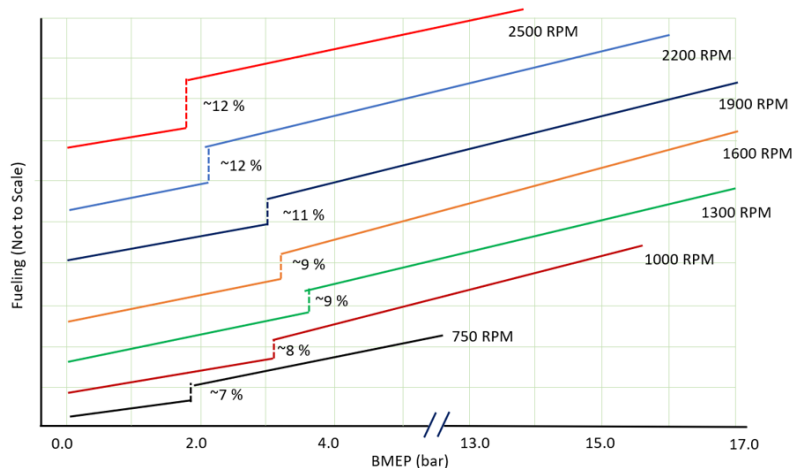


Figure 10. CDA Transition Load and Fuel Efficiency Change versus Engine Speed

The results are further summarized in Figure 10. While not drawn to scale, the figure shows the three-cylinder-to-six-cylinder transition load at each speed, and the approximate fuel efficiency change. As engine speed increases from 750 to 1300 rpm, the load that can be produced with three cylinders increases to nearly four bar BMEP. At higher speeds the maximum load achievable with three cylinders again drops. This occurs due to engine breathing becoming more restrictive at high speed, reducing the amount of fresh air that can be inducted. The turbocharger was not able to provide significant boost in the three-cylinder operating mode, which limits the BMEP that can be achieved while firing on three cylinders.

2.5 Mechanical Friction Reduction

Friction reduction has a fuel consumption benefit that is a function of both speed and load. The benefit of friction reduction tends to decrease with load, since FMEP grows only slowly with load, while BMEP is directly proportional to load. Friction increases with speed, so the worst case for friction is at high speed and light load. Report DOT 812 146 from 2015 explored the benefit of friction reduction in several vehicle types and over a range of drive cycles. The report shows that there is some benefit to be had from friction reduction even in heavily loaded long-haul applications, although the benefits are much greater in lightly loaded vehicles operating in stop-and-go conditions.

The impact of reduced mechanical friction and parasitic loads was assessed. A similar rationale was applied for both the medium- and heavy-duty engine evaluations. Figure 11 shows the friction reduction versus engine speed and load used for the 15-liter heavy-duty analysis. The same friction reduction assumptions were used in for both the medium- and heavy-duty engines, scaled to match the different rated power and torque peak speeds. The maximum friction reduction was applied at

lower speeds and light loads, where it was determined that reduced water pump speed and oil pump displacement could be applied. The smallest projected friction reductions were applied at high speeds and at high loads. In both operating regimes, the opportunities for friction reduction are limited to sliding friction reduction through coatings and lubricant formulation.

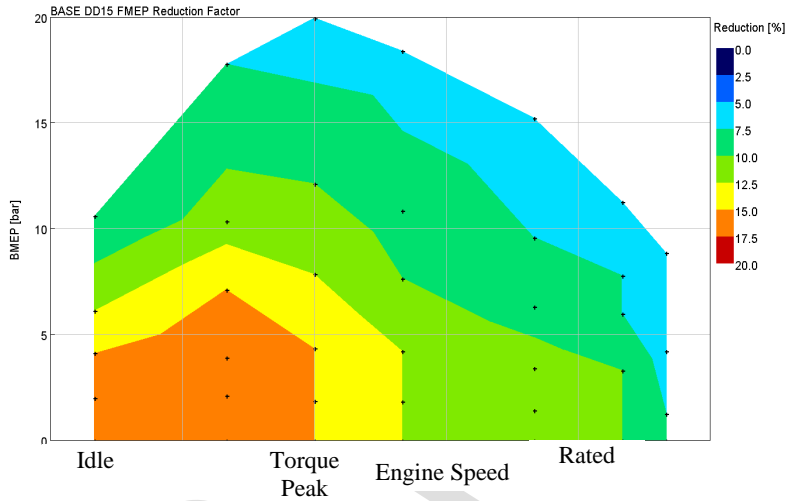


Figure 11. Friction Reduction Rationale Applied to Heavy- and Medium-Duty Engines

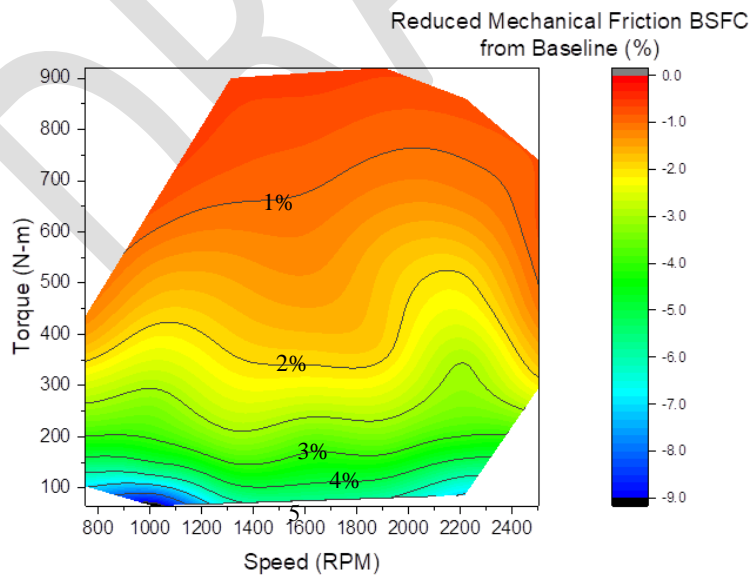


Figure 12. BSFC Percentage Improvement From Baseline with Reduced Friction

The projected BSFC improvement resulting from reduced friction is shown as compared to the baseline in Figure 12. The benefits seen at low speeds are accentuated based on water and oil pump power reductions. At higher engine speeds the sliding friction contribution increases, and reducing that contribution shows an increasing benefit. This drops off at the highest engine speeds based on the assumption that the opportunity to reduce friction is reduced, as discussed in the previous paragraph.

2.7 EGR Pump with High-Efficiency Fixed Geometry Turbo

When first replacing the VGT with a fixed geometry turbocharger, a simulation was run to assess the possibility of hitting EGR targets without requiring additional hardware. Figure 16 shows that, while a negative pressure differential exists between the intake manifold and the turbine for most of the full-load operating range, it is insufficient to provide the same EGR flow as the VGT. As turbocharger efficiency increases, the engine will tend towards greater pressure in the intake manifold than in the exhaust manifold, requiring an EGR pump or other means to force EGR to flow.

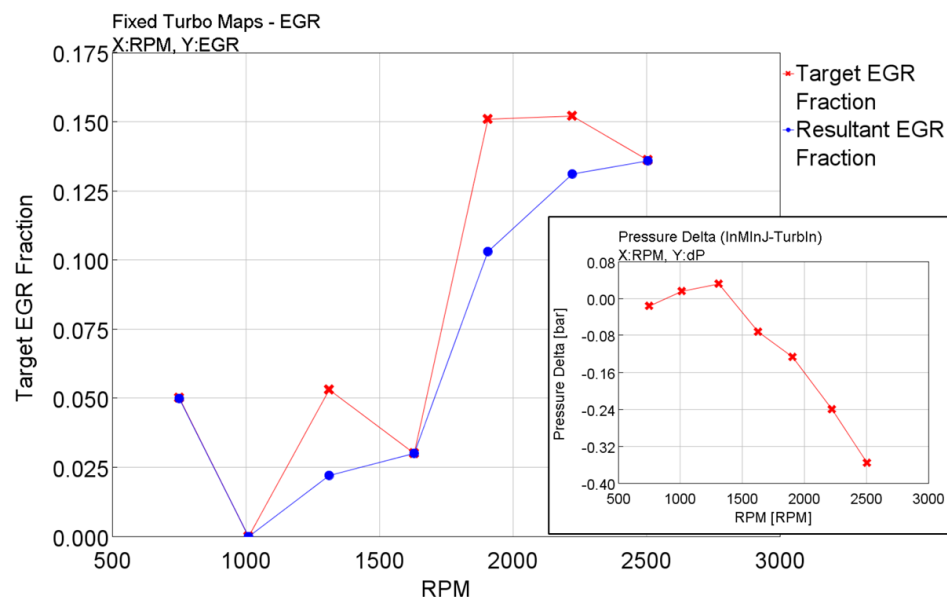


Figure 16. Pressure Differential and Resulting EGR Flow Using a Fixed Geometry Turbo

Therefore, an EGR pump is required to provide the necessary levels of EGR throughout the operating range. Data for a 200-cc EGR pump was provided by Eaton. The pump was inserted downstream of the EGR cooler, replacing the baseline model's EGR valve system. The EGR pump operation is only required when the engine's pressure differential provides insufficient EGR flow.

If excess EGR flow is being generated by the engine, that flow can be used to drive the EGR pump and provide power back to the engine in the Conventional setup described below. In these conditions the pump functions as a flow regulator and at low EGR demand rates, typically at low engine loads, the pump acts as a restriction or blockage. To overcome this, the pump is operated at a minimum speed of 1000 rpm. This means that the EGR rate may be slightly increased under some light load conditions.

For the analysis performed in this project, the energy required to power the EGR pump was accounted for in two ways. The Conventional EGR Pump approach assumed that the engine supplied the energy to power the EGR pump, and this power demand is considered as a power draw on the crankshaft, directly affecting the fueling result. When the EGR pump is being driven by excess EGR flow, that power contribution is considered as a power benefit back to the crankshaft which also affects the fueling result. In each case, a flat 80% energy conversion efficiency was assumed, in addition to the mechanical efficiency map that is built into the EGR pump model.

The Hybrid EGR Pump approach assumed that the energy was supplied by another source such as a battery system that is recharged by another means. Therefore, the power requirement of the Hybrid EGR pump was not accounted for in the engine fueling calculation. Excluding the no-load case where engine power is approximately zero, the EGR pump uses at most 0.15% of the engine power and produces as much as 0.5% additional engine power after conversion efficiencies are accounted for. Figure 17 shows the EGR pump operation, where power is required at about half load or greater at all but the highest engine speeds. The EGR pump is producing power throughout more than half of the operating map, as indicated by the negative EGR pump power.

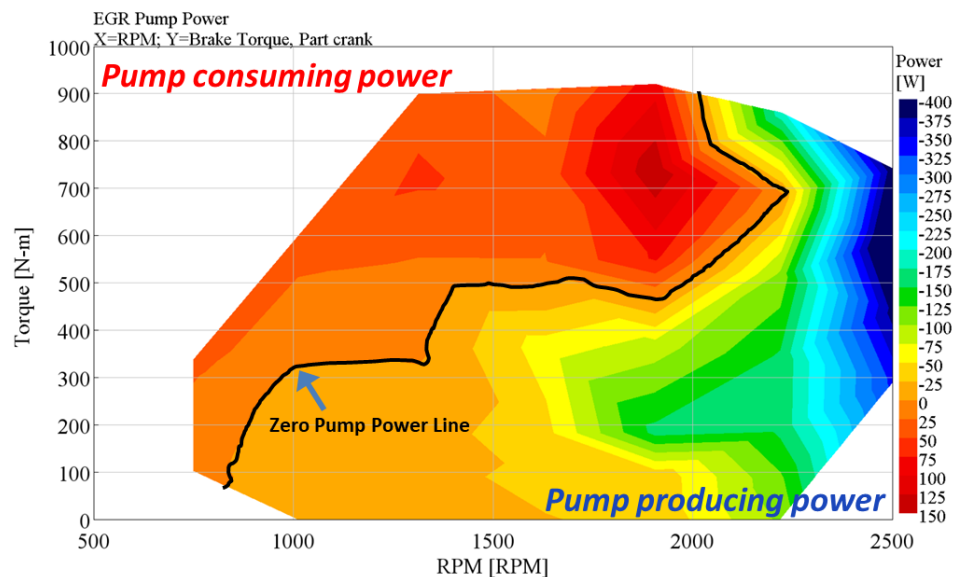


Figure 17. EGR Pump Power Consumption or Production

Figure 18 shows the fueling requirements compared to the baseline engine for both the Hybrid and the Conventional EGR pump approaches. The results show a nearly indistinguishable difference between the two methods. The difference between the two approaches is less than 0.5% at the most extreme case. The Conventional EGR pump is returning a similar percentage of power as it requires, resulting in a net effect that is nearly the same as the Hybrid EGR pump. This indicates that a Conventional EGR pump setup can be implemented on the 6.7L ISB with a very small fueling penalty or the need for hybridization.

DRAFT

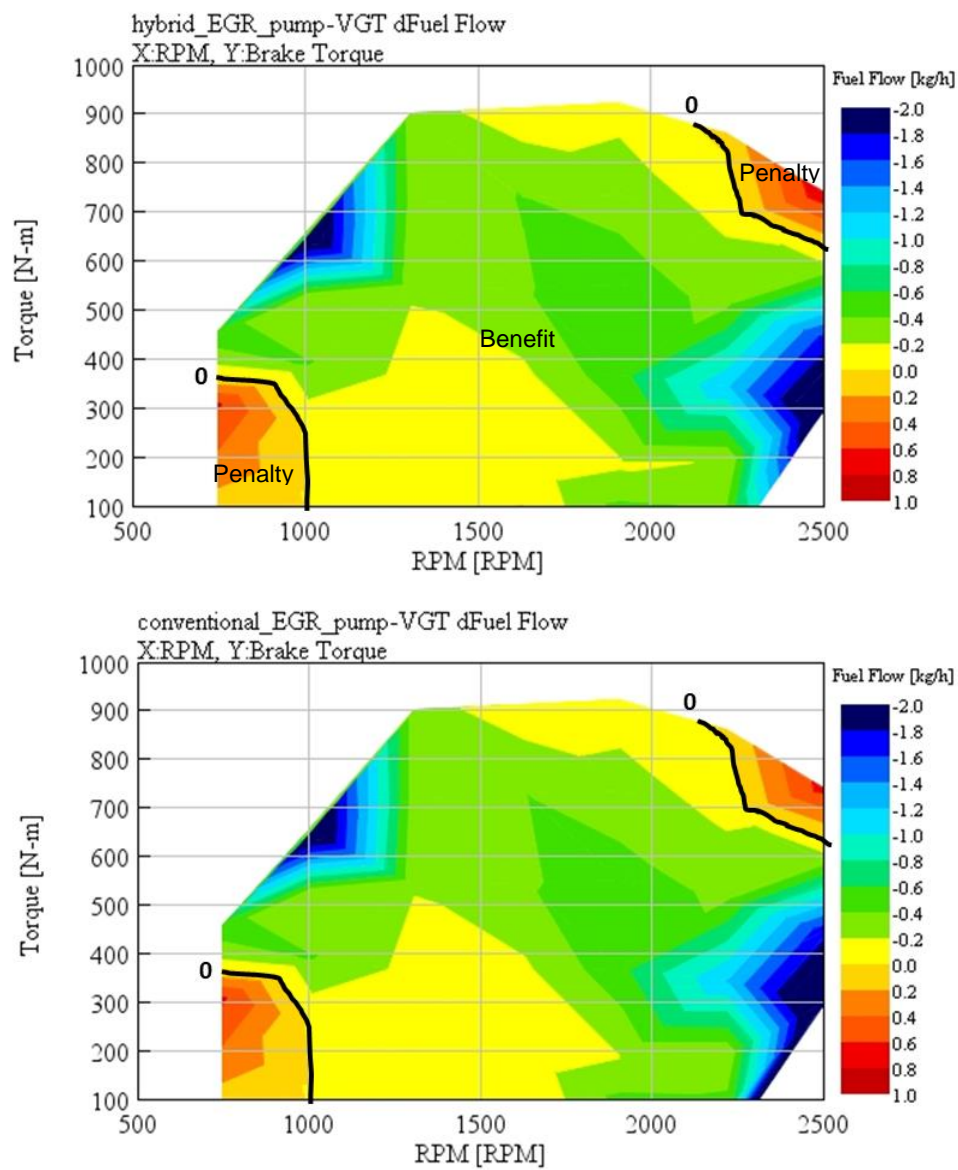


Figure 18. Fueling Change over Baseline, Hybrid EGR Pump Approach (top) and Conventional EGR Pump Approach (bottom)

2.8 Technology Combo: EGR Pump and Cylinder Deactivation with High-Efficiency Fixed Geometry Turbo

The final analysis added cylinder deactivation to the Conventional EGR Pump model. The same process was followed as on the previous CDA where three cylinders were deactivated at low load conditions. Starting from zero load, fueling was increased at each speed while maintaining an air-to-fuel ratio above 19. Figure 19 shows the combined BSFC reduction with the EGR pump and utilizing CDA at low loads, compared to the baseline. Note the increased fueling at the lowest engine speeds as seen previously in the change from the VGT to the fixed geometry turbocharger with wastegate. The results show an overall decrease in fueling requirements throughout most of the operating map, with the most significant improvements at low loads.

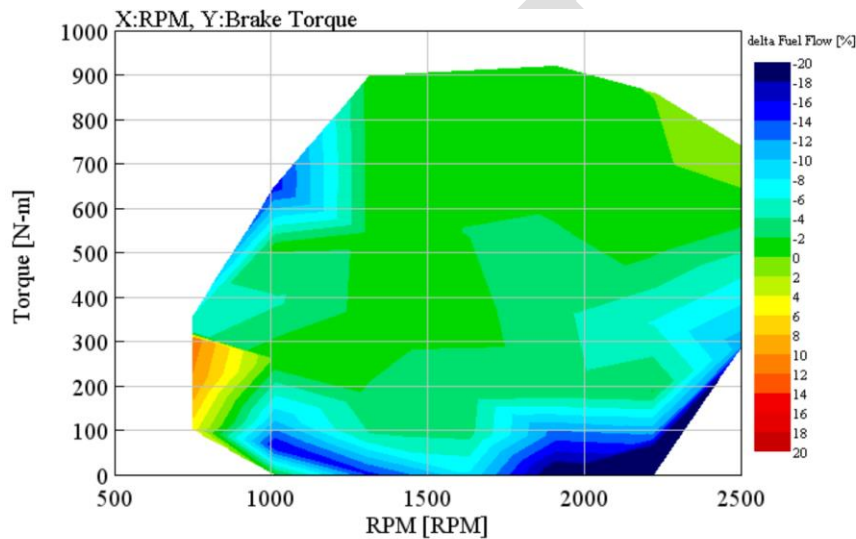


Figure 19. Percentage Fueling Change over Baseline when Combining the Conventional EGR Pump with Cylinder Deactivation

Figure 20 shows that by adding CDA to the EGR pump model, an additional 2-16% BSFC reduction can be realized at low load conditions, compared to the Conventional EGR pump alone. Compared to the baseline model, the configuration including a high efficiency fixed geometry turbo with wastegate, an EGR pump, and CDA provides the most significant reduction in fueling requirements. Figure 21 shows BSFC maps for the baseline and each variation of the fixed geometry turbocharger model, indicating that each alternative configuration provides a reduction in BSFC compared to the baseline VGT.

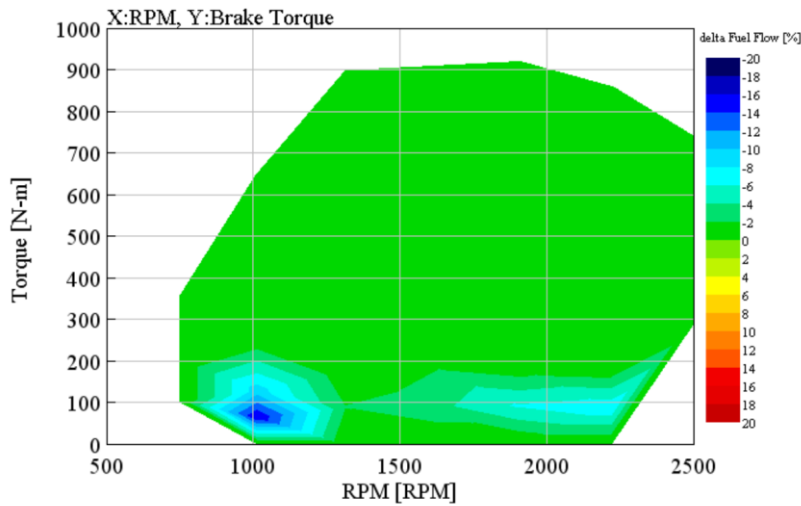


Figure 20. CDA Fueling Changes Added to the Conventional EGR Pump Model

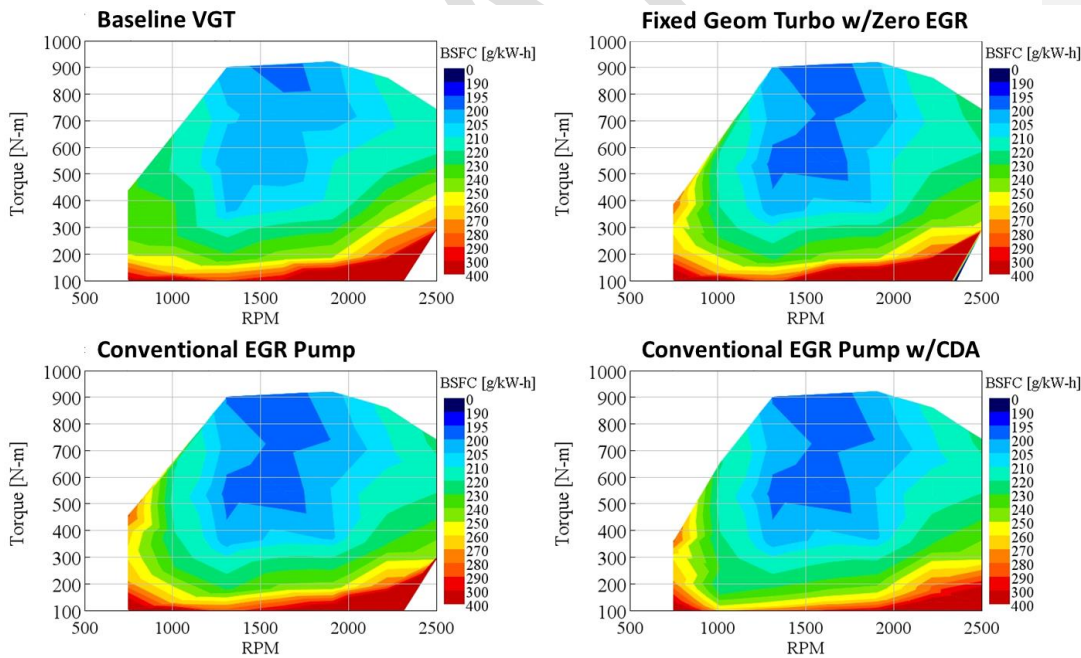


Figure 21. BSFC Comparisons for the Fixed Geometry Turbo Configurations Compared to Baseline (top left)

3.0 DD15 HEAVY-DUTY DIESEL ENGINE

Error! Reference source not found. **DD15** Error! Reference source not found.

- **Basic engine specifications:**
 - Diesel 14.8 Liter inline 6 cylinder
 - Single Fixed Geometry Twin Asymmetric Entry Turbocharger
 - Diverter valve on the smaller turbine entry that can direct exhaust flow to the turbine or to the EGR system
 - 4 valves per cylinder
 - Power rating: 300 kW @ 1600 rpm
 - Torque rating: >2300 Nm @ 1000-1200 rpm (2360Nm @ 1100rpm)

A GT Power model was built using the geometry of a DD15 model from the previous NHTSA project that was completed in 2016. The results of this project are available in reports DOT HS 812 146 and DOT HS 812 194. The model from the previous project was updated to reflect the development of the DD15, particularly the asymmetric turbo arrangement, the revised EGR system, and the fuel deactivation and 50% EGR strategy applied to the front 3 cylinders at low speed & load operating conditions. With this strategy, the diverter valve is set to deliver 100% of the exhaust flow from the front 3 cylinders to the EGR stream, providing an overall engine EGR rate of 50%. At the same time, the fueling of the front 3 cylinders is reduced or turned off depending on load. When the fuel to the front 3 cylinders is shut off, this control strategy effectively provides cylinder deactivation without requiring VVA valvetrain hardware. All intake air going into the front 3 cylinders is recirculated through the EGR system, reducing the overall exhaust flow going to the aftertreatment by nearly 50%. This approach also increases exhaust temperatures, since only 3 cylinders are fired, and only their exhaust flow goes to the aftertreatment.

To calibrate the model, test data from a SwRI benchmarking program was used. Not all the required data was present, and where necessary, data from the original NHTSA DD15 model was carried over due to the similarity in the engine. Overall, there was sufficient information and data to produce a well correlated model. Figure 22 shows a schematic of the GT model. The most significant missing data included:

- **Combustion data – from analysis of high-speed cylinder pressure data**
 - **50% Mass Fraction Burned Timing**
 - **10-90 Burn Duration**
- **Turbo performance maps**
- **Geometry of asymmetric turbine inlet, diverter valve, and EGR system**

The GT Power model was then run over a speed range of 600 – 1900 rpm at 10, 20, 40, 60, 80 & 100% load (see figure 23), and validated by the following operating parameters:

- **BMEP, IMEP, PMEP**
- **BSFC**
- **Air and Fuel Flow**
- **Pre/Post compressor pressures and temperatures**
- **Pre/Post Turbine pressures and temperatures**
- **EGR Rates**

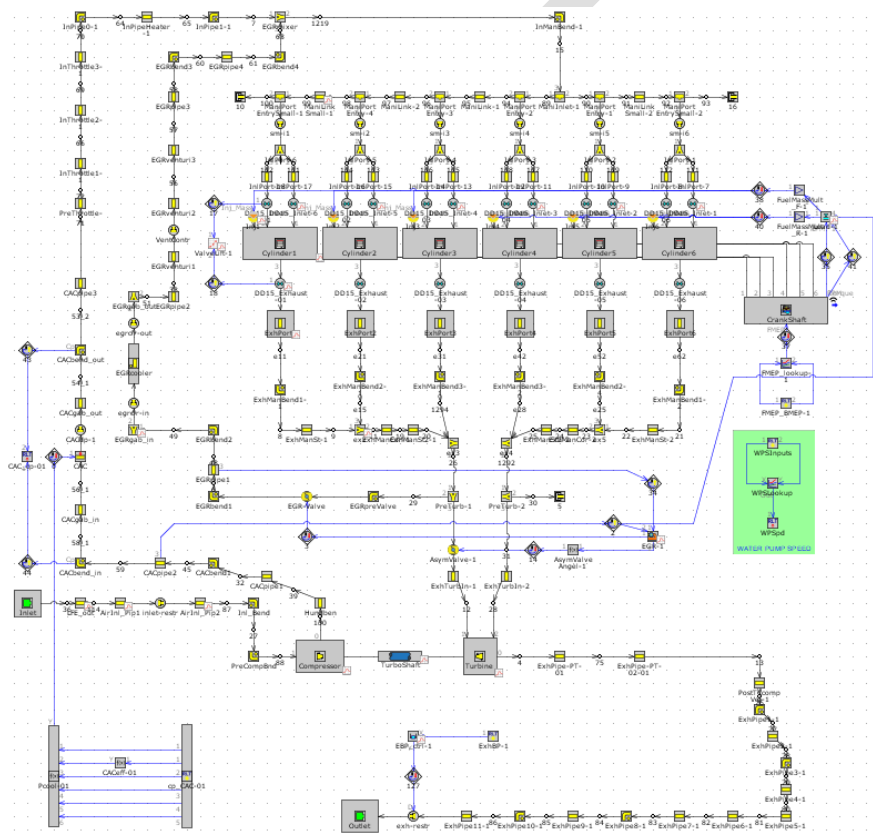


Figure 22. DD15 GT Baseline Model

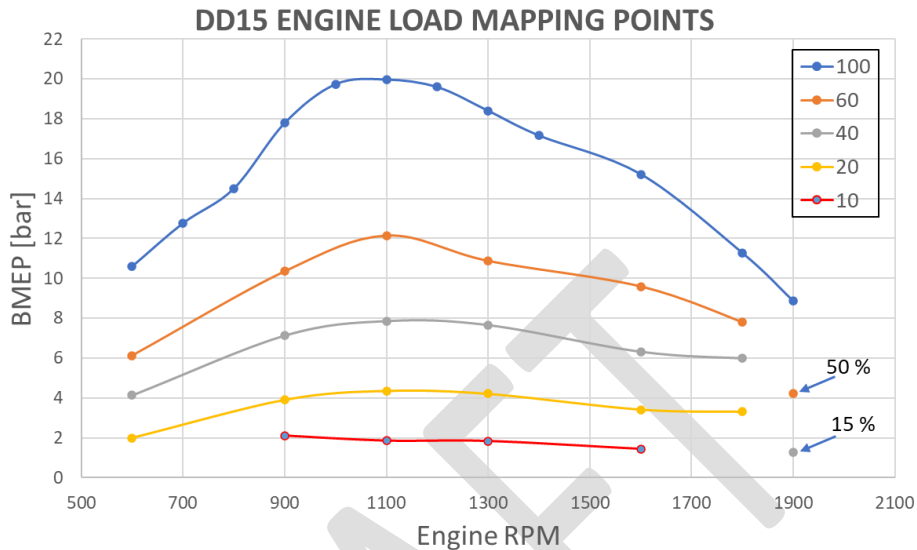


Figure 23. DD15 GT Baseline Operating Points

The geometry was originally constructed from measurements of the real engine hardware. Port flow data and valve lift data came from flow-rig tests, and as the core engine has not changed, this information was carried over from the previous project. For the EGR diverter valve, which for this version of the DD15 is incorporated into front entry of the twin entry turbine housing, published data was used to model the geometry. The system operates in such a way that a single valve controls the flow to either the turbine or the EGR. This means that at the extremes of travel, the valve can either divert all the exhaust gasses of the front 3 cylinders to the EGR system and none to front turbine entry or none to the EGR system and all to the turbine. The valve position is modulated throughout the engine's speed/load range to achieve the target EGR flow.

The actual turbo maps for the asymmetric turbo were not available, so the existing maps from the original model were used and scaled so that the measured inlet & outlet conditions were matched to test data. Using the test data pressures it was possible to tune the asymmetry ratio and EGR valve geometry to produce simulation results that match the available test data.

A review of published data indicated that a match of +/- 3% should be achievable with a correctly setup GT model. Two examples of papers relating to models for similar medium duty engines are:

- "Creation and Validation of a High Accuracy, Real-Time-Capable Mean-Value GT-Power Model" by Tim Prochnau, International Truck & Engine Corporation. Presented at the 11th GT-Suite Users' Conference, November 13, 2007
- "Transient engine modeling at John Deere using GT-Power" by John Deere. Presented at GT-Suite North American Conference 2009

Further papers showing the modelling, accuracy and application of GT Power models can be found at <https://www.gtisoft.com/knowledgebase> .

With the "matched" operating conditions, the operating points were run again to confirm that the simulated BSFC was within $\pm 3\%$ of the experimental results. Shown below in Figure 24 is the comparison between the engine data and model reported BSFC. Also shown is the full range of matched data for the model operating on the full load torque curve. The accuracy of the model was also evaluated by comparing simulated and experimental air flow, EGR rate, peak cylinder pressure, as well as turbocharger pressures and temperatures. See Figures 25-27 for comparison plots of these parameters.

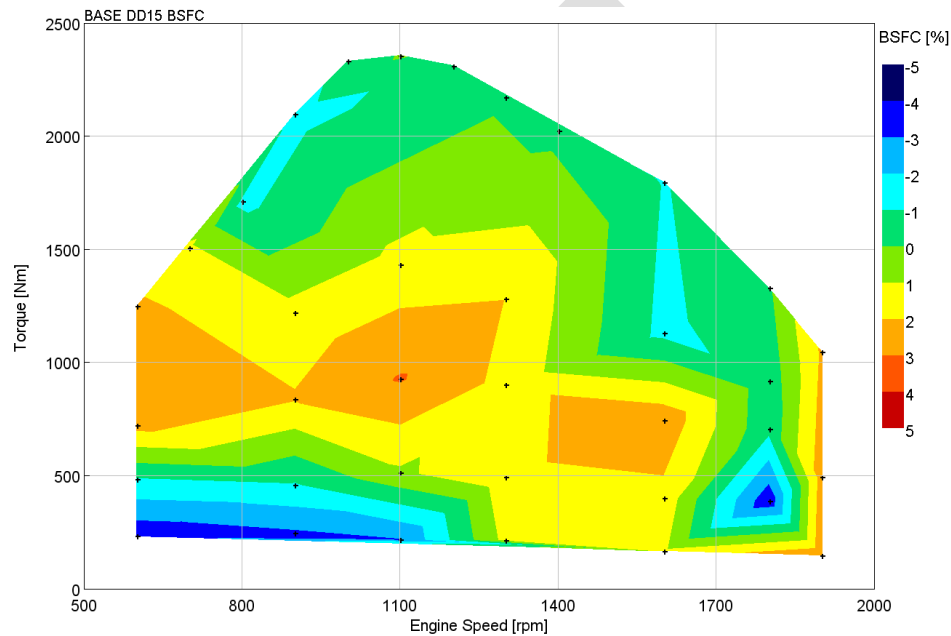


Figure 24. Comparison of BSFC Predicted by the GT Model Against 2019 Engine Test Data

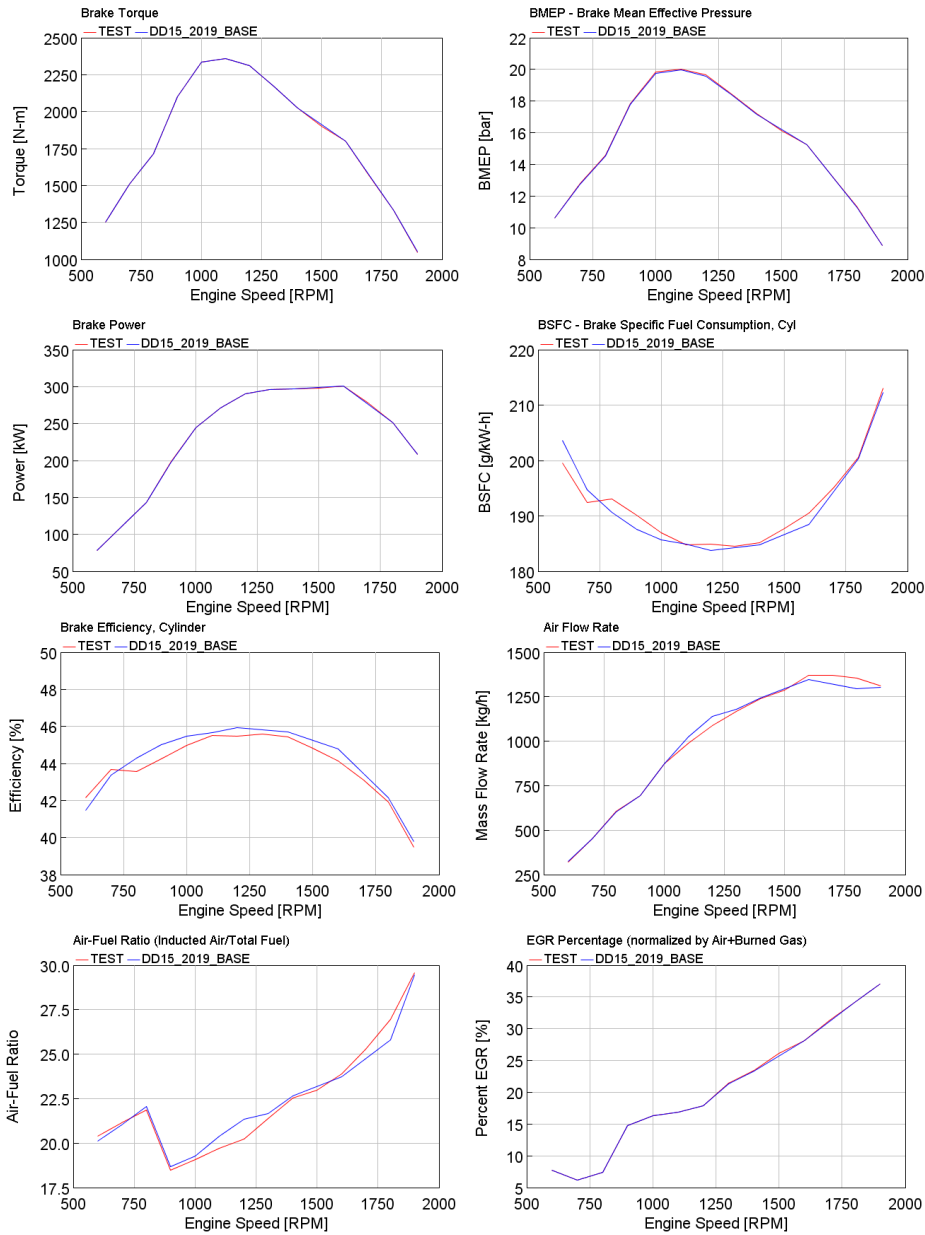


Figure 25. (Part 1) Baseline Model Data Correlation at Full Load. Note that where only one line can be seen, there is a near-perfect match between model and test data.

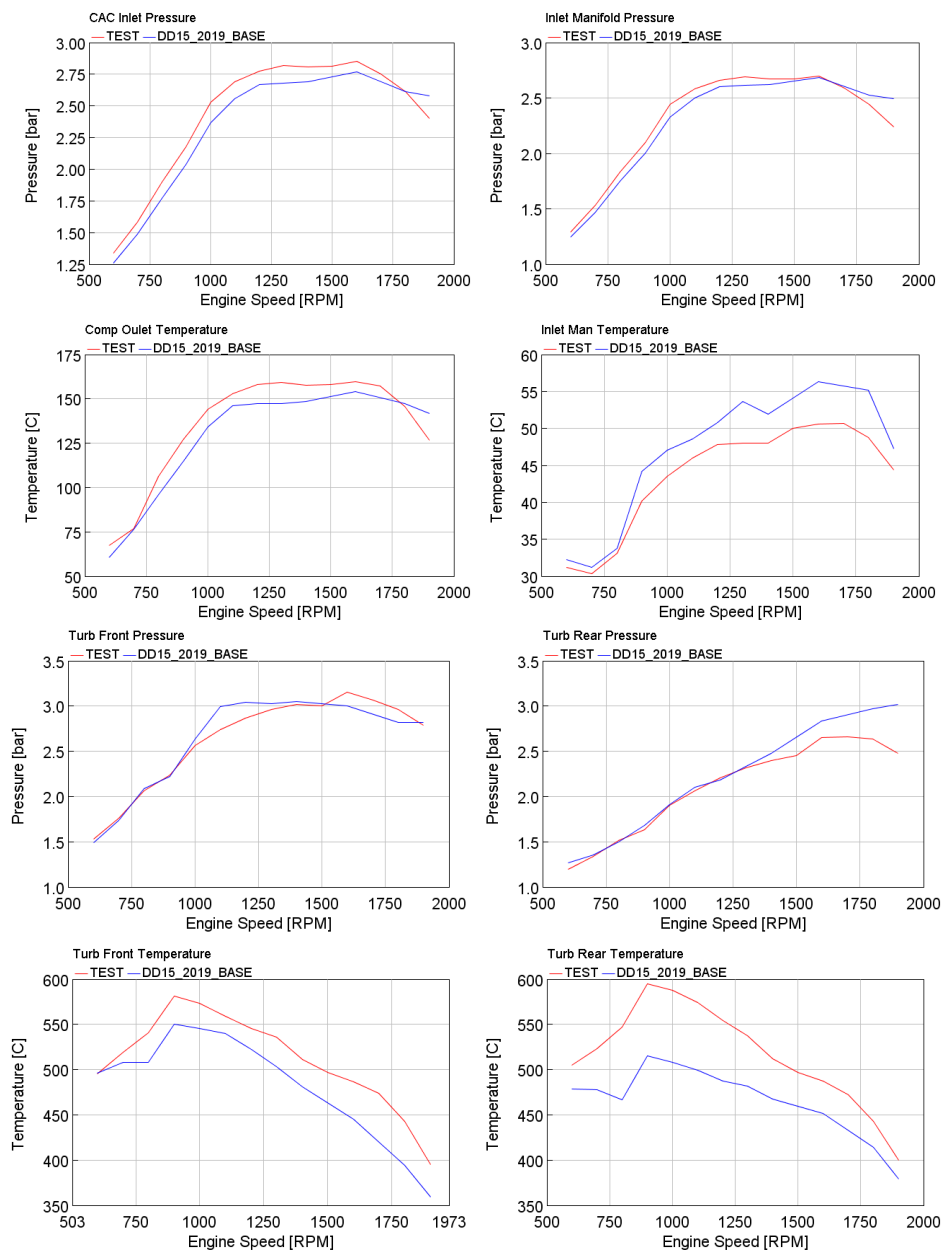


Figure 26. (Part 2) Baseline Model Data Correlation at Full Load

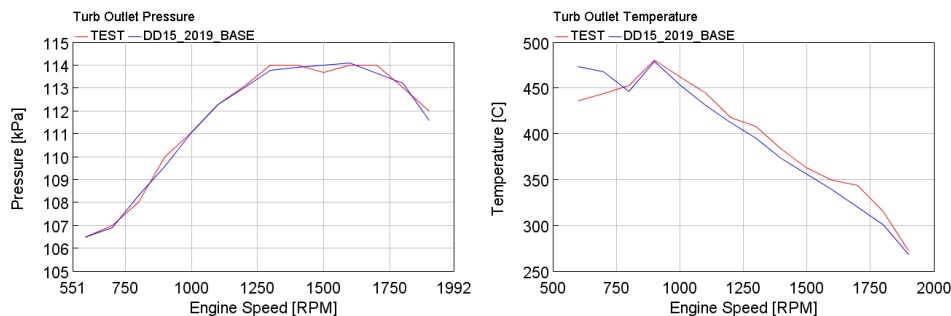


Figure 27. (Part 3) Baseline Model Data Correlation at Full Load

3.2 Reduced Engine Friction (FMEP)

The baseline engine model with a reduced friction map was run under the same conditions as the baseline model. The friction (FMEP) was reduced on a speed-load relationship, with full load reductions of 5% and part load reduction of up to 17.5% (see Figure 28). As expected, the largest benefits occur at light load and lower engine speeds, as shown in Figure 29.

Reducing engine friction can be achieved in several ways, such as low viscosity oils, smaller bearings, ring/piston/liner interface improvements, a more efficient high pressure fuel pump, as well as electronically controlled oil and water pump speed or displacement. In this study, all the friction improvements were lumped together to produce a reduced FMEP map. Note that these would be a lot of development required to achieve the sort of friction reductions modelled here, and it is not certain that this size of benefit could be achieved without risking reliability/durability issues.

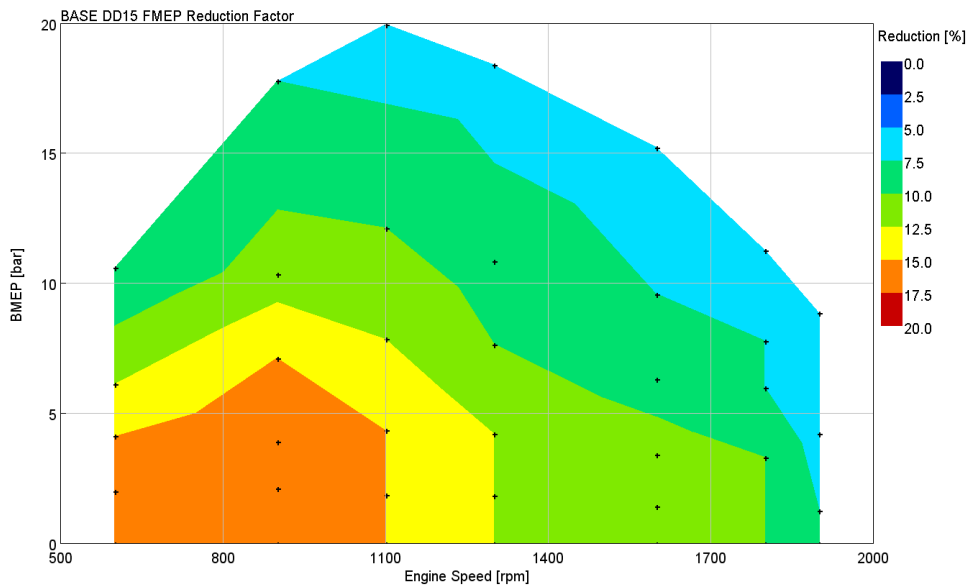


Figure 28. Friction (FMEP) Reduction Assumptions

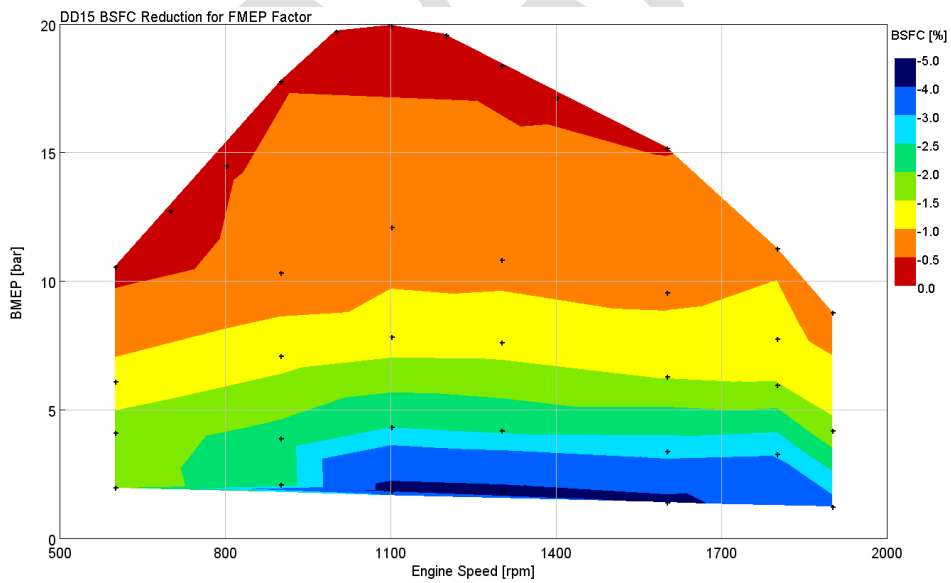


Figure 29. Friction reduction BSFC Improvement over Baseline

3.3 Down Speeding with Increased BMEP

A common approach to improving the drive cycle fuel consumption is engine downspeaking. Typically, the peak torque engine speed is reduced and max torque available is increased. This allows the engine to run at a lower speed for a given vehicle speed. For this study, 2 downspeaking cases were assessed,

- Downspeed A: 1850 lb.ft. (2508 Nm) from 930-1144 rpm, and 400 hp from 1144-1500 rpm
- Downspeed B: 2050 lb.ft. (2779 Nm) from 930-1032 rpm, and 400 hp 1032-1500 rpm

The higher torque levels were achieved by increasing injected fuel quantities and resizing the turbocharger to match the new higher power levels. Cylinder pressure was allowed to increase to observe what levels were reached and to judge whether this was within the limits of current technology. Compression ratio was left unchanged. In both downspeaking cases, the turbo systems were re-sized to achieve comparable minimum AFR ($\sim 19:1$) and the same EGR as the base engine. As a result, the engine speed for the vehicle operating in top gear while cruising on the highway are reduced from about 1150 RPM @ 65 MPH for the baseline case, to around 1100 RPM for Downspeed A, and around 1000 RPM for Downspeed B. Figure 30 shows the effect of Downspeed A on engine performance, and Figure 31 shows the effect on fuel consumption.

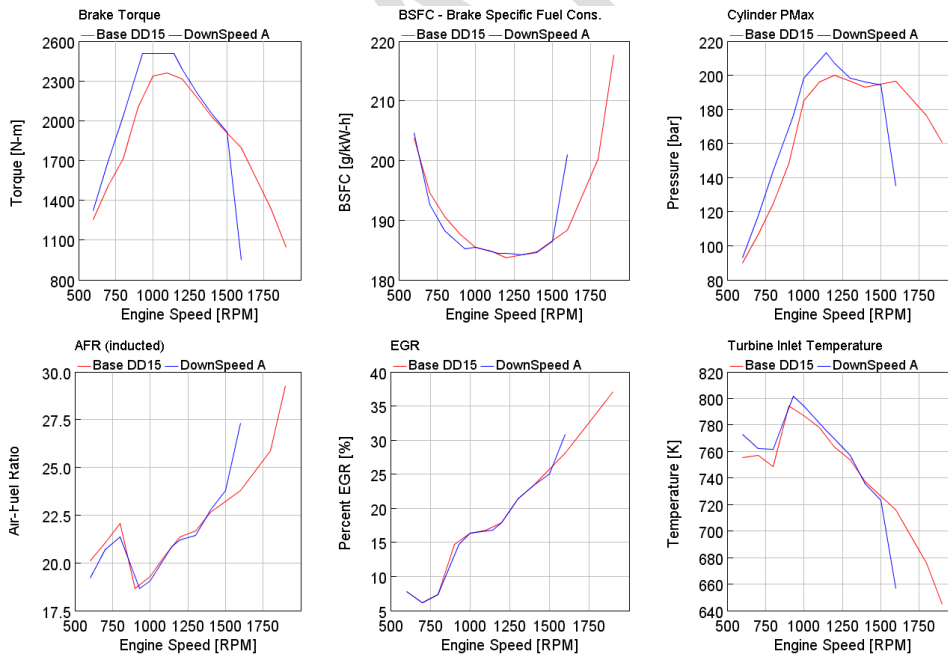


Figure 30. Effect of DownSpeed 'A' on Engine Performance at Full Load

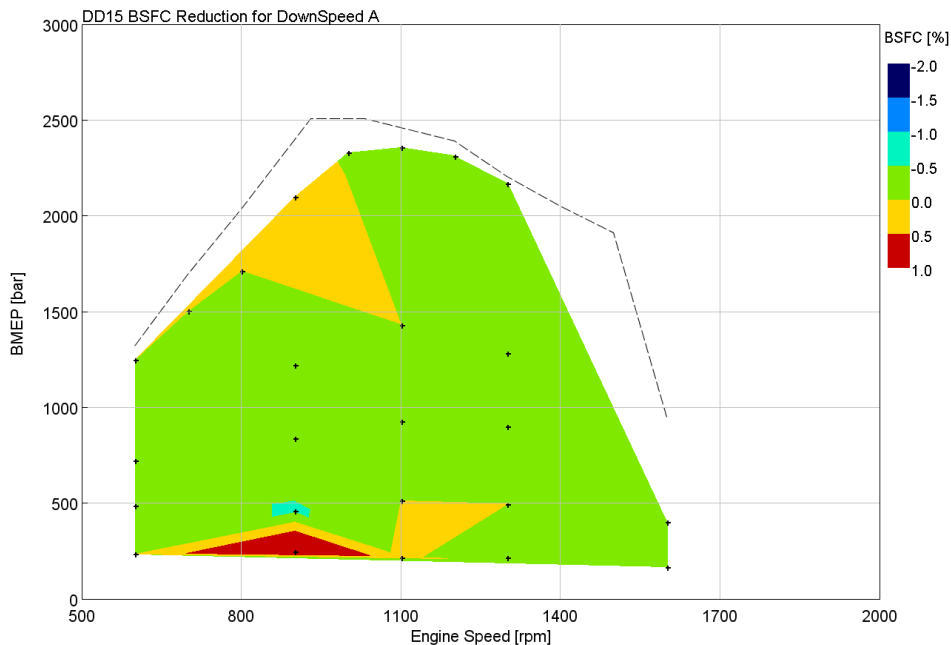


Figure 31. DownSpeed ‘A’ BSFC improvement. Green and blue areas represent an improvement, while orange and red show an increase in fuel consumption.

Downspeed A involves an increase in peak cylinder pressure from about 200 bar to about 215 bar, and Downspeed B drives a peak cylinder pressure increase to about 225 bar. The existing engine design may be capable of handling some level of PCP increase, but design changes and additional development are likely to be required to sustain PCP levels over 210 or 215 bar. This engine is rated at 400 HP, but there are versions of the DD15 that provide up to 600 HP and 2050 lb-ft of torque. SwRI has data to indicate that the high-power variants do run slightly higher cylinder pressure, but that PCP is limited to the 210 to 215 bar range. A reduced compression ratio, retarded timing, and other changes can be made to limit PCP as power increases. All engines have conditions such as low ambient temperature and high altitude where PCP can exceed normal limits. This is accounted for in the design of the engine. The PCP limit is set for “normal” operating conditions, with margin built in to allow for more severe conditions that may be encountered in service. As an alternative, measures such as retarded injection timing or reduced EGR flow could be used to stay within PCP limits, although these approaches are likely to come with a fuel consumption penalty and/or engine-out NO_x penalty under high load conditions. Another option is to reduce the compression ratio to limit PCP, but this would increase fuel consumption slightly.

Figure 32 shows the effect of Downspeed B on engine performance, and Figure 33 shows the effect of Downspeed B on fuel consumption. Downspeed B is more aggressive and produces larger effects.

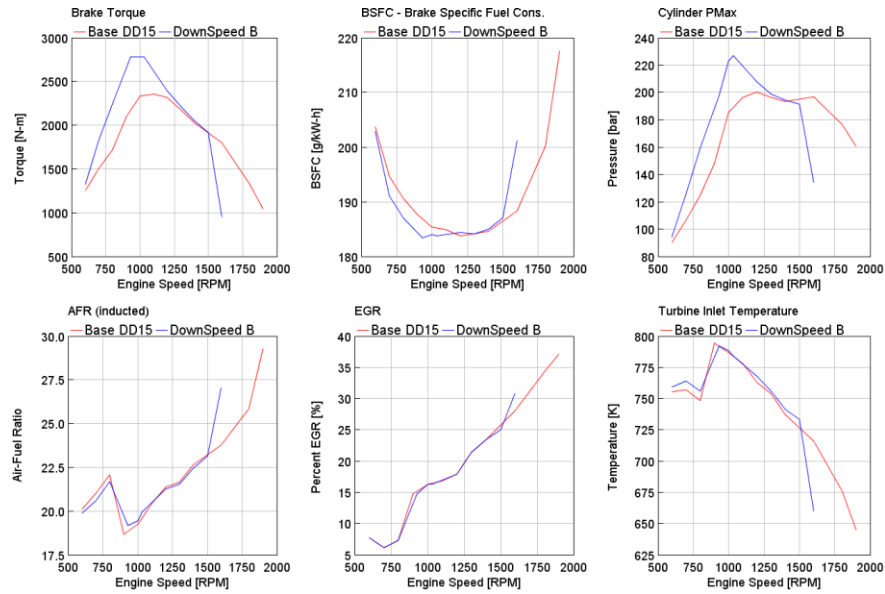


Figure 32. Effect of DownSpeed 'B' on Engine Performance at Full Load

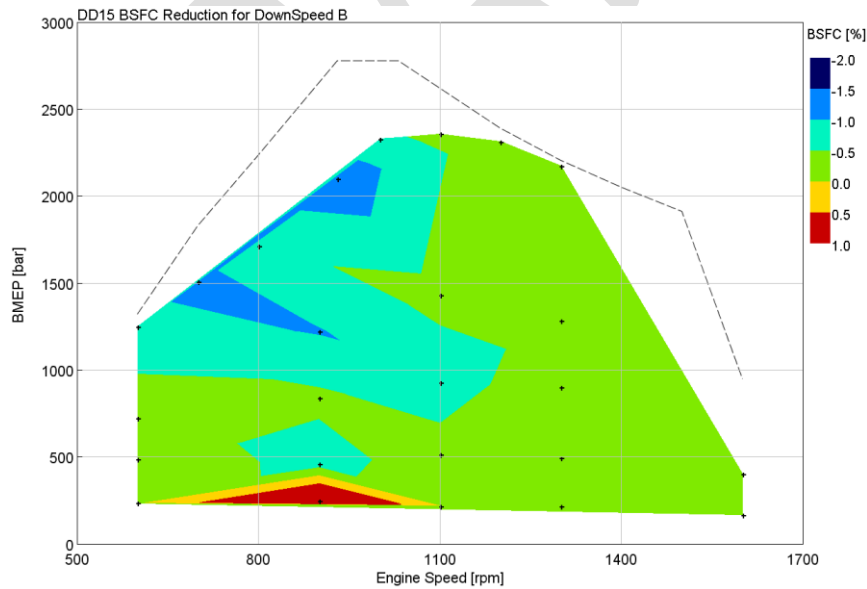


Figure 33. DownSpeed 'B' BSFC improvement. Green and blue areas show a reduction in fuel consumption compared to the baseline, while orange and red show an increase.

3.4 Downsizing with Constant BMEP

A 12.5L displacement version of the DD15 was constructed to assess the effect of downsizing. The approach taken was to remove 1 cylinder, so making the engine a 5-cylinder unit. This method was chosen because it was simpler to reconfigure the manifold layouts rather than re-size all the ports, valves & associated pipework. An ideal approach would be to model a smaller diesel engine, such as the Volvo D13 or the Detroit DD13. Unfortunately, this approach would require the purchase and testing of an engine to provide input data for the model, building a new GT-POWER model, and calibrating it. This effort was beyond the scope of the project. In our experience, the performance differences between a 5 and 6-cylinder of comparable displacement will be small. With a 5-cylinder layout, the firing order has several options, but the order previously chosen for the 2016 NHTSA project when this technology was assessed of 1-4-3-2-5 was carried over.

The main complication with this approach is the asymmetric arrangement of the turbine & EGR system. It was decided that the split would be arranged such that the 2 front cylinders fed the EGR system, and the rear 3 cylinders went directly to the turbine. Additionally, the turbine entry flow area ratio was changed from 29% front to 22% in the front. This setup allowed for sufficient EGR capacity to deliver the EGR rates required.

The FMEP values are the same as for the base engine, so the friction torque or power at a given operating point is reduced by 1/6, due to the smaller displacement and cylinder count. The engine was run at the same BMEP as the base engine, which results in a lower torque and power. The turbo was re-sized to achieve comparable Air Fuel Ratios as the base engine, and this has a slightly detrimental effect on PMEP. The start of injection (SOI), compression ratio and EGR rates were maintained the same as for the base engine.

The results show that the down sized engine is marginally better at part load conditions, but worse at higher loads and speeds due to the increased PMEP. This high load BSFC penalty can be assigned to the reduced performance of the turbocharger set up for downsized operation, compared to the more efficient dual entry turbo setup that is used on the baseline 6-cylinder engine. Figure 34 shows the BSFC delta on a like-for-like torque basis. In other words, differences in fuel consumption are shown at the same torque level for the two engines, rather than at the same BMEP level.

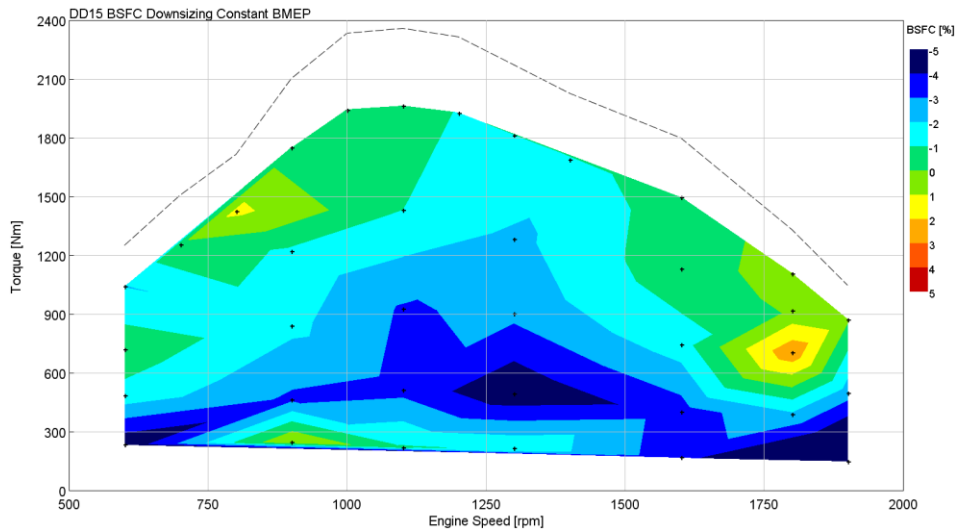
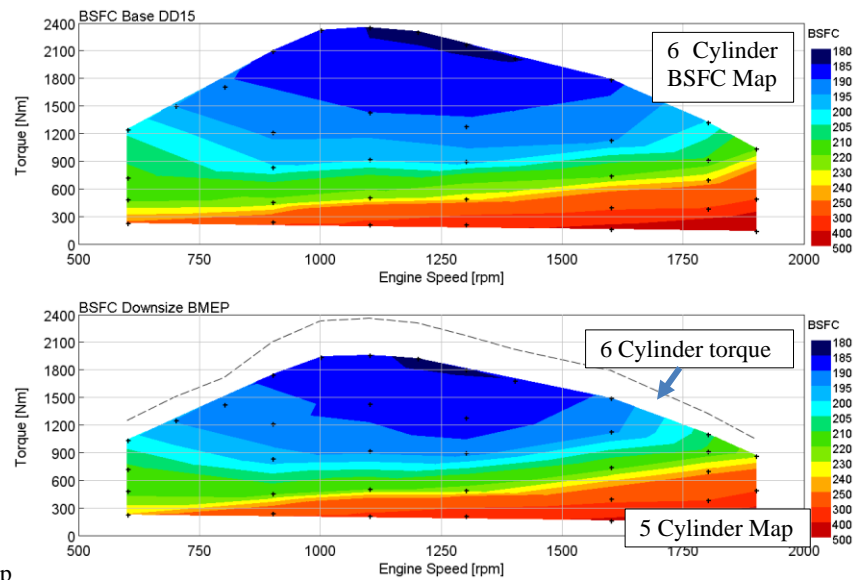


Figure 34. BSFC Improvement of Downsized 5 Cyl. Engine with Constant BMEP. Pale Green, Yellow, and Orange Reflect Increases in Fuel Consumption, While Dark Green and Blue Represent Improvements

Figure 35 compares BSFC maps on an equal BMEP basis. Since the downsized engine has a lower torque curve, the comparison is only shown up to the maximum torque of the downsized variant (the dotted line is the base engine torque curve). These look similar at first glance (other than the lower maximum torque of the downsized engine), but a look at the light load portion of the maps (Figure 36) shows significant advantages for the 5-cylinder. This figure shows that there is a BSFC penalty at low RPM and high torque, but the downsized version generally benefits from a BSFC advantage across most of the operating range, especially at mid to light load which is where the vehicle would be operating much of the time on transient drive cycles. Because the BMEP of the 5-cylinder version is the same as for the original 6-cylinder version, there are no limitations or changes in terms of cylinder pressure or turbocharger pressure ratio. There is, of course, a decrease in vehicle performance due to the reduced availability of power and torque. For Class 8 application, this might not be acceptable due to safety and other customer needs, such as vehicle speed when climbing a grade.



ap

Figure 35. Comparison of 6 Cyl. vs. 5 Cyl. BSFC Maps

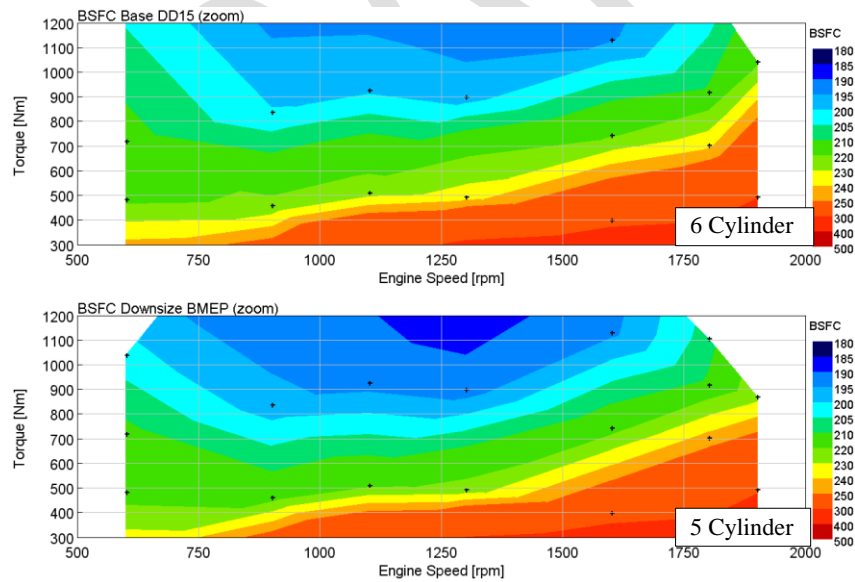


Figure 36. Comparison of 6 Cyl. vs. 5 Cyl. BSFC Maps – Zoomed to Look at 300 to 1200 Nm Torque.

3.5 Downsizing with Constant Torque

The engine model developed in section 1.4 was then run at the same torque levels as the base engine, which results in higher BMEP levels. The base turbo was rescaled to maintain the base engine minimum AFR, and thus higher boost levels were required. PMEP is higher and FMEP is also higher on a per-cylinder basis, as the engine is running at a higher BMEP on the speed-load friction lookup map.

The results show that the down sized engine is significantly better at part load conditions, but slightly worse at higher loads and speeds due to the increased FMEP & PMEP. Figure 37 shows the BSFC delta on a like-for-like torque basis, while Figure 38 show the actual BSFC for both the baseline 6-cylinder engine & the downsized 5-cylinder engine. Figure 39 zooms in on the light load section of the BSFC curve to highlight the improvement. Figure 40 highlights the performance for the full load torque curve, where the downsized engine is achieving the same performance as the 6-cylinder engine but is running at higher boost, turbine pressures and maximum cylinder pressure.

It should be noted that the combustion model is setup so that a fixed set of Wiebe functions are used for a given speed and percent load per cylinder condition: for example, the 1400 rpm 10% load combustion data is the same for both models even though the value of 10% load per cylinder is 16.7% higher for the downsized model. At low load conditions the combustion duration can change by several degrees with a small change in load, so this approach introduces some uncertainty in light load fuel consumption values.

The Wiebe functions are a commonly used method zero-dimensional empirical method for representing the combustion burn-rate characteristics of internal combustion engines for modeling purposes. The Wiebe model uses a series of parameters to simulate a burn-rate heat release curve which can be adjusted and fitted to match measured data without the complex chemistry solvers typically needed for combustion prediction.

The parameters required for the Wiebe setup used in this project are burn duration, a burn midpoint, and a shape factor. Multiple Wiebe functions can be combined to simulate to improve combustion heat release matches or for more complex burn rates experienced with multi-shot injection profiles– the example above indicates how this is achieved. For this project a maximum of a two Wiebe functions were combined.

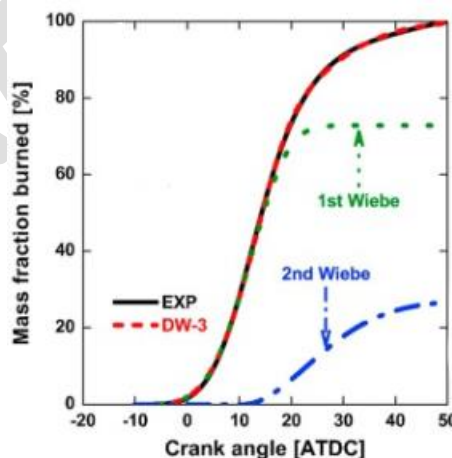


Figure XX. Example of using two Wiebe functions to match experimental cylinder pressure

Commented [A3]: A footnote or reference for this?

Figure 41 (part 2) shows that the 5-cylinder variant with power and torque matching the original 6-cylinder requires a substantial increase in peak cylinder pressure from 200 bar to over 240 bar. Achieving this level of cylinder pressure would require considerable modification to the engine design and extensive validation testing before being introduced to production. As an alternative, the downsized engine could employ measures such as retarded injection timing and reduced EGR rates to limit maximum cylinder pressure. These measures, however, would increase fuel consumption and/or engine-out NO_x under high load conditions, and provide results less attractive than the ones shown here. The higher requirements for boost pressure in the 5-cylinder variant would also have the effect of limiting the engine's altitude capability, so it is possible that a 2-stage turbocharger arrangement would be required in a production implementation.

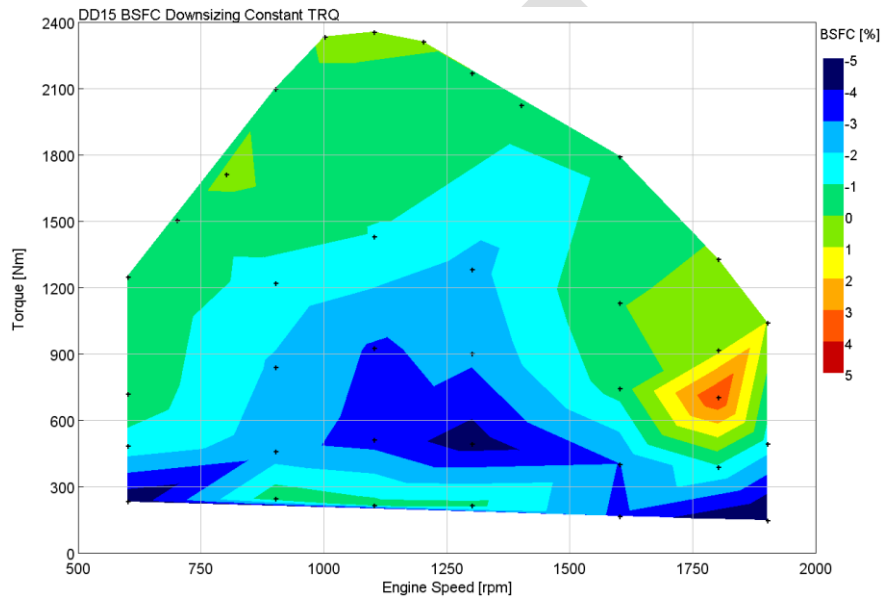


Figure 37. BSFC improvement of Downsize Engine with Constant Torque

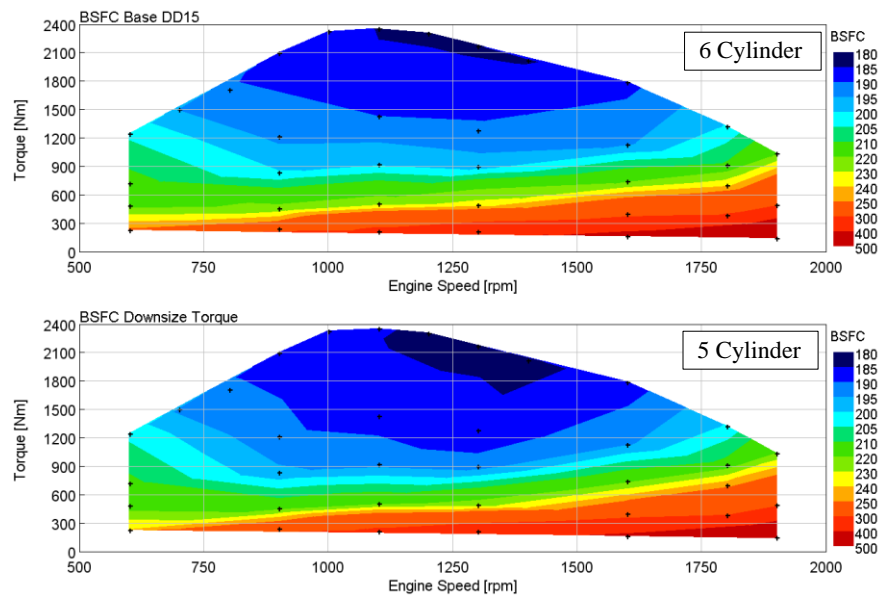


Figure 38. Comparison of 6 Cyl. vs. 5 Cyl. BSFC Maps.

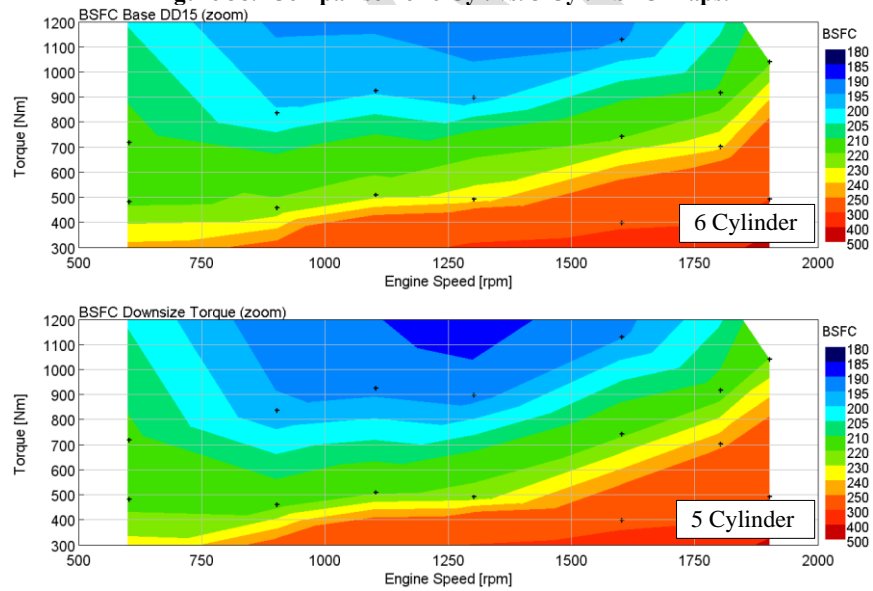


Figure 39. Comparison of 6 Cyl vs. 5 Cyl. BSFC on a Torque Basis – Zoomed to Look at 300 to 1200 Nm Torque.

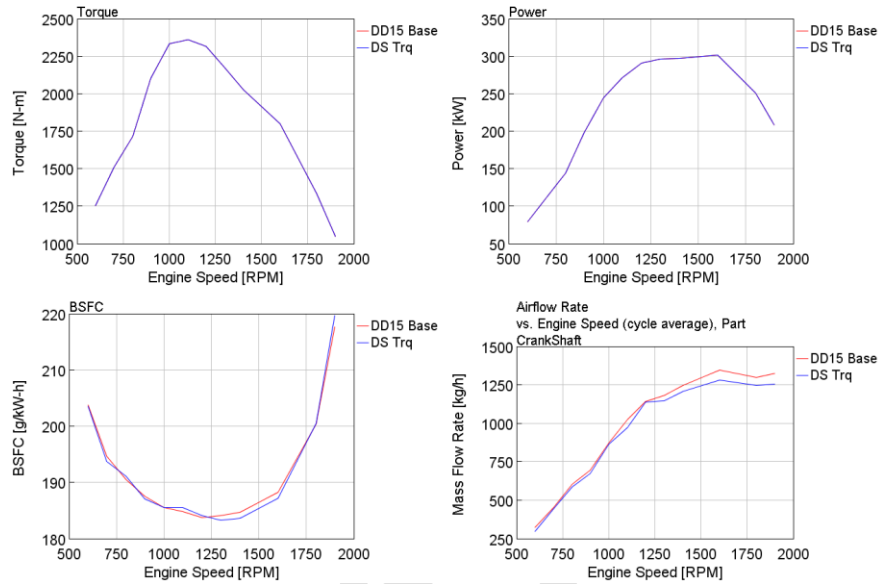
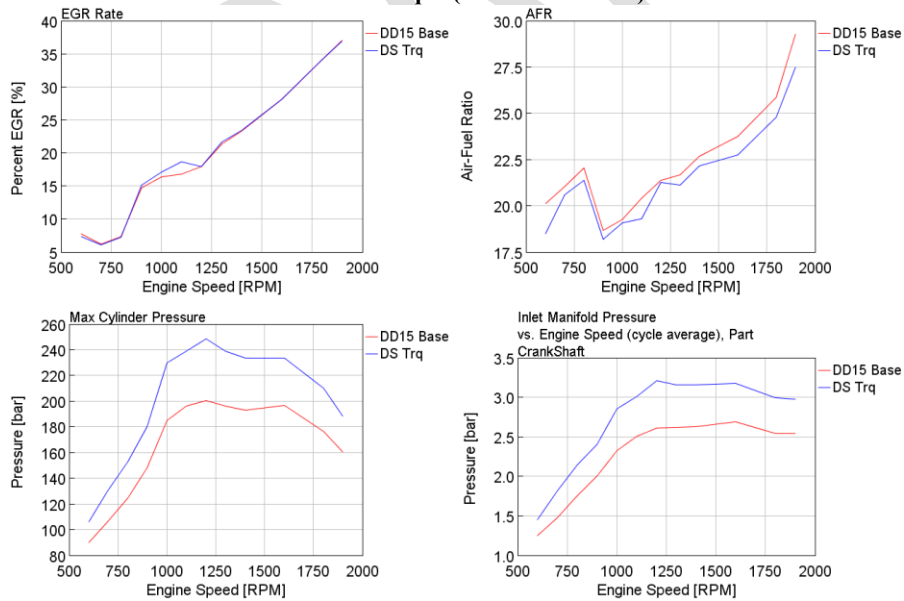


Figure 40. (Part 1). Comparison of 6 Cyl vs. 5 Cyl. Full Load Performance with Constant Power and Torque (Increased BMEP).



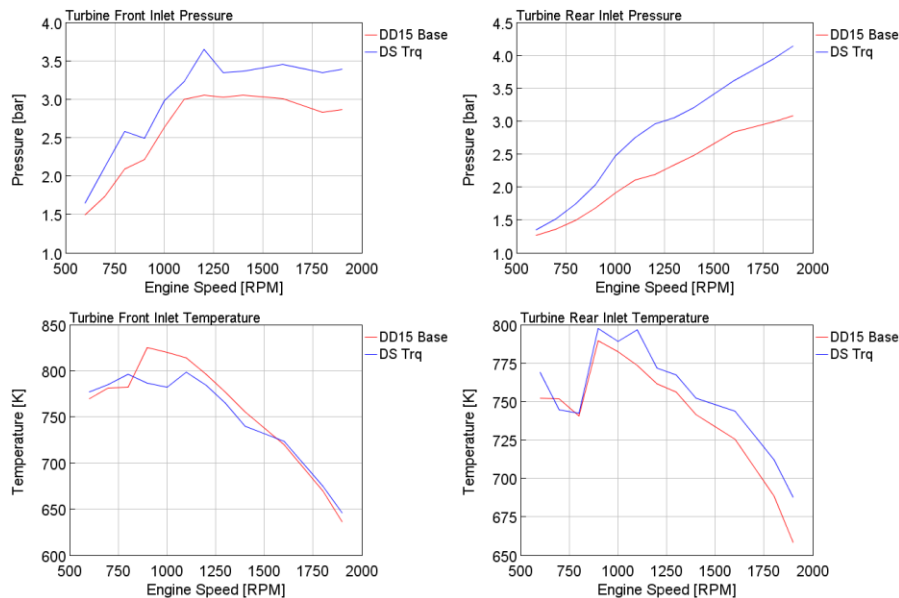


Figure 41. (Part 2). Comparison of 6 Cyl vs. 5 Cyl. Full Load Performance.

3.6 Waste Heat Recovery

Waste heat recovery systems are an attempt to recoup some of the heat energy that is rejected from the engine and transform it into useful energy to do the work desired and therefore reduce the fuel consumption of the vehicle. In this program, the type of waste heat recovery applied was an Organic Rankine (bottoming) Cycle (ORC), which has been studied and researched in the last decade but has yet to show up on a production HD engine. The details of the Rankine cycle applied to this engine are given in Appendix A. Briefly, the configuration of this cycle was to use pure ethanol as the working fluid and to limit the low-pressure side of the system to no lower than atmospheric pressure.

For this analysis, the ORC was determined to not provide significant output below 20% load and those points were all taken as having no contribution from the WHR system. In addition, heat rejection to the ORC condenser was arbitrarily limited to 80 kW to limit the impact on fan load and/or vehicle aerodynamics. The final bottoming cycle selected was a system equipped with a recuperator.

The benefits on the base engine configuration are shown in Figures 42 and 43 below. As shown, the bottoming cycle improves the engine system efficiency by 2 to 5.5% across broad areas of the operating map including the lower engine speed area where the most efficient operation is typically already found and where the vehicle spends a lot of operating time. The benefits are greatest at high load, so applications with sustained moderate to high load will gain the most advantage. However, at least 4.5% improvement is found at engine loads above about 35%, so the gains are

reasonably widespread with regards to engine load. The bottoming cycle is also more conducive to efficiency gains on operating cycles that have relatively steady load rather than highly transient operation, as there are system thermal lags that can be problematic to optimizing gains.

In Figures 42 and 43, there are two data points that appear anomalous. At around 1600 RPM and 400 Nm load, there is data point where the WHR performs very well at light load, while at 1800 RPM and 850 Nm, there is a data point where WHR offers a smaller benefit compared to other speeds at the same load. This variation in WHR performance is due to changes in the EGR rate of the base engine. The higher EGR rate at 1600 RPM / 400 Nm provides more high-quality energy to the system, improving its performance, while a lower EGR rate at the 1800 RPM / 850 Nm point lowers WHR performance. This brings up an important point: the WHR system benefits greatly from an engine calibration that uses high EGR rates, although in many cases, calibrators try to minimize EGR rate to minimize pumping work and thus maximize engine efficiency.

The bottoming cycle was also applied to the best engine configuration in section 3.15. A more thorough discussion of the details of the bottoming cycle benefits is provided there and in Appendix A.

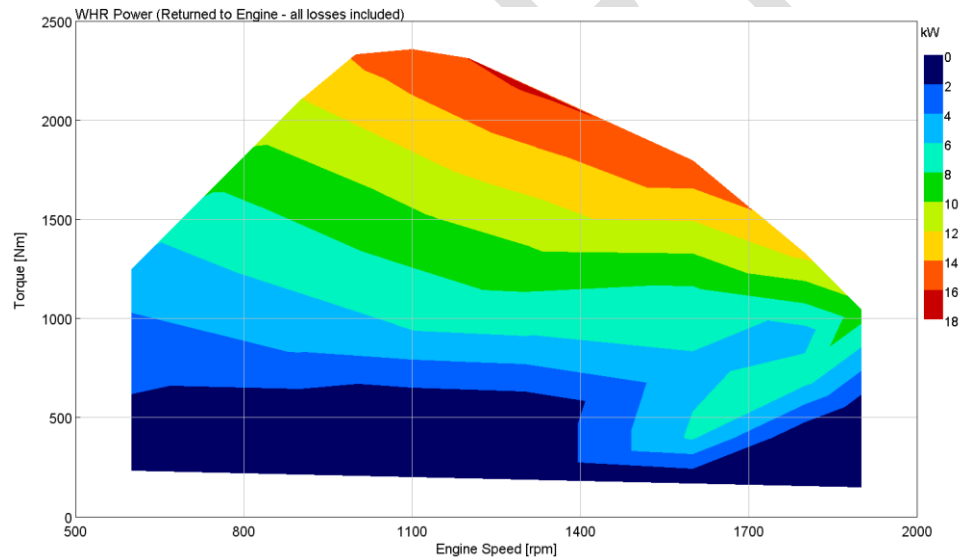


Figure 42. Power Recovered by WHR

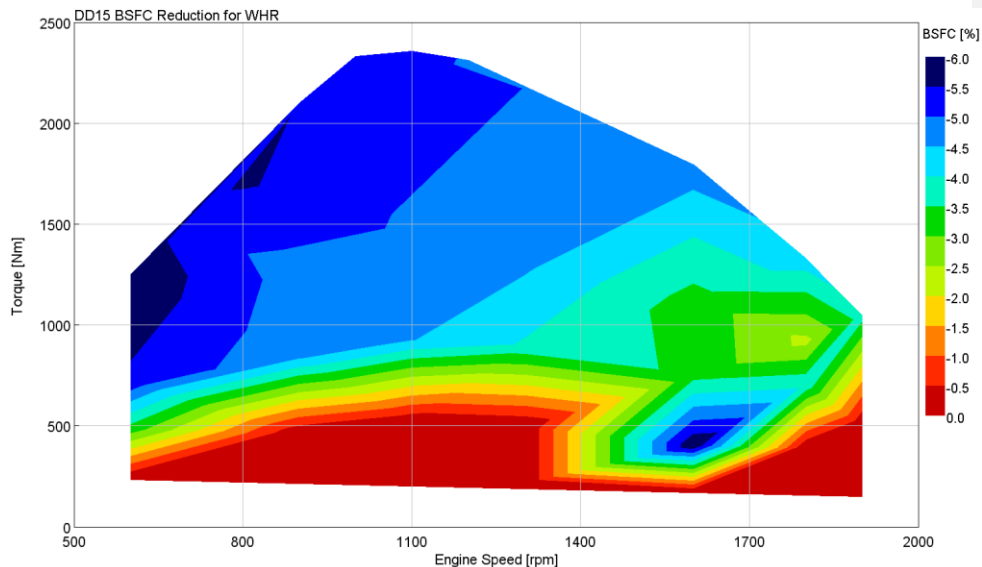


Figure 43. BSFC Improvement From WHR

3.7 Electric EGR Pump with High Efficiency Turbo

The base engine model was modified to replace the existing asymmetric turbo and EGR system with an electrically powered EGR pump and high efficiency twin entry turbo (also called a twin scroll turbo). EGR pump data was supplied by Eaton and the high efficiency turbo data came from Garrett. The base engine EGR flow was controlled by the pressure differential between the exhaust side of the engine and the intake side. To flow EGR at any engine operating condition meant that the exhaust side pressure would always need to be higher than the intake side, and to regulate the flow rate a control valve is used. The EGR flow is taken pre turbine, and in this application from the front entry of the turbine. To further increase the pressure delta, the turbine entries are setup asymmetrically, so the front entry has a smaller, more restrictive flow area than the rear cylinders' entry. This arrangement contributes to reducing the overall engine pumping work, PMEP, since only the front 3 cylinders need to work with the pressure differential required to drive EGR flow. The electric EGR pump does not require a pressure drop to function, since it is a positive displacement unit, and this removes the requirement for the exhaust side of the engine to operate at higher pressure. This allows the use of high efficiency turbos which, in combination with the EGR pump, reduces the PMEP and leads to a fuel consumption improvement.

For the analysis performed in this project, the energy required to power the EGR pump was accounted for in two ways. The first approach assumed the engine supplied the energy to power the EGR pump, and this power demand directly affects the BSFC result. An 80% power conversion efficiency was assumed in both directions. In other words, if the EGR pump power demand was 1 kW, the engine had to provide 1.2 kW to the motor/generator. If the EGR pump was providing

1 kW back to the engine, the engine got credit for 800W coming back from the motor/generator. The second approach assumed the energy was supplied by another source such as a battery system, which was not powered by the engine and was thus not accounted for in the engine BSFC calculation. Assuming that a 48V mild hybrid system is used, a battery size of 1 to 2 kW-h is typical and adequate for use with an EGR pump.

The EGR pump uses at most ~1.5kW, which is 0.5% of engine rated power. Also, over a large portion of the engine operating map, the pump is delivering power back to the engine or external power source, due to the higher pressure on the exhaust side (despite the PMEP reductions). When the exhaust manifold pressure is higher than the intake manifold pressure, the pressure difference drives the EGR pump, which can then provide power back to the engine. In these conditions the pump functions as a flow regulator and at low EGR demand rates, typically at low engine loads, the pump acts as a restriction or blockage. To overcome this, the pump is operated at a minimum speed of 1000 rpm. This means that the EGR rate is slightly increased under some light load conditions.

Figure 44 shows the BSFC improvement resulting from the application of the electric EGR pump, where the engine supplies power to the motor/generator to drive the pump. The engine also gets back power if the EGR pump is making power. The results show a fuel consumption benefit over most of the operating range, particularly at light to mid load. Results for the alternative setup where the energy for the pump is supplied externally are not presented here, because they are so similar in value to those shown. However, two separate fuel maps were produced and supplied. Figure 45 highlights some of the EGR pump operating performance parameters. The comparison of the EGR demand and EGR delivery plots clearly shows the effect of raising the EGR pump minimum speed to 1000rpm, and that the pump over-supplies the engine with EGR at light load. Note that a negative EGR pump power indicates that the pump is being drive by the pressure and is generating power that is either returned to the engine or external power source.

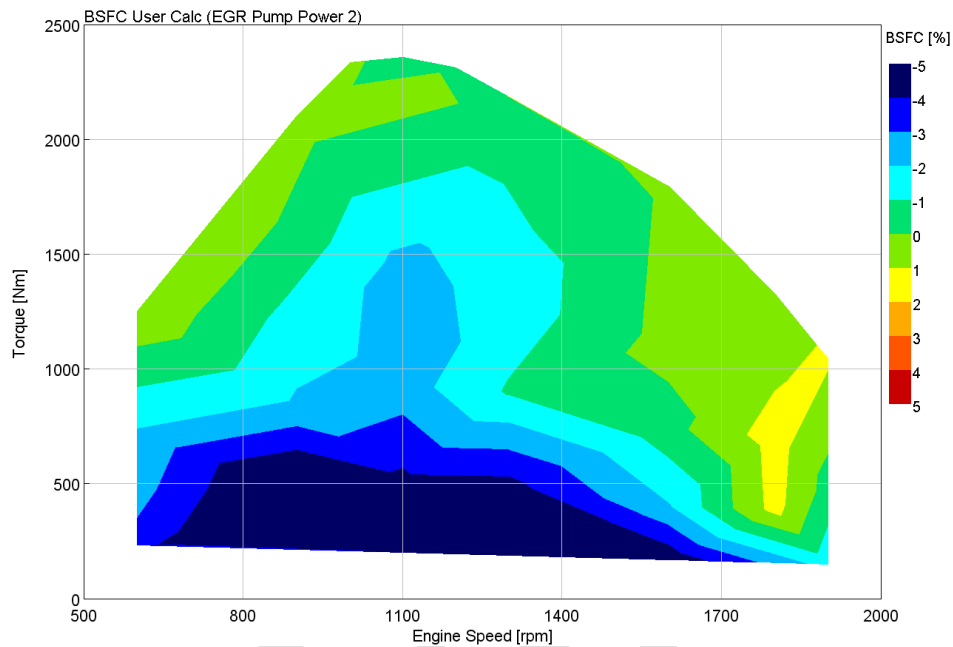


Figure 44. BSFC Improvement With Electric EGR Pump. Pale Green and Yellow Indicate an Increase in Fuel Consumption, While Dark Green and Blue Shades Show a Benefit.

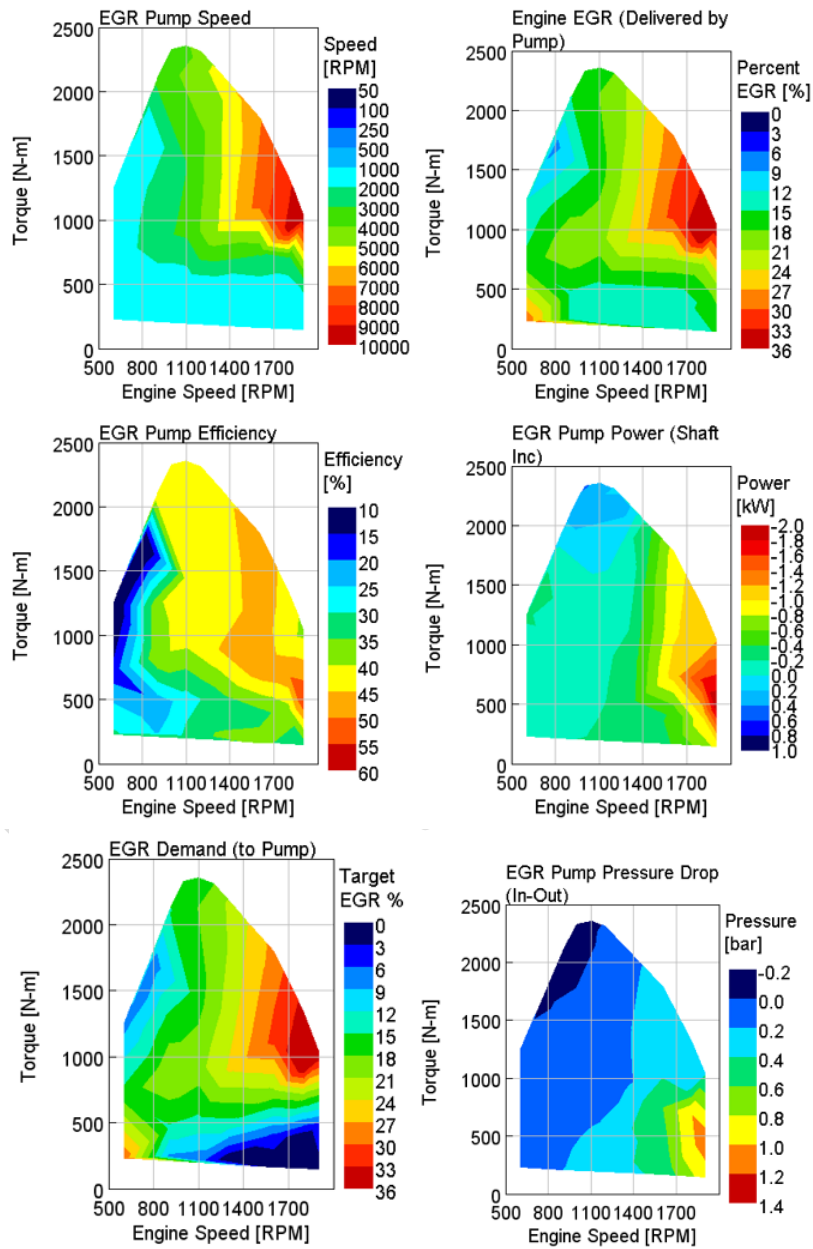


Figure 45. Operating Parameters of Electric EGR Pump

3.8 Cylinder Deactivation

The base engine was modified to represent the technology used for a typical cylinder deactivation (CDA) strategy, where the valve train for certain cylinders, the front three in this case, is deactivated and the combustion is turned off. CDA is only activated at low engine speeds and loads, typically under 4 bar BEMP. It is used to improve both fuel consumption and thermal management of the exhaust aftertreatment system. By running a lower number of cylinders at a given load condition, each cylinder must work at a higher specific output to achieve the same total torque, and in doing so operates at an improved efficiency condition. Additionally, by running at a higher cylinder load, the exhaust temperature is also higher, thus benefiting the overall exhaust temperature. Total exhaust flow rate is reduced, since only 3 cylinders are breathing when CDA is active.

The DD15 used for this project features as standard a form of CDA which works in conjunction with the EGR & turbo asymmetry setup. This is an unusual technology not used by any other engine in the North American truck market except for the DD13 engine which is also made by Detroit. In the DD15, only the fueling is cut-off and the EGR diverter valve is set to guide 100% of the exhaust from the front 3 cylinders to the EGR loop to achieve what amounts to cylinder deactivation. Under these conditions, the valve train is still active and the cylinders that now have no combustion still must pump air through the system, so pumping losses are still present.

When the analysis was performed it was found that there was no advantage to a traditional CDA approach compared the system used by the existing DD15, and in fact the efficiency was marginally worse when applied to this engine due to the asymmetric EGR and turbocharger setup. As a result, the technology was not pursued, and a fuel map was not produced.

3.9 Mild Miller Cycle

The Miller cycle is an over-expanded cycle which provides a higher expansion ratio than compression ratio, with the advantage of providing improved thermal efficiency compared to conventional internal combustion engine operating conditions. In practice, this difference in expansion ratio can be achieved through a compression stroke which includes a late or early closing of the intake valve. This effectively reduces the compression stroke but keeps the combustion and expansion process as normal, enabling extraction of additional energy before the exhaust process. For a naturally aspirated engine, the Miller Cycle increases the expansion ratio to improve thermal efficiency, but with a trade-off of reduced BMEP. To combat the effect of this shortening of the compression stroke, turbochargers or superchargers are used to keep BMEP levels stable, to uphold the advantages of this cycle. Therefore, the Miller cycle uses the boost system to recover the lost charge resulting from the smaller displacement on the compression stroke.

To investigate a mild version of the Miller cycle, the application of variable valvetrain actuation (VVA) was not used, but instead a revised valve event, fixed at all operating conditions, was determined. Previous experience and analysis of VVA/Miller technology on large diesel engines had shown that minimal performance gains were achievable without extensive additional changes

Commented [A4]: Reference to these? Is this from modeling perspective? Real world experiments?

to the engine setup, and this more inclusive approach was studied with the Strong Miller analysis described in section 3.10.

The analysis indicated that the system could be tuned to achieve BSFC improvements in different areas of the operating map, but not across the entire map, as shown in Figure 46. Additionally, by modifying the valve event it was also necessary to re-scale the turbo size to achieve comparable AFRs to the base model, and the effect of turbo scaling contributed more to the effect on BSFC than the revised valve event. The results indicated that a maximum of just of 2% BSFC improvement was achievable. Subsequently, a mild Miller approach was not considered feasible and not further investigated, although a fuel map was produced to allow use this technology to be assessed in the vehicle model. This map uses a turbo map that is biased to reduce fuel consumption at speeds below about 1400 RPM, at the expense of increased fuel consumption at higher speeds.

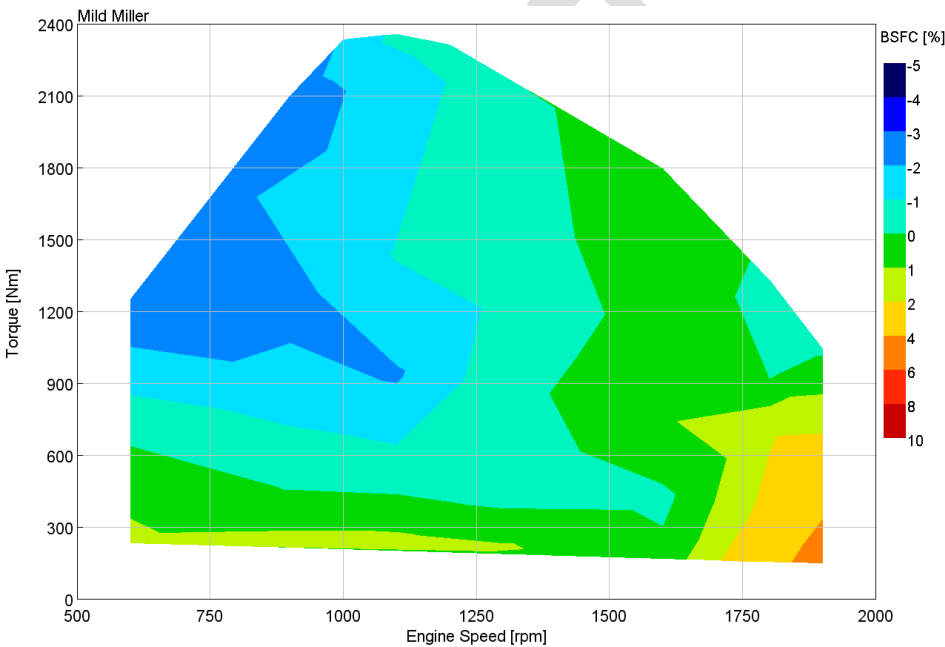


Figure 46. BSFC Improvement From Mild Miller Valve Event and Revised Turbocharger Match

3.10 Strong Miller with EGR Pump, VVA, and 2-Stage Turbocharger

To investigate the effect of Strong Miller valve events, the base model was significantly revised and updated. A full control variable valvetrain actuation (VVA) was added to the inlet valvetrain, where lift, duration, and timing were all adjustable. Additionally, the turbo system was replaced with a 2-stage intercooled setup with no asymmetry, and the EGR system was replaced with the electric EGR pump described in section 1.7. The light load cylinder fuel cut-off feature was also deleted. These changes effectively turned the engine into a more conventional, HD diesel and removed the complexity and influence of the asymmetric turbo, the EGR diverter valve, and any differences from cylinder to cylinder in fueling. Note that the asymmetric turbo, EGR diverter valve, and variations in fueling between cylinders are features unique to Daimler heavy duty diesels and are not currently used on any competing engine. It should be noted that the aim of the analysis was not to develop a VVA system, but to demonstrate what could be achieved by one.

The model was run within existing engine performance limits, including the same max torque curve, equal minimum AFR and equal maximum cylinder pressure. The model featured a wastegate on the high-pressure turbine, which was active at full load conditions to maintain the same AFR or PCP as the base engine, and then was inactive at part load to minimize pumping losses.

The model was then run at a series of fixed operating conditions and the inlet valve events optimized for best BSFC. The inlet valve opening timing range was limited to $\pm 10^\circ$ of the base engine, and as the results indicate this parameter varied only slightly across the operating range. Inlet duration was either increased by adding up to 20° of dwell at peak lift, or reduced by up to 50% duration, while at the same time reducing lift proportionally by applying a relationship of lift proportional to the square root of duration (as shown in Figure 47).

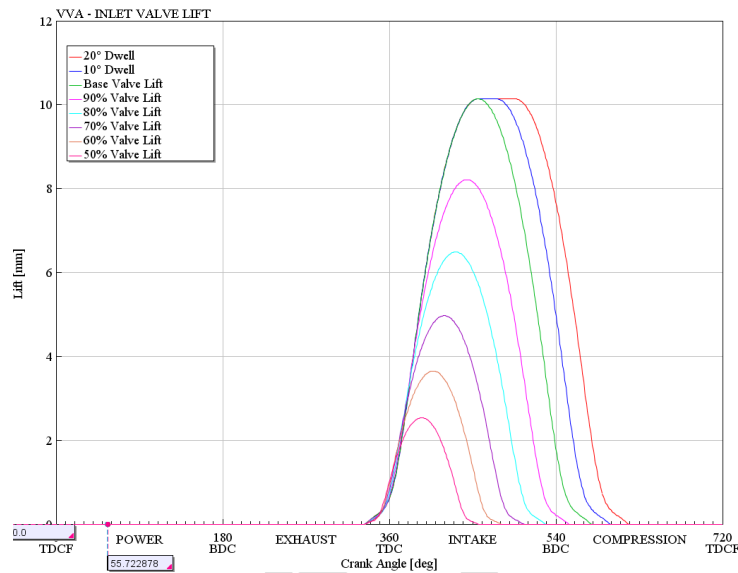


Figure 47. Inlet Valvetrain Scaling Range

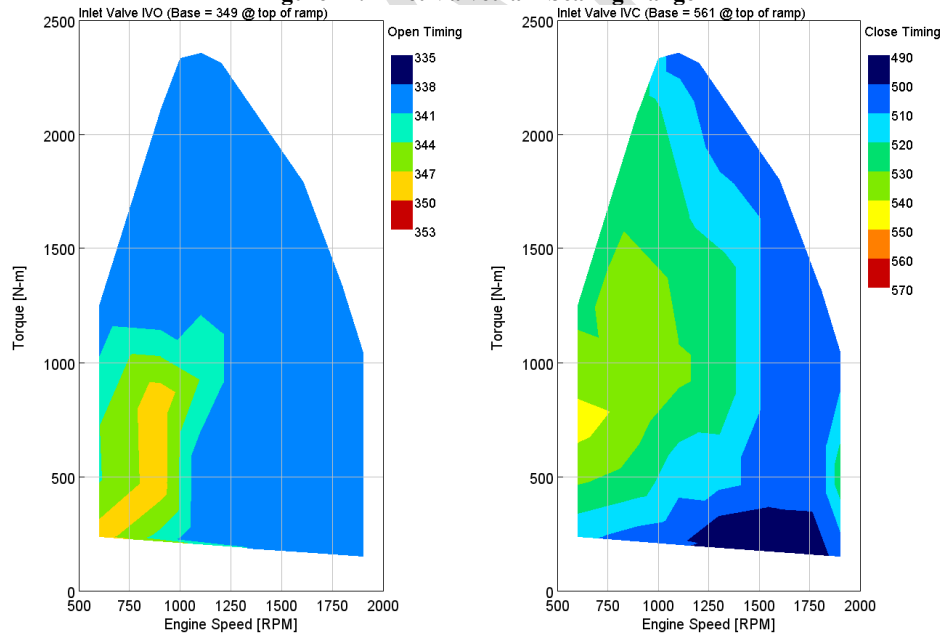


Figure 48. Resulting Inlet Valve Opening & Closing Optimized

The results showed that for the setup used and the constraints imposed, duration was always shorter than for the base engine by a factor of between 75-95% (Figure 48). If an increase in BMEP had been allowed for this study, then it is possible that an increased intake valve opening duration may have been a feasible solution. Figure 49 shows the cylinder pressures and AFR across the operating range. The max PCP was kept within the base value of 200 bar and the minimum AFR did not drop below 18.5:1, although due to the wastegate strategy AFR did exceed the base engine values at some part load conditions by up to 10%. When AFR is low (below 20 or 21), an increase in AFR will drive an increase in NO_x, but at higher AFR values, a 10% change in AFR will have minimal effect on NO_x.

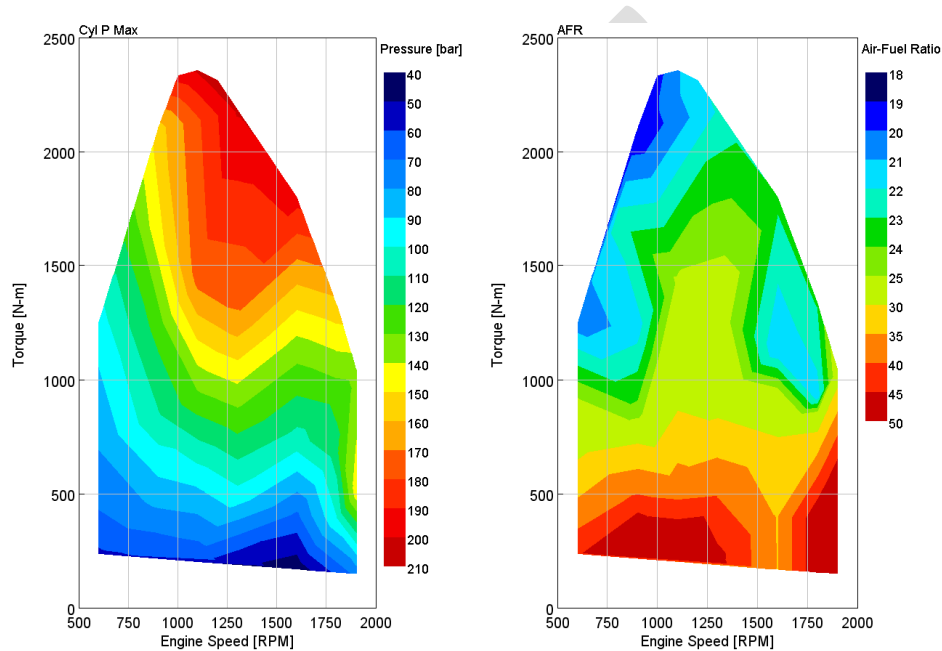


Figure 49. Strong Miller Cylinder Pressures & Air Fuel Ratios

The results of the Strong Miller setup are shown in the following figures. Figure 50 shows the BSFC improvement relative to the baseline engine model, with gains of over 10% attained at light load. A more realistic comparison is with the EGR pump equipped engine (see section 3.7), which also featured a high efficiency, non-asymmetric turbocharger. This comparison shows that the Strong Miller setup can achieve some useful BSFC gains across the operating map. It should be noted that the EGR pump energy requirements and associated efficiencies (both when absorbing and providing energy) are accounted for in the overall BSFC result.

Figure 51 shows the fuel consumption of the strong Miller cycle engine compared to the version with a high efficiency turbo and EGR pump (both components are used by the strong Miller engine,

so this is a good basis for comparison). Modest BSFC reduction can be seen across much of the map, with a larger benefit at high speed and light load.

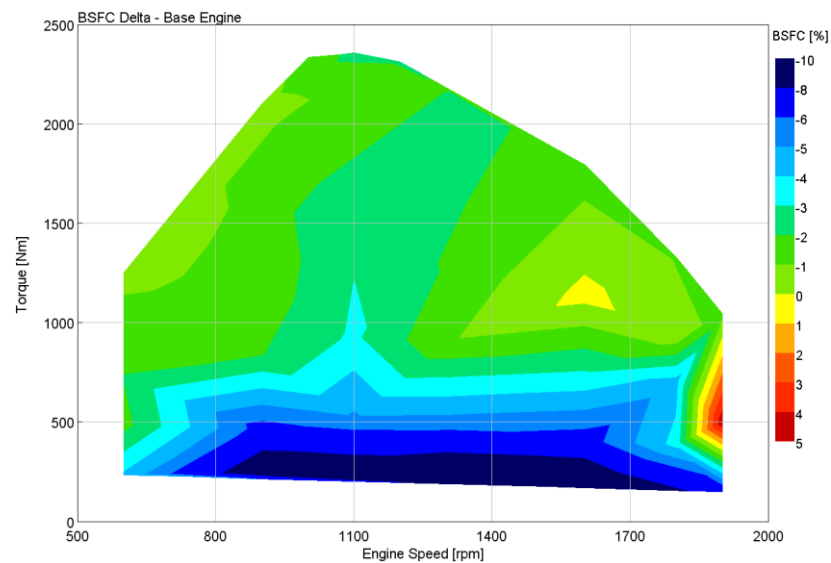


Figure 50. Strong Miller BSFC Improvement vs. Base Engine. Yellow and Orange Areas Show Increased Fuel Consumption, Green and Blue Areas Show Reduced Fuel Consumption.

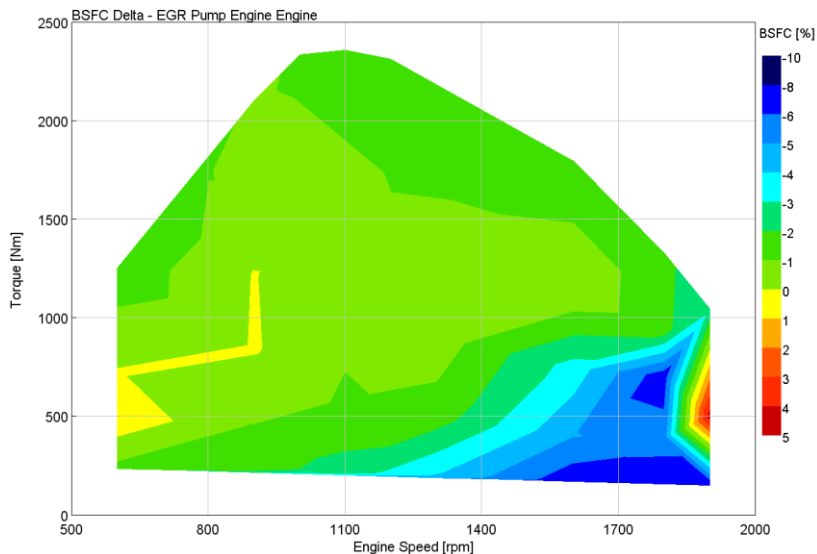


Figure 51. Strong Miller BSFC Improvement vs. EGR Pump + High Efficiency Turbo Engine

3.11 Mechanical Turbocompound

Daimler was the first company to put a turbocompound system on a heavy-duty engine in production, with the launch of the DD15 engine in 2008. For the 2013 update of the DD15, Daimler chose to delete the turbocompound, although it is still used on the low volume DD16 engine that is aimed at the heavy-hauler market. Volvo added a turbocompound option to its D13 engine in 2017 and updated it in 2021. There are no other turbocompound heavy-duty diesel engines on the market.

The basic idea of a turbocompound system is to capture some of the exhaust energy and put it back into the crankshaft, so a turbocompound can be considered a form of waste heat recovery. Turbocompound systems have the advantage of applying some backpressure to the normal turbocharger, so even a very efficient turbo will run with exhaust manifold pressure higher than the intake manifold pressure, allowing EGR to flow. In engines without turbocompound, the efficiency of the turbo must be degraded to the point where exhaust manifold pressure is always above intake manifold pressure. A disadvantage of the turbocompound system is that it makes life harder for an SCR aftertreatment system. The thermal inertia of the power turbine slows catalyst warmup, and because the power turbine is extracting energy from the exhaust, aftertreatment inlet temperatures are lower. This may require thermal management strategies that increase fuel consumption during warmup and light load operation. As was found in DOT HS 812 146, turbocompound engines provide a significant BSFC benefit only when operating at high load, so they are most effective in heavy-haul applications where the load factor (average load over the drive cycle) is high. Long haul applications with vehicle weights of 80,000 pounds or less tend to run at load factors in the 40% range, which limits the benefit of turbocompound.

The base engine model was modified to incorporate an Auxiliary Power Turbine unit (APT) to enable the recovery of exhaust gas energy after it has passed through the main engine turbocharger. The APT is connected to the engine crankshaft via a gearbox & fluid coupling. It should be noted that an earlier generation of DD15 engine sold from 2008 through 2012 did include an APT as a standard feature, and that this was later replaced by the asymmetric turbo arrangement used on the current production engine. Analysis from the previous NHTSA project had indicated that the removal of the APT had provided little impact on the BSFC performance (~1%), so adding the APT back was not expected to deliver significant improvements.

To optimize the setup, both APT sizing and gear ratios of the connection back to the engine were optimized. The analysis showed that the APT could generate up to 8kW of energy, which is less than 3% of maximum engine power. The power turbine output was subject to transmission losses, so there is ~2.5% effective power return at the best operating point. The addition of the APT resulted in a 0.5-1% BSFC improvement over much of the operating range, as shown in Figure 52. There is a slight fuel consumption penalty around 1000 Nm and 1100 rpm.

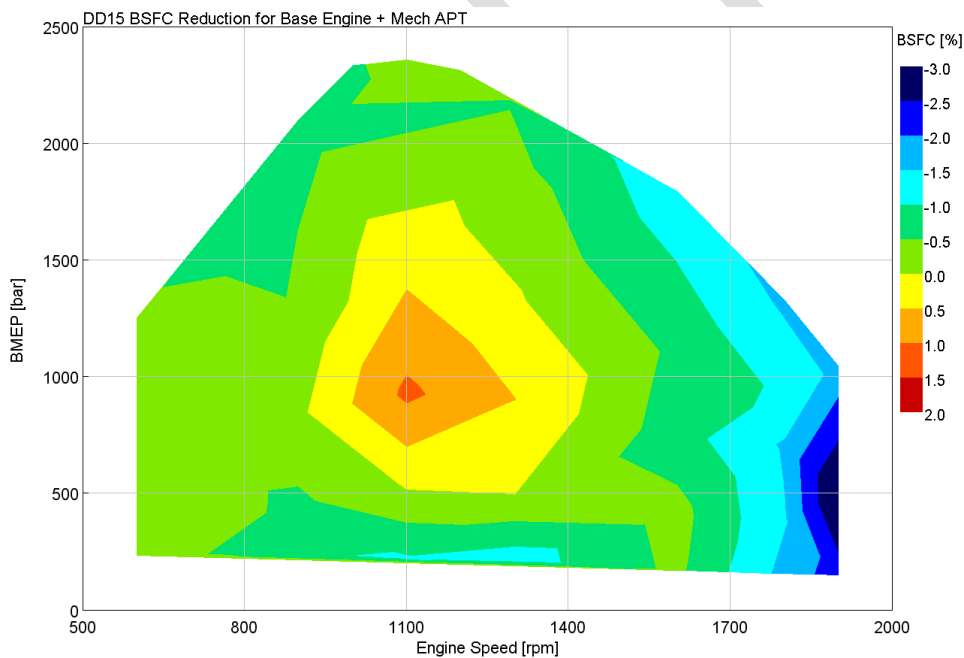


Figure 52. BSFC Improvement from Mechanical APT

3.12 Electric Turbocompound

The base engine model was modified to incorporate an Auxiliary Power Turbine unit (APT) as described in section 3.11. For this analysis the APT output was connected to an electric generator

through a geared system. Energy from the power turbine could be either recycled back to the engine through an electric drive or used to power other electric devices, such as an EGR pump. In this case, the energy was fed back to the engine with a total system efficiency of ~80%. The logic behind doing an electric turbocompound arrangement is to decouple the power turbine speed from the engine crankshaft speed, which allows the power turbine to operate more efficiently over parts of the engine map.

To optimize the setup, APT sizing was optimized to balance power generation against backpressure on the engine. The analysis showed that the APT & generator could generate up to 7kW of energy, which is 2.5 % of maximum engine power, but this is subject to transmission and system efficiency losses, so the maximum net power is ~2.0% of crankshaft power. Two sets of results are presented. Figure 53 show the BSFC improvement for the electrical APT running with the base EGR rates, and Figure 54 shows the BSFC improvement running with some EGR points in the mid-load portion of the operating range reduced by up to 5 percent. Figure 55 presents a comparison of the 2 EGR rates used in the simulation work. Note that a reduction in EGR rate will lead to an increase in engine-out NOx, so higher aftertreatment performance would be required.

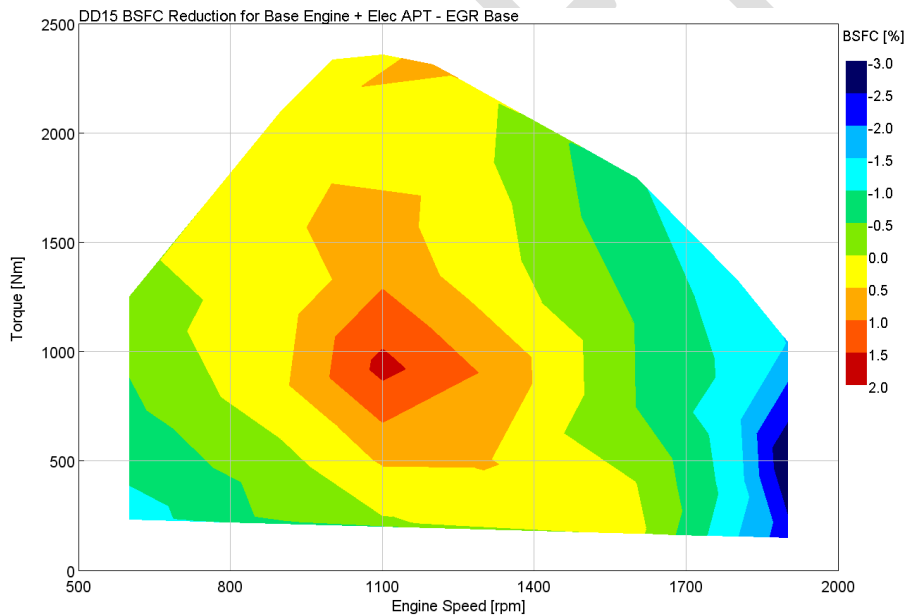


Figure 53. BSFC Improvement of Electric Turbocompound With Base Engine EGR

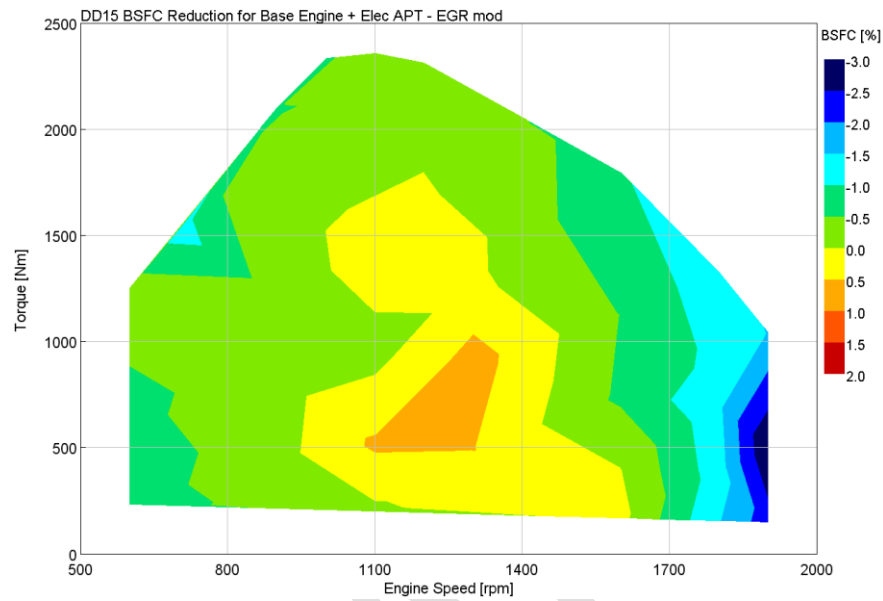


Figure 54. BSFC Improvement of Electric Turbocompound With Reduced EGR

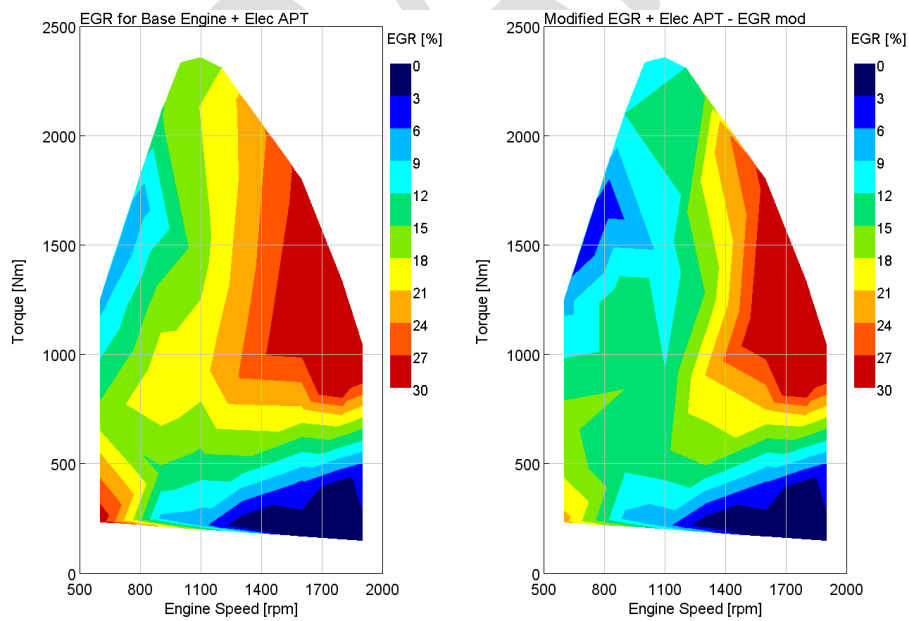


Figure 55. Comparison of Electric Turbocompound EGR Rates

3.15 Error! Reference source not found.

On completion of the individual technology simulations, the results were analyzed, and a model constructed featuring the combination of the best performing technologies. Two model configurations were chosen:

1. Strong Miller with EGR Pump & 2 Stage Turbo + Downsized High Torque (2050 lb.ft)
2. As (1) + Waste Heat Recovery (WHR)

Both these setups feature high specification and high-cost technologies. All are mature technologies but have yet to be combined on a production engine platform. The Strong Miller requires VVA, the EGR Pump is a new emerging technology that should be ready for production in a few years, and WHR is costly and complex. However, to achieve the largest improvements in fuel consumption and engine efficiency, it is necessary to apply these technologies.

The original Strong Miller option included a compression ratio increase to maintain 200 bar PCP with the baseline torque curve. Because of the higher BMEP of the combo version, PCP increased to just over 220 bar at 1050 RPM. PCP then falls with increasing speed to below 200 bar by 1400 RPM. For a production application, the Strong Miller valve events could be tweaked to maintain a 200 bar PCP, with a small fuel consumption increase at low speed and high load. When waste heat recovery is added to the package, the peak cylinder pressure drops to just over 210 bar at 1050 RPM, because the engine BMEP is reduced to compensate for the contribution from the WHR system. Again, the system could be tuned to maintain the original 200 bar PCP limit. In this case, there would be a slight BSFC penalty at low speed, high load, but there could be BSFC improvements at higher speed where the engine is running well under 200 bar.

Figures 60 and 61 show the relative BSFC for the base engine and the 2 combination builds. The best BSFC points are:

- Base Engine: 183.7 g/kW.hr @ 1200rpm @ 2314 Nm
- Combination 1: 179.5 g/kW.hr @ 1200rpm @ 2310 Nm
- Combination 2: 171.8 g/kW.hr @ 1200rpm @ 2310 Nm

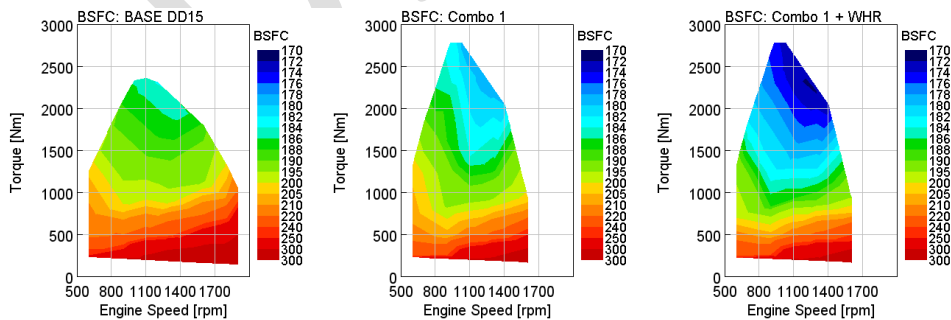


Figure 60. BSFC of Base Engine vs Technology Combinations 1 & 2

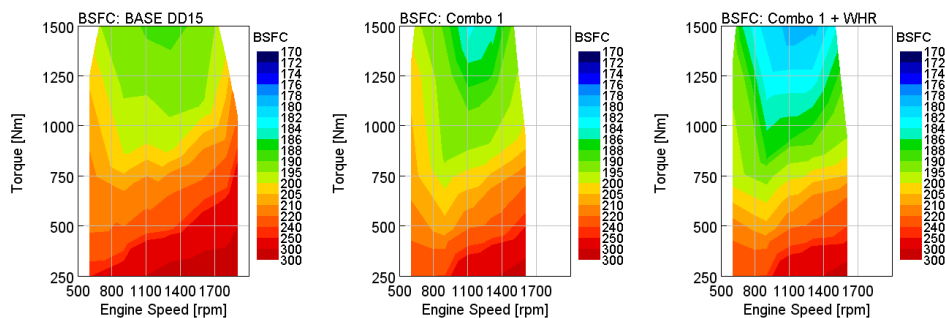


Figure 61. BSFC of Base Engine vs Technology Combinations 1 & 2 at Low Load

Figures 62 and 63 below show the BSFC for each of the 2 combination builds and their improvement relative to the base engine build. Figure 64 shows the full load performance of a range of key parameters, and compares the combination builds with the base engine and the downspeed engine with otherwise standard setup.

Both options achieve gains across the entire operating map. Combination 1 achieves >2% improvement over 75% of the map and Combination 2 achieve >5% improvement over 75% of the map. It should be noted that the best improvements for both models are at high speed, low load conditions which will probably have only a small effect on a drive cycle result, as the engine would rarely operate in this region. The addition of the WHR system makes significant improvements at the higher load conditions, where the engine is operating at its hottest and as has the most opportunity to recovery energy. At lower loads, below 500 Nm, the results are very similar, since little energy is recovered. Given the high add-on cost of a WHR system, this trade-off may help determine which applications could benefit most from a WHR system. Another factor to keep in mind is the poor transient response of WHR systems, which makes them unsuitable for use in transient operations such as urban driving and many vocational applications.

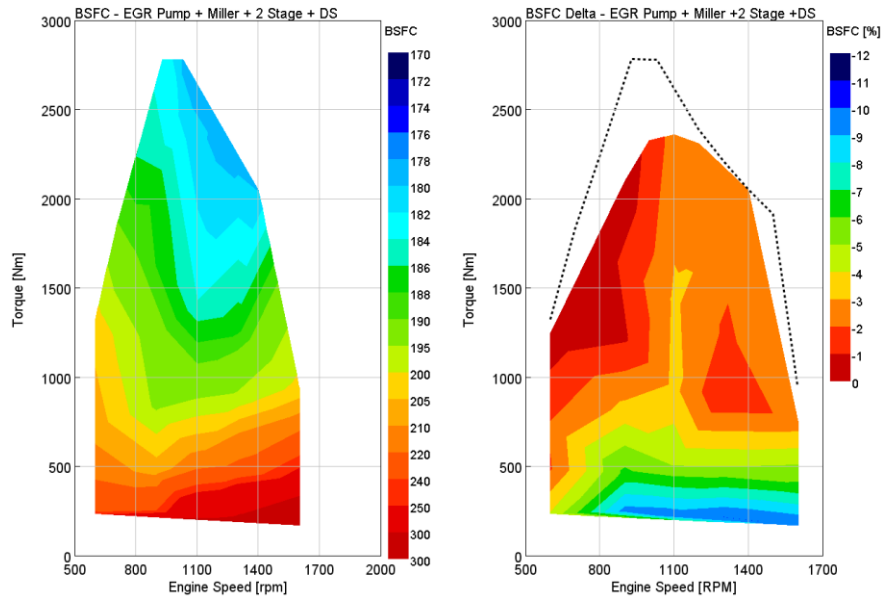


Figure 62. BSFC & BSFC Improvement of Technology Combination 1

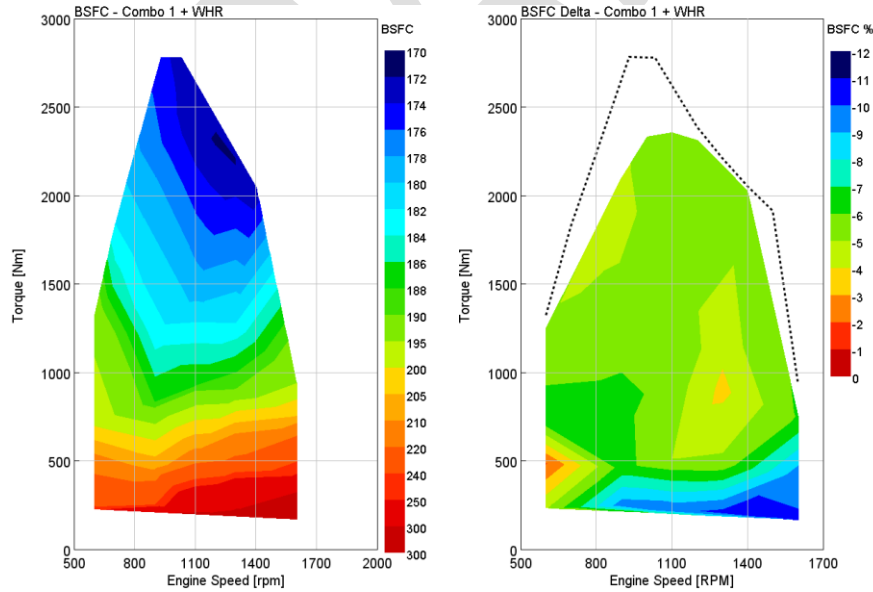


Figure 63. BSFC & BSFC Improvement of Technology Combination 2 vs. Baseline

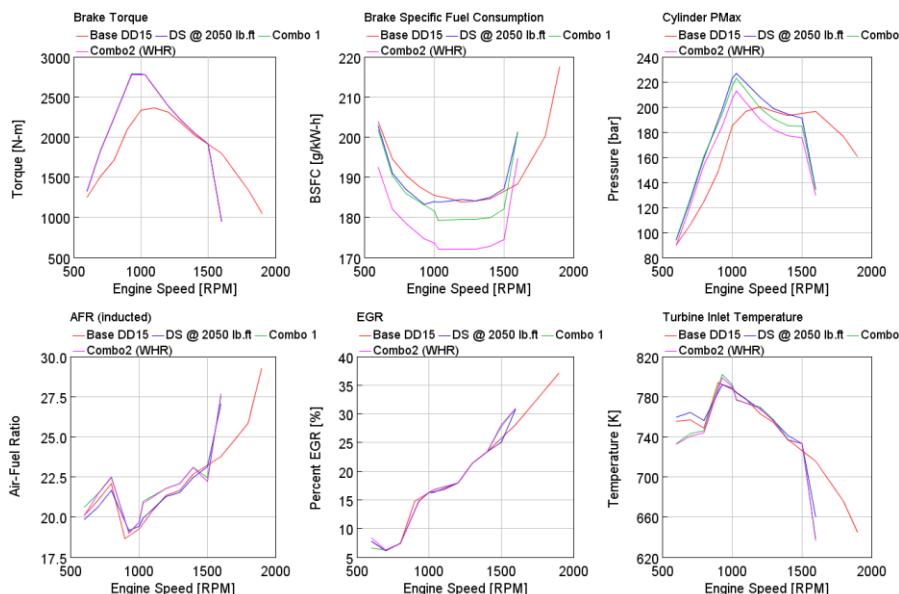


Figure 64. Full Load Performance of Base v Downspeed v Combination Build Engines

Figure 65 shows the operating regions of a sleeper truck on the ARB transient cycle, supplied by Argonne. The highest density points are grouped along the 1200-1400 rpm speed range band, which if scaled and aligned to the downspeed engines would be operating around 1000-1200 rpm region. This would indicate that Combination 2 could give a minimum fuel consumption reduction of 5%, with up to 10% at the low load conditions.

It is important to keep in mind that these BSFC reduction are for steady-state operating conditions. In reality, the contribution of the WHR system to BSFC reduction would be much less on a cycle like the ARB transient cycle. Much of the heat for the WHR system comes post-aftertreatment. The aftertreatment has a very high thermal inertia, so it will take a long time for WHR system power to increase after a step increase in engine load. It will also take some time for WHR system power to decrease to zero after a drop to no load. The thermal inertia issue is even a problem for cruise cycles. Slight changes in road grade can drive large changes in power demand on the engine. If these changes occur over a short period of time, the performance of the WHR system will be reduced. There is likely synergy between the WHR system and a hybrid, where energy storage could mitigate the thermal inertia and response issues of the WHR system. Investigation of such a combination was outside the scope of this work.

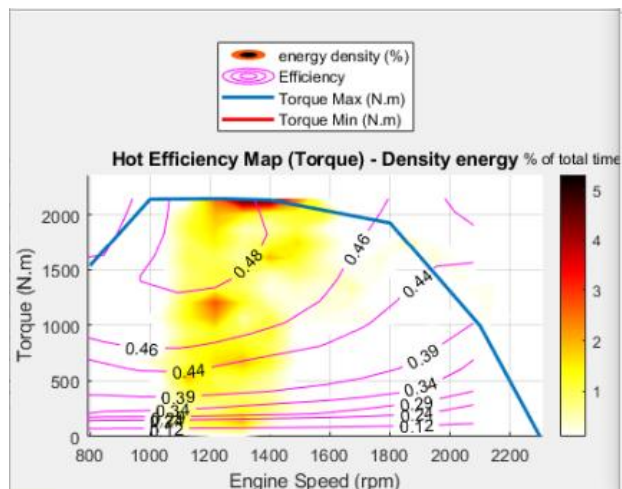


Figure 65. Argonne Data for Operating Region of Sleeper Truck (ARB Transient Cycle)

For vehicle simulations, SwRI suggests applying a 150 second first order time constant to the WHR power produced from a step increase in load, and a 30 second first order time constant to the WHR power produced from a step decrease in load. Results could be compared to simulations without a time constant to gauge the impact of thermal inertia on a given test cycle.

4.0 GM DURAMAX 3.0 LITER LIGHT DUTY DIESEL

The engine selected as representative of North American light-duty diesel truck applications is the General Motors 3.0-liter Duramax. It is an in-line six-cylinder four-stroke engine with 84 mm bore and 90 mm stroke. The engine uses cooled low-pressure-loop and un-cooled high-pressure-loop EGR systems with a variable geometry turbine, water-to-air charge air cooling that uses a separate low temperature coolant loop, and a variable intake manifold with dual air intake paths.

The engine produces 206 kW at 3750 rpm and a maximum torque of 620 Nm at 1500 rpm. The torque curve is relatively flat from 1500 to 3000 rpm, and the engine has a compression ratio of 15:1. This compression ratio is low by medium- and heavy-duty engine standards but is common in high BMEP light duty diesels. The lower compression ratio allows high BMEP with relatively modest peak cylinder pressure, at the expense of some efficiency.

4.1 Baseline Model Match

All the engine configurations evaluated were simulated using a Gamma Technologies GT Power® model provide by General Motors, depicted in Figure . The model was extensively adjusted to match to GM's engine performance and emissions data set. Available measurements included air and fuel flow versus engine speed, EGR mass flow rate, pressures and temperatures throughout intake and exhaust system, peak cylinder pressure and crank angle degree MFB 50, mean effective pressures, and brake specific NOx. GM's model included a predictive combustion Di-Pulse sub-model, a NOx model, and turbine performance maps. Model validation focused on matching the baseline fuel consumption, indicated and brake mean effective pressures, and air-fuel ratio.

The resulting fuel efficiency match achieved with the model is presented in Figure and Figure . In Figure , the percent difference between measured and modeled fuel consumption is presented across the speed and load map. The match was within four percent for majority of points on the map, with mid and high load operation often within two percent. The difference between measured and modeled results exceeds four percent under light load conditions where a small difference in fuel flow can show up as a large percentage error and at very low-rpm, high-load conditions, where it was deemed that little or no time would be spent by an engine coupled with an automatic transmission.

In Figure , the percent difference between measured and modeled brake thermal efficiency (BTE) is presented. The match was within four percent for majority of the speed and load map. The error exceeds four percent at light loads ($\text{BMEP} \leq 1$ bar), no-load and at one low-speed, high-load point (1000 rpm and 14 bar). With challenges involved in measurement accuracy at light loads, this error was deemed acceptable. And for the low-speed high-load point, it was assumed that the engine would spend little to no time before shifting to a more efficient speed-load condition.

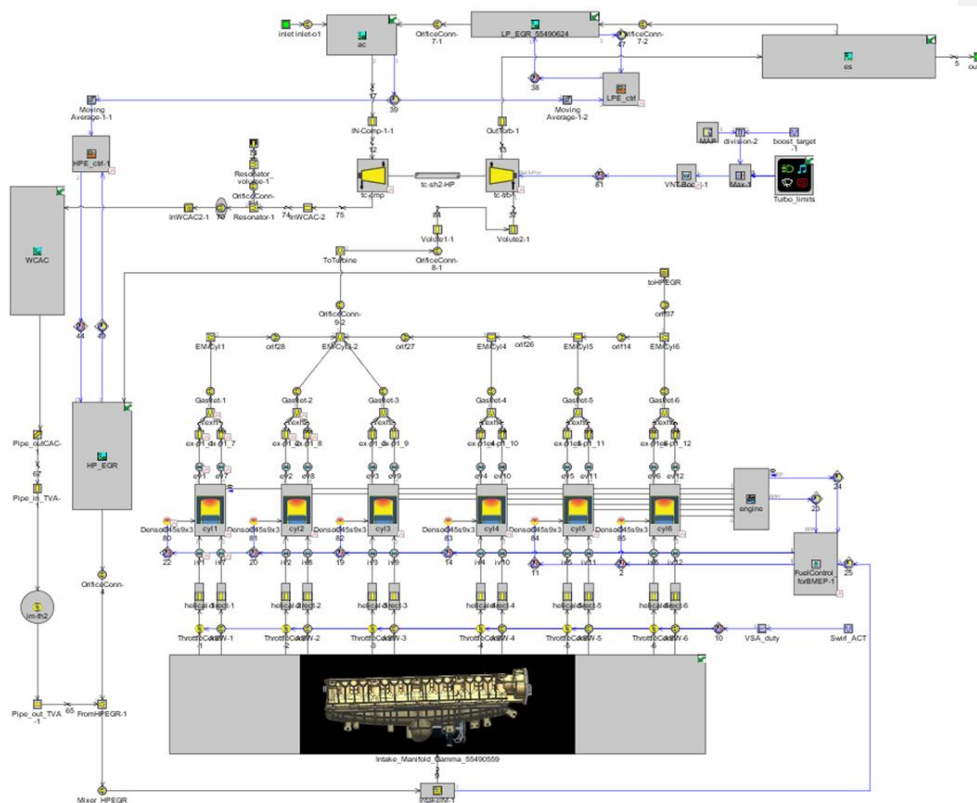


Figure 66. GT-Power® Model of the Duramax 3.0L Engine

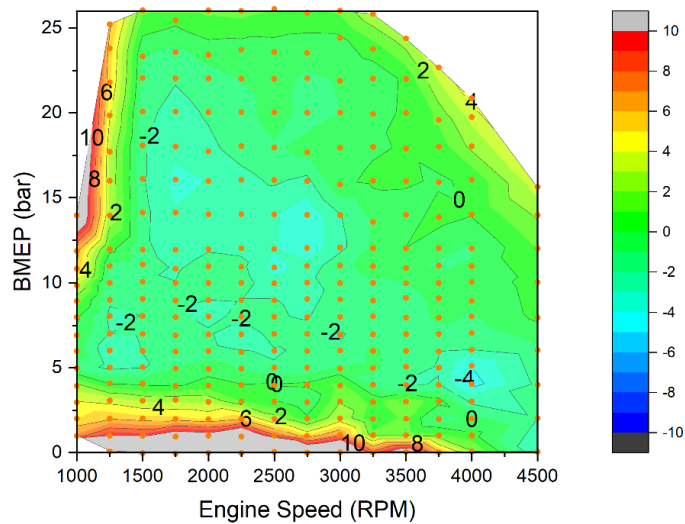


Figure 67. Fuel Flow Rate Percentage Difference at Various Operating Points. Yellow and Red Values Indicate That the Model Overpredicts Fuel Consumption, While Blue Areas Under-Predict Fuel Consumption. Green Areas Show Good Agreement Between Model and Test.

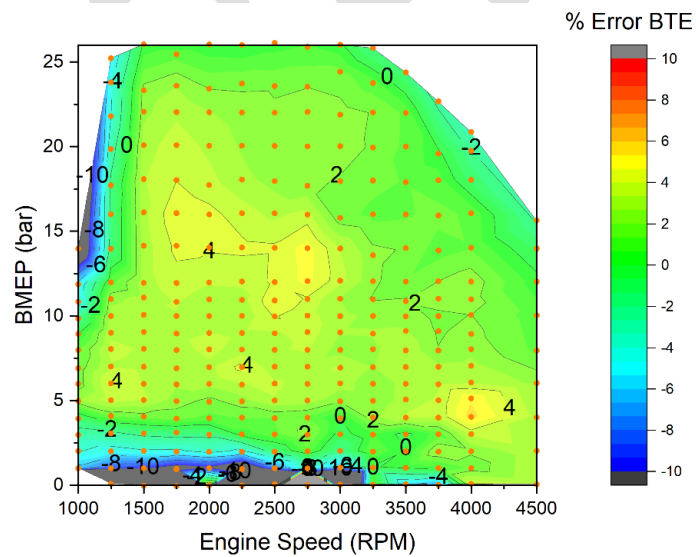


Figure 68. BTE / BSFC Percentage Difference between Measurement and Model

The EGR map applied to the model is presented in Figures 69 and 70. As noted previously, this engine uses cooled low-pressure loop and hot high-pressure loop EGR. As shown in Figure 70, high pressure EGR is active only at light loads, with peak EGR rate of 35% at low-speed and low-load conditions.

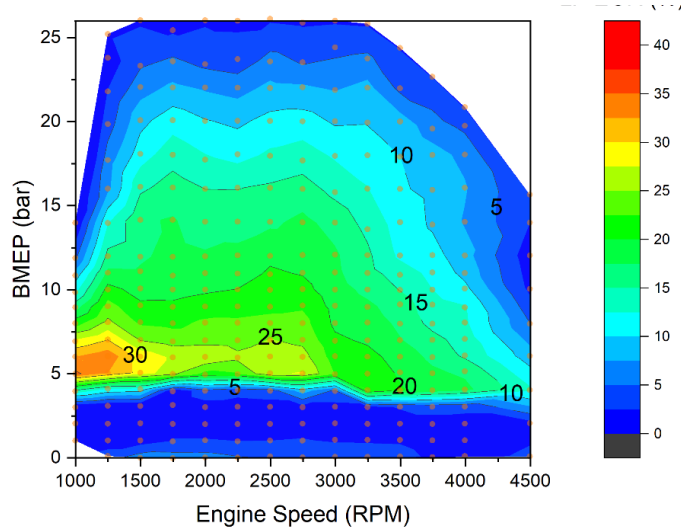


Figure 69. Low Pressure Loop EGR Map Used in the Engine Model

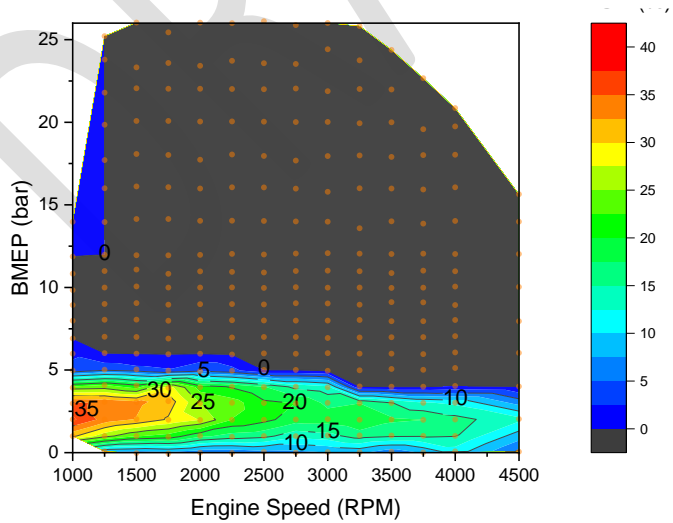


Figure 70. High Pressure Loop EGR Map Used in the Engine Model

Turbine and variable geometry compressor maps provided by GM were used in the model. The peak efficiency on this compressor map was just above 76 percent. Figure shows the experimentally determined motoring torque curve.

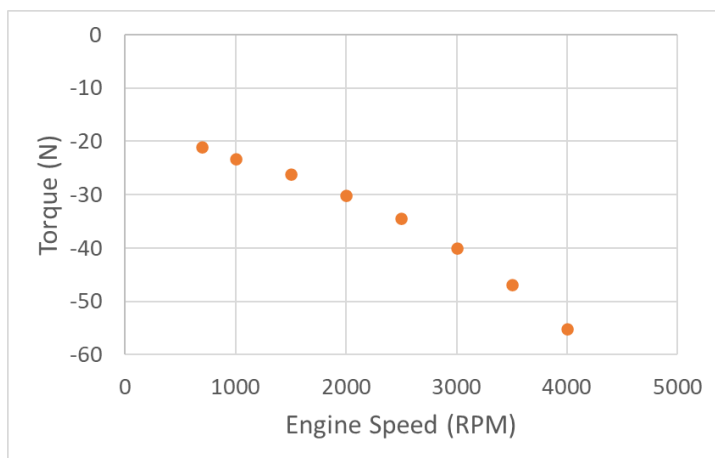


Figure 71. Duramax 3.0 Motoring / Minimum Torque Curve

The baseline validation shows good match to measured data and fulfills the objective of this study, which requires the engine model to be a good representation of current technology in a light duty truck diesel engine. Hardware limits like Peak Cylinder Pressure, compressor and turbine outlet temperatures rail pressure and turbo speeds limits supplied by the manufacturer are used to define modeling limits during various technology evaluation studies.

4.2 Reduced Friction

The impact of reduced mechanical friction and parasitic losses on fuel consumption was assessed. Multiple technologies like variable speed or variable displacement accessories, crank designs with reduced oil flow¹, reduced piston cooling^{2,3}, coatings and lubricant formulation can be applied to the engine to gain meaningful reductions in friction. For this study, a 20% friction reduction across speed-load map with respect to baseline was assumed, with reduced parasitic losses contributing to friction reduction at low speeds and light loads and a combination of reduced parasitic losses and lower sliding friction helping at high speed and load conditions. Figure shows the percent friction reduction versus engine speed and load used for 3.0-liter light duty engine analysis. Note that this reduction in FMEP is different from the ones applied to medium- and heavy-duty engines in the other sections of this report.

1 Bitsis, D. and Miwa, J., "Optimization of Heavy-Duty Diesel Engine Lubricant and Coolant Pumps for Parasitic Loss Reduction," SAE Technical Paper 2018-01-0980, 2018

2 Morris, A. and Bitsis, D., "Reduced Piston Oil Cooling for Improved Heavy-Duty Vehicle Fuel Economy," SAE Technical Paper 2021-01-0387, 2021

3 Denton, B., Smith, E., Miwa, J., and Bitsis, D., "Evaluation of Zero Oil Cooling for Improved BTE in a Compression Ignition Engine," SAE Technical Paper 2020-01-0284, 2020

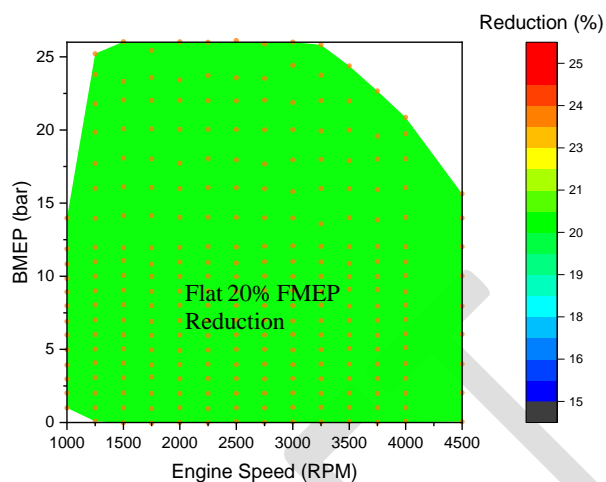


Figure 72. Friction Reduction Rationale Applied to Light-Duty Engine

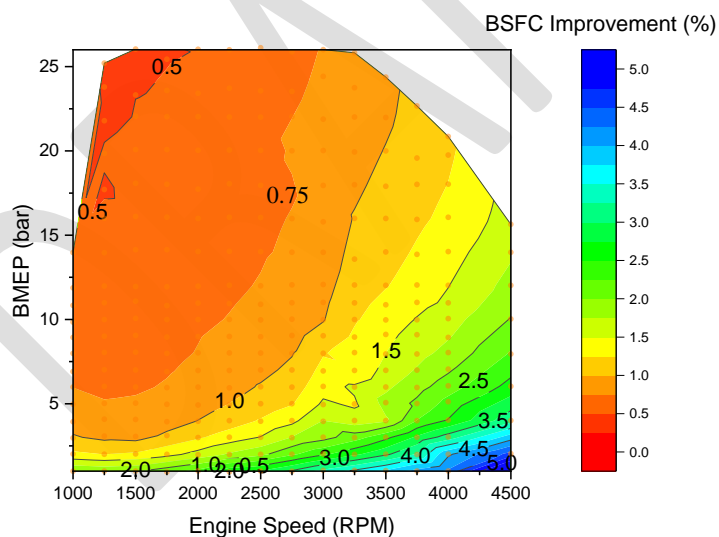


Figure 73. BSFC Percentage Improvement form Baseline with Reduced Friction

The impact of reduced friction on BSFC as compared to baseline is shown in Figure . Maximum benefits are seen at higher speeds and lighter loads due to reduction in hydrodynamic bearing friction and parasitic losses from oil and water pumps which increase as a function of speed. At higher engine speeds and loads, the sliding friction contribution increases and reducing that

contribution shows some benefit. At lower engine speeds and high loads, the baseline friction power as a percentage of brake power is already low, this drops the scope for BSFC improvement by reducing friction.

4.3 Cylinder Deactivation

The cylinder deactivation study was conducted using three-cylinder deactivation at light loads, and then switching to normal six-cylinder operation at higher loads. The approach was to operate three cylinders and gradually increase fueling at each speed, from no-load until either the engine was not able to meet brake mean effective pressure (BMEP) target or BSFC was higher than baseline. Minimum air fuel ratio was limited to 20:1. Figure shows the region where three-cylinder deactivation was beneficial, and the upper load threshold for three-cylinder deactivation generally increases with speed until 4000 rpm.

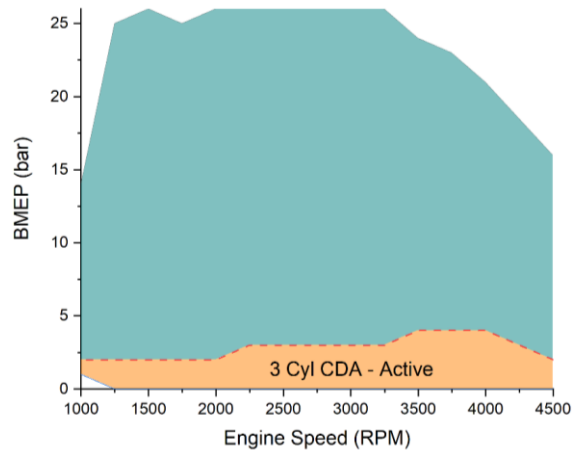


Figure 74. Cylinder Deactivation Boundary

The resulting light load fuel efficiency improvement is shown in Figure and a zoomed in fuel efficiency improvement plot is shown in Figure . At low speeds, the engine is limited to about 2.4 bar BMEP. As the speed increases beyond 2250 rpm, the engine can sustain 3 bar BMEP with three cylinders. The load that can be produced with three cylinders continuous to increase nearly to four bar in the 3500 - 4000 rpm range, before dropping again by 4500 rpm. The increase till 3500 rpm is primarily due to reduction in pumping losses at these speeds as shown in Figure .

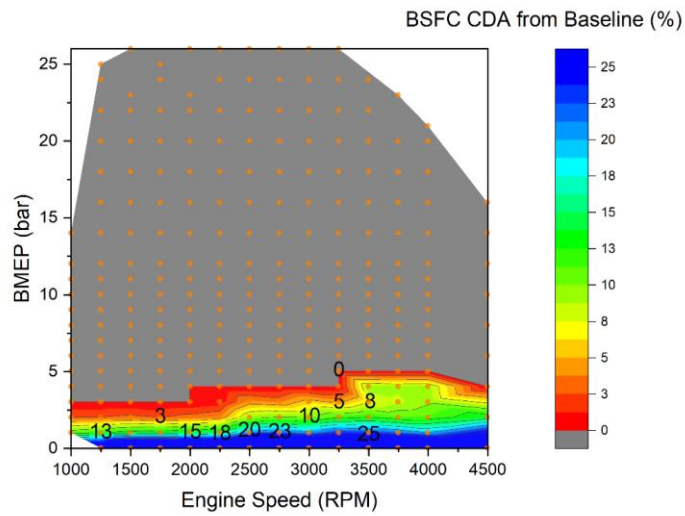


Figure 75. BSFC Percentage Fuel Consumption Reduction with Three Cylinder Deactivation

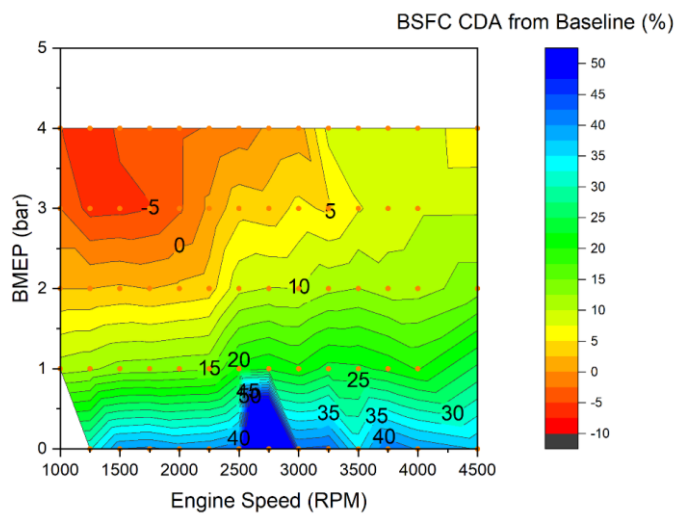


Figure 76. BSFC Percentage Fuel Consumption Reduction with Three Cylinder Deactivation (Zoomed in to Light Load)

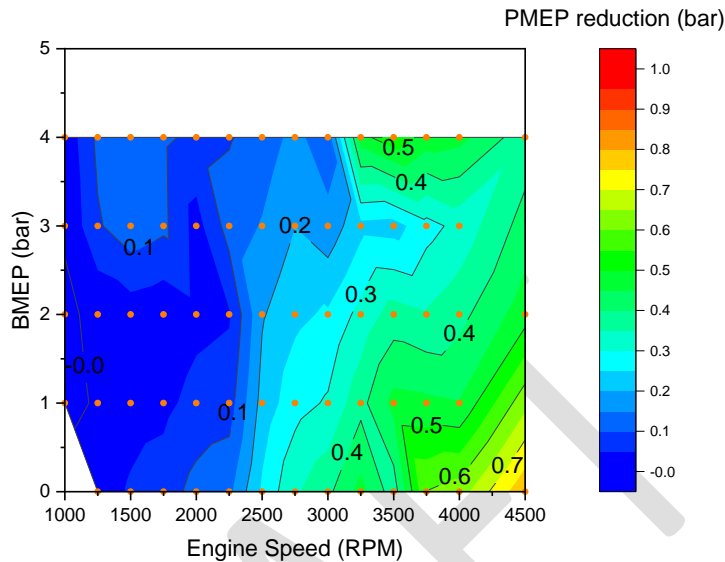


Figure 77. Reduction in Pumping Losses with Three Cylinder Deactivation

4.4 Series Sequential with High Efficiency Fixed Geometry Turbos

One way of increasing engine efficiency is to increase the turbocharger efficiency. Variable geometry turbos are generally less efficient on the turbine side than a fixed geometry turbo, so one route to consider is a move to fixed geometry turbos. However, for an engine like the 3.0 diesel which has a high BMEP and wide speed range, it is not possible to match a single fixed geometry unit that will give satisfactory results across the whole speed range. This leads to the idea of using two different size fixed geometry turbochargers, one sized to be most efficient at lower engines speeds, and the other sized for high engine speeds.

In the GT-Power model, the stock variable geometry turbocharger was replaced with a series sequential arrangement with two differently sized fixed geometry turbochargers in series. A smaller high pressure (HP) stage can be leveraged to achieve high torque at low engine speeds, while a larger unit is used in the low pressure (LP) stage for efficient exhaust energy extraction up near rated power. Compared to two-stage turbocharging, in a series sequential arrangement the smaller unit can be bypassed completely to avoid choking and over-speed of the smaller turbo, and the larger low-pressure stage can be regulated by a wastegate to control boost level, AFR, and peak cylinder pressure.

Model modifications for series sequence arrangement are presented in Figure . A passive compressor bypass valve and active turbine bypass valve are used to regulate flow through high pressure stage, while a wastegate is used to control the low-pressure stage turbo. A turbocharger matching exercise was carried out to identify optimum turbocharger sizes for the interacting high-pressure and low-pressure stages. For a good match, the HP stage should be able to provide

necessary air flow and boost pressure at low engine speeds. In the middle of the engine speed range, both stages are used to provide necessary boost, and the work share between HP and LP stage is critical for engine performance and low pumping work. In this medium speed range, the air system controls operate using bypass valves and wastegate to balance the contribution of the two turbos. At high engine speeds, the smaller high-pressure stage should be phased out to reduce pumping losses, and the LP stage should be adequately sized to meet air flow demand at peak power.

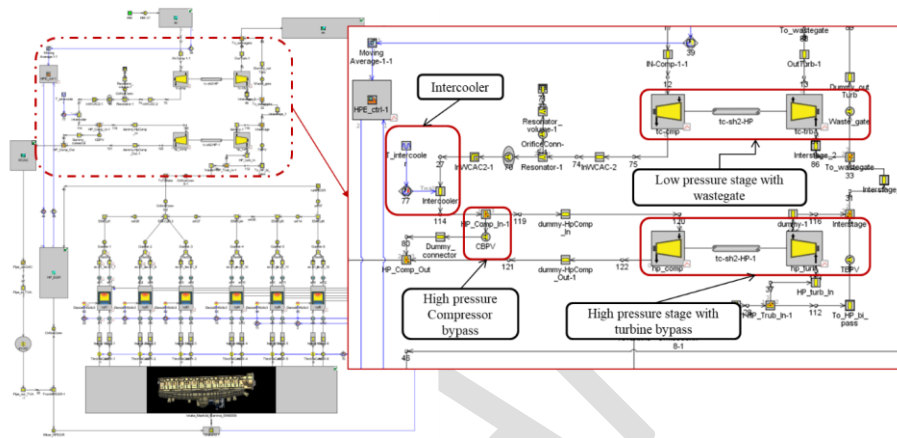


Figure 78. GT-Power® Model Modifications for Series Sequential Arrangement

The map for LP stage was generated by fixing the vane position on baseline variable geometry turbine and scaling the turbine maps solely for fuel efficiency. Maps for high pressure stage were provided by Garrett, and these maps were scaled to find a good match between high pressure and low-pressure stages. The model was further modified by adding an intercooler between low pressure and high-pressure compressor stages, and coolant temperature for the intercooler was assumed to be same as for the charge air cooler. At speeds above 1250rpm, the engine with a series sequential arrangement has higher backpressure than baseline due to the small high-pressure stage. To leverage the higher pre-turbine pressure, EGR routing was modified by eliminating low-pressure loop and moving to a cooled high-pressure loop EGR system. EGR cooler coolant temperature was assumed to be same as engine coolant temperature.

Once the turbocharger matching exercise was completed, bypass and wastegate valve positions were mapped across the speed and load points to identify optimal valve positions, while still operating within engine hardware limits like allowable peak cylinder pressure, exhaust temperatures, and turbocharger speed limits. Depending on the bypass and wastegate valve positions, the engine speed-load map can be divided into four distinct modes of operation as shown in Figure . At low load and low speed points, it was observed that operating as a naturally aspirated engine, with both turbine bypass and wastegate full open, allows for maximum fuel efficiency gains. At low speed and moderate to high loads, the engine uses both HP and LP stages to provide the required boost, and this mode of operation is represented as HP+LP in Figure . From 2250rpm

to 2750 rpm from moderate to high loads, the engine operates in Mixed mode where the HP stage is partially bypassed, and the work is slowly handed over to the LP turbo. At high speeds for optimum efficiency, it was beneficial to run the in LP only mode, where the HP stage is completely bypassed and a wastegate is used to regulate boost from the LP stage.

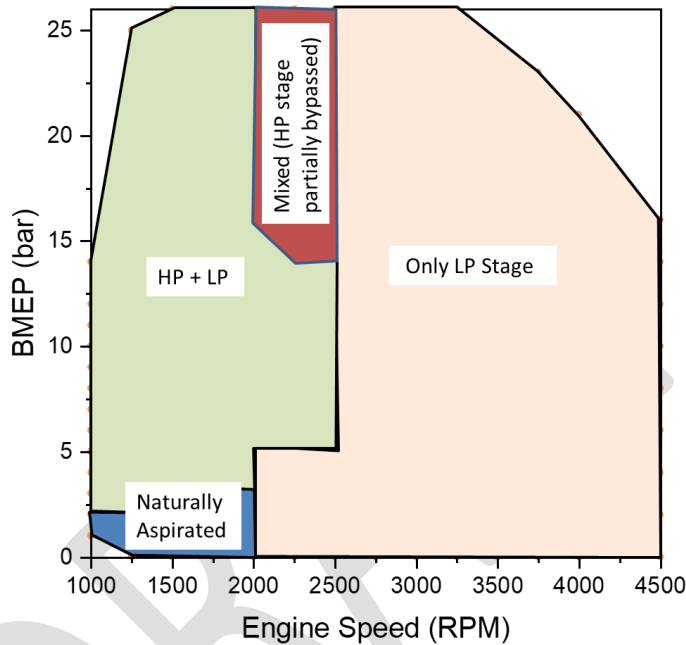


Figure 79. Valve Control Modes for Series Sequential Turbocharging

The resulting fuel efficiency improvement from series sequential turbochargers is presented in Figure . Considerable fuel efficiency benefit is seen across the map, especially below 2250 rpm, because the HP unit can utilize the limited exhaust energy that is available. Under the same conditions, the VGT must throttle its turbine to generate enough boost, which leads to higher backpressure and subsequently higher pumping losses. At mid to high speed (above 2750 rpm), the two-stage system is still advantageous, as it is operating in high efficiency region of LP unit. It must be noted that although the efficiency is better at higher speed and low load regions, the air-fuel ratio drops below 20:1. The simulated improvement at high speed and light load is not realistic, due to the low AFR, but this error was considered acceptable because this region is outside where the engine normally operates or will be simulated to operate. Efficiency with the VGT rivals the series sequential system when the two-stage system is switching between stages, in other words mixed-mode operation at high loads from 2250 rpm to 2750 rpm, and when VGT has higher

efficiency than the wastegated LP stage at 4500 rpm and moderate load. These results are in line with what was observed in literature^{4,5}.

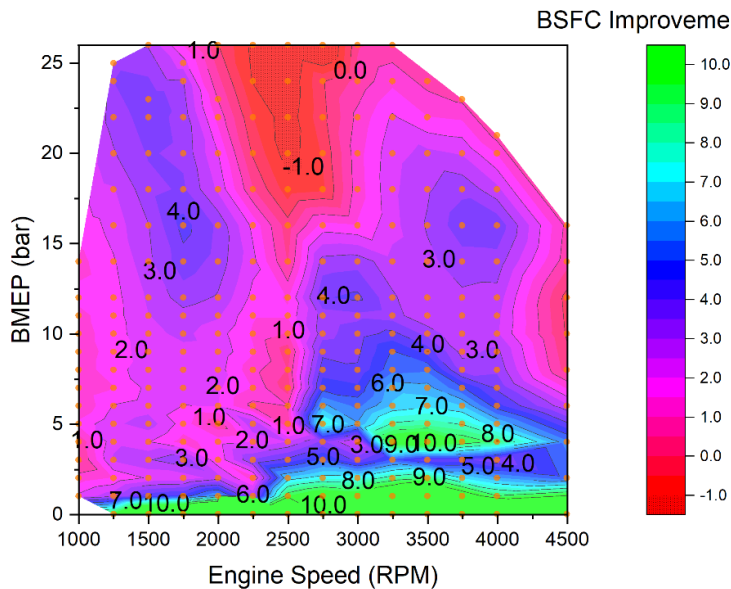


Figure 80. BSFC Percentage Improvement from Baseline with Series Sequential Turbos

4.6 High-Efficiency Fixed Geometry Turbocharger with e-Compressor

A single high-efficiency fixed geometry turbocharger with wastegate was evaluated in combination with an e-compressor for boost at low engine speeds. Fixed turbine and compressor maps were tuned to the engine's peak power and peak torque operation at high speeds, with the compressor efficiency map shown in Figure . For the chosen fixed geometry turbocharger option, peak cylinder pressure is maintained below the 180-bar base engine design limit without any wastegate operation. As seen in Figure , the fixed geometry turbocharger does not generate enough boost at low engine speeds.

⁴ Zhang, Q., Brace, C., Akehurst, S., Burke, R. et al., "Simulation Study of the Series Sequential Turbocharging for Engine Downsizing and Fuel Efficiency," SAE Technical Paper 2013-01-0935, 2013

⁵ Zhang, Q., C. Brace, S. Akehurst, R. Burke, G. Capon, L. Smith, S. Garrett, and K. Zhang. "Control Strategy Study of the Series Sequential Turbocharging Using 1-D Simulation." Proceedings of the ASME Turbo Expo 5 (2013): Proceedings of the ASME Turbo Expo, 2013, Vol.5. Web.

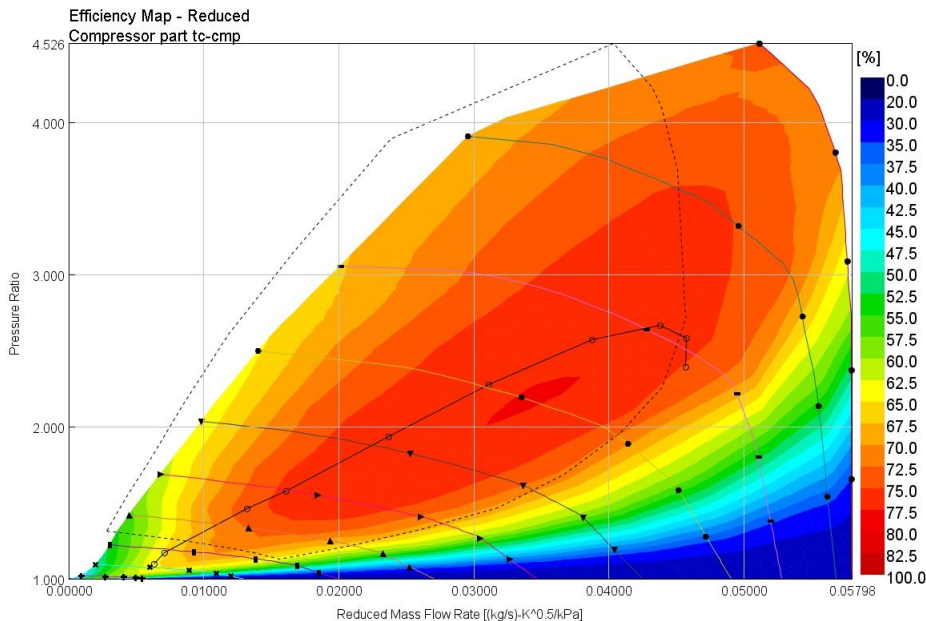


Figure 83. Fixed Geometry Turbo Compressor Efficiency Map

An e-Compressor is added to provide boost assist when required. Data for the e-Compressor was provided by Garrett. The e-Compressor was placed downstream of the charge air cooler, and e-compressor speed is controlled to maintain target air-fuel ratio. Intake air flow is diverted to a bypass path when boost assist is not required from the e-Compressor. For the analysis performed in this project, it is assumed that the energy required for e-Compressor is supplied from a 48V hybrid battery system that is recharged by another means. Therefore, the power requirement for the e-Compressor is not captured in the engine fueling calculations.

As can be seen in Figure 85, the maximum power demand from the e-Compressor is 6 kW at an operating condition of 1500 RPM and 22 bar BMEP. For speeds from 1000 RPM to 2,500 RPM and loads above 15 bar, the power demand is 4 kW or more. Power demand rapidly drops off at higher engine speed or at loads below 15 bar. A typical 48V mild hybrid system with a 1 or 2 kWh battery pack would be able to provide the required power.

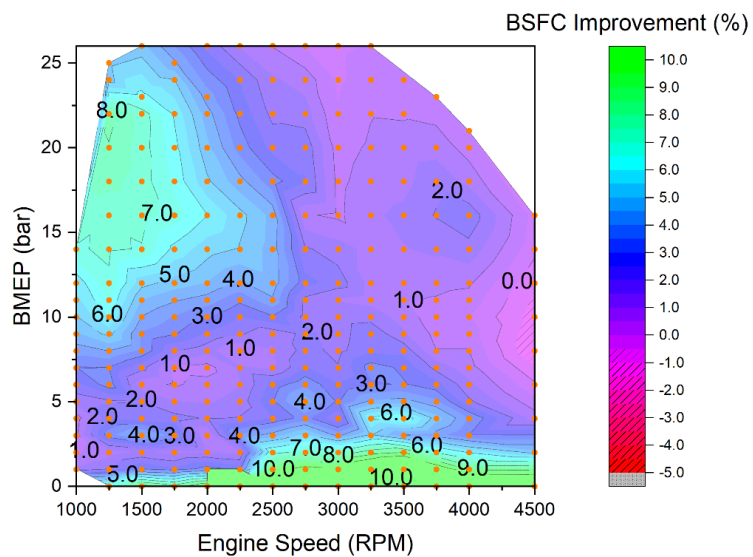


Figure 84. Percentage BSFC Improvement Compared to the Baseline, with Fixed Geometry Turbo and e-Compressor

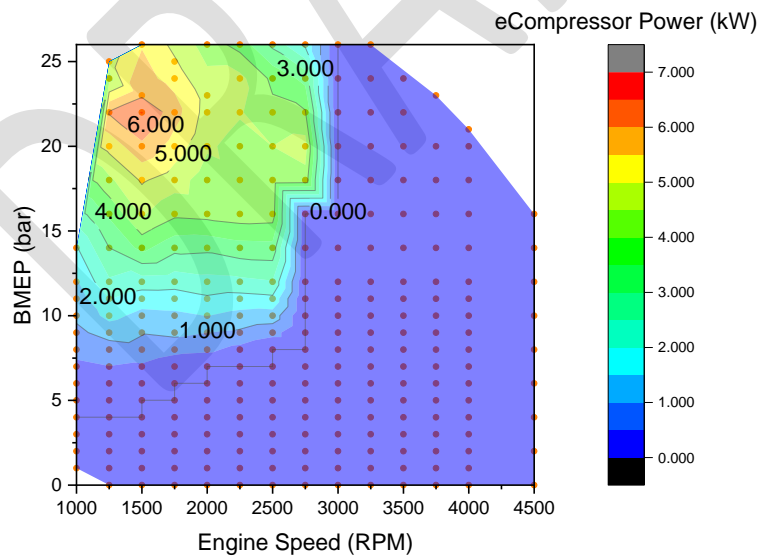


Figure 85. e-Compressor Power Consumption

The results from fixed geometry high efficiency turbocharger coupled with e-Compressor are shown in Figure , and e-Compressor power consumption across speed-load map is shown in Figure . This configuration gives good fuel efficiency benefits across the map without having the complex control issues involved in a series sequential approach. It is important to note that the benefits at low engine speed and moderate to high load points where the e-Compressor provides boost assist are inflated, since the e-Compressor power consumption is not accounted for in the fuel efficiency calculation. Figure 85 shows that the maximum E-Compressor power demand is about 6 kW at 1500 RPM and 22 bar BMEP. The compressor requires 4 kW or more over the range up to 2500 RPM any time load is above 15 bar. Outside of this area, power demand rapidly falls off, since the exhaust driven turbine can provide the required power. E-Compressor power demand is lower at full load than at 22bar BMEP because of reduced EGR flow at full load.

4.7 High-Efficiency Fixed Geometry Turbocharger with e-Compressor and Moderate Down Speeding

The high-efficiency fixed Geometry Turbocharger with e-Compressor analysis is repeated with moderate down speeding, with the hope of pushing the operating envelope to a more beneficial fuel efficiency zone. Power and torque curves for the baseline and downspeed engine variants are shown in Figure . For down-speed points, the peak power was maintained around 215 kW (same as baseline), but peak torque was increased from 620Nm to 715Nm and maximum speed at peak torque is reduced from 3300rpm to 2750rpm. Maximum BMEP for the downspeed version is limited to 30 bar, and it is assumed that the engine can sustain peak cylinder pressures around 200 bar, a 20 bar increase from 180 bar base engine limit. The maximum engine speed is reduced from 5000 rpm to 4500 rpm.

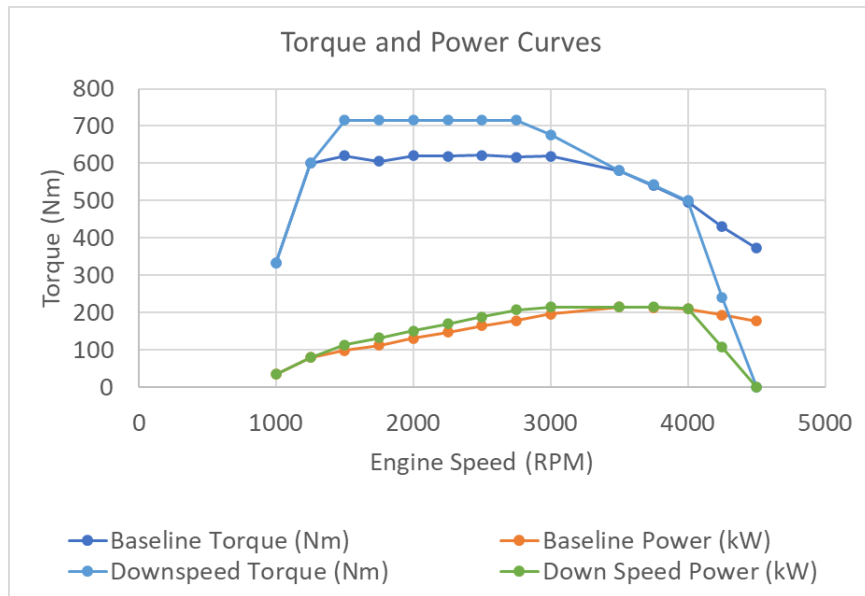


Figure 86. Baseline and Down-Speed Power and Torque Curves

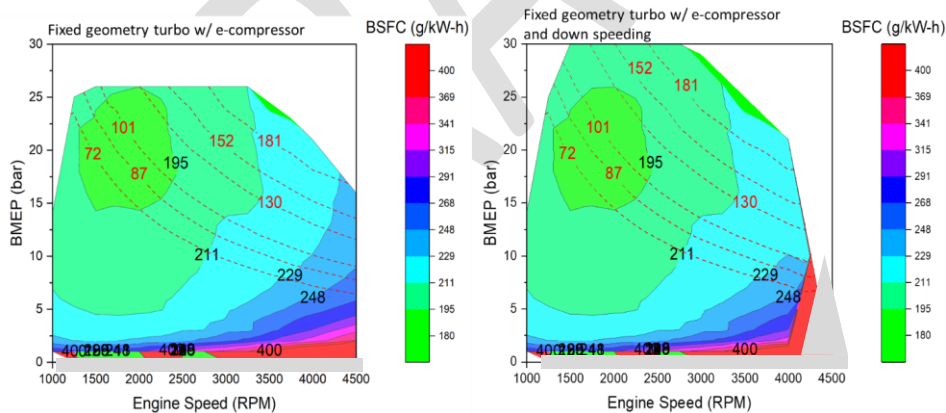


Figure 87. BSFC Comparison for Fixed Geometry Turbo w/e-Compressor, With and Without Down Speeding

The results from the analysis with down speeding are compared to the case without down speeding in Figure . Constant power curves in red are overlaid on BSFC map to show how down speeding helps to move engine operation at high power around 150kW to 180kW to a more beneficial BSFC island. Vehicle transmission and drive ratios also need to be modified to leverage the fuel

efficiency benefits from down speed map. Note that for light loads, the transmission shift schedule should not be changed, because there is still limited torque below 1500 RPM. However, at higher loads, the shift schedule can move shift points down to lower RPM. The axle ratio should also be adjusted to compensate for the lower speed range and higher torque of the downspeed engine. Figure shows e-compressor power consumption over the downspeed map. The e-compressor can provide additional boost requirements at high torque points. Figure 88 shows the power demand required by the e-compressor. The maximum peak cylinder pressure observed during this analysis was 190 bar.

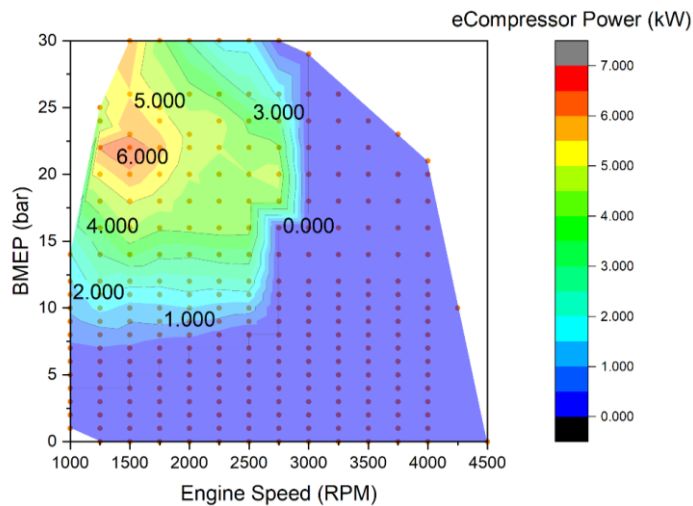


Figure 88. e-Compressor Power Consumption Over Down Speed Map

4.8 High-Efficiency Fixed Geometry Turbocharger with e-Compressor, Moderate Down Speeding and CDA

The final analysis added cylinder deactivation to Fixed Geometry Turbocharger Model with e-Compressor and down speeding. The same process was followed as on the previous CDA application, where three cylinders were deactivated at low load conditions. Starting from zero load, fueling was increased at each speed while maintaining an air-to-fuel ratio above 20. Figure shows the combined BSFC map with the e-Charger and moderate down speeding and utilizing CDA at low loads.

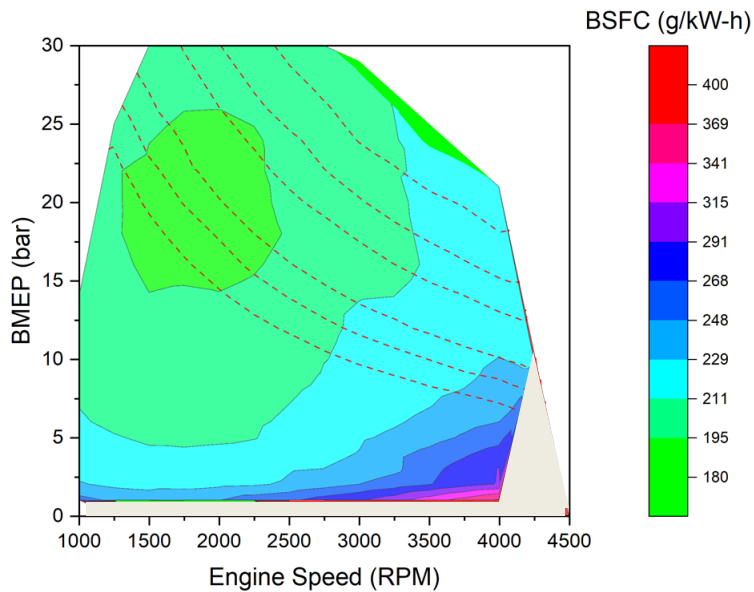


Figure 89. BSFC Map When Combining Fixed Geometry Turbocharger Model with e-Compressor and Down Speeding with CDA

The resulting BSFC benefit from CDA at light loads is shown in Figure Figure , at light loads below three bar good improvement in BSFC is observed across the speed range, while the e-Compressor power requirement remained same with or without CDA, as shown in Figure .

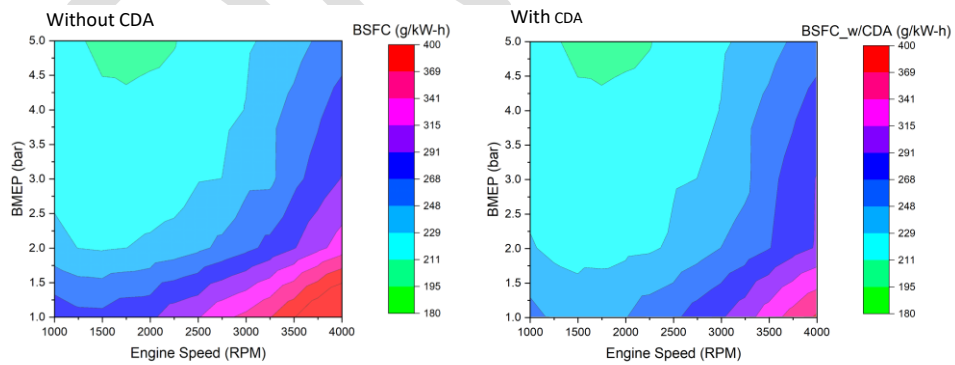


Figure 90. BSFC Comparison at Light loads for Down Speed Configuration with CDA Compared to Configuration without CDA

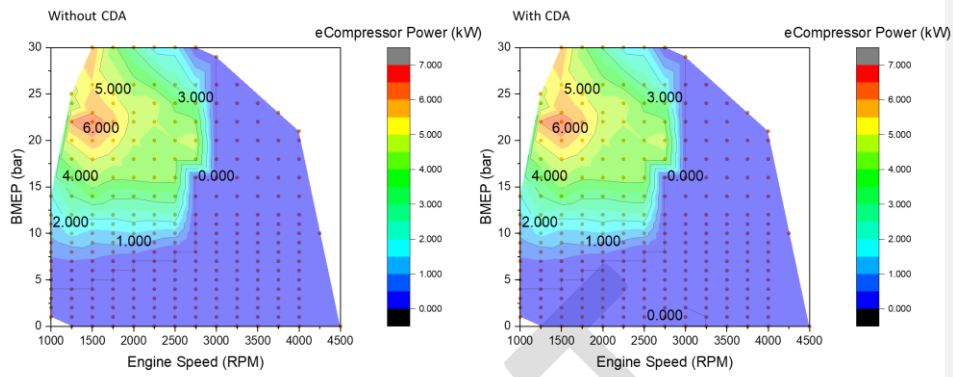


Figure 91. e-Compressor Power Consumption for Down Speed Configuration With CDA

5.0 FORD 7.3 LITER MEDIUM DUTY GASOLINE ENGINE

5.1 Baseline Engine Validation

A baseline model was provided by Ford for the 7.3L Godzilla engine in a Ricardo WAVE format. Gamma Technologies converted the WAVE model into a GT-Power model. The provided baseline model was only configured to simulate wide-open throttle operation with power enrichment. Ford also provided steady state experimental data to validate the model. The model used a Wiebe function for describing the combustion. The CA50 was set from the steady state data provided, and the burn duration (MFB 10-90) was set as an equation dependent on engine speed ranging from 20 to 25° CA. For the baseline model, the friction was directly input as FMEP for each speed-load point to match the steady state test data. An orifice was added in the exhaust stream and tuned to give the same backpressure as the catalysts, based on the test data. The heat transfer model was tuned last to match the BTE within +/- 5%. Figure 92 shows that most of the map met this criterion.

Above about 8.8 bar BMEP, the engine uses power enrichment, as shown in Figure 93. At high speed, additional enrichment is added for engine and catalyst thermal management. The best BTE for the baseline engine was right at 36% at 2000 rpm, 7 bar BMEP, as shown in Figure 94. Figure 95 shows the combustion phasing (CA50) for the baseline simulation results. There are two areas with high amounts of combustion phasing retard. The first is in the low-speed, high load region and the second is in the high-speed, high load region. Knock is time dependent, so the slow engine speeds have longer durations on a time basis, making knock more likely. Knock generally gets better at higher speeds because the time durations for the same crank angle delta are shorter. However, the airflow increase is restricted based on the orifice in the exhaust, increasing the backpressure and resulting residuals. The hot residuals appear to cause the engine to have a higher knock tendency at high loads.

If the hypothesis is correct that high speed backpressure causes increased residuals, and that these in turn create a high-speed knock issue, there is the possibility of improving high speed knock. A free-flowing, low-restriction exhaust system could reduce the tendency towards high-speed knock. Achieving lower exhaust restriction would require a larger, more expensive catalyst and a larger exhaust system. This would allow more advanced combustion phasing at high speed and load, which in turn would reduce fuel consumption at high speed and load. This potential fix for the high-speed knock issue becomes particularly important in the case of a hybrid system, where high speed knock limits the potential for making the engine more efficient by increasing compression ratio.

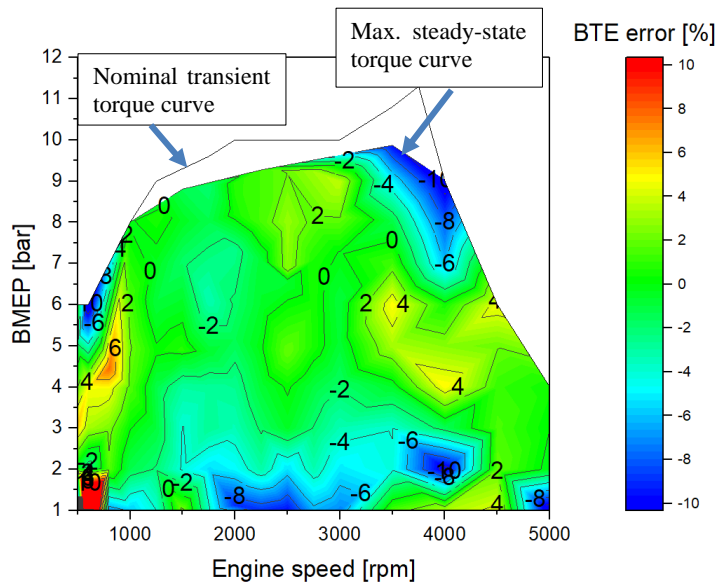


Figure 92. Difference Between Model and Test Data for BTE / BSFC. Green areas show good agreement, while blue areas show the model to under-predict fuel consumption, and yellow or red areas are where the model over-predicts fuel consumption.

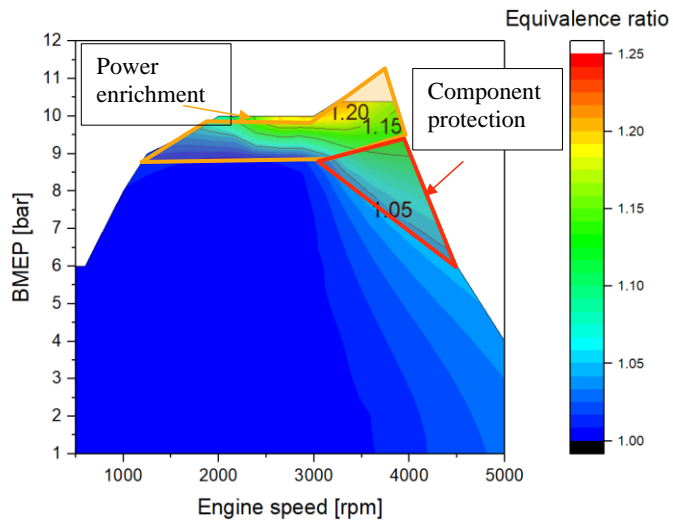


Figure 93. Equivalence Ratio of the Base Engine, Showing Power Enrichment and Component Protection

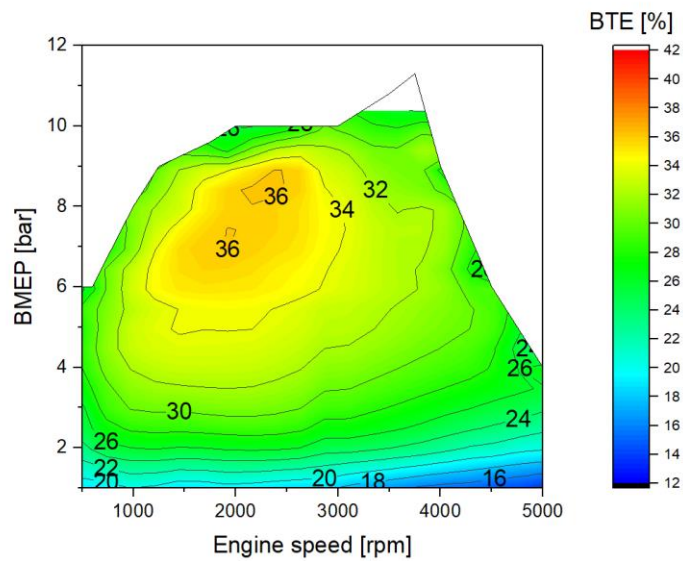


Figure 94. Ford 7.3 Baseline BTE, from GT Model

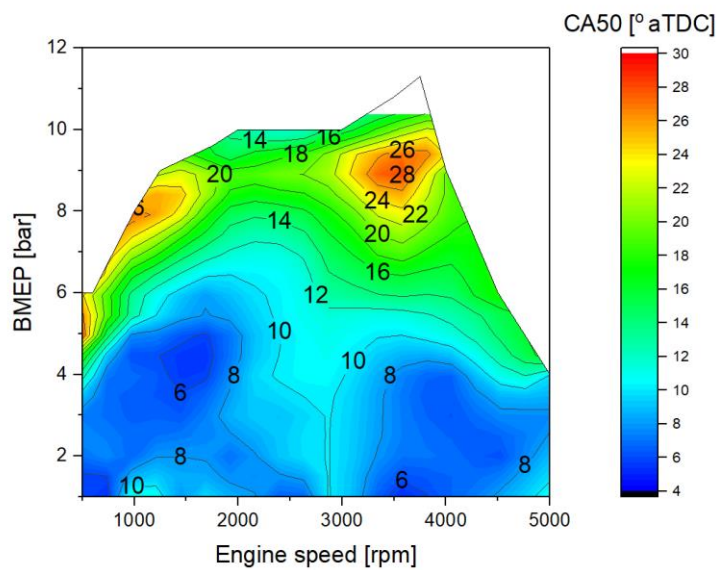


Figure 95. 7.3 V-8 Baseline CA50 Timing

5.2 Changes to Model to Predict Engine Technology Performance

The steady-state test data from Ford included enrichment for component protection at the higher loads. Under transient operation, the engine only uses enrichment to boost the maximum available torque. This can be seen in Figure 92, where the gap between the maximum transient torque curve (black line) and the maximum steady-state torque (top of the colored area) is filled by using enrichment.

Most engine ECU's have a timer that must expire before enrichment for component protection starts. The thermal inertia of an engine means that sustained high load operation is required to reach critical component temperatures, so brief periods of high load operation can be tolerated without enrichment. Maintaining stoichiometric operation also limits criteria emissions for test cycles that do not require sustained high load operation. For transient operating cycles, it is uncommon to see sustained runtime in the high-power regions that would result in enrichment. Comparing the engine's baseline steady-state data to models with varying technology packages could thus show an unrealistic benefit from eliminating enrichment. Data in the component protection region was kept stoichiometric for all provided fuel maps. Data including the power enrichment is part of all provided maps.

A knock model was developed in GT to predict the combustion at high loads if enrichment were not used. This model was also used to predict the combustion for each of the technology packages investigated. The knock model used was a GT-Power built in model called the Kinetics-Fit-Gasoline Knock.

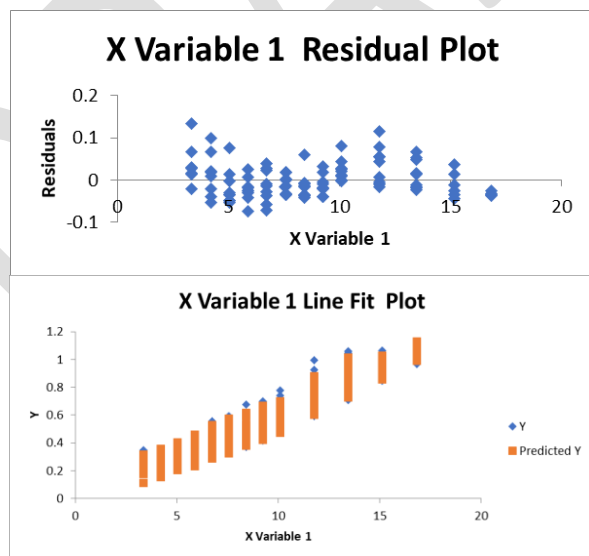


Figure 96. Friction Model Correlation

A friction model was also developed based on the baseline test data provided by Ford. FMEP was calculated from IMEP and brake torque. The baseline simulation directly input the FMEP for each operating condition. The Chen-Flynn Friction model is a correlation for friction based on engine speed and peak cylinder pressure. The peak cylinder pressure was not provided in the baseline dataset, so these values were selected from the corresponding simulation results. A regression of FMEP was built from the mean piston speed, mean piston speed squared and the peak cylinder pressure, as shown in Figure 96. The adjusted R^2 value was greater than 0.93 with a max residual of less than 0.2 bar. This friction model was then used for all additional technology packages to predict differences in FMEP based on changes to the peak cylinder pressure from dilute operation, turbocharging, or various other changes to combustion.

5.3 GDI with CR 10.5

The first technology change applied was a GDI system to replace the standard port injection used on the production 7.3 V-8. DI provides better volumetric efficiency, since only air is flowing through the ports. The injection timing can be optimized to provide a degree of charge cooling, which in turn provides a knock benefit. The baseline engine has a CR of 10.5. The GDI engine maintained the 10.5 CR while advancing the combustion phasing by about 5° CA at knock limited loads. The injection timing and fraction of fuel vaporized were tuned so the knock model predicted the 5° CA advance. This matches experimental data SwRI has from converting a PFI system to DI on an engine with a similar size bore. Note: The friction model did not add any losses for the higher power requirements of the DI fuel pump. It is typical that the efficiency will be slightly worse at low loads for the DI version compared to the PFI version.

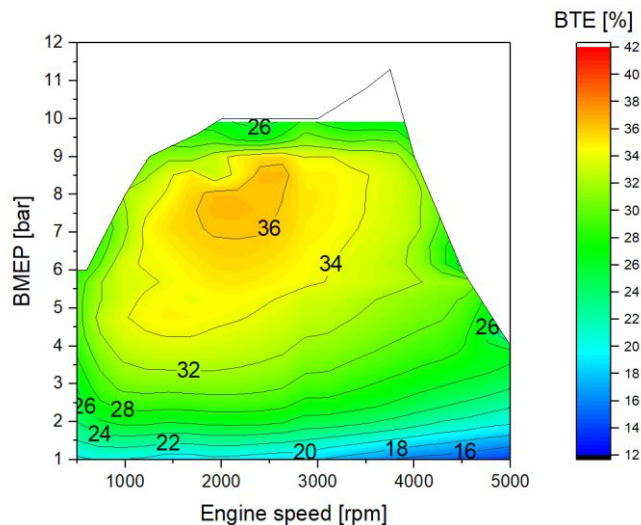


Figure 97. BTE Map for GDI with 10.5 CR

Figure 97 shows the BTE map for the engine with GDI and a 10.5 CR. The area with a BTE of 36% or more is larger than the baseline engine of Figure 94. Figure 98 shows the CA50 timing of

the engine with GDI and a 10.5 CR, and Figure 99 shows the percent BTE improvement provided by the DGI system. A one percent improvement in BTE is equal to a one percent reduction in fuel consumption. There is no change in efficiency over a wide area of the map, but at high loads where spark advance could be applied, the improvement is up to 4%.

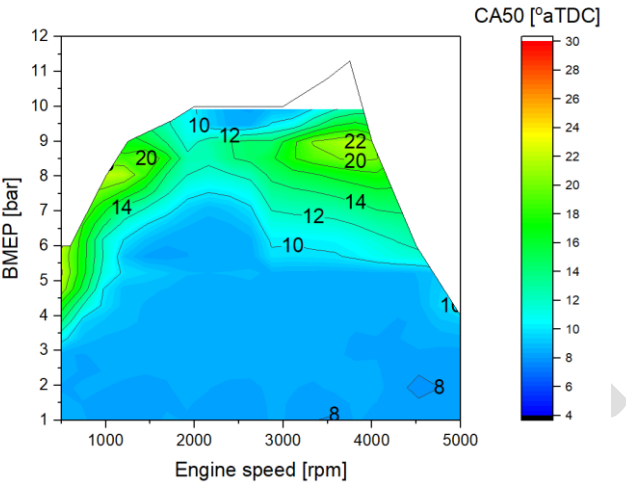


Figure 98. CA50 Timing for GDI with 10.5 CR

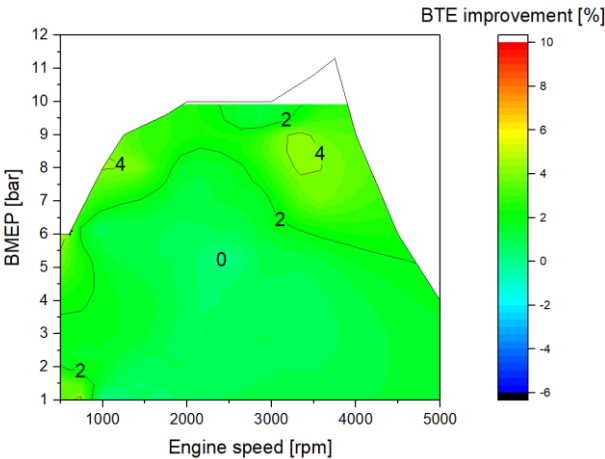


Figure 99. BTE Improvement of GDI with 10.5 CR Relative to Baseline

5.4 GDI with 11.5 CR

The GDI modeled was simulated again with a one-point CR increase from the baseline. With a CR of 11.5, the combustion phasing of the knock limited loads was retarded to nearly the same as the baseline simulation, to match the knock performance of the base engine. The higher CR provides additional efficiency, especially at medium and low loads.

Figure 100 shows the BTE map for the engine with GDI and 11.5 CR. Figure 101 shows the CA50 timing of the engine with GDI and 11.5 CR, which can be compared to the baseline engine CA50 map in Figure 95. Finally, Figure 102 shows the percent improvement in BTE that is provided by the GDI engine with 11.5 CR. Over a large portion of the map, improvements of 2% to 3% are shown.

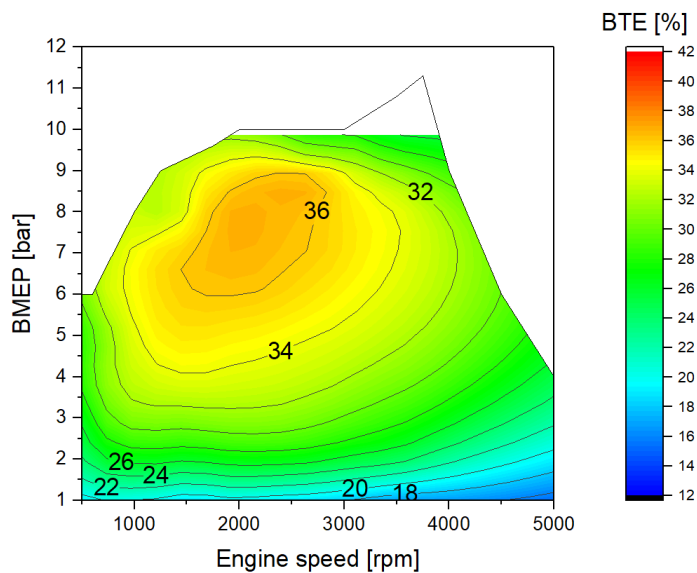


Figure 100. BTE Map for GDI with 11.5 CR

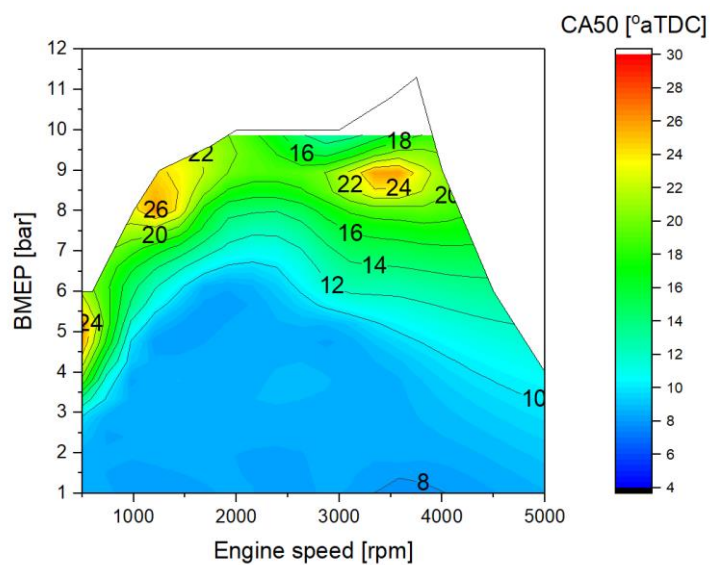


Figure 101. CA50 Timing for GDI with 11.5 CR

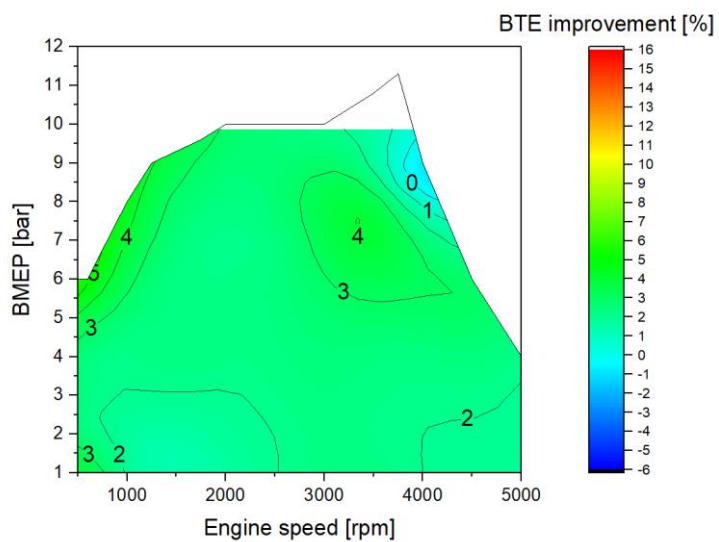


Figure 102. BTE Improvement of GDI with 11.5 CR Relative to Baseline PFI with CR 10.5

5.5 GDI with CR 12 and 4V Head

One way to improve knock resistance is to increase the charge air motion, which in turn shortens combustion duration. SwRI used experience comparing the charge motion available from 2-valve and 4-valve high tumble configurations to create a 4-valve version of the GT model. On this naturally aspirated engine, the higher charge motion allowed an additional 0.5 compression ratio points, to a total of 12:1.

Figure 103 shows the BTE map for the 4-valve engine with GDI and a 12.0 CR, and Figure 104 shows the CA50 map for this engine. Figure 105 shows the percent improvement in BTE, not against the baseline engine, but against the 2-valve engine with GDI and 11.5 CR. This comparison is done to show just the benefit of a high tumble 4-valve engine, compared to 2-valve. Figure 105 shows that the 4-valve engine is slightly less efficient at speeds below about 1500 RPM at loads up to 7 bar, but it offers benefits above 1500 RPM and at high loads across the entire speed range.

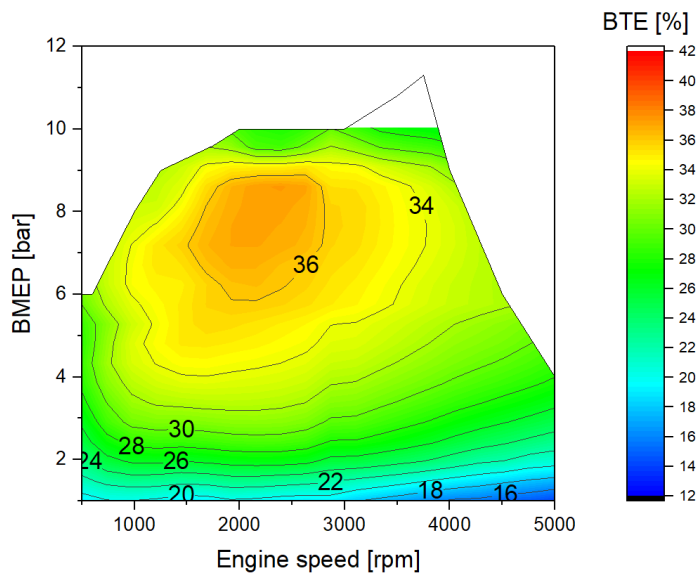


Figure 103. BTE Map for 4-Valve GDI with 12.0 CR

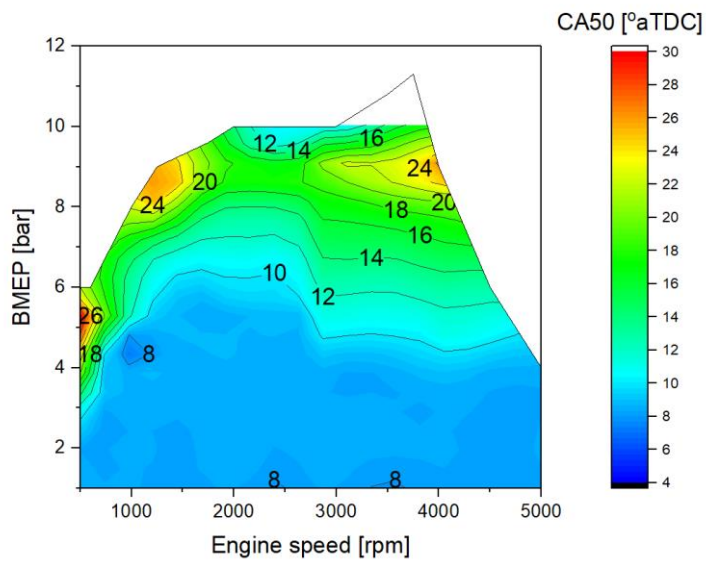


Figure 104. CA50 Timing for 4-valve GDI with 12.0 CR

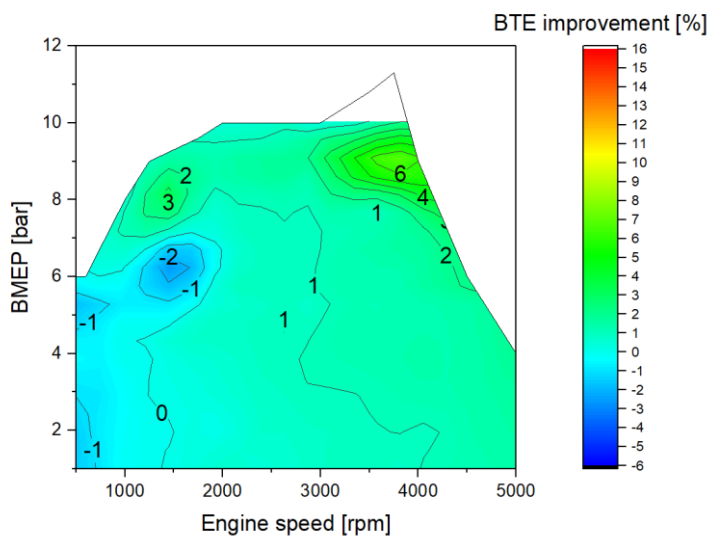


Figure 105. BTE Improvement of 4-valve GDI with 12.0 CR, Relative to GDI with 11.5 CR

5.6 Lean Burn NA Engine with GDI

Lean burn engines require a different aftertreatment approach. The normal 3-way catalyst used with stoichiometric engines loses its ability to reduce NO_x emissions when the engine runs lean. Therefore, lean burn engines use a combination of an oxidation catalyst (to eliminate CO and HC emissions) with an SCR aftertreatment for NO_x control, like what is used on diesel engines. The SCR system would require additional development to withstand the high exhaust temperatures that can occur at high load. These lean burn aftertreatment systems would be substantially more expensive than the traditional 3-way catalyst.

The lean model shows the largest BTE improvements over the baseline, with a peak BTE of 38% (Figure 106). Since the engine is naturally aspirated, the lean air-fuel ratio tapers back to stoichiometric and eventually power enrichment as the load increases, as shown in Figure 107. The model also used a correlation to adjust the burn durations for leaner mixtures. Both data taken at SwRI and data published by other organizations was used to determine this correlation. Without changes to the combustion system or piezo injectors for a stratified lean approach, the lean limit is around lambda 1.6, based on combustion stability. This was the maximum simulated AFR at low loads around 3 bar BMEP. The baseline engine used enrichment to reach higher torques than are available under steady state conditions. This is shown in Figure 92 near the transient torque curve, where lambda is less than 1. These enrichment points are the same as in the GDI 11.5 CR model, as shown in Figure 108.

The lean model improves efficiency by reducing throttling losses and improving the gamma. At very lean conditions, the combustion temperatures are lowered, and this can provide a combustion phasing benefit. SwRI has data to show that at lambda 1.4 the combustion phasing is nearly equal to stoichiometric. As the air-fuel ratio is controlled leaner than 1.4, the combustion phasing can be advanced. For the NA aspirated model, the loads where the conditions were that lean were not at knock limited loads. Figure 109 shows the percentage improvement in BTE (or percent reduction in fuel consumption), compared to the GDI engine with 11.5 CR. Double digit gains can be seen at low speed and light load, and a large portion of the map shows at least a 5% improvement. The improvement tapers to zero at high load.

Commented [A5]: Do you have reference for the other sources?

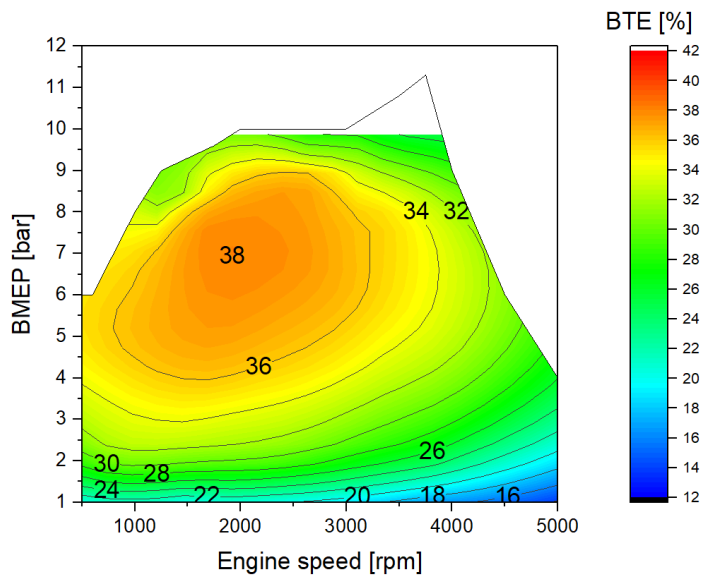


Figure 106. BTE Map for Lean Burn GDI with 11.5 CR

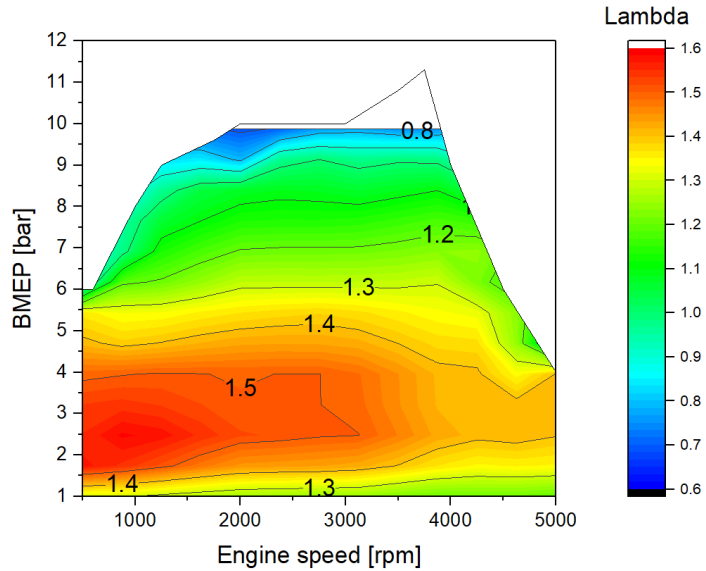


Figure 107. AFR Map for Lean Burn GDI with 11.5 CR

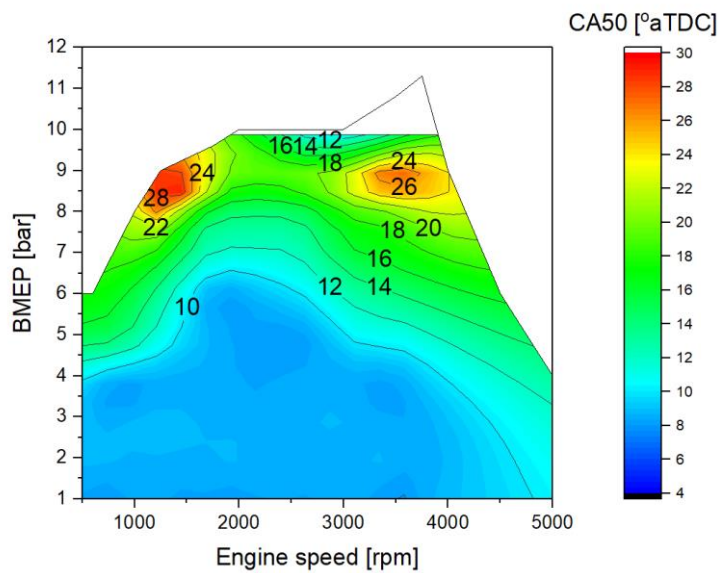


Figure 108. CA50 Map of Lean Burn GDI with 11.5 CR

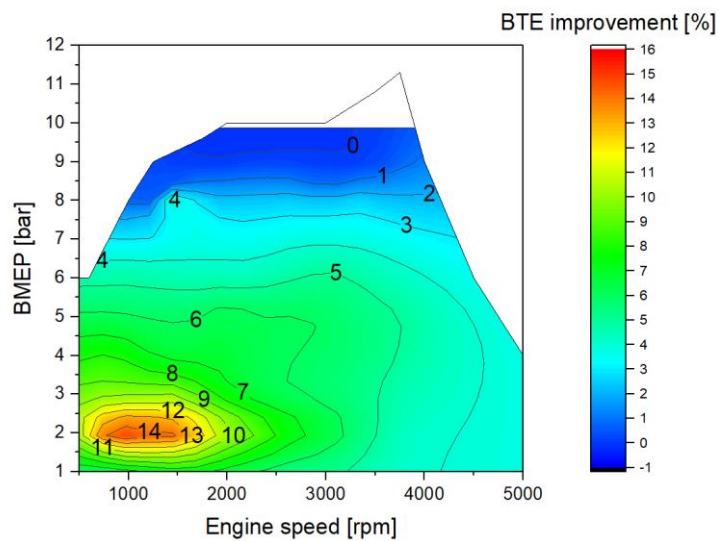


Figure 109. BTE Improvement of Lean Burn GDI with 11.5 CR, Relative to GDI 11.5 CR

5.7 NA GDI with Independent Cam Phasers (VVT)

The baseline engine has 2-valve heads, with a single block-mounted cam operating all valves on both heads. The cam phasing actuation starts in the parked position and retards the valve opening. Intake and exhaust events are phased together. An Atkinson cycle approach is used at part load, with a late intake valve closing for reduced pumping work. Because of these features, making a change to a dual cam will only provide marginal improvements in PMEP over the baseline.

For this technology option, the 2-valve heads are retained, but the phasing of intake and exhaust valves is done independently. This could be done with a single cam using a cam-in-cam arrangement, or more readily with two separate cams, one for intake and one for exhaust.

Figure 110 shows the BTE map for the engine with GDI, 11.5 CR, and independent cam phasers, and Figure 111 provides the CA50 map. Figure 112 shows the percent BTE improvement for the engine with GDI and 11.5 CR and independent cam phasers, compared to the GDI engine with 11.5 CR but the baseline single phaser. Large improvements can be found at light load, but by about 4 bar BMEP, the improvement is generally 1% or less.

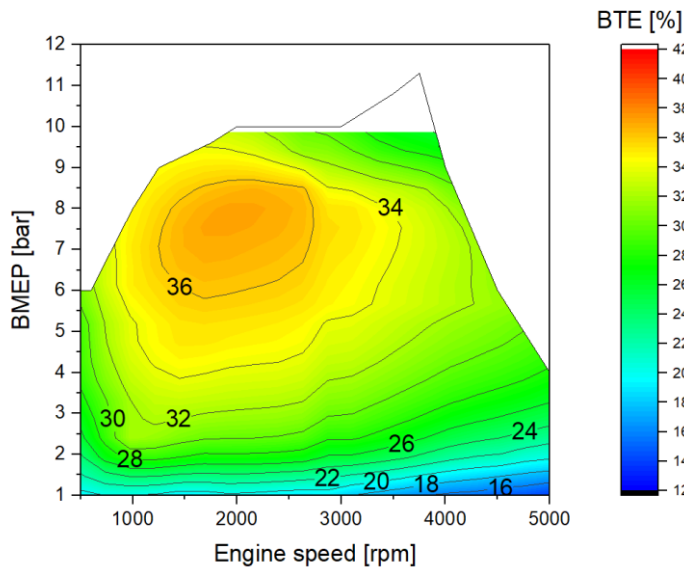


Figure 110. BTE Map for GDI with 11.5 CR and Independent Cam Phasers

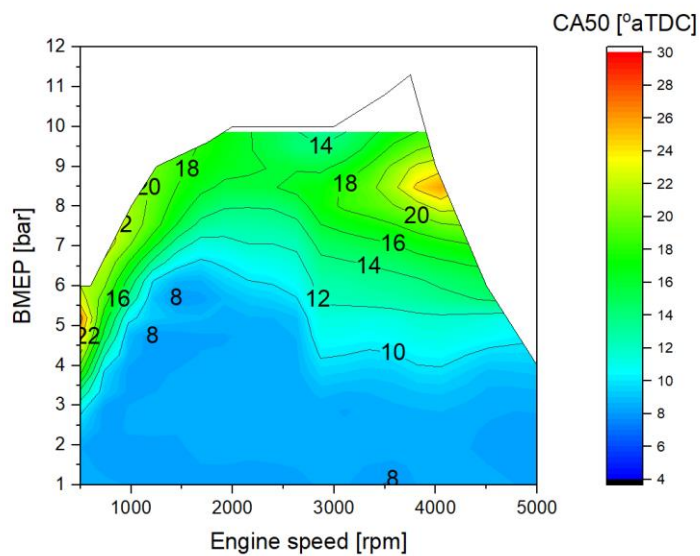


Figure 111. CA50 Map of GDI with 11.5 CR and Independent Cam Phasers

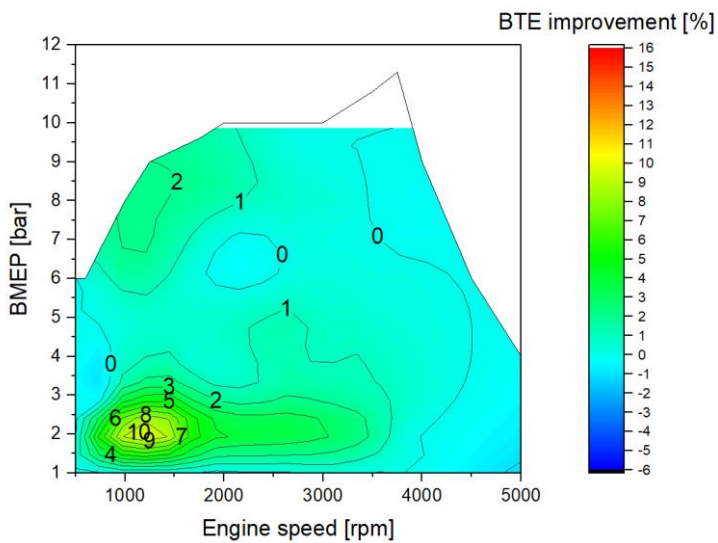


Figure 112. BTE Improvement of GDI with 11.5 CR and Independent Cam Phasers, Relative to GDI with 11.5 CR

5.8 NA GDI with LPL EGR

A naturally aspirated low-pressure loop EGR configuration is similar in concept to the NA lean configuration. At high loads the engine is air limited, so the EGR rates taper off to zero at full load, as shown in Figure 114. The resulting BTE map, shown in Figure 113, has a large area of 36% or higher BTE. Along the torque curve, the engine still needs to use enrichment just as the baseline engine did. Because the engine performance along the torque curve is the same as the baseline engine there was no possibility to increase the CR higher beyond what could be gained from the DI injection. The CR was therefore maintained at 11.5:1 for the LPL EGR simulations.

In the mid load range, the engine was simulated with up to 20% EGR. One of the benefits of adding EGR to an engine is that the knock mitigation that normally allows better combustion phasing. The combustion phasing was a few degrees advanced in the 6 to 8 bar BMEP region, to take advantage of the knock mitigation benefits of LPL EGR. The MBT line was pushed slightly higher in the load range, as shown in Figure 115. As the EGR rates are tapered, the combustion phasing differences are also reduced. At lighter loads, the addition of EGR reduces the pumping loss because of the higher trapped mass in-cylinder. At idle and very low load, the EGR was removed to prevent misfire. A typical calibration will start the flow of EGR above a certain manifold pressure. Below that pressure, the combustion stability is too poor while running with EGR.

Figure 116 shows the percentage BTE improvement or fuel consumption reduction provided by LPL EGR, compared to the GDI engine with 11.5 CR.

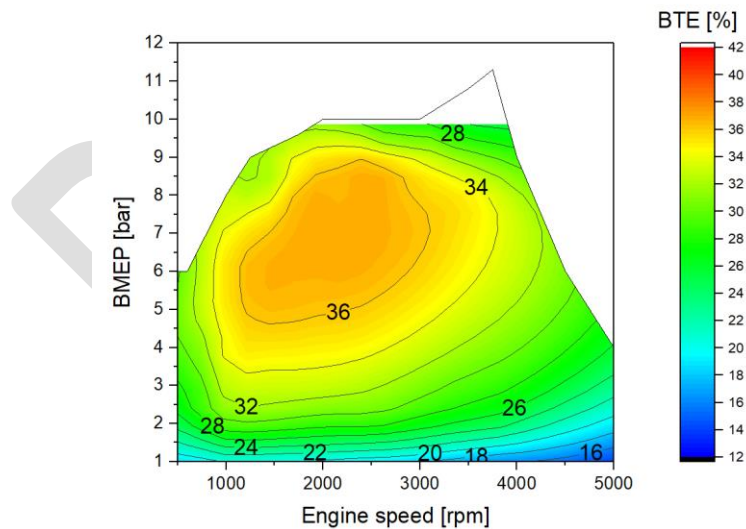


Figure 113. BTE Map for GDI with 11.5 CR and LPL EGR

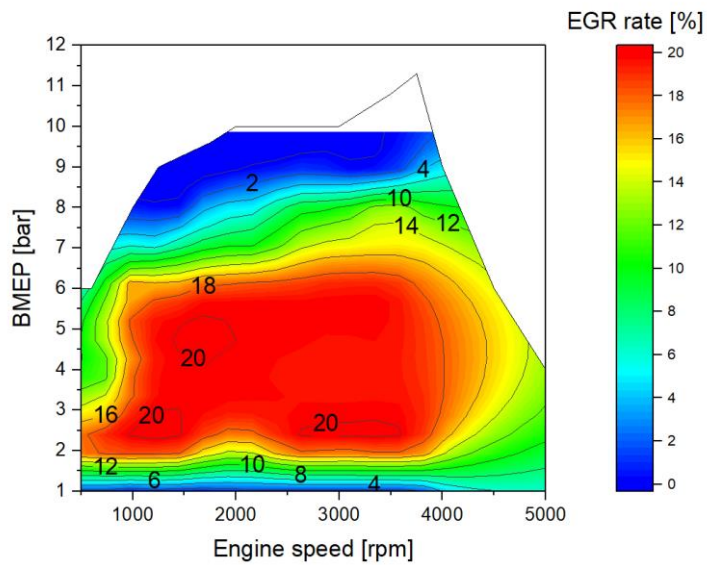


Figure 114. EGR Rate Map for GDI with 11.5 CR and LPL EGR

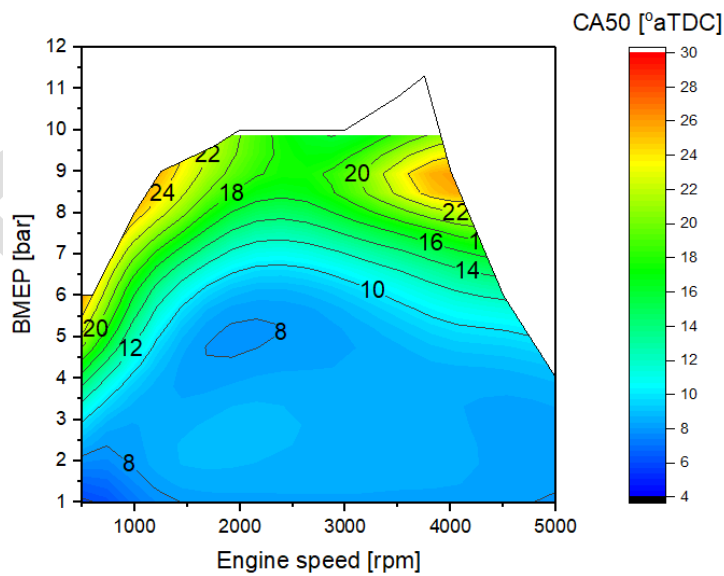


Figure 115. CA50 Map for GDI with 11.5 CR and LPL EGR

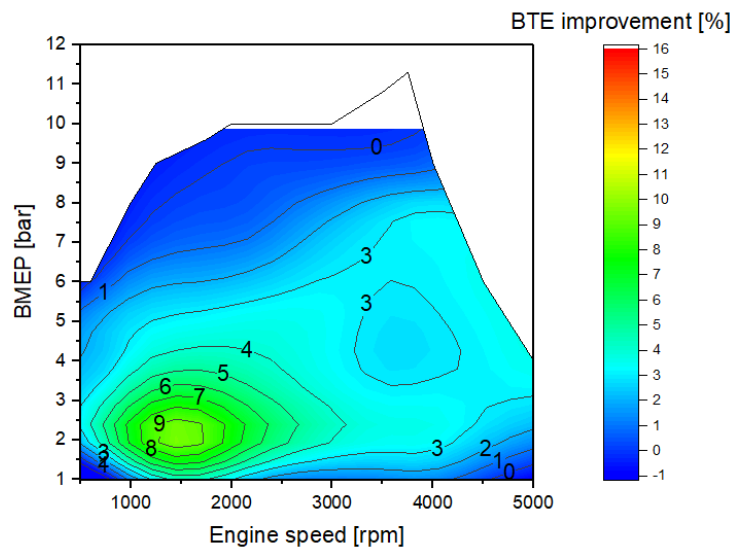


Figure 116. BTE Improvement of GDI with 11.5 CR and LPL EGR, Relative to GDI 11.5 CR

5.9 Technology Combo: NA GDI with LPL EGR and 10% Lower Friction

A friction reduction was to be applied to the NA engine configuration with GDI, 11.5 CR, and LPL EGR. The coefficients for the Chen-Flynn friction model were recalculated, targeting a 10% reduction. Because the engine has rather low FMEP to start with, a 10% FMEP reduction seems like a reasonable expectation for the benefit that could be obtained with additional friction reduction features. The modified friction model was used to re-run the LPL EGR technology simulation. At higher loads, the lower friction loss enables the engine to operate at a lower IMEP for the same BMEP, providing some additional combustion phasing benefit compared to the LPL EGR model, as shown in Figure 118.

Figure 117 shows the resulting BTE map for the technology combination. Figure 119 shows the resulting percent improvement in BTE, compared to the original PFI baseline engine. Fairly substantial improvements can be seen across most of the map. Figure 120 shows the incremental BTE benefits of friction reduction. At high loads the lower friction resulted in a slightly lower manifold pressure and therefore extended the area of the map using EGR before it is fully tapered off at full load. The additional EGR provides a combustion phasing benefit and provides a larger BTE improvement at medium load than over the rest of the map.

Figures 121, 122, and 123 show the FMEP maps for the following configurations: baseline engine, GDI engine with 11.5 CR and LPL EGR, and finally, the GDI engine with 11.5 CR, LPL EGR, and FMEP reduction of 10%.

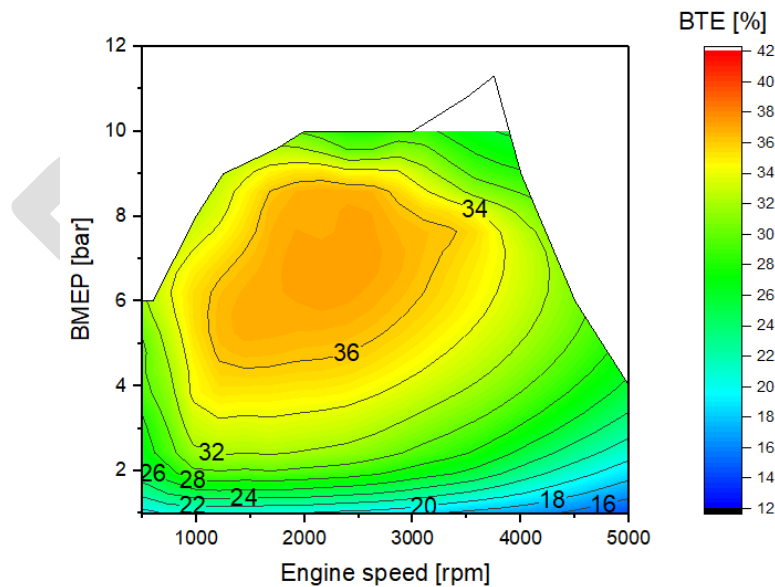


Figure 117. BTE Map for GDI with 11.5 CR, LPL EGR, and FMEP Reduction

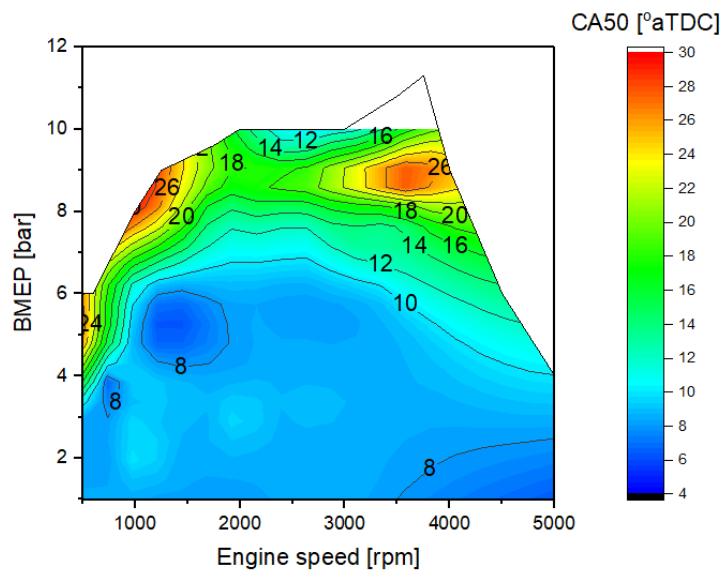


Figure 118. CA50 Map for GDI with 11.5 CR, LPL EGR, and FMEP Reduction

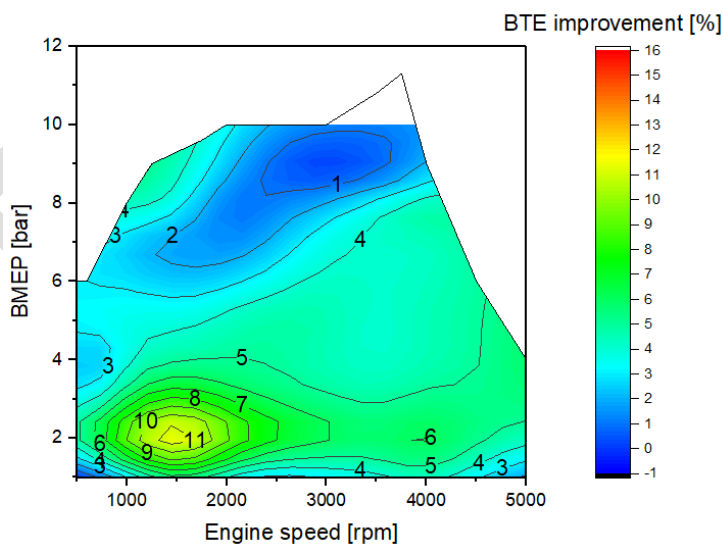


Figure 119. Change in BSFC of for GDI with 11.5 CR, LPL EGR, and FMEP Reduction, Relative to Baseline

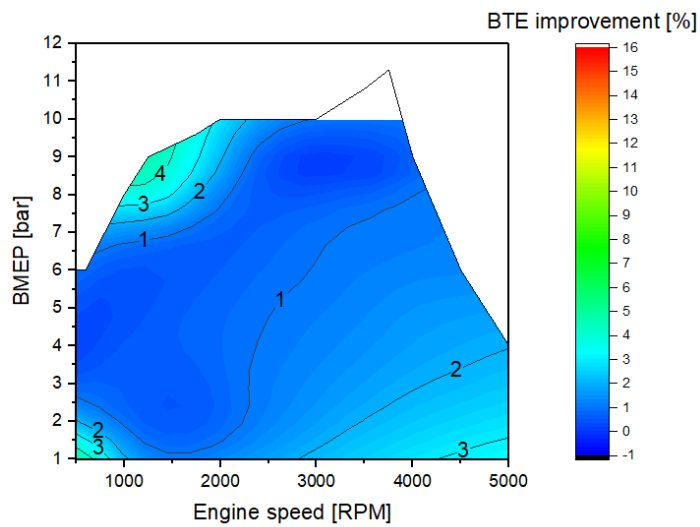


Figure 120. BTE Improvement for GDI with 11.5 CR, LPL EGR, and FMEP Reduction, Relative to the Same Engine without FMEP Reduction, Showing the Incremental Benefit of Friction Reduction

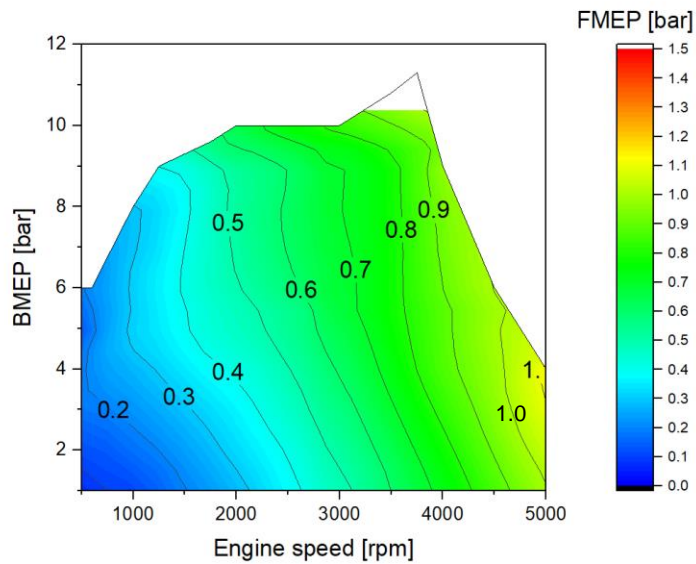


Figure 121. FMEP Map for the Baseline Engine

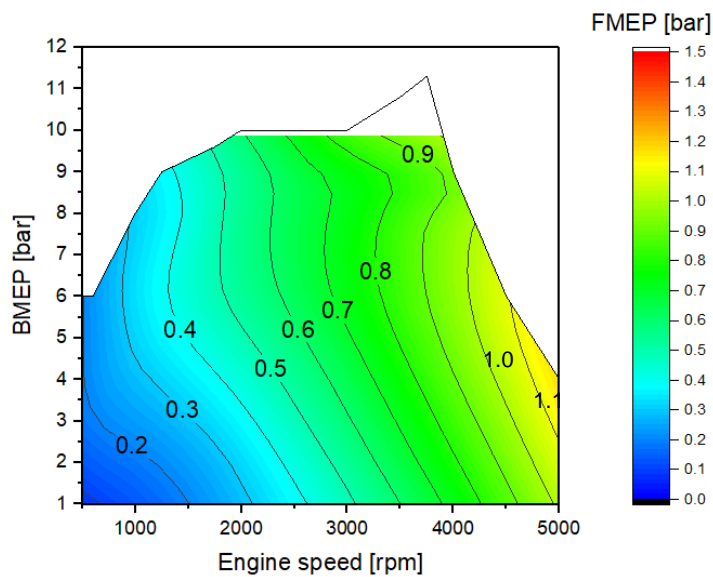


Figure 122. FMEP Map for GDI with 11.5 CR and LPL EGR

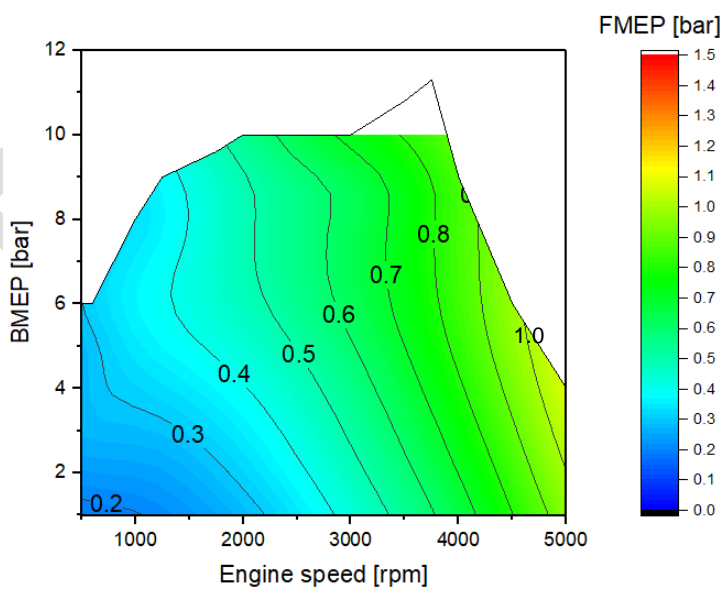


Figure 123. FMEP Map for GDI with 11.5 CR, LPL EGR, and Reduced FMEP

5.10 NA GDI with Higher CR for Hybrid Applications

As hybrid vehicles are gaining market share, more research is being performed on what can be done to improve the engine efficiency when some of the demands on the engine change, because the electric motor can supplement some of the power demand. Figure 124 shows a few torque curves that are lowered by the amount of torque than can be supplied by the given motor power. These are theoretical curves which assume the batteries have enough charge to supply the full e-motor power.

It is SwRI's experience that it will always be possible to identify an aggressive drive cycle where battery will be fully depleted. The most conservative approach is then to calibrate the engine to still be able to meet the original torque curve, so no vehicle performance would be lost under any conditions. An example of a drive cycle where the battery could be depleted would be pulling a heavy trailer up a long grade. More aggressive hybrid engine calibration approaches would weigh the efficiency higher but would require vehicle power derates when the battery SOC gets too low. Higher engine efficiency can be achieved if vehicle performance is sacrificed under certain unusual operating conditions.

Typically, the compression ratio of an engine is limited by the knock performance in the low speed, high torque region. It is possible (for a hybrid configuration) to reduce the engine torque requirements at low speeds but still meet the same peak torque input to the transmission. At low engine speed, a relatively small amount of e-motor power is required to make up for an engine torque derate. This can be accomplished by delaying intake valve closing at low engine speeds. This would allow an increase in CR compared to a conventional ICE only vehicle. Unfortunately, the dataset provided by Ford showed a strong knock response up near the rated speed. This is shown by the high CA50's near 9 bar, and 3750 rpm in Figure 95. The retarded combustion phasing is caused by the increased backpressure and residuals as the engine speed increases, which in turn causes a higher propensity to knock. This leads to the conclusion that even though the CR might be increased for the low-speed region, the high-speed region becomes a second limiting factor.

The combustion phasing for the baseline engine is already retarded at high BMEP, so the conservative hybrid engine would maintain the GDI engine CR with 11.5:1. Fuel maps for GDI versions with a CR of 12.5 and 13.5:1 have been provided for additional investigation. Argonne can use these maps to determine the battery capacity and motor requirements that would be suitable for these configurations. The torque curve for these maps have been trimmed compared to the baseline engine to prevent knock and excessive combustion timing retard. A limiting factor in combustion retard is temperature. As the CA50 is retarded, engine and exhaust temperatures increase, so running an extended time with a strong retard will result in excessive temperatures and a shorter system life. SwRI chose to limit CA50 to no more than 32 degrees after TDC in this study.

To help explore what benefits could be obtained with different e-motor sizes, Figure 125 shows the base engine torque curve in dark blue, along with three potential derates of 25, 75, and 100 kW. Note that there is no need to use all the available derate at all speeds, since even for the 25 kW derate, there are portions of the speed range where the engine can provide some power at a higher CR.

Commented [A6]: A torque derate does not need to be driven by delayed intake valve closing – that's just one option. A change in throttle position is another option, and early intake valve closing is a third option. The idea here is that a hybrid would allow you to avoid knock, which is most prevalent at low speed and high load, by reducing the engine torque contribution and increasing the e-motor contribution. By taking low speed, high load operation off the table, you can then do things to make the engine more efficient at other conditions, such as increase compression ratio. I recommend deleting this added line.

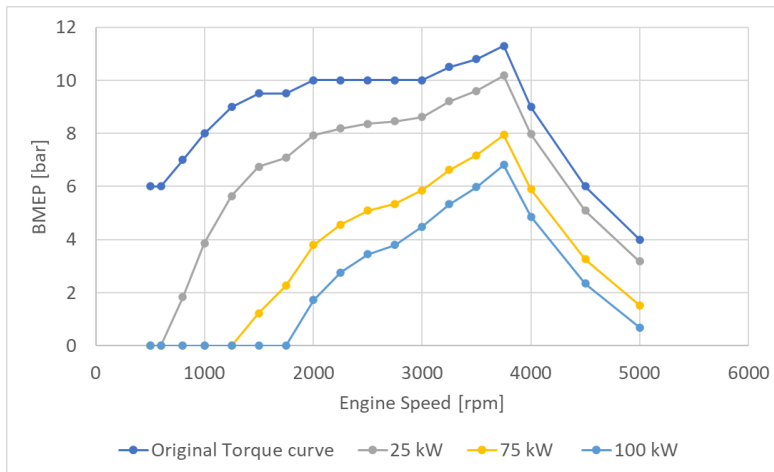


Figure 124. Engine Derate Options for 25, 75, and 100 kW e-motors

In Figure 125, the CR 12.5 and 13.5:1 torque curves are trimmed to their stoichiometric range to achieve the highest possible efficiency. Simulations were also run with enrichment to extend the power rating, and if necessary, enrichment could be used to limit the amount of derating.

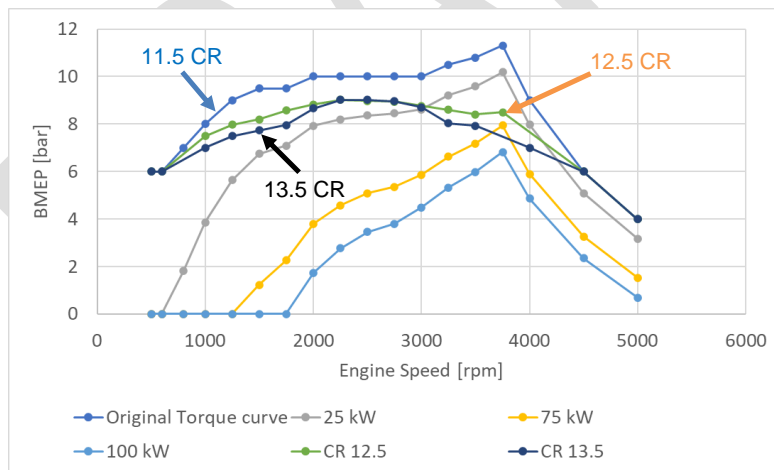


Figure 125. Engine Torque Curves for 11.5, 12.5, and 13.5 CR with GDI

As can be seen in Figure 125, a 25-kW e-motor would be able to fully compensate for the 13.5 CR torque curve up to 3,000 RPM. However, at rated speed, electric assistance of more than 75 kW would be required to maintain the original vehicle performance. The differences between the 12.5

and 13.5 CR curves are apparent at low speed, where only a small amount of assistance is needed, but also at the rated power point of 3,800 RPM.

A more extensive analysis of possible options would be helpful. For example, would it be acceptable to tolerate a reduction in power availability at rated speed for most vehicle applications? The answer may well be yes. Another evaluation, which would best be performed experimentally, would be to evaluate the potential for a less restrictive exhaust system and catalyst. Lower back pressure would reduce residuals in the cylinder, helping avoid knock. This could reduce the amount of derate required at high speed, and thus relax the amount of e-motor power required. There may be a combination of factors that would allow even higher CRs than 13.5 to be considered in a future study.

Similarly, a series hybrid would ideally target the best possible efficiency of the engine at one small operating region. The selection of this operating region is dependent on the charging requirements that would need to be determined by vehicle simulations. As a starting point for simulations, the engine could be simulated with the 13.5 CR at 2000 rpm, 7 bar.

Figure 126 shows the BTE map and torque curve reduction for the GDI engine with a 12.5 CR. Figure 127 shows the CA50 map for this configuration, and Figure 127 shows the improvement in BTE compared to an 11.5 CR. The improvement is typically around 1%, but there is a penalty at high loads.

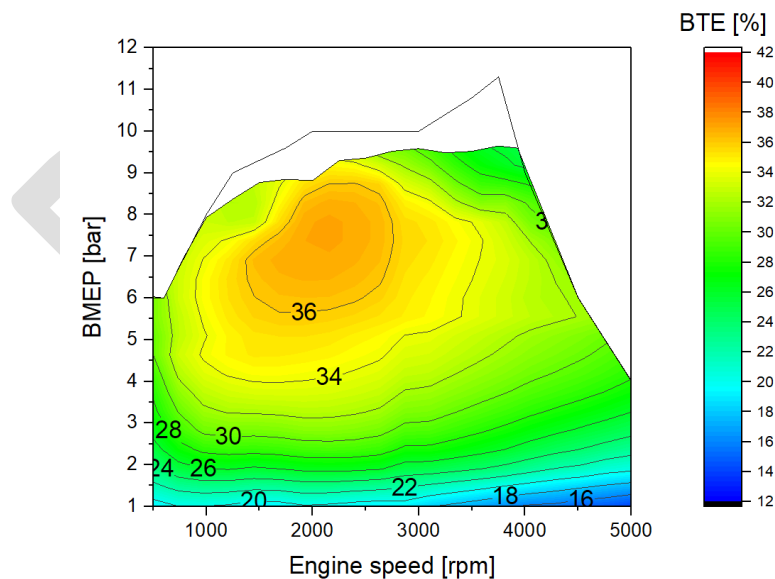


Figure 126. BTE Map for GDI with 12.5 CR for Hybrid Applications

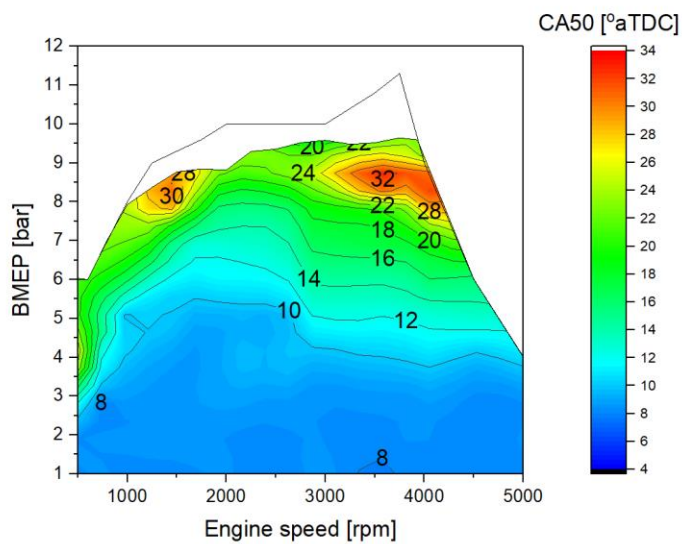


Figure 127. CA50 Map for GDI with 12.5 CR for Hybrid Applications

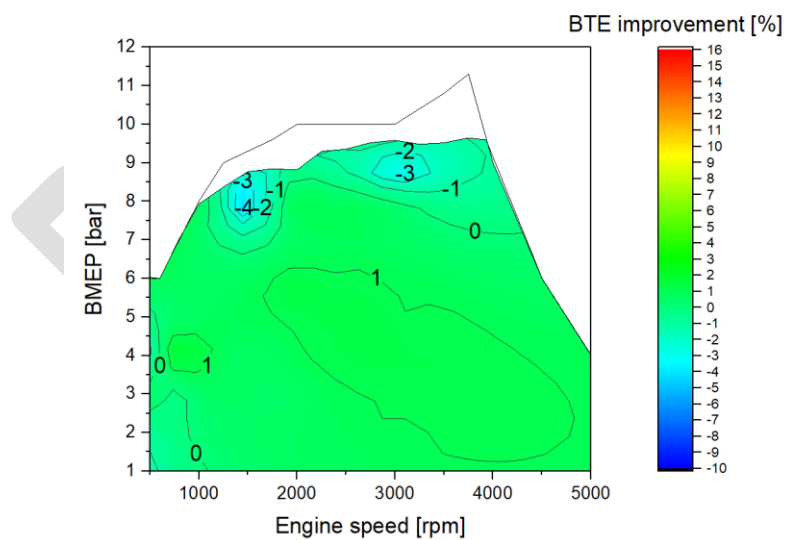


Figure 128 BTE Improvement of for GDI with 12.5 CR Relative to GDI with 11.5 CR

5.10.1 CR 13.5

Figure 129 shows the BTE map and torque curve reduction for the 13.5 CR engine. Figure 130 provides the CA50 map for the 13.5 CR engine, and Figure 131 shows the BTE improvement for the 13.5 CR engine compared to the 11.5 CR GDI version. Improvements of 1% to 2% across most of the map can be seen, although there are high load penalties at low speed and especially at high speed.

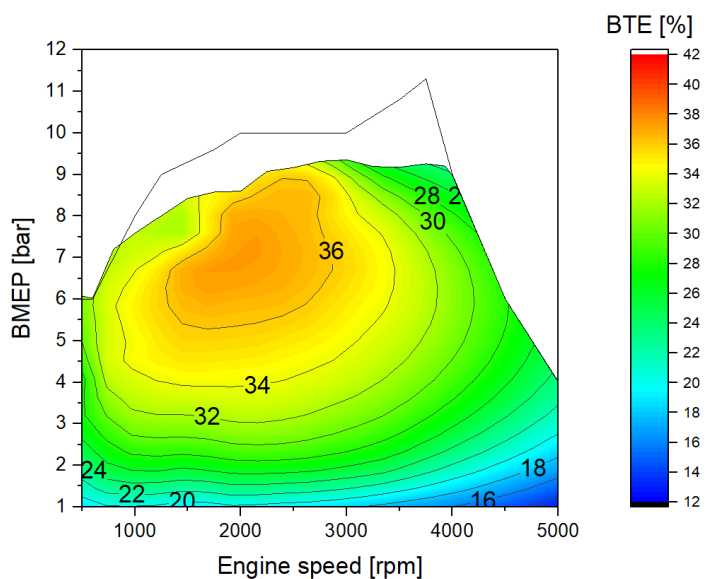


Figure 129. BTE Map for GDI with 13.5 CR for Hybrid Applications

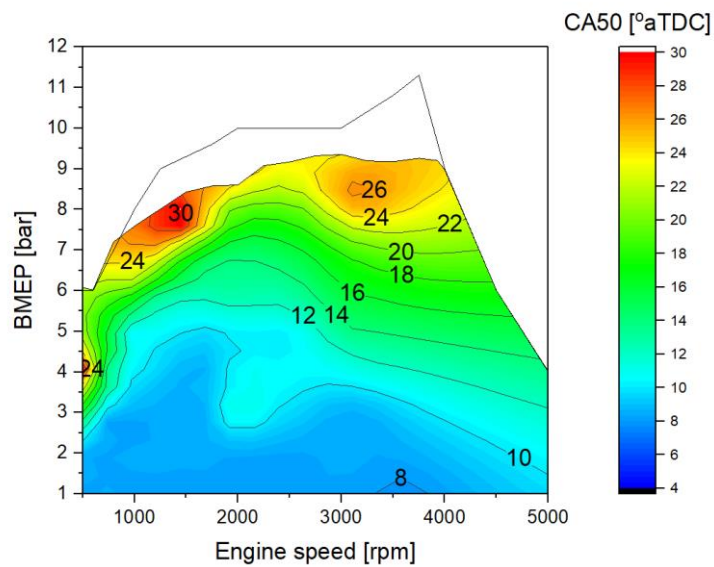


Figure 130. CA50 Map for GDI with 13.5 CR for Hybrid Applications

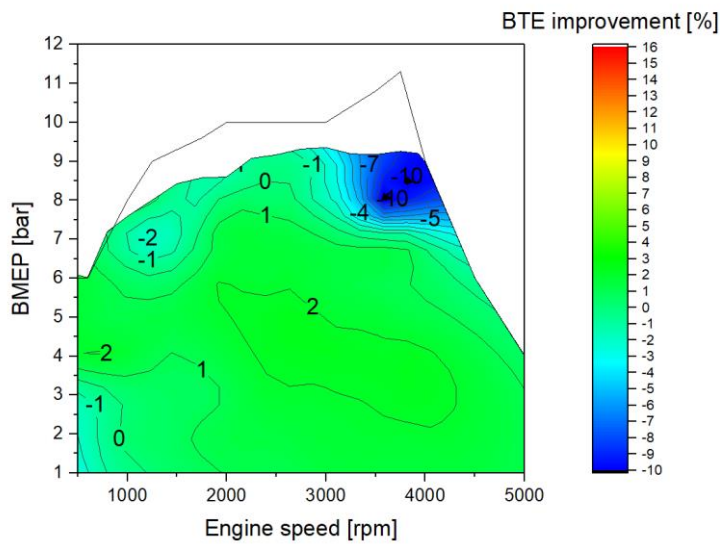


Figure 131. BTE Improvement for GDI with 13.5 CR Relative to GDI with 11.5 CR

5.11 Turbocharged Versions with a Narrower Speed Range

It has been shown that downspeeding engines can improve the drive cycle efficiency of vehicles. A range of power curves were studied to determine the best speed range for boosted versions of the 7.3L engine. The base engine had a power rating of 260 kW with the rated power near 3900 rpm. To keep the same vehicle performance, the same power was needed within the narrower speed range. The iso-power line in Figure 132 shows the BMEP level for varying degrees of downspeeding. The BMEP level at the rated power was maintained back to the peak torque speed. A sweep of CR and BMEP was simulated at a range of speeds. As a practical limitation, a minimum CR of 9.5 was also considered. Based on the knock model, the results showed that downspeeding to achieve a peak torque of 16 bar BMEP was too aggressive – it would require a CR below 9. It was determined that with a CR of 9.5:1, the 2-valve engine could achieve the power targets at a BMEP of 13.5 bar and 3100 rpm.

Figure 133 shows the actual torque curves used in this project. The 4-valve engine has better knock tolerance, so it was able to run higher BMEP than the 2-valve version. The 2-valve engine used a peak torque of 13.5 bar BMEP, while the 4-valve engine was able to run at 14.5 bar. The power curves used in this project are shown in Figure 134. Note that for all speeds between the torque peak and rated power conditions, the boosted engines will give better vehicle performance. This is because the boosted engines run a constant peak torque across the range from torque peak to rated, while the baseline naturally aspirated engine loses torque as speed drops from rated. The baseline engine has a very unusual torque curve, with torque peak and rated power occurring at the same engine speed. This is not a good feature from a drivability perspective. SwRI speculates that the reason for this torque curve is that Ford did not develop a revised, longer runner intake manifold for the medium-duty version of the engine, so it retained the high peak torque speed of the light duty version.

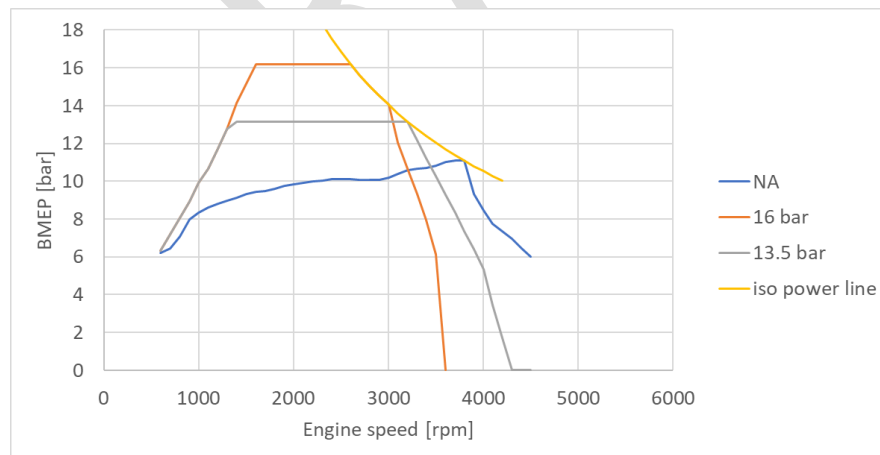


Figure 132. Torque Curve Options Considered for a Boosted Version with Downspeeding

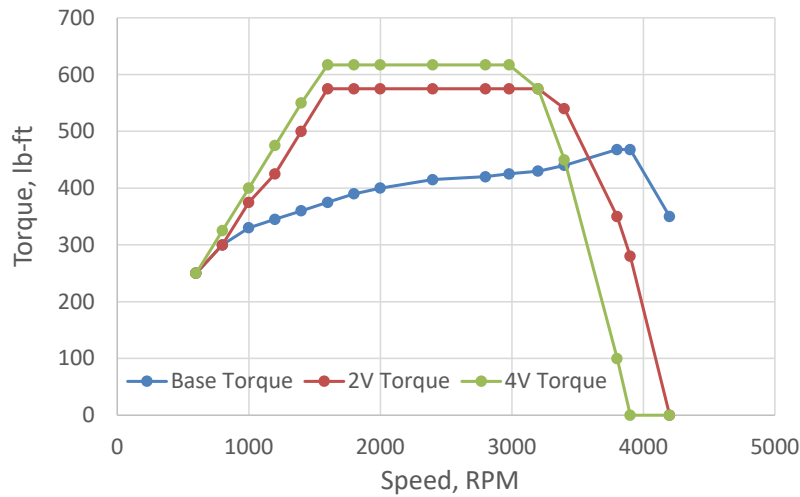


Figure 133. Comparison of Turbocharged (2V and 4V) and NA (Base) Torque Curves

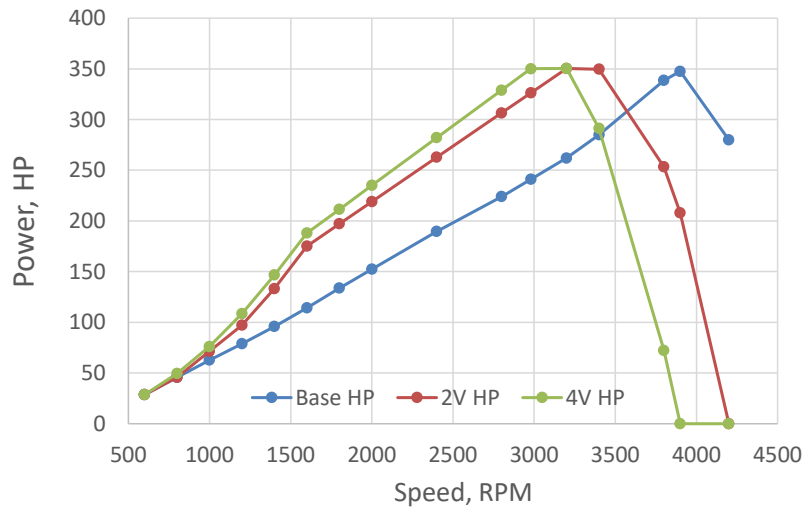


Figure 134. Comparison of Turbocharged (2V and 4V) and NA (Base) Power Curves

One of the technologies to be evaluated is a turbocharged version with LPL EGR or lean burn operation. It has been SwRI's experience that 2-valve heads do not have a high EGR tolerance or dilution tolerance. For the best results, a new pent-roof, 4-valve head would increase the EGR tolerance and the overall efficiency. A pent-roof head provides higher tumble flow and faster burn

rates. EGR and air dilution both slow down burn rates, so the high tumble is necessary to mitigate the negative effect of EGR or dilution. Compared to the 2-valve head, the 4-valve head was considered to have similar surface area to volume ratios, so the heat transfer changes were considered negligible.

For each of the turbocharged versions both 2 and 4-valve heads were simulated. The 2-valve head maintained the burn durations from the baseline naturally aspirated data of around 20 -25° CA. The 4-valve head was simulated with a burn duration of 15° CA, like other high tumble fast burn engines. The shorter burn durations also help reduce the knock intensity. At the onset of knock, more of the fuel has been consumed in a fast burn engine, so the resulting knock is less severe. The difference in knock propensity from the differences in burn durations gives two potential options to improve the efficiency. The CR can be increased a little higher or the load could be pushed higher to utilize more downspeeding. It was found that the latter option gave more benefits over most of the map. A very highly loaded drive cycle could reverse this trend, but most regulatory cycles are not highly loaded. The 4-valve simulations start with the same 9.5:1 CR, but with a peak torque of 14.5 bar BMEP. This provides the rated power at 2900 rpm, compared to 3,900 RPM for the baseline naturally aspirated engine.

5.11.1 Turbocharged and Downsped with GDI 2V

Figure 135 shows the BTE map for the boosted GDI engine with 2 valves and a 9.5 CR, and Figure 136 shows the CA50 map for this version. The best point BSFC is just below 36%, which is slightly worse than the baseline engine. A turbocharged engine could still offer better vehicle fuel consumption, despite the efficiency penalty. At lower vehicle power demands, the boosted engine will be operating at lower RPM because of taller gearing. This means that a small power demand will be met at a higher, more efficient BMEP level.

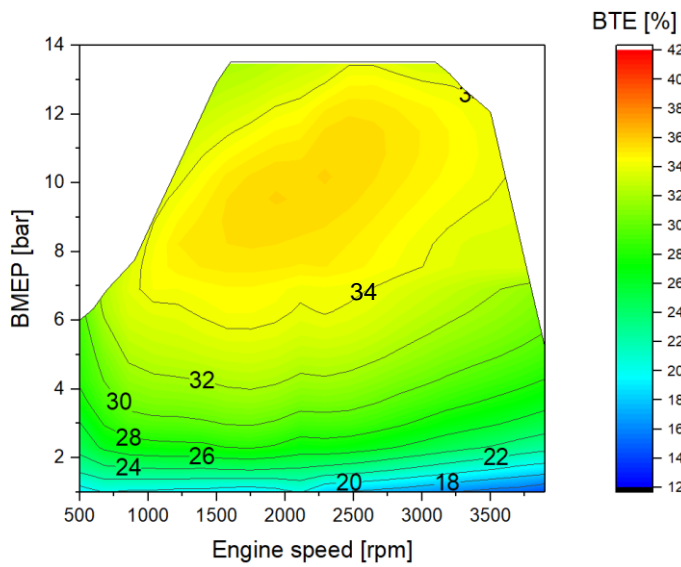


Figure 135. BTE Map of Turbocharged GDI 2V Engine

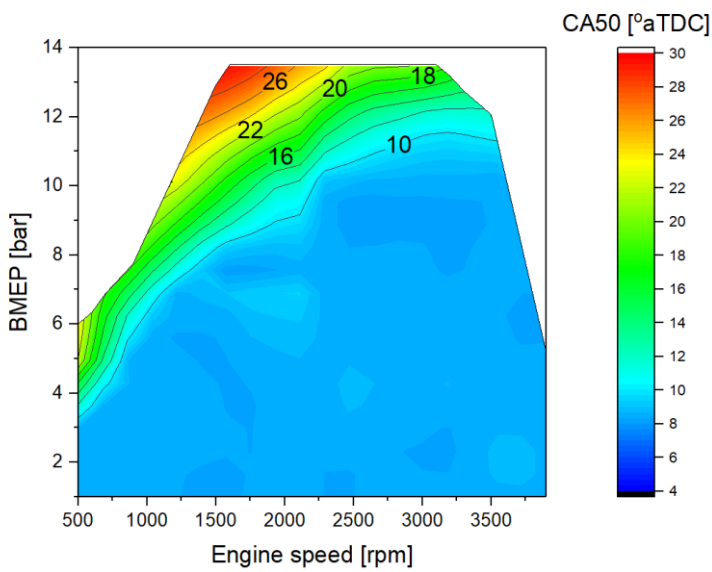


Figure 136. CA50 Map of Turbocharged GDI 2V Engine

5.11.2 Turbocharged Downsized with GDI 4V

Figure 137 shows the BTE map for the boosted GDI engine with 4 valves and a 9.5 CR, and Figure 138 shows the CA50 map for this version. The best point BSFC is just below 36%, which is slightly worse than the baseline engine. This result is also no more favorable than for the 2-valve version, but the 4-valve allows more downspeeding, which should help vehicle fuel consumption under light load conditions.

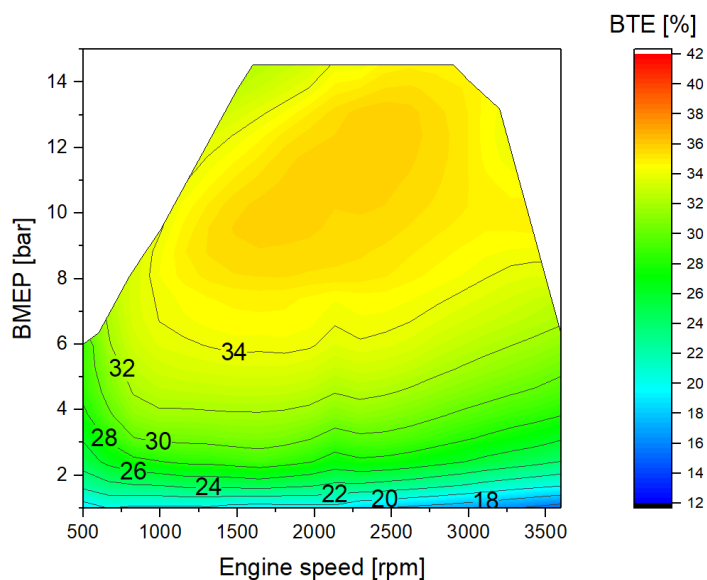


Figure 137. BTE Map of Turbocharged GDI 4V Engine

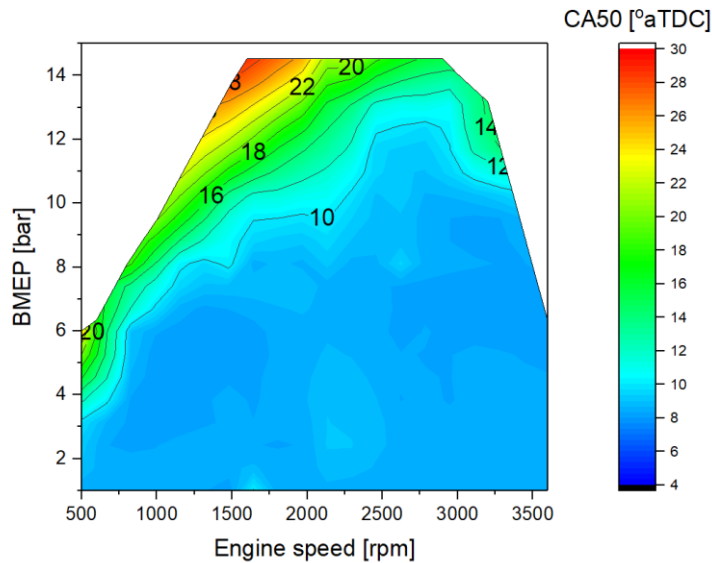


Figure 138. CA50 Map of Turbocharged GDI 4V Engine

5.11.3 Turbocharged Downsized with GDI 2V, Lean Burn

Lean combustion has a high potential for improving fuel economy of vehicles. Air dilution has a stronger beneficial impact on gamma than EGR dilution. However, the exhaust aftertreatment is more expensive, requiring an SCR. Lean combustion also differs from EGR in terms of knock mitigation. Any amount of EGR added reduces the knock propensity, while combustion that is slightly lean actually has a higher knock propensity. This is because the combustion temperatures are the hottest and oxygen is readily available for combustion at slightly lean conditions. As the mixtures are controlled leaner, the combustion temperatures cool and the burn rates slow. Around a lambda of 1.4, the combustion phasing is the same as stoichiometric, but with the benefits of the excess air on gamma. Lean limits for homogenous mixtures with a conventional ignition system are in the lambda 1.4 to 1.6 range. Based on the turbocharger match, the engine was boost limited in the low-speed, high torque region, resulting in a lean limit of lambda 1.4. Because at lambda 1.4 the knock propensity is like the baseline turbocharged stoichiometric model, the CR was maintained at 9.5:1 for both the 2 and 4V versions.

Figure 139 shows the lambda map for the 2V lean burn boosted engine, and Figure 140 shows the fuel map. The map features a large area of efficiency above 36%, but the peak efficiency is below 38%. Figure 141 shows the CA50 map for this version, while Figure 142 compares the efficiency of the 2V lean burn boosted engine to the baseline 2V boosted engine. Double digit gains at low speed gradually taper to no benefit at high speed, high load conditions.

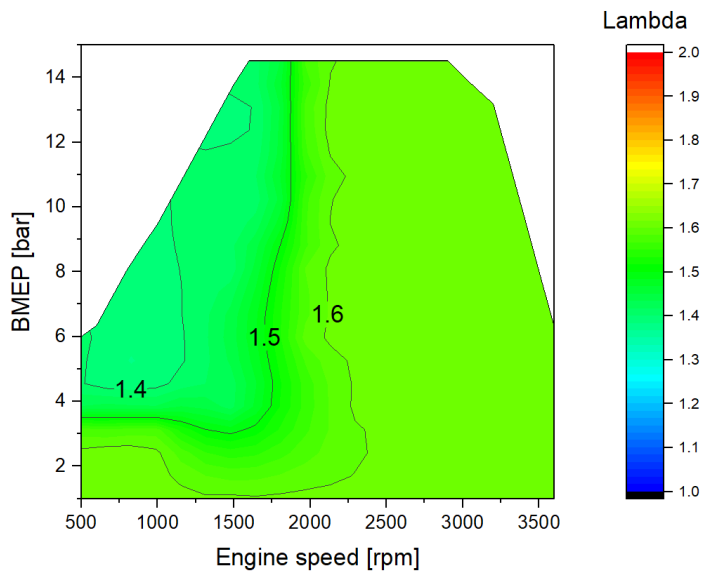


Figure 139. Lambda Map of the TC lean GDI 4V Engine

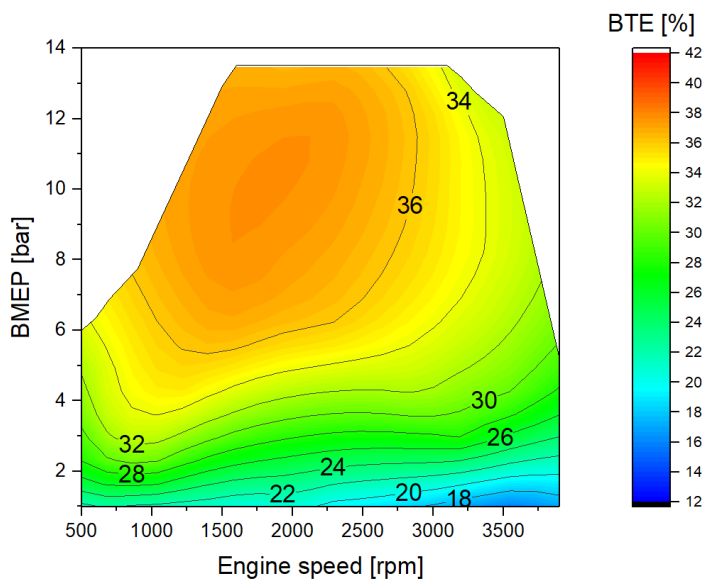


Figure 140. BTE Map of Turbocharged, Lean Burn GDI 2V Engine

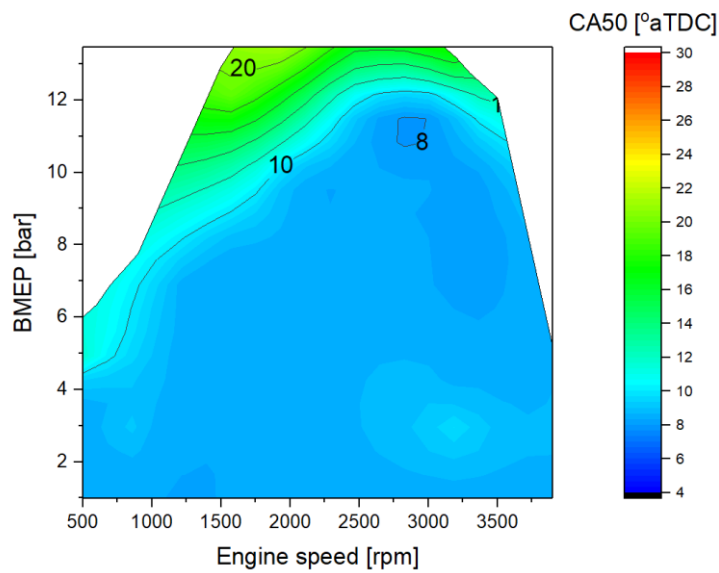


Figure 141. CA50 Map of Turbocharged GDI, Lean Burn 2V Engine

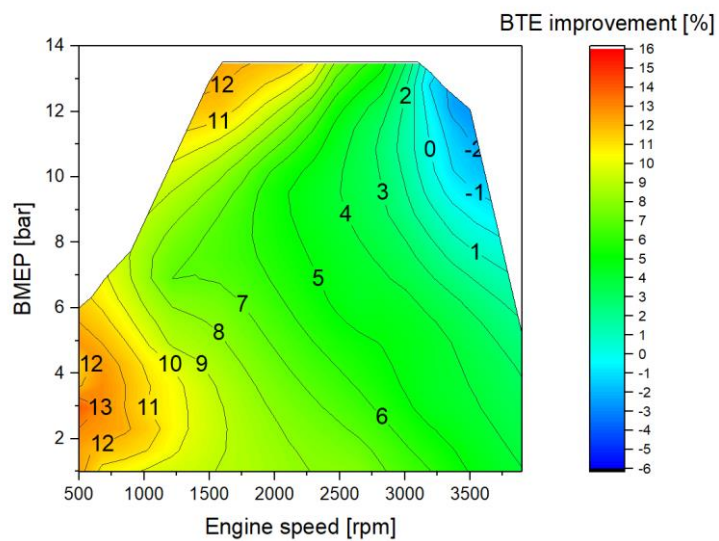


Figure 142. Change in BSFC of for Turbocharged GDI, Lean Burn 2V Engine Relative to the Turbocharged GDI Stoichiometric 2V Engine

5.11.4 Turbocharged Downsized with GDI 4V, Lean Burn

Figure 143 shows the fuel map for the lean burn, boosted, 4V engine. The map features a large area of efficiency above 36%, and the peak efficiency is better than 38%. Figure 144 shows the CA50 map for this version, while Figure 145 compares the efficiency of the 4V lean burn boosted engine to the baseline 4V boosted engine. Double digit gains at low speed gradually taper to no benefit at high speed, high load conditions.

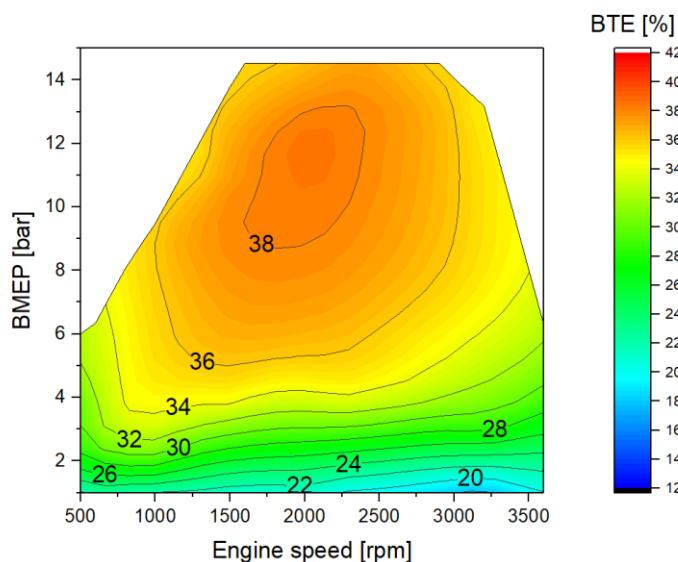


Figure 143. BTE Map of Turbocharged, Lean Burn GDI 4V Engine

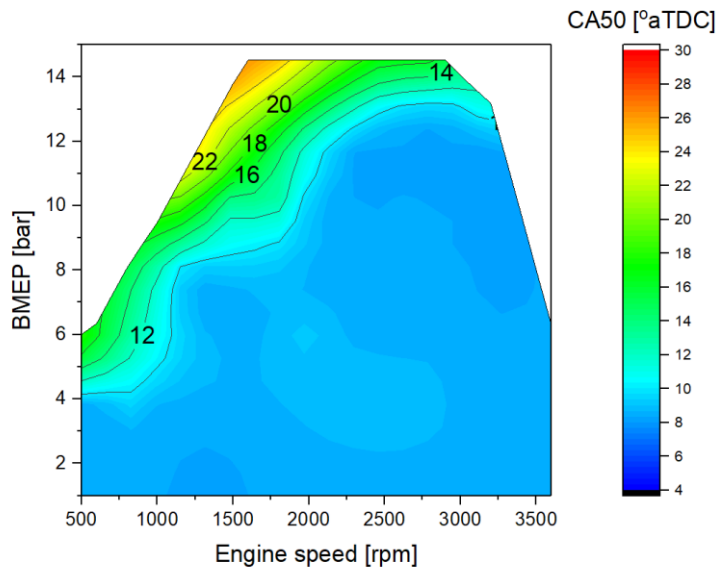


Figure 144. CA50 Map of Turbocharged, Lean Burn GDI 4V Engine

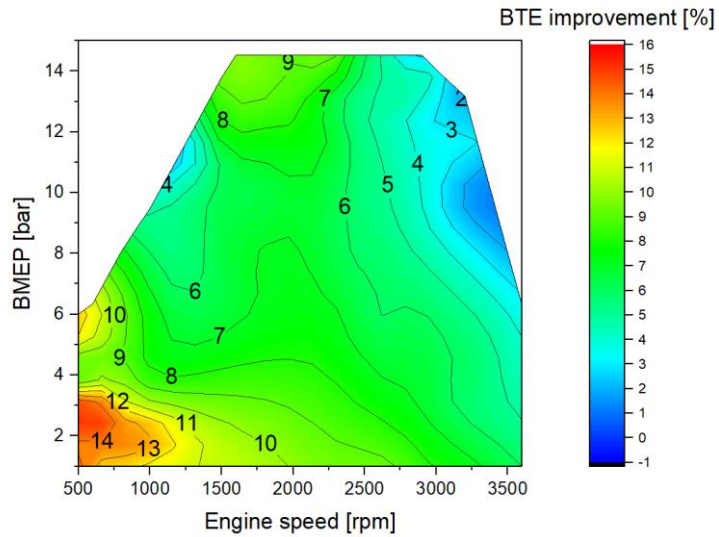


Figure 145. Change in BSFC for Turbocharged GDI, Lean Burn 4V Engine Relative to the Turbocharged GDI, Stoichiometric 4V Engine

5.11.5 Turbocharged Downsized with GDI 2V, Independent Cam Phasers (VVT)

The TC GDI model used the same cam authority as the baseline engine, with the intake and exhaust cams phased together. The phasing was swept to determine the best timing for different regions of the map for the turbocharged models. In this section, the VVT model phases the intake and exhaust cams separately. The parked positions were advanced by 20 degrees to prioritize overlap and residuals. The TC GDI base model prioritized LIVC. The maximum residual level targeted was 35%, based on SwRI's testing experience, which shows that this is the maximum before reaching the combustion stability limit. Increased residuals primarily help with reducing pumping losses at low loads. At higher loads, the hot residuals make the knock propensity worse, so the amount of overlap is reduced. Since the knocking characteristics are not improved compared to the turbocharged baseline, the CR was maintained at 9.5:1 for both the 2 and 4 valve configurations. The results show the cam phasing for LIVC is more beneficial than phasing to obtain residuals. These maps were not provided to Argonne, since the turbocharged baseline results were better.

Figure 146 shows the BTE map for the turbocharged, GDI 2V engine with independent cam phasers. Figure 147 shows the CA50 map for this version, while Figure 148 shows the percent BTE improvement compared to the baseline boosted GDI 2V engine with a single cam phaser. Figure 148 shows that dual independent phasers can provide some benefits at low speeds and light loads, but there is a 1% to 3% fuel consumption penalty across a wide area of the map.

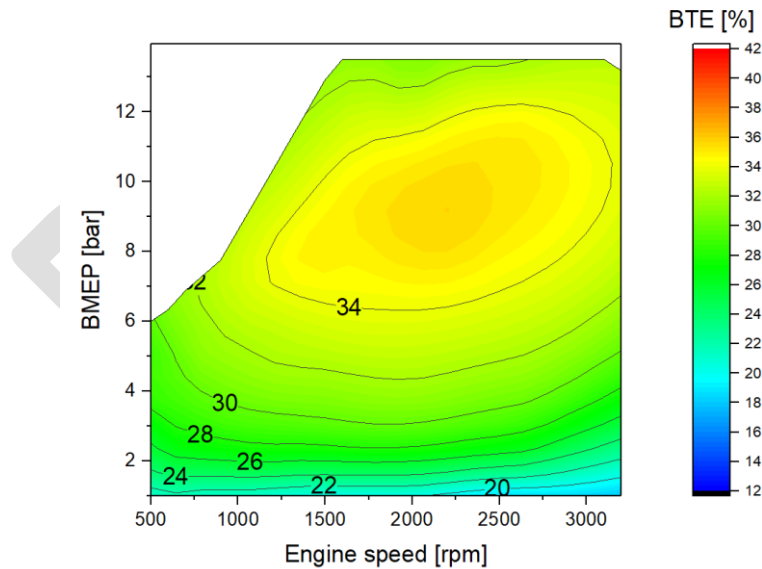


Figure 146. BTE Map of Turbocharged, GDI 2V Engine with Independent Cam Phasers

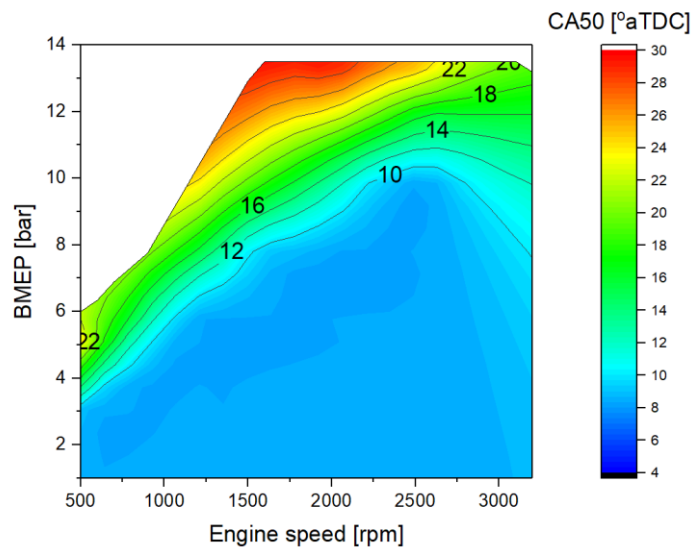


Figure 147. CA50 Map of Turbocharged, GDI 2V Engine with Independent Cam Phasers

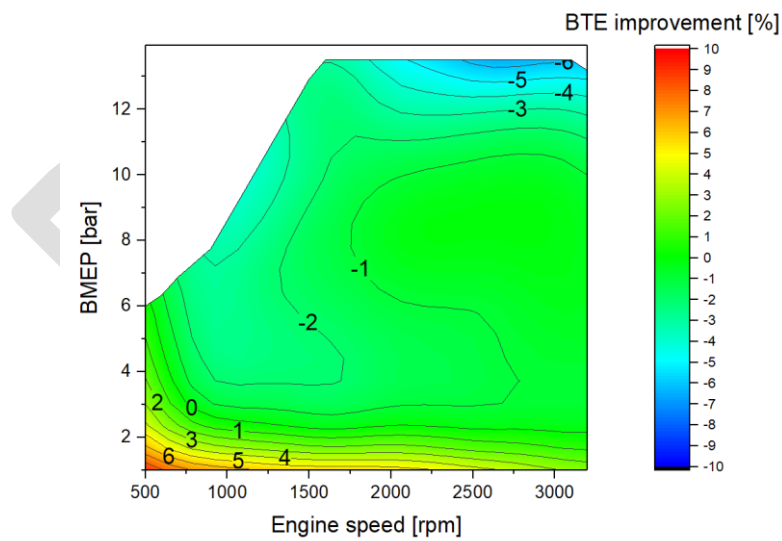


Figure 148. BTE Improvement for Turbocharged, GDI 2V Engine with Independent Cam Phasers, Relative to Turbocharged GDI Stoichiometric 2V Engine

5.11.6 Turbocharged Downsized with GDI 4V, Independent Cam Phasers (VVT)

Figure 149 shows the BTE map for the turbocharged, GDI 4V engine with independent cam phasers. Figure 150 shows the CA50 map for this version, while Figure 151 shows the percent BTE improvement compared to the baseline boosted GDI 4V engine with a single cam phaser. Figure 151 shows that dual independent phasers can provide some benefits at light loads below 2 bar BMEP, but there is a 0% to 3% fuel consumption penalty across a wide area of the map.

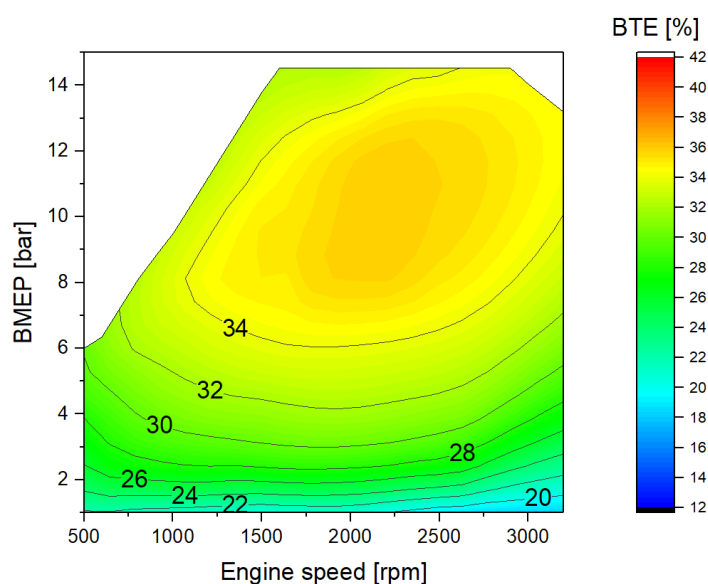


Figure 149. BTE Map of Turbocharged, GDI 4V Engine with Independent Cam Phasers

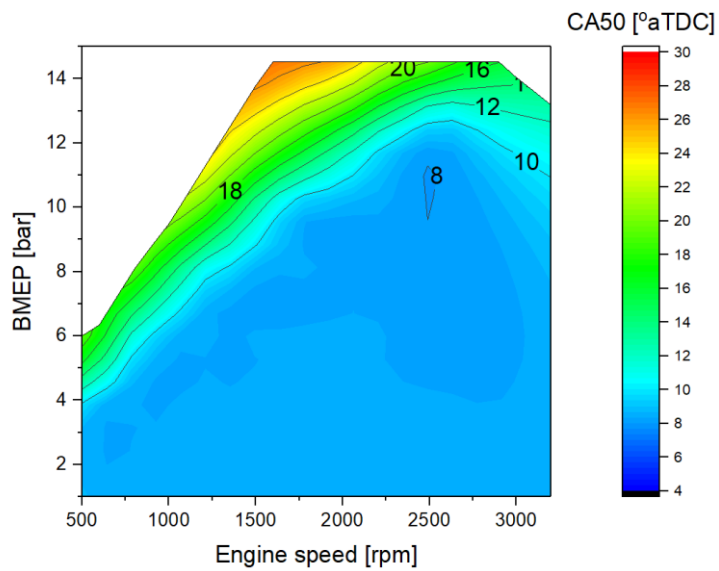


Figure 150. CA50 Map of Turbocharged, GDI 4V Engine with Independent Cam Phasers

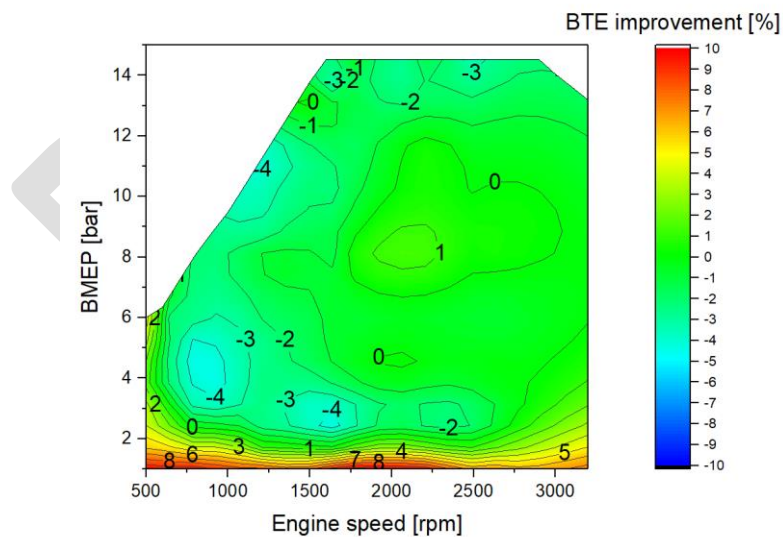


Figure 151. BTE Improvement for Turbocharged, GDI 4V Engine with Independent Cam Phasers, Relative to Turbocharged GDI Stoichiometric 4V Engine

5.11.7 Turbocharged Downsized with GDI 2V, VVT and LPL EGR

The VVT with LPL configuration uses the same phasing authority as the TC VVT model. The configuration uses a mix of internal residuals and external low-pressure loop cooled EGR. At low to intermediate loads the valve timing was set to target a total EGR plus residuals of 35%. The 2-valve configuration uses 20% external EGR while the 4-valve version uses 25% EGR. The external EGR reduces the knock propensity and enabled a CR increase to 10.5:1.

Figure 152 shows the BTE map for the boosted GDI 2V engine with independent cam phasers and LPL EGR. There is a reasonably large island of BTE above 36%, but the peak is below 38%. Figure 153 shows the CA50 map for this configuration, while Figure 154 shows the BTE improvement compared to a baseline boosted GDI 2V configuration. Benefits of 3% to 6% are shown at loads below 2 bar BMEP, while benefits of 1% to 3% show across a large area of the map.

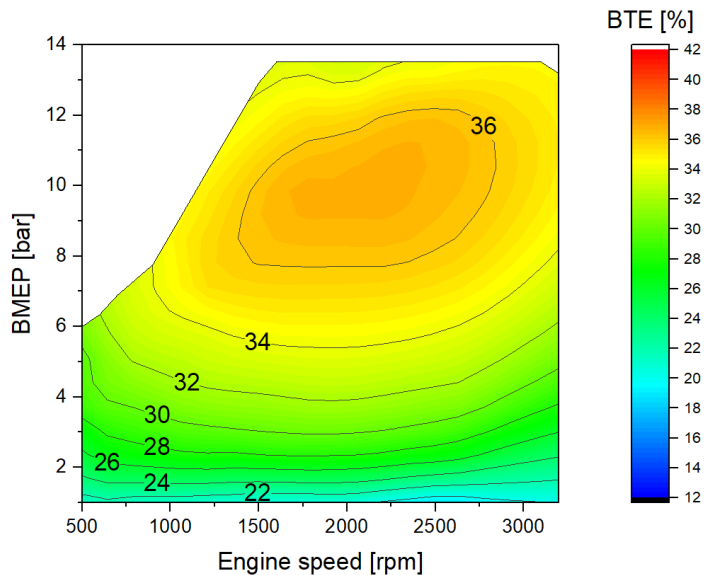


Figure 152. BTE Map for Turbocharged GDI 2V with Cam Phasers and LPL EGR

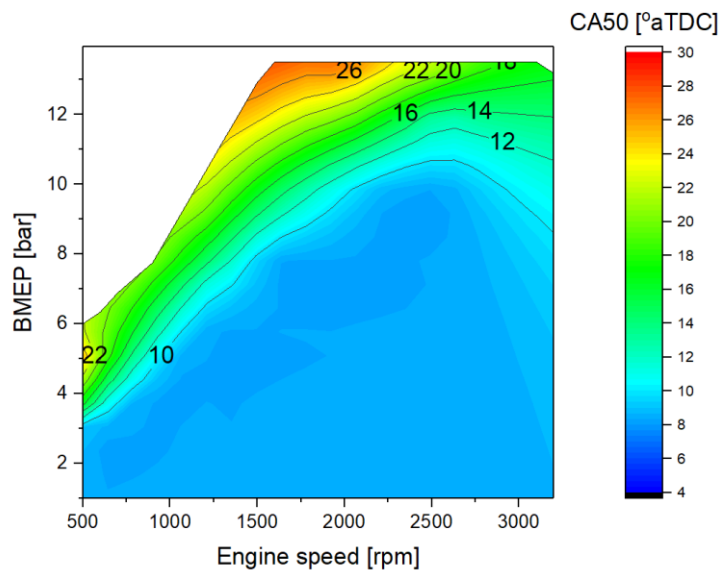


Figure 153. BTE Map for Turbocharged GDI 2V with Cam Phasers and LPL EGR

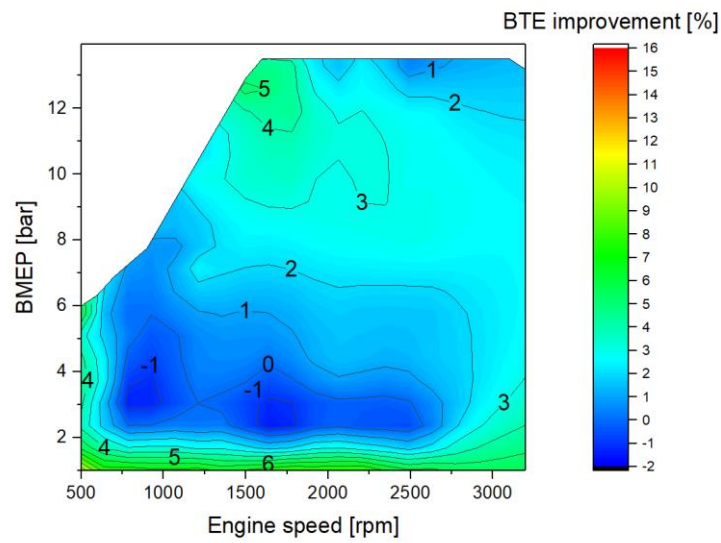


Figure 154. BTE Improvement Turbocharged GDI 2V with Cam Phasers and LPL EGR, Relative to the Turbocharged GDI Stoichiometric 2V Engine

5.11.8 Turbocharged Downsized with GDI 4V, Cam Phasers, and LPL EGR

Figure 155 shows the BTE map for the boosted GDI 4V engine with independent cam phasers and LPL EGR. As with the 2V version, there is a reasonably large island of BTE above 36%, but the peak is below 38%. Figure 156 shows the CA50 map for this configuration, while Figure 157 shows the BTE improvement compared to a baseline boosted GDI 2V configuration. Benefits of 3% to 8% are shown at loads below 2 bar BMEP, while benefits of 1% to 4% show across a large area of the map.

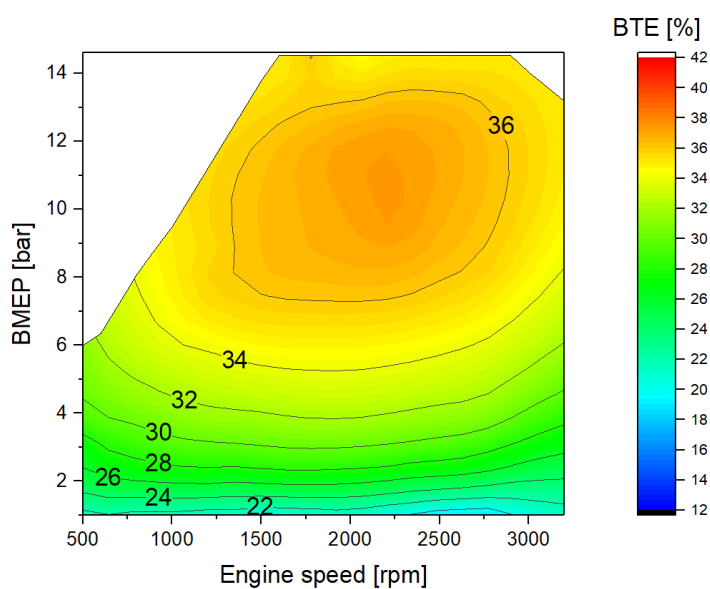


Figure 155. BTE Map for Turbocharged GDI 4V with Cam Phasers and LPL EGR

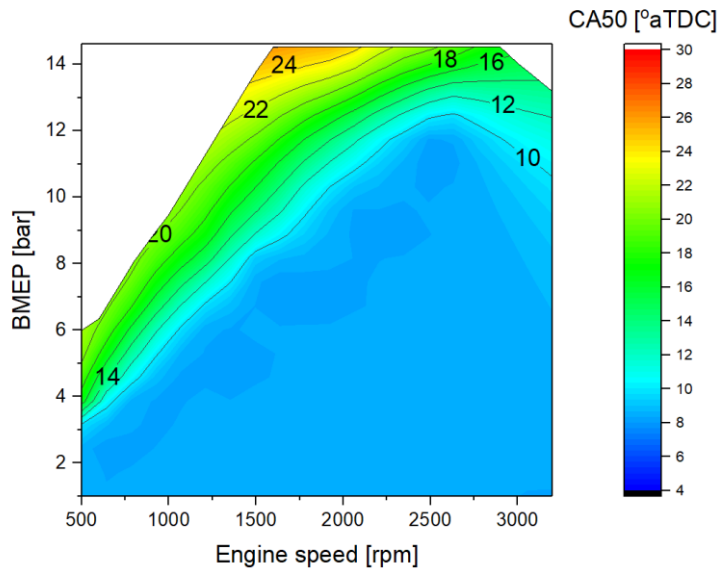


Figure 156. BTE Map for Turbocharged GDI 4V with Cam Phasers and LPL EGR

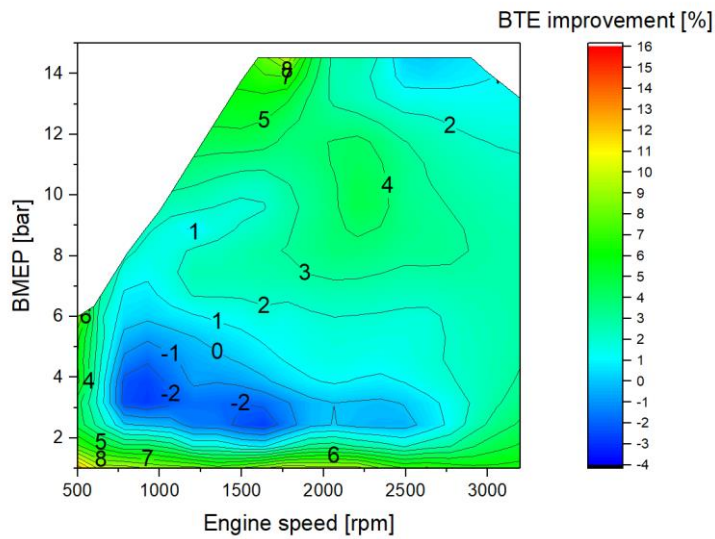


Figure 157. BTE Improvement Turbocharged GDI 4V with Cam Phasers and LPL EGR, Relative to the Turbocharged GDI Stoichiometric 4V Engine

5.12 NA GDI with CDA and 11.5 CR

The cylinder deactivation model was run in a NA configuration to show the maximum potential improvement for fuel economy. The model uses the baseline model plus GDI and an increased CR of 11.5:1. Cylinder deactivation is used at loads up to 4 bar BMEP. One bank of four cylinders was deactivated for simplicity rather than employing a dynamic skip fire approach. The intake and exhaust valves were deactivated for the deactivated bank to minimize the pumping work. The firing cylinders benefit from operating at a higher IMEP. The manifold pressures are also much higher, which significantly reduces the pumping loss.

The BTE map for this configuration is shown in Figure 158, while Figure 159 shows the CA50 map. The CA50 map has a characteristic of showing significant combustion retard to avoid knock as the engine approaches 3 and 4 bar BMEP. Above 4 bar BMEP, 8-cylinder operation with standard CA50 values is used. Figure 160 shows a large benefit at low loads from CDA. Above 4 bar BMEP, the efficiency is the same as the NA GDI model with 11.5 CR. Note that the plotting routine is not very good at handling abrupt transitions in fuel consumption, so some smoothing will be seen. All improvement values above 4 bar BMEP should be zero. The delivered fuel maps do not suffer from this issue.

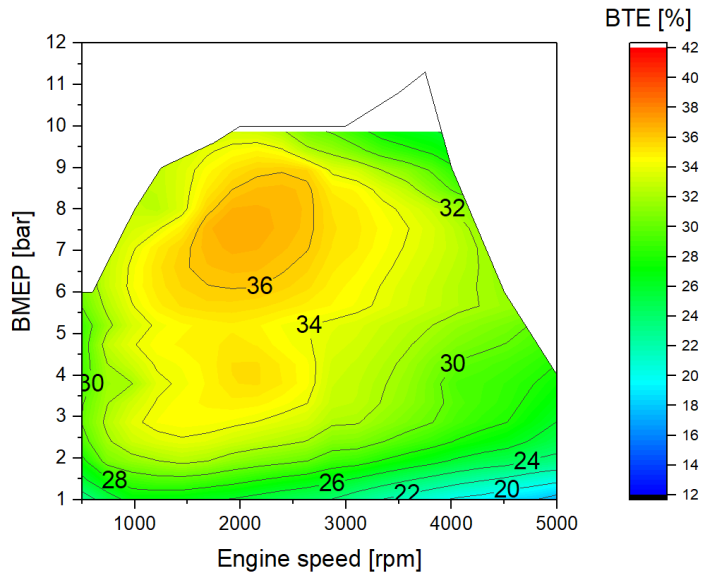


Figure 158. BTE Map for GDI with 11.5 CR and CDA

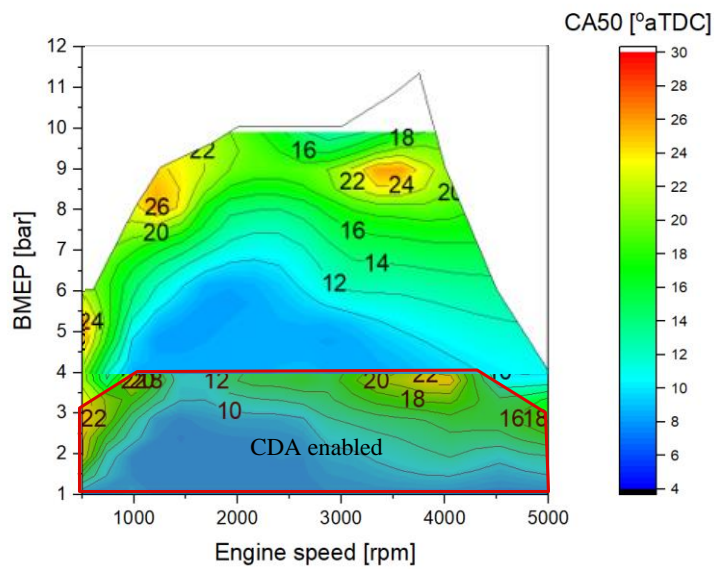


Figure 159. CA50 Map for GDI with 11.5 CR and CDA

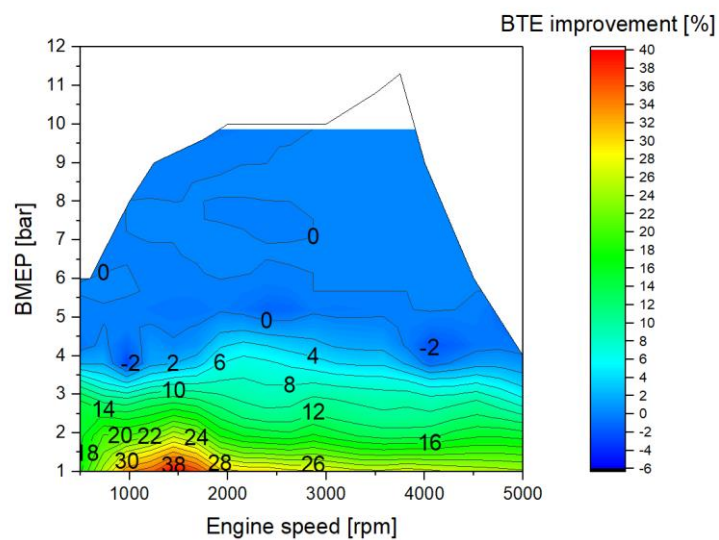


Figure 160. BTE Improvement for GDI with 11.5 CR and CDA, Relative to GDI and 11.5 CR without CDA

5.13 Turbocharged Downsized with GDI 2V, Independent Cam Phasers, D-EGR

The D-EGR model is like the TC GDI model with dual independent cam phasers (VVT) plus LPL EGR. It was determined that CDA was not viable to use in conjunction with D-EGR, however, due to the risk of misfire. D-EGR used two dedicated cylinders out of the eight for a 25% EGR rate. The dedicated cylinders are run rich, which produces some H_2 and CO in the EGR stream. Both these species increase the reactivity of the EGR, enabling better combustion stability with the high EGR rates. The reformation also serves to effectively increase the octane rating of the fuel. The engine out emissions are maintained by having the exhaust stream run stoichiometric for all conditions. This allows the standard 3-way catalyst to be applied. For simplicity, the simulations ran all cylinders stoichiometric with a small octane rating increase. The higher octane enabled another half point of CR increase compared to LPL EGR, so the D-EGR models used a CR of 11:1. The 4V version was estimated to be able to use more dedicated cylinder enrichment and therefore was given a larger octane rating increase than the 2V version.

Figure 161 shows the BTE map for the 2V D-EGR engine, while Figure 162 shows the CA50 map. A large area of better than 36% BTE is shown, but the best point is just below 38%. Figure 163 shows the BTE improvement of the 2V D-EGR engine compared to the 2V turbocharged baseline. Improvements of 3% to 6% cover a wide area of the map, with higher benefits at very light load and at very low speeds.

In the next section, Figure 164 shows the BTE map for the 4V D-EGR engine, while Figure 165 shows the CA50 map. A large area of better than 36% BTE is shown, but the best point is just below 38%. Figure 166 shows the BTE improvement of the 4V D-EGR engine compared to the 4V turbocharged baseline. Improvements of around 5% cover a wide area of the map, with higher benefits at very light load.

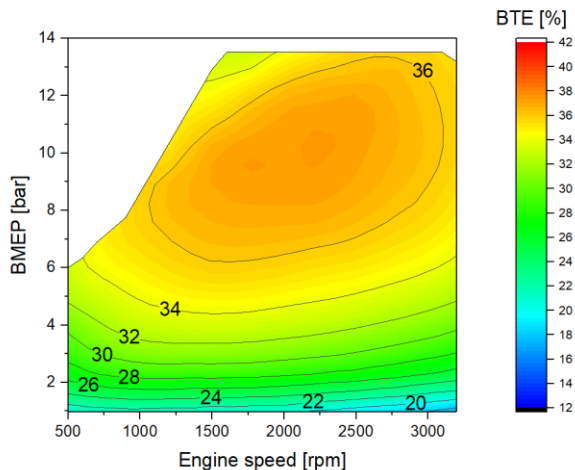


Figure 161. BTE for the 2V D-EGR CR 11 Map

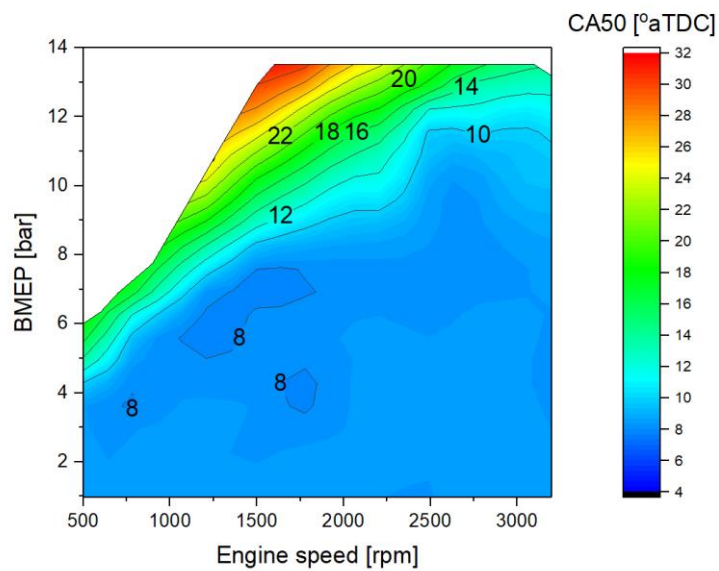


Figure 162. CA50 Map for the 2V D-EGR CR 11 Model

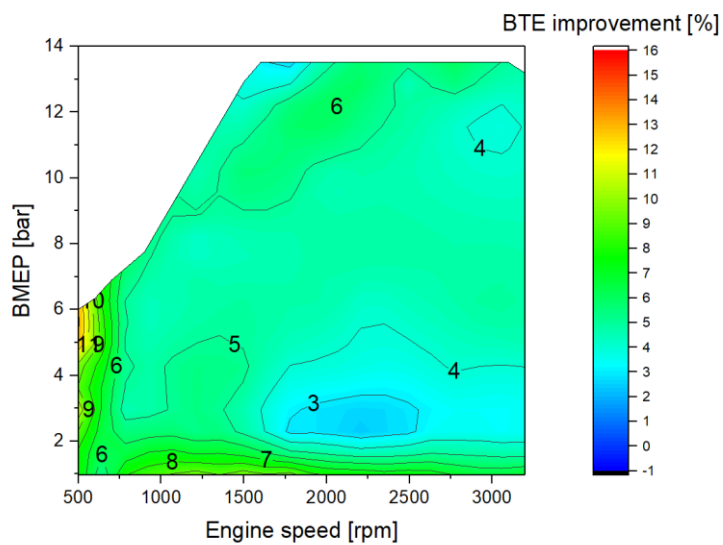


Figure 163. BTE Improvement for the 2V D-EGR CR 11 vs the Turbocharged GDI 2V CR 9.5 Engine

5.14 Turbocharged Downsized with GDI 4V, VVT, D-EGR, CDA

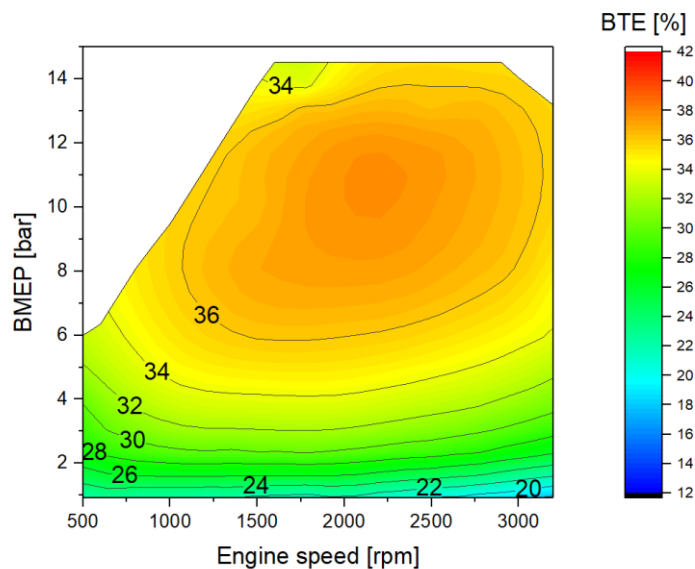


Figure 164. BTE Map for the 4V D-EGR Engine with CR 11

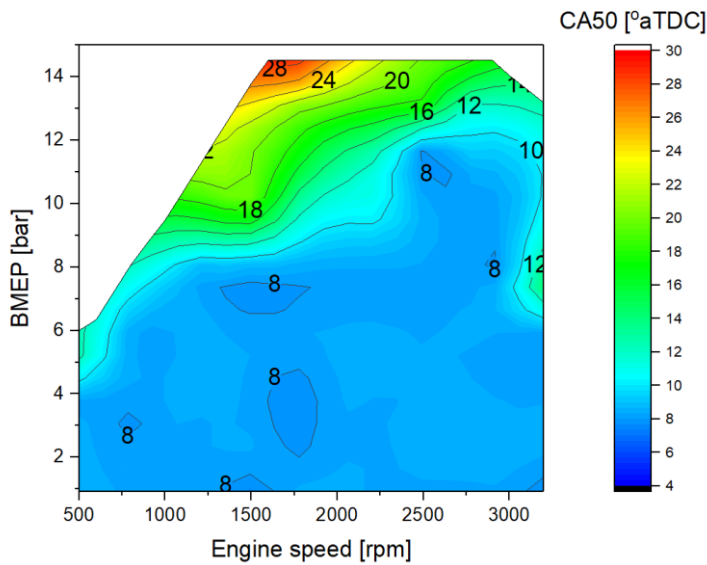


Figure 165. CA50 Map for the 4V D-EGR Engine with CR 11

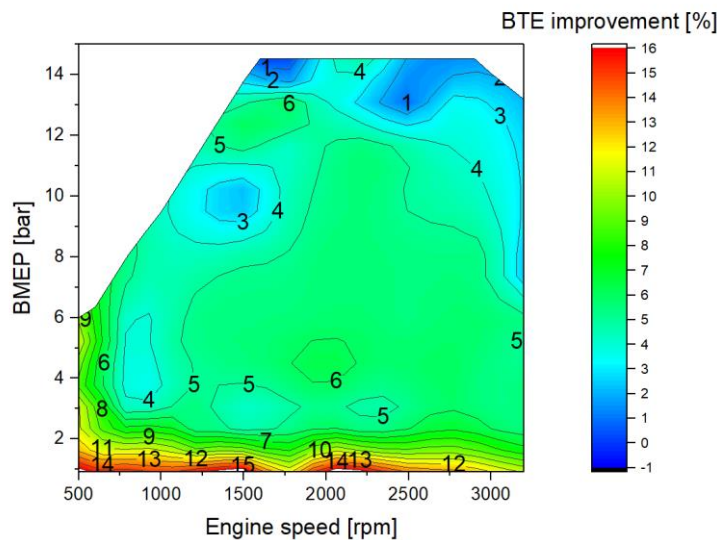


Figure 166. BTE Improvement for the 4V D-EGR Model Relative to the Turbocharged GDI 4V CR 9.5 Model

5.15 NA GDI with Full Authority Variable Valve Timing and Duration (VVA)

The VVA model expands on the capability of the VVT model. The VVT model has control of both the intake and exhaust timing but uses fixed valve lift and duration. The VVA model adds the capability to adjust the lift and duration as well. There are current production valvetrain systems available that can shorten the valve event duration and reduce the lift. The VVA configuration can be used to eliminate the throttle. The manifold pressure for each case is effectively always at atmospheric pressure, so the system controls load by shortening the valve duration. The base valve timing uses LIVC. The shortened valve lifts and durations changes it to use EIVC.

Figure 167 shows the BTE map for the naturally aspirated GDI engine with 11.5 CR and full authority VVA, while Figure 168 shows the CA50 map. Figure 169 shows the increase in efficiency allowed by the full authority VVA system, compared to the baseline of a naturally aspirated GDI with 11.5 CR. Double digit benefits can be seen at light load, primarily because of reduced throttling losses. The benefits at higher load are in the low single digits.

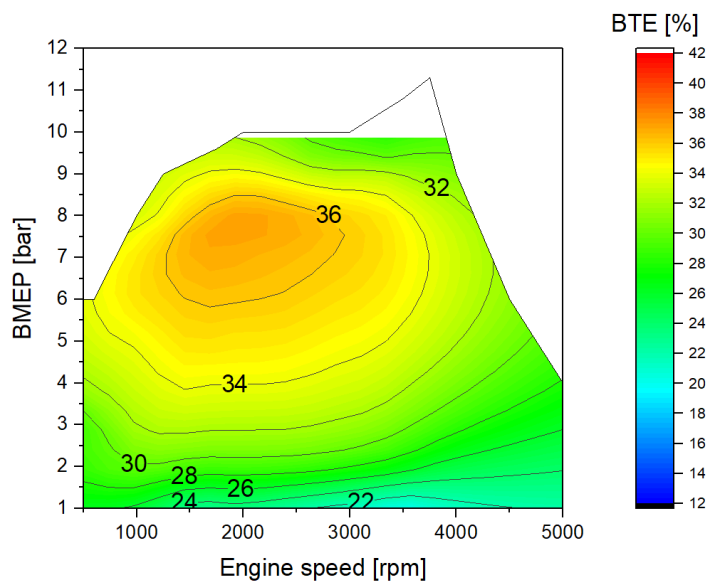


Figure 167. BTE Map for the NA GDI 11.5 CR with VVA

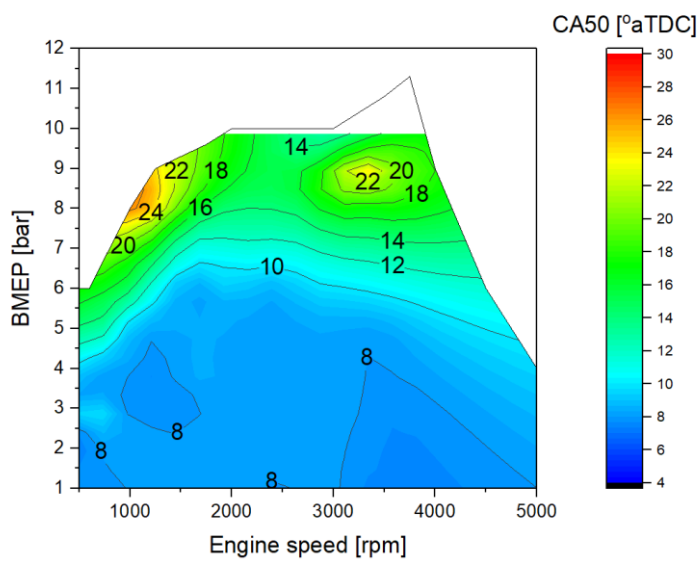


Figure 168. CA50 Map for the NA GDI 11.5 CR with VVA

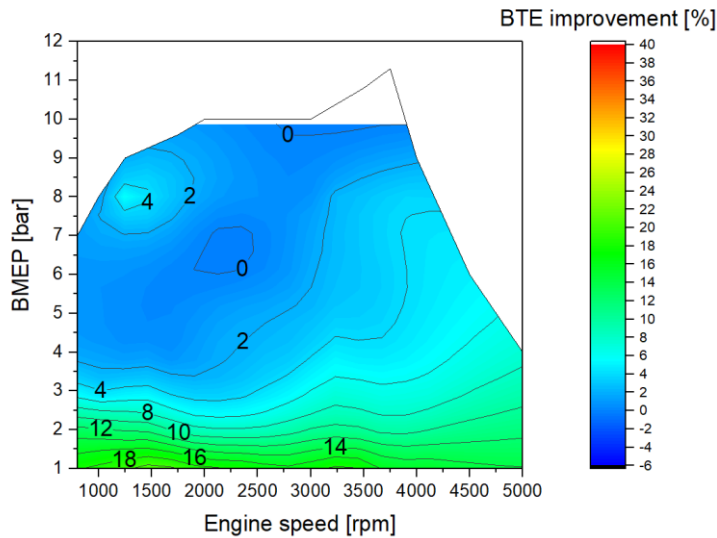


Figure 169. BTE Improvement for the NA GDI 11.5 CR with VVA Relative to the NA GDI 11.5 CR

5.16 TC GDI 2V, with Full Authority Variable Valve Timing and Duration (VVA) and LPL EGR

The turbocharged versions that use VVA can take advantage of it only in the naturally aspirated range of BMEP. Once the engine needs to be boosted to meet the target loads, the valve durations return to the full duration and the same valve timing as the VVT models. LPL EGR can be used across the map, except at very light load.

Figure 170 shows the BTE map for the turbocharged 2V GDI engine with full authority VVA and LPL EGR, and Figure 171 shows the CA50 map for this configuration. Figure 172 compares the efficiency of the 2V engine with VVA and LPL EGR to the baseline of a single cam phaser. VVA + LPL EGR provides a 2% to 4% benefit across much of the map, with much larger benefits at light load and at lower speeds.

In the following section, Figure 173 shows the BTE map for the turbocharged 4V GDI engine with full authority VVA, and Figure 174 shows the CA50 map for this configuration. Figure 175 compares the efficiency of the 4V engine with VVA to the baseline of a single cam phaser. The LPL EGR provides a 2% to 4% benefit across the turbocharged region where the VVA lift is returned to its max lift. The VVA system provides much larger benefits at light load and at lower speeds.

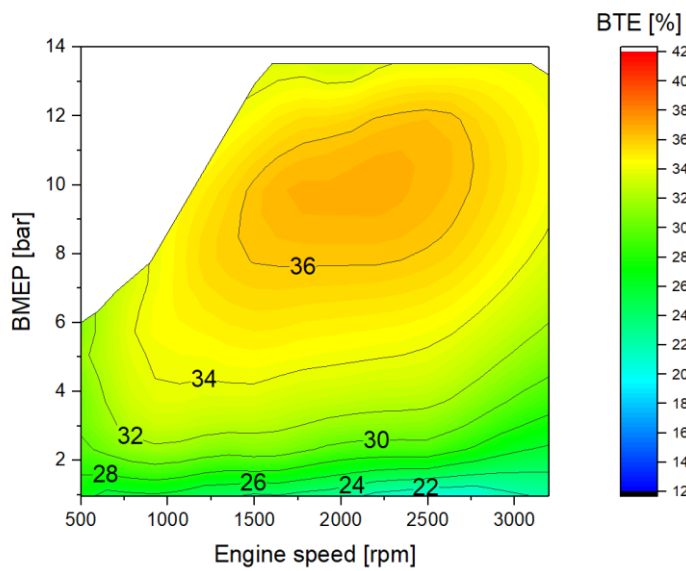


Figure 170. BTE Map for the TC GDI 2V Model with VVA

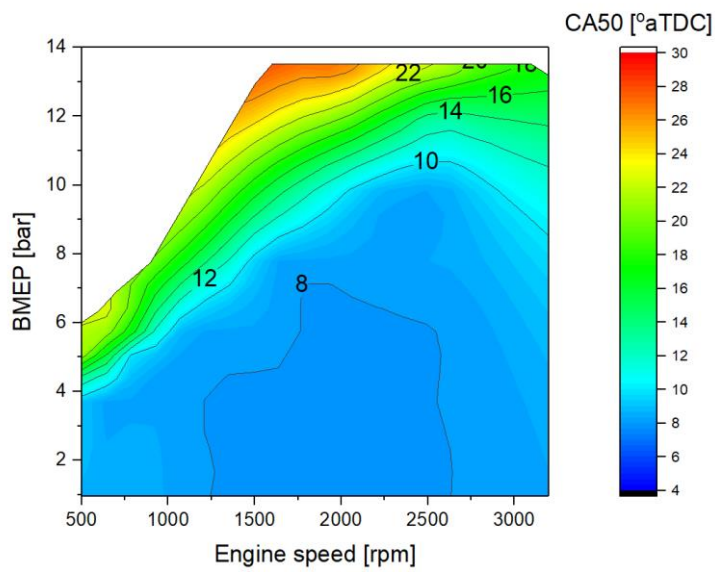


Figure 171. CA50 Map for the TC GDI 2V Model with VVA

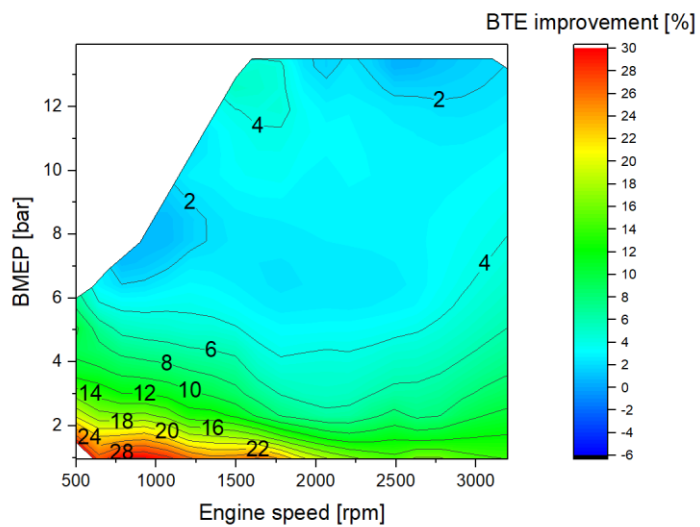


Figure 172. BTE Improvement for the TC GDI 2V Model with VVA Relative to the Turbocharged GDI 2V Engine

5.17 TC GDI 4V, with Full Authority Variable Valve Timing and Duration (VVA) + LPL EGR

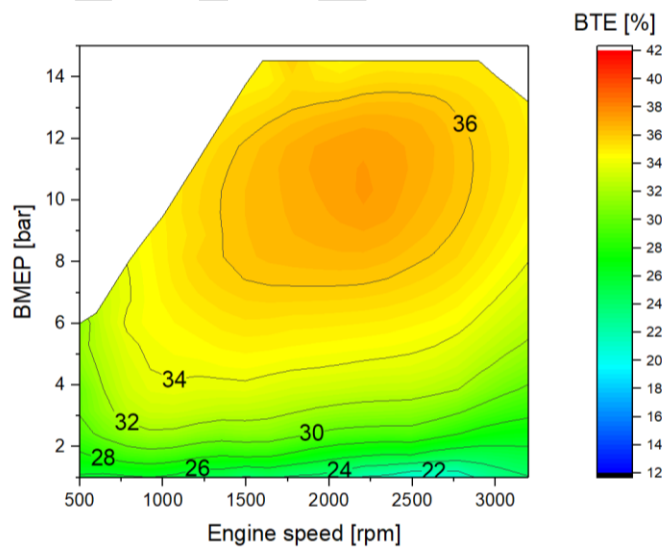


Figure 173. BTE Map for the Turbocharged GDI 4V Model with VVA

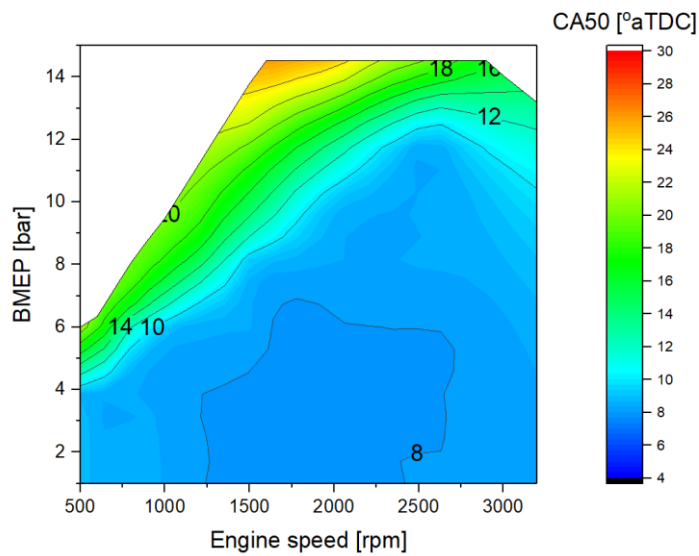


Figure 174. CA50 Map for the Turbocharged GDI 4V Model with VVA

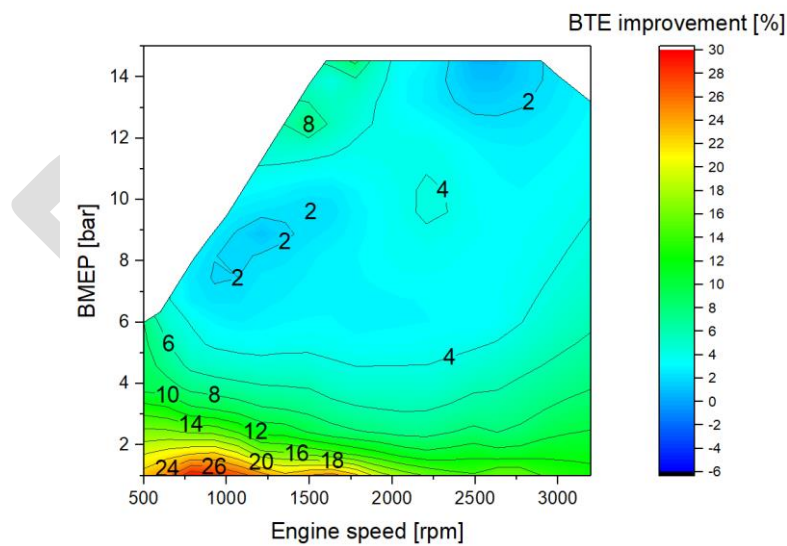


Figure 175. BTE Improvement for the Turbocharged GDI 4V Model with VVA Relative to the Turbocharged GDI 4V Engine

6.0 CONCLUSIONS AND RECOMMENDATIONS

6.1 B6.7 Medium Duty Diesel

Section 2 provides details on the B6.7 engine technologies. The baseline engine model matched well with experimental data, except at low speed and light load and at high speed and light load, where the model tends to overpredict fuel consumption. The high-speed light load area is unlikely to be used to any significant extent on actual drive cycles. The model match was deemed adequate for the task of evaluating new technology options.

An extensive evaluation of mild Miller cycle with fixed valve events failed to achieve any significant fuel consumption benefit, so a map of this technology was not provided. Cylinder deactivation (CDA) provides a 7% to 12% reduction in light load fuel consumption. These benefits generally come in below about 3 bar BMEP, or 15% load. Note that CDA also provides a substantial thermal management effect, so this is a rare technology that can heat the aftertreatment without using extra fuel to do it. A reduction in engine FMEP (friction) provides a benefit of about 1% in fuel consumption at 75% load, with less than 1% benefit at higher loads. Below 50% load, the benefit increases to 2% or more.

Replacement of the conventional VGT / High Pressure Loop EGR system with a fixed geometry turbo and an EGR pump provides a 0% to 2% fuel consumption reduction across most of the operating range. The benefit is independent of whether the EGR pump power is provided by the engine or by an external power source. This is because the EGR pump actually contributes power in the higher speed area of the map, balancing its need for power at lower engine speeds. The final technology combination added CDA to the EGR pump. This combination provides 1% to 2% benefit at most loads above 3 bar BMEP, with much larger benefits of 7% to 13% at light load.

Overall, cylinder deactivation was the most attractive technology, combining light load thermal management with substantial light load BSFC reduction. Friction reduction is also worth pursuing, especially since many medium duty applications run at relatively low load factors. The cost of an EGR pump can be partially offset by switching from an expensive variable geometry turbocharger to a less expensive fixed geometry turbo. To the extent that turbo efficiency can be further increased, the EGR pump will ensure that the proper EGR rate is always available. However, none of the technologies evaluated here are likely to provide drive cycle fuel consumption benefits of 5% or more, except in cycles with low average load.

6.2 Detroit DD15 Heavy-Duty Diesel

Section 3 provides details on the DD15 technologies that were evaluated. The baseline GT model matched experimental fuel consumption data within 3% over almost the entire speed and load range, which was the target for this study. In the critical speed range of 1000 to 1400 RPM, the agreement was generally within 2%. A reduction in FMEP provided a BSFC reduction of about 1% at half load, with the benefit decreasing to less than 0.5% at full load. Reduced FMEP was more effective at light load, with benefits greater than 2% at 25% load or less.

Two levels of downspeeding were evaluated. The more aggressive downspeed option provided fuel consumption reductions of 0 to about 1% over much of the map. However, because the downspeed options allow for taller gearing of the vehicle, larger improvements are expected from the vehicle simulations. For a given power demand, the engine will be running at lower RPM and higher BMEP. For lightly loaded operating conditions, this will push the engine up into a more efficient part of its operating map. It should be noted that use of downspeeding, and especially of the more aggressive option, will require the use of larger, heavier, and more expensive driveline components (transmission, drive shafts, U-joints, and axle) to handle the higher torque.

Two approaches to downsizing were evaluated: one with constant BMEP (and thus lower power and torque) and one retaining the original torque curve (and thus using higher BMEP). Both approaches have little benefit at higher load, but at light load the smaller engines benefit from their reduced overall friction (5/6 of the original friction power). The constant BMEP option has the penalty of reduced vehicle performance.

The organic Rankine cycle WHR system provides 4.5% to 5.5% fuel consumption reductions from half load to full load. These benefits tail off as load is reduced, because of lower exhaust gas temperatures. The critical issue with WHR is its slow transient response. In order to get a realistic estimate of WHR system performance on drive cycles, a transient model that reflects the changes in EGR flow rate and temperature as well as exhaust tailpipe flow rate and temperature is needed. This model would incorporate a thermal model of the aftertreatment system to estimate tailpipe temperature under transient conditions. SwRI strongly recommends development of this model in order to make future evaluations of WHR systems more accurate.

Another technology explored on the DD15 was to replace the asymmetric turbo arrangement with a high efficiency, dual entry, fixed geometry unit. An electrically powered EGR pump provided the required EGR flow. This system provides no fuel consumption benefit at full load, and even a small penalty at speeds over 1600 RPM. On the other hand, at cruise speed there is a 2% benefit at half load, increasing to 5% at light load. Vehicle simulation will be needed to determine the value of the EGR pump under different applications and drive cycles.

Cylinder deactivation did not provide a benefit on this engine because the DD15 already has a form of cylinder deactivation that does not involve shutting the valves off. No map for this technology was provided. Similarly, attempts to implement a mild Miller cycle were unable to obtain a useful benefit. There is a map provided, but it mainly reflects the result of a change in turbocharger match. The new match offers modest BSFC reduction below 1200 RPM, in exchange for fuel penalties above 1200 RPM. The strong Miller cycle required a number of changes: a two

stage fixed geometry turbo system with intercooling, an EGR pump, and variable valve actuation. This system provides 2% or more fuel consumption reduction across a large portion of the operating map, and more at light loads.

As was found in the 2015 study, both mechanical and electrical turbocompound provide little or no benefit, and actually perform worse than the base engine at many conditions. The situation can be improved a little by reducing the EGR rate, but there still doesn't appear to be any justification for the cost and complexity of a turbocompound system.

The final two technology combinations included downspeeding along with the strong Miller (2-stage turbo, VVA, and EGR pump). This combination provides modest benefit at higher load, but up to 10% at light load. Vehicle modeling will be required to quantify the benefit as a function of drive cycle. The last combination added WHR to the previous combination package. This combination provides 5% to 6% BSFC reduction across a wide operating range. However, as previously noted, the slow transient response of the WHR system means that using steady state fuel maps to project vehicle BSFC reduction is very risky. Therefore, SwRI recommends development of a transient WHR system model.

6.3 GM Duramax 3.0 Liter Light Duty Diesel

Section 4 provides detailed information on the technologies that were evaluated on the Duramax 3.0. Figure 67 shows the match between the Duramax 3.0 GT model and experimental results provided by GM. The match is almost always within +/- 3 percent except at very low RPM and at loads below 2 bar BMEP (8% load). At very light load, the model over-predicts fuel consumption.

An across-the-board 20% reduction in FMEP was simulated. This provided a benefit of less than 1% across much of the operating range, but as much as 5% at high speed, light load. With the normal operation of the engine being confined to lower speed under most drive cycles, the benefit of friction reduction will be small. It should also be noted that the Duramax has very low FMEP values for a diesel engine, so achieving a significant reduction in friction would be technically challenging.

Cylinder deactivation provides a double-digit percentage reduction in fuel consumption at light loads, generally below about 3 bar BMEP or 12% load. This should provide benefits in lightly loaded drive cycles, and it also has the benefit of keeping the aftertreatment warmer under light load conditions.

Replacing the single variable geometry turbo with series sequential turbos provides a 2% to 4% benefit below 2,000 RPM and again above 3,000 RPM. Around 2,500 RPM at high load, during the hand-off between the smaller high-pressure turbo and the low-pressure turbo, fuel efficiency suffers slightly.

A second two-stage boosting system was evaluated. This combined a single fixed geometry high efficiency turbo with an e-charger to supply boost support at low engine speeds. The e-charger provided a strong 6% or higher BSFC reduction at low speed and high load, with about 2% savings over a wide area of the map. These results somewhat overstate the benefit of the e-booster,

however, since the energy required to drive the e-boost system was not charged back to the engine. The e-boost system allows an increase in maximum BMEP to 30 bar (from 26), and this was used to create a downspeed torque curve. This would allow the transmission shift points to be lower under high power demand conditions and would also allow a taller axle ratio for the vehicle. These two changes should provide measurable benefits in vehicle drive cycles. The maximum E-Compressor power demand is about 6 kW at 1500 RPM and 22 bar BMEP. The compressor requires 4 kW or more over the range up to 2500 RPM any time load is above 15 bar. Outside of this operating range, the power demand of the e-compressor is minimal.

The final configuration evaluated combined the downspeed engine with e-boost and CDA. This combination provides 3% or more benefit across a wide speed/load range, more than 6% benefit at low speed and high load, and more than 10% benefit at loads less than 3 bar. For this combination, the vehicle model will need adjusted transmission shift points and axle ratio.

6.4 Ford 7.3 Liter Medium-Duty Gasoline Engine

Section 5 provides details of the Ford 7.3-liter engine technologies that were evaluated. The turbocharged variants were somewhat less efficient than their naturally aspirated counterparts, especially if one only considers best point brake thermal efficiency. The benefits of a boosted engine are expected to come in vehicle simulation. The lower rated speed of the boosted variants means that for a given power demand, the boosted engine will run at a lower speed and higher torque than the naturally aspirated engine. At low to moderate loads, this pushes the boosted engine up into a more favorable part of the operating map. SwRI expects that relatively light vehicles and lightly loaded duty cycles will show the best results for boosted engines, but highly loaded vehicles or duty cycles may show a fuel consumption penalty for boosted compared to NA engines.

The addition of GDI is a relatively straightforward change, providing slight benefits across most of the map, but more at higher load. GDI allows a 1-point compression ratio improvement. Dual PFI / GDI systems can be considered to eliminate valve carboning and the light load parasitic power penalty of GDI. Converting from a 2-valve to 4-valve cylinder head means an almost entirely new engine. The 4-valve version provides shorter combustion duration, which allows a half point CR increase for the naturally aspirated engine, and higher BMEP for turbocharged variants (at a constant CR).

Lean burn combustion offers the largest potential for BSFC reduction, especially on boosted variants where the engine can run lean up on the torque curve. Unfortunately, lean combustion would require a NOx aftertreatment system capable of handling the high exhaust temperatures experienced under high load operation. Dual independent cam phasers can provide some light load BSFC reduction, but no benefit at higher loads. Full authority VVT provides across the board BSFC reduction that are largest at light load.

The benefits of low-pressure loop EGR are 3% to 6% below about 6 bar BMEP, but they taper to zero at full load in the naturally aspirated version, where EGR needs to be turned off to achieve full load. Low pressure loop EGR can be used right up to full load on boosted engines, but the

benefits fall in the 1% to 3% range over much of the map. Finally, cylinder deactivation provides large efficiency gains below about 4 bar BMEP, including double digit percentage savings below 3 bar.

6.5 Recommendations for Future Work

There is a large gap in our information on the diesel side between the medium-duty 6.7-liter engine and the heavy-duty 15-liter engine that is generally used for long haul applications. There are many Class 8 vocational applications that use engines in the 9-to-13-liter range, so selecting and evaluating an engine in that size range would help fill in a gap in our existing information portfolio.

The existing waste heat recovery model provides only steady-state operating performance. Long-haul applications have a lot of load transients due to things like mild grades, fluctuations in wind, traffic congestion, and overpasses. Because the transient response of waste heat recovery systems is very slow, it is important to understand how the system performs under real-world conditions. For example, after a step increase in load, it will take more than a minute for a WHR system to reach full output, and WHR output continues for tens of seconds after load demand drops off. This performance will tend to reduce the fuel economy benefits of WHR under transient operating conditions. SwRI recommends a task to expand the current WHR model to include transient performance. This will enable a much more realistic evaluation of WHR's contribution to fuel efficiency over a wide range of drive cycles and payloads.

Turbocharged versions of the 7.3-liter gasoline engine offer slightly lower best point BTE than comparable naturally aspirated versions. However, for a given power demand, the boosted engine will operate at lower speed and higher BMEP, which means the boosted engine will be more efficient under many low and medium power demand conditions. Determining which alternative performs best in vehicles requires vehicle drive cycle simulation, with careful attention to matching the proper axle ratio and shift schedule to each engine variant. SwRI can help review vehicle simulation results to make sure that each engine configuration is evaluated with the axle ratio and shift schedules that will give the best results.

One issue that appeared on the 7.3 liter gasoline engine is high speed knock sensitivity. Because the engine is prone to knock at high RPM, any hybrid system combined with a high compression ratio version of the engine would need to provide substantial power, so that the engine could avoid high speed, high load operating points. SwRI believes that this issue is due to relatively high backpressure from the exhaust and aftertreatment system, and that this backpressure could be reduced at a relatively small cost. To understand the impact of reduced backpressure on knock, SwRI recommends some additional analysis. The knock models available in GT-Power are not accurate enough to provide good guidance, so SwRI recommends using GT to determine the exhaust residual fraction as a function of backpressure, and then using combustion computational fluid dynamics (CFD) software to determine the knock reduction provided by a given change in exhaust backpressure. The goal of this exercise would be to determine if it is possible to achieve a high efficiency hybrid engine configuration that would need only modest support from the electric motor, making a hybrid system both more efficient and lower cost.

DRAFT

APPENDIX A
Waste Heat Recovery System Details

Appendix A – Waste Heat Recovery System Details

For this study, the following configuration of Rankine bottoming cycle was selected and thermodynamically modelled:

- Ethanol working fluid
- Low pressure side (condenser outlet) set at 1.03 bar-abs and 79.0°C. This pressure is selected to be slightly above atmospheric, avoiding the potential of air leakage into a sub-atmospheric pressure system, which would result in a flammable mixture of ethanol and air. This selection also results in a high temperature delta between the condenser outlet and ambient, allowing for a smaller, less complex heat exchanger to be utilized and a possible reduction in frontal area and/or the need for engine cooling fan assistance to keep the system operating satisfactorily.
- High pressure level fixed at 350 bar-abs in consideration of maintaining reasonable cost hardware for sealing and managing the pressure
- Pressures and flowrates are independent of engine operating point, implying a variable speed/capacity pump and expander
- Flowrate is adjusted at each point to provide maximum bottoming cycle output
- Minimum “approach temperature” for every heat exchanger is assumed to be 25°C. This means that on a counterflow heat exchanger, for example between the exhaust stack gas and bottoming cycle fluid, the bottoming cycle fluid outlet cannot be hotter than 25°C below the incoming exhaust stack gas.
- Each heat exchanger (HX) is presumed to have a pressure drop of 10 kPa which is fixed independent of flowrate
- The expander details are not specified but a fixed 70% isentropic efficiency is applied to the device
- Electrical efficiencies are assumed to be 91% for generator and motor. Therefore, to take the power from the bottoming cycle output to the crankshaft, the transport efficiency is $(91\%)^2$ or 82.8%.
- The configuration is as shown in Figure A1 below:
 - Pump
 - Stack pre-heater
 - EGR cooler/final heater
 - Expander
 - Condenser
 - Optionally, a recuperator is applied, transferring heat from the expander outlet to the pump outlet fluid

No efforts were made to recover heat from either the aftercooler or jacket water systems on the engine, since previous studies found those sources to be too low in temperature to contribute in a favorable manner to the bottoming cycle performance. Heat was recovered from a post-aftertreatment exhaust stack heat exchanger and then from the EGR cooler, where heat quantities

and temperatures are both high and facilitate an effective and efficient bottoming cycle. Because the EGR cooler is the higher temperature source of heat, it is placed second in the flow path to maximize expander inlet temperature. It is noted that there will need to be additional EGR cooling, since at most conditions the bottoming cycle fluid leaving the EGR cooler is too hot to bring the EGR down to the final target EGR cooler outlet temperature.

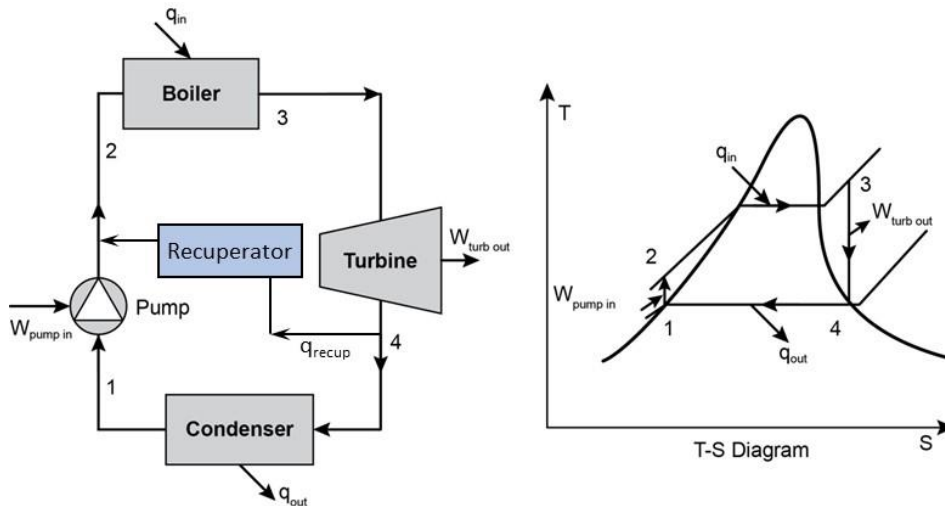


FIGURE A1. SCHEMATIC AND T-S DIAGRAM OF WHR SYSTEM

As mentioned earlier in section 1.6, the ORC was determined to not provide significant output below 20% load and those points were all taken as having no contribution from the WHR system. In addition, heat rejection to the ORC condenser was arbitrarily limited to 80 kW in an attempt to limit the impact on fan load and/or vehicle aerodynamics.

The impact of this limitation is shown in Figure A2, where the contribution to crankshaft power is given for three configurations of the bottoming cycle applied to the best combination engine build: Base, Base with Qrej-ltd (basic configuration with condenser heat rejection limited to 80 kW), and Recup with Qrej-ltd (recuperator configuration with condenser heat rejection limited to 80 kW). The upper portion of Figure A2 gives the bottoming cycle final power output to the cranktrain after electrical conversion losses and the lower portion of Figure A2 gives that power as a percentage of the engine's brake power at the given operating point. Results for the base case are shown as blue bars, while results for the base case with Qrej-ltd are shown in red. Limiting the heat rejection to 80 kW has little or no effect on the output power at most operating conditions. Results for the recuperator with Qrej-ltd are shown in green. The recuperator improves system performance at most operating conditions.

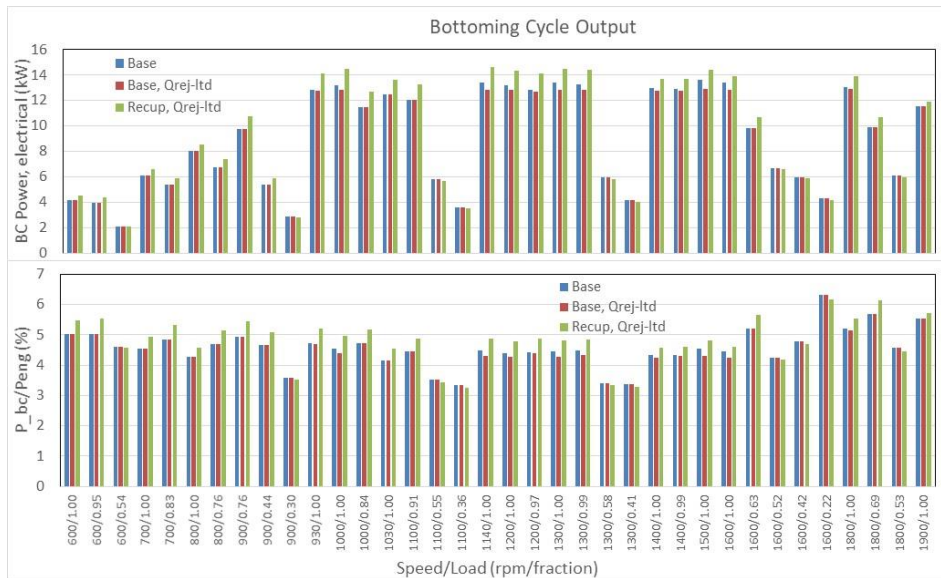


FIGURE A2. BOTTOMING CYCLE OUTPUT IN KW AND AS A PERCENTAGE OF ENGINE POWER, ALL AS A FUNCTION OF ENGINE SPEED AND LOAD

As the figure shows, the bottoming cycle contributes over 12 kW to the engine system at high loads, with bottoming cycle output decreasing with decreasing engine power, as would be expected due to lower exhaust flow rates and temperatures. Figure A2 demonstrates that the bottoming cycle output as a percentage of base engine power is on the order of 3-6% for the operating points shown. This value represents the fuel consumption reduction that would be provided by the addition of the bottoming cycle to the engine system.

The marginal improvement provided by the recuperator is also apparent in Figure A2. At part loads, the recuperator provides little to no benefit in terms of bottoming cycle power output and can even result in minor reductions in power due to the pressure drop of two additional heat exchanger passes. In many of the low load points, the recuperator is non-functional; that is, the temperature coming out of the expander is not high enough to be able to transfer heat to the pump outlet fluid. At high loads, the recuperator compensates for the loss that the simple cycle experiences when constrained to 80 kW of condenser heat rejection, and it accomplishes some additional gain. Critically for the vehicular application of the bottoming cycle, the recuperator significantly reduces the condenser heat rejection, therefore improving the power output at a given heat rejection level. This is represented in figures dpb2 and dpb3 where the full load data is provided showing the BC power output reduction when the condenser heat rejection is limited to 80 kW for the basic BC. However, the recuperated version (which also has limited condenser heat rejection) is not only able to recover that loss but to provide significantly more power than even the unlimited non-recuperated version.

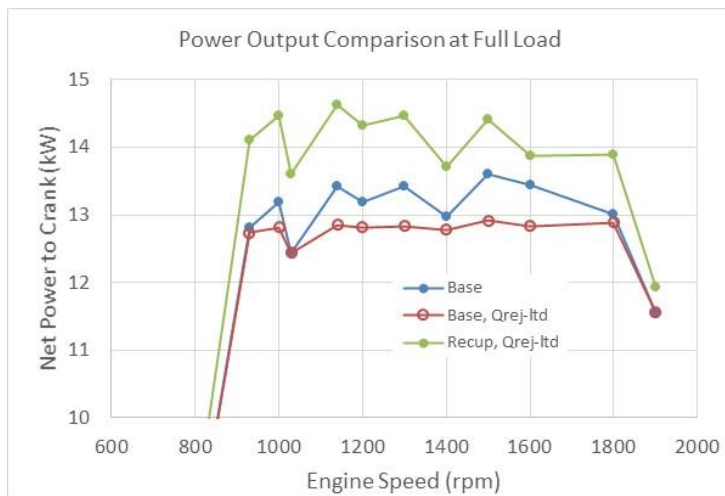


FIGURE A3. BOTTOMING CYCLE POWER OUTPUT AT ENGINE FULL LOAD CONDITIONS

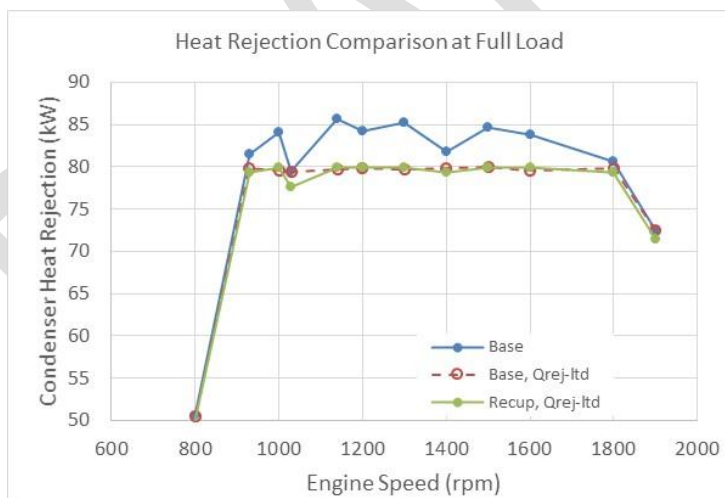


FIGURE A4: BOTTOMING CYCLE CONDENSER HEAT REJECTION AT ENGINE FULL LOAD CONDITIONS

The actual condenser heat rejection for full load operation with the three different BC configurations is shown graphically in Figure A4, showing that nearly all the full load points were limited, but the reductions were moderate, on the order of 5%.

The ratio of bottoming cycle power output divided by heat rejection is given in Figure A5, which shows an improvement of ~0.02 (or 12%) in the power/heat rejection ratio on average. Because vehicle heat rejection is of considerable importance to the truck cooling system design, the improved power per unit heat rejection offered by the recuperator is a significant advantage.

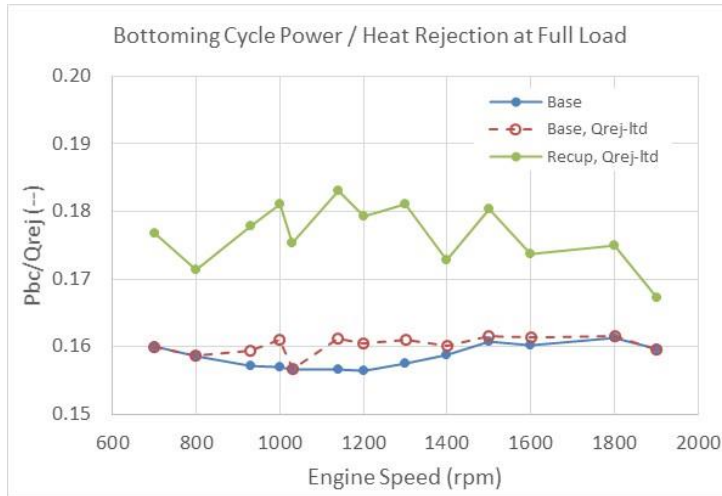


FIGURE A5. BOTTOMING CYCLE NET POWER / CONDENSER HEAT REJECTION AT ENGINE FULL LOAD CONDITIONS

Figure A6 demonstrates that the recuperator adds about 0.5% additional system power output at full load at the 80-kW heat rejection limit, equivalent to a 0.5% reduction in fuel consumption. This, along with the heat rejection advantage provided by a recuperator, would allow financial benefits to be computed for a given driving cycle or application to determine the desirability of the recuperator.

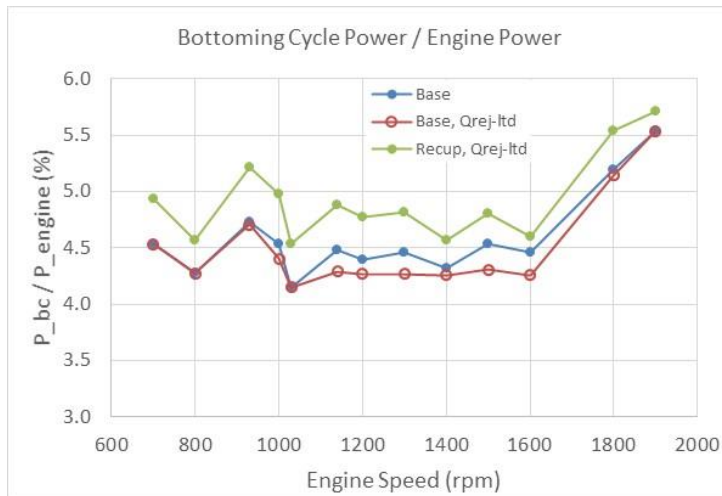


FIGURE A6. BOTTOMING CYCLE PERCENT POWER CONTRIBUTION AT FULL LOAD CONDITIONS

There are two limitations of WHR systems that must be accounted for when using the fuel maps provided by this project in vehicle simulations. First, if the additional heat rejection from the bottoming cycle causes the engine cooling fan to come on, the result would be a net negative impact on fuel consumption. The engine cooling fan takes more power to operate over most of the engine speed range than the WHR system can contribute, so the control system would need to disable the WHR if its use would cause the fan to come on. This can only be modelled using a sophisticated vehicle cooling system model such as can be found in GT-Suite.

The second limitation of WHR systems is their very slow transient response. Engine aftertreatment has a very high thermal inertia, so a step change in engine load (and engine exhaust temperature) takes a long time to show up as a change in aftertreatment outlet temperature. This means that when engine load increases, it takes time (minutes) for the WHR system to produce its full potential power. When engine power demand drops to zero, the WHR system will continue to produce some power for minutes. This power must be thrown away if it is not needed unless an energy storage system is available. A 48V mild hybrid system could accommodate the power of a WHR system and serve as an energy storage buffer. Again, detailed vehicle simulation modelling would be required to accurately assess WHR performance on any drive cycle that is not entirely steady state.

Figure A7 shows the response of a production aftertreatment system to an increase in engine load. The data shown is taken from a segment of the FTP transient emissions certification cycle for heavy-duty diesel engines. The engine power ramps up from 75kW to 360 kW starting at Time = 0 (black curve). The engine exhaust temperature increases fairly rapidly, but not as fast as the load increase, due to the thermal inertia of the engine components and turbocharger (grey curve). Aftertreatment inlet temperature tracks exhaust temperature but shows a loss of about 10°C from

the engine outlet (red curve). Finally, the aftertreatment outlet temperature responds very slowly to changes in exhaust temperature or aftertreatment inlet temperature (blue curve).

The aftertreatment outlet temperature is actually higher than the inlet temperature from Time -60 to +20 seconds, because the thermal inertia of the system warms the exhaust after a decrease in load (an event that happened before the beginning of the figure). Once the exhaust and aftertreatment inlet temperatures increase after Time = 0, the aftertreatment outlet temperature lags behind for 200 seconds. The yellow curve is referenced to the secondary Y-axis, and it shows the difference between engine out and aftertreatment outlet temperatures.

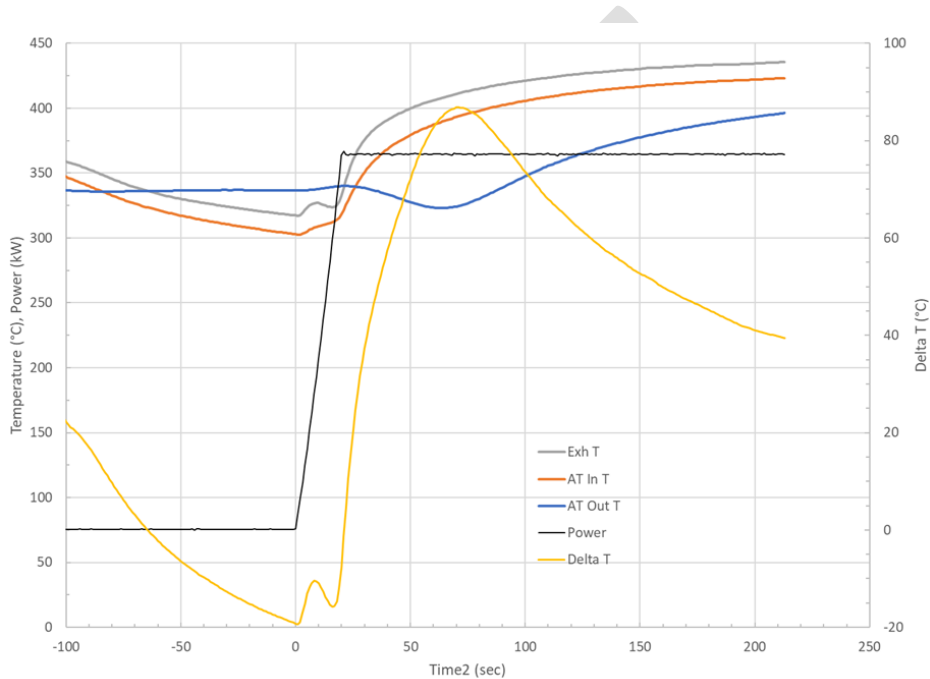


FIGURE A7. THERMAL RESPONSE OF A PRODUCTION AFTERTREATMENT SYSTEM.

The bottoming cycle is clearly one of the largest improvements that can be made to the engine in terms of fuel consumption reduction and BTE improvement. Unfortunately, it also has a high cost and high impact to the engine installation.